Dissertation

Submitted to the

Combined Faculties for Natural Sciences and for Mathematics

of the Ruperto-Carola University of Heidelberg, Germany

for the degree of

Doctor of Natural Sciences

presented by

Stephanie Hoppe, M.Sc. Molecular Biosciences

born in Achim, Germany

Oral Examination: 18.06.2015

Identification of target T cell epitopes for a therapeutic HPV16 vaccine

Referees: Prof. Dr. Martin Müller

PD Dr. Dr. Angelika Riemer

The work described in this thesis was performed from November 2010 to January 2015 under supervision of PD Dr. Dr. Angelika Riemer in the group Immunotherapy and -prevention at the German Cancer Research Center (DKFZ) in Heidelberg, Germany.

Conference and workshop presentations based on this study:

Hoppe, S., Blatnik, R., Grabowska, A.K., Wühl, M., Link, S., Warnken, U., Ruppert, T., Schnölzer, M. and Riemer, A.B. *Identification of HPV T cell epitopes for therapeutic vaccine design by mass spectrometry*. (09/2011): Poster presentation at the 16th International Summer School on Immunology by the Federation of European Biochemical Societies (FEBS), Hvar, Croatia

Hoppe, S., Blatnik, R., Grabowska, A.K., Wühl, M., Link, S., Rösli, C., Warnken, U., Ruppert, T., Schnölzer, M. and Riemer, A.B. *Identification of HPV T cell epitopes for therapeutic vaccine design by mass spectrometry*. (09/2011): Poster presentation at the 2011 Joint Annual Meeting of the Italian Society of Immunology Clinical Immunology and Allergology (SIICA) - German Society for Immunology (DGfI), Riccione, Italy

Hoppe, S., Blatnik, R., Grabowska, A.K., Wühl, M., Link, S., Warnken, U., Ruppert, T., Schnölzer, M. and Riemer, A.B. *Identification of HPV T cell epitopes for therapeutic vaccine design by mass spectrometry*. (02/2012): Poster presentation at the 2nd Heidelberg Forum for Young Life Scientists, Heidelberg, Germany

Hoppe, S., Blatnik, R., Grabowska, A.K., Wühl, M., Link, S., Warnken, U., Ruppert, T., Schnölzer, M. and Riemer, A.B. *Identification of HPV T cell epitopes for therapeutic vaccine design by mass spectrometry*. (07/2012): Poster presentation at the DKFZ PhD retreat, Weil der Stadt, Germany

Hoppe, S., Blatnik, R., Grabowska, A.K., Wühl, M., Ruppert, T., Warnken, U., Schnölzer, M. and Riemer, A.B. *A mass spectrometry approach to identify HPV16 T cell epitopes for therapeutic vaccine design*. (09/2012): Poster presentation at the European Congress of Immunology 2012, Glasgow, UK

Hoppe, S., Blatnik, R., Grabowska, A.K., Wühl, M., Ruppert, T., Warnken, U., Schnölzer, M. and Riemer, A.B. *A mass spectrometry approach to identify HPV16 T cell epitopes for therapeutic vaccine design*. (11/2012): Poster presentation at the DKFZ PhD Poster Presentation, Heidelberg, Germany

Hoppe, S. and Blatnik, R. *A mass spectrometry approach to identify HPV16 T cell epitopes*. (04/2013): Talk at the ATV retreat (Infection & Cancer) 2014, Bad Kreuznach, Germany

Hoppe, S., Blatnik, R., Wühl, M., Ruppert, T., Warnken, U., Schnölzer, M. , Rösli, C. and Riemer, A.B. *A mass spectrometry approach to identify HPV16 T cell epitopes for therapeutic vaccine design.* (06/2013): Poster presentation at the 7th International PhD Student Cancer Conference, London, UK

Hoppe, S., Blatnik, R., Wühl, M., Ruppert, T., Schnölzer, M. and Riemer, A.B. *A mass spectrometry approach to identify HPV16 T cell epitopes for therapeutic vaccine design.* (11/2013): Talk and poster presentation at the Cold Spring Harbor Asia (CSHA) Tumor Immunology and Immunotherapy Conference, Suzhou, China

Hoppe, S. *Identifying HPV16 T cell epitopes for therapeutic vaccine design*. (05/2014): Talk at the ATV retreat (Infection & Cancer) 2014, Schöntal, Germany

Hoppe, S., Blatnik, R., Schessner, J.P., Dressler, L., Steinbach A., Winter, J., Wühl, M., Klevenz, A., Khallouf, H. and Riemer, A.B. *Identification of target T cell epitopes for a therapeutic HPV16 vaccine*. (12/2014): Poster presentation at the American Association for Cancer Research (AACR) conference Tumor Immunology and Immunotherapy: A New Chapter, Orlando, USA

I. Abstract

To rationally design therapeutic human papillomavirus (HPV) vaccines, it is important to know which T cell epitopes are present on HPV-transformed cells. HPV affects the cellular antigen processing machinery, thus not every epitope derived from viral proteins is necessarily presented by human leukocyte antigen (HLA) molecules on the cancer cell surface.

HPV16 has been identified as the causative agent in 50% of all cervical cancer cases and in approximately 95% of all extra-cervical mucosal HPV-induced tumors. The transforming potential of high-risk HPVs is mediated by two consistently expressed viral oncoproteins, E6 and E7. As the induction and maintenance of the malignant phenotype depend on these two proteins, they are ideal targets for immunotherapy. A therapeutic vaccine that is applicable to everyone without prior HLA typing needs to contain epitopes for the major HLA types. To date, HPV T cell epitopes have mostly been determined for the most prevalent HLA type, HLA-A2. We now aim to identify HPV16 E6 and E7 T cell epitopes for the HLA-A3, HLA-A11 and HLA-A24 supertypes.

Different *in silico* prediction algorithms were used to predict prospective epitopes from the E6 and E7 proteins derived from the HPV16 reference sequence for the mentioned HLA supertypes. In total, 74 epitopes, comprised of 8 to 11mer peptides, were predicted for HLA-A3, 96 epitopes for HLA-A11 and 95 epitopes for HLA-A24. In competition-based cellular binding assays, 22 previously known binding peptides were confirmed and 78 novel binding peptides were identified. Additionally, HPV16 variants harbored in our HPV16-positive cell line collection were determined and peptide binding to HLA-A24 was shown for seven out of 20 tested HPV16 variant peptides.

Evaluation of prediction server performance based on the generated data suggested different optimal prediction servers depending on peptide length and on the HLA type. NetMHC and NetMHCcons were shown to be the best predictors overall.

Immunogenicity of identified binding peptides was investigated by screening long-term memory responses in healthy donors. To this end, peptide-specific short-term T cell lines were generated from peripheral blood mononuclear cells, which were HLA typed, stimulated with HLA-matching peptides and cultured for twelve days. Several peptides were identified to be immunogenic. Immunogenicity of the four most promising candidate peptides for HLA-A24 could be further confirmed by generation of peptide-specific long-term T cell lines from healthy HLA-A24-positive donors and subsequent co-culture with autologous B cells pulsed with the respective peptide. Functional assays, such as IFNγ ELISpot assays and cytotoxicity assays, determined the best vaccine candidates.

In conclusion, several novel HPV16 E6 and E7 $CD8^+$ T cell epitopes were identified. Verified epitopes are the basis of rational therapeutic vaccine design and are also important for immunomonitoring purposes. In addition, they can be employed as a tool for the development of other immunotherapies such as adoptive T cell transfer with transgenic T cell receptors.

II. Zusammenfassung

Für die Entwicklung eines effizienten therapeutischen Impfstoffs gegen humane Papillomviren (HPVs) ist es wichtig zu wissen, welche T Zell Epitope auf HPV-transformierten Zellen präsentiert werden. HPV beeinflusst die zelluläre Prozessierung von Antigenen und deshalb wird nicht jedes Epitop der viralen Proteine zwangsweise auch von humanen Leukozytenantigen (HLA)-Molekülen auf der Oberfläche von Krebszellen präsentiert.

HPV16 wurde als kausal in 50% aller Gebärmutterhalskrebsfälle und in ungefähr 95% aller anderen mukosalen HPV-induzierten Tumoren identifiziert. Das transformierende Potential von Hochrisiko-HPV-Typen ist durch die beiden konstitutiv exprimierten Onkoproteine E6 und E7 gegeben. Da die Induktion und das Aufrechterhalten des malignen Phänotyps auf diesen beiden Proteinen beruht, sind sie ideale Ziele für Immuntherapien. Ein therapeutischer Impfstoff, der ohne eine vorherige HLA-Typisierung für jeden verwendbar ist, muss Epitope für mehrere HLA-Typen beinhalten. Allerdings wurden bisher hauptsächlich HPV T-Zell-Epitope für den häufigsten HLA-Typ, HLA-A2, bestimmt. Das Ziel dieser Studie war die Identifizierung von HPV16 E6 und E7 T-Zell-Epitopen für die HLA-Supertypen HLA-A3, HLA-A11 und HLA-A24.

Verschiedene *in silico* Algorithmen wurden verwendet um potentielle 8- bis 11mer Epitope der E6 und E7 Proteine der HPV16 Referenzsequenz für die obengenannten HLA-Supertypen vorherzusagen. Insgesamt wurden 74 Epitope für HLA-A3 vorhergesagt, sowie 96 Epitope für HLA-A11 und 95 Epitope für HLA-A24. In kompetitiven Peptid-Bindungs-Tests konnten 22 bekannte bindende Peptide bestätigt und 78 neue bindende Peptide identifiziert werden. Zusätzlich wurden HPV16-Varianten, die in unserer HPV16 positiven Zellkultursammlung vorkommen, bestimmt. Die Peptidbindung an HLA-A24 konnte in sieben von zwanzig getesteten HPV16-Variantpeptiden gezeigt werden.

Basierend auf den generierten Daten von bindenden und nicht bindenden Peptiden wurde eine Evaluation der Leistung der Vorhersageserver wurde durchgeführt. Hierbei stellten sich verschiedene Vorhersageserver als führend bei unterschiedlichen Peptidlängen und bei verschiedenen HLA-Typen heraus. Generell konnten NetMHC und NetMHCcons in dieser Studie als die beste Vorhersageserver bestimmt werden.

Um die Immunogenität der identifizierten bindenden Peptide zu untersuchen, wurden Langzeit-Gedächtniszellantworten in gesunden Spendern überprüft. Zu diesem Zweck wurden Peptid-spezifische Kurzzeit-T-Zelllinien aus mononukleären Zellen des peripheren Blutes generiert und die HLA-Typen der Spender bestimmt. Daraufhin wurden die Zellen mit HLA-passenden Peptiden stimuliert und für zwölf Tage kultiviert. Etliche Peptide waren immunogen. Die Immunogenität der vier vielversprechendsten Peptidkandidaten wurde durch Peptid-spezifische Langzeit-T-Zelllinien bestätigt, welche zu diesem Zweck mit autologen B Zellen co-kultiviert wurden, die zuvor mit den selben Peptiden gepulst worden waren. Funktionelle Tests, wie IFNγ-ELISpot-Assays oder Zytotoxizitäts-Experimente, wurden verwendet um die besten Impfstoffkandidaten zu bestimmen.

In der vorliegenden Studie konnten neue HPV16 E6 und E7 T-Zell-Epitope identifiziert werden. Verifizierte Epitope sind die Basis für die rationale Entwicklung von therapeutischen Impfstoffen und zudem wichtig für Immunomonitoring-Ansätze. Zusätzlich können sie genutzt werden, um andere Immuntherapien, wie zum Beispiel adoptiven T-Zelltransfer mit transgenen T-Zellrezeptoren, zu entwickeln.

III. Acknowledgements

An dieser Stelle möchte ich mich bei allen Personen bedanken, die bei der Umsetzung dieser Doktorarbeit durch fachliche und persönliche Hilfestellung mitgewirkt haben.

Zu allererst möchte ich mich bei PD Dr.Dr. **Angelika Riemer** bedanken, die mir die Möglichkeit gegeben hat, meine Doktorarbeit in ihrer Arbeitsgruppe anfertigen zu können. Besonders möchte ich mich für das Vertrauen und den großen wissenschaftlichen Freiraum bedanken, den ich während meiner Promotion hatte. Sie hat mich über das Projekt hinaus voll unterstützt und mir die Chance gegeben mich sowohl menschlich als auch wissenschaftlich weiterzuentwickeln.

Bei Prof. Dr. **Martin Müller** möchte ich mich herzlich für die Übernahme des Erstgutachtens bedanken und dafür, mir als TAC Mitglied zur Seite zu stehen. Zudem möchte mich mich bei PD Dr. **Suat Ötzbeck** und Dr. **Steeve Boulant** dafür bedanken, dass sie meine Prüfer in meiner Disputation waren. Ein weiteres Dankeschön geht an Dr. **Volker Lohman**, der mich als TAC Mitglied unterstützt hat.

Ein ganz besonderer Dank geht an unser gesamtes Labor mit der alten und etwas neueren Stammbesetztung aus **Renata Blatnik**, Dr. **Aginieszka Grabowska,** Dr. **Hadeel Khallouf**, **Alina Steinbach**, **Martin Wühl** und **Alexandra Klevenz**. Danke für die vielen Ratschläge, Meinungen, Diskussionen, die Offenheit und Direktheit, die Hilfe im Labor und vor allem für die fantastische Atmosphäre. Egal was war, wir hatten so viel Spass und ihr wart immer für mich da.

Renatka möchte ich hvala sagen dafür, dass wir das Abenteur PhD von Anfang an gemeinsam durchgestanden haben. Vielen Dank für alles über das Labor hinaus, dafür dass Du mir deine Heimat gezeigt hast, für unseren letzten genialen Skiurlaub und und und... Bei **Hadeel** möchte ich mich speziell für die wissenschaftlichen Diskussionen, die Hilfe im Labor und für deinen Input zu dieser Arbeit bedanken, zudem für unsere ganzen gemeinsamen Konferenzen, vor allem unser Trauma Mickey Mouse. Außerdem für deine motivierende Art und dein Verständnis und dafür, dass Du ein treuer Spinning- und Unisportpartner bist, شكرا. Ein ganz dickes Dankeschön an **Alina**, dafür dass Du einfach du bist. Wenn man dich sieht, geht die Sonne auf. Vielen Dank für die ganze theoretische und praktische Hilfe bei den T und B cells und fürs Korrekturlesen. Bei **Martin** möchte ich mich für die ganze Unterstützung in der Zellkutur bedanken, dafür dass ich mit allem zu Dir kommen konnte und Du immer ein offenes Ohr hattest. **Alex** möchte ich für die wertvollen Tipps, tatkräftige Unterstützung und Ideen im letzten Jahr ganz speziell danken. Im Besonderen auch dafür, dass Du selbst in stressigsten Situationen und sonst auch immer gut gelaunt bist. Bei **Agi** möchte ich mich für die Hilfe und Tipps im Labor bedanken. Dziękujemy, für deine einmalige Art und auch für all unsere Labtrips nach Stuttgart bzw Bad Cannstatt. Ein weiteres Dankeschön geht an **Jan Winter** für die ganzen Ideen und Unterstützung in puncto Bioinformatik bei den T cell predictions und für deine beruhigende Art.

Vielen Dank auch an all unsere Praktikanten und Studenten die über die Jahre bei uns waren, **Marc Pfeil**, **Aakanksha Jain**, **Victoria Hentschke**, **David Kranz**, **Fanny Georgi**, **Johannes Stortz**, **Kinga Grabowska**, **Sina Knapp**, **Jasmin Mangei, Miriam Bertrant** und **Sebastian Utz** und ganz speziell an meine Bachelor und Master Studenten: Vielen Dank an **Johanna Dickmann**, die meine erste Bachelorette war und mir bei der Story um die HPV16 Varianten sehr geholfen hat. Danke an **Marius Küpper**, der es fast ein ganzes Jahr mit mir und seiner Masterarbeit bei uns ausghalten hat. Ein dickes Dankeschön an **Julia Schessner** und **Lisa Dreßler**, die mir im letzten Sommer bei den ELISpots geholfen haben. Danke, dass ihr euch mit mir die Nächte vorm FACS und in der Zellkultur um die Ohren geschlagen habt.

Für die Unterstützung bei allem Bürokratischen möchte ich mich bei **Angelika Schmidt-Zitouni** und **Monika Bock** herzlich bedanken.

Auch unseren alten und neuen **Labornachbarn**, den **Hoppe Seylers** und den **de Villiers**, möchte ich sehr für die Unterstützung und tolle Nachbarschaft danken. Zudem vielen Dank an die **Krammers**, die uns in ihren Journal Club aufgenommen haben und für die ganzen Antikörper und Co. Zudem möchte ich mich bei all meinen **Blutspendern** bedanken, ohne die diese Arbeit nie zustande gekommen. Vielen Dank an Prof. **Michael Pawlita** für die unzähligen Male Blut abnehmen.

Vielen Dank auch an **Hans-Henning Schmidt** und **Jasmin Quandt** von den **Beckhoves** dafür, mich jahrelang an das FACS mit dem 96-well plate reader gelassen zu haben.

Ausserdem möchte ich meinen Freunden, die mir das Leben nebem dem Labor versüßt haben danken.

Ein dickes Dankeschön geht an **Lisa Thill** dafür dass, wenn Du auch im weit, weit entfernten Amsterdam, Trier, Köln oder auf irgendwelchen thüringischen Wiesen warst, trotzdem immer in Kontakt geblieben bist und für dein spontanes Korrekturlesen. Ganz speziell möchte ich mich bei **Bettina Fiege** bedanken, für unsere letzten gemeinsamen Jahre in Heidelberg. 1000 Dank dafür, dass Du mich immer wieder daran erinnert hast, dass es auch ein Leben ausserhalb des Labs gibt, für unsere ganzen Kaffeepausen und Wein-, Koch- und Partyabende. Danke auch fürs Korrekturlesen. Ein ganz spezieller Dank geht an **Nadine Hertrich**. Vielen, vielen Dank, dass Du Tag und Nacht für mich da warst. Ohne die tausenden Kilometer die wir zusammen gelaufen sind, wären wir wohl beide noch mehr abgedreht, als wir es eh schon sind. Danke fürs Zuhören, Ertragen und die ganzen Dinge die wir in den letzten fast sieben Jahren erlebt haben. Außerdem natürlich fürs Korrekturlesen und die Fernunterstützung in den letzten 4 Monaten.

Abschließend danke ich meiner Familie, **Nils**, **Gabi** und **Günter Hoppe**, die mich während des gesamten Studiums und während meiner Promotion bedingungslos unterstützt haben. Vielen, vielen Dank für eure Geduld mit mir, fürs Zuhören und eure Ratschläge in allen Lebenslagen. Danke dafür, dass ihr einfach immer für mich da seid.

IV. Table of Contents

V. List of Figures

VI. List of Tables

1. Introduction

In 3000 BC, cancer was first described as a disease (Hajdu, 2011) and despite of considerable progress in development of therapy, cancer still remains the second-leading cause of death in the industrialized world today (WHO, 2008). After cardiovascular diseases, cancer is also the second most common cause of death for women and men in Germany (DKFZ, 2012). In 2012, cancer globally accounted for 8.2 million deaths (Ferlay et al., 2012; WHO, 2014) and it is estimated that annual cancer cases will increase further from 14 million in 2012 to 22 million cases within the next two decades. Moreover, the WHO indicates that 60% of the global new annual cases will occur in less developed countries.

Incidences of most cancer entities increase with age and thus, cancer is often referred to as a disease of the advanced age. Taking into consideration that medical progress also accounts for a steadily increasing life expectancy, cancer has been becoming a growing major public health problem (Jemal et al., 2011; Soerjomataram et al., 2012).

Cancer can be described as a large group of diseases comprising the formation of neoplasms or malignant tumors in any part of the body (Ferlay et al., 2012). Abnormal cells grow unlimited beyond their normal boundaries and thus form tumors. If they invade adjacent tissue and spread to other organs, this process is called metastasis and is actually the major cause of death from cancer. The origin of cancer is multifaceted, including inherited genetic causes as well as environmental factors such as tobacco smoking, diet, obesity and infections (Ferlay et al., 2012). Infectious agents causing cancer include bacteria and viruses such as the human papillomaviruses (HPV), the hepatitis B and C viruses (HBV and HCV), human herpes virus 8 (HHV8) and Epstein-Barr virus (EBV) (Parkin, 2006).

Since cancer cells are altered cells of one's own body, treatment is difficult. For successful treatment, it is crucial to distinguish cancerous cells from nonmalignant cells and elucidate the underlying mechanisms that lead to the development of cancer. During the last decades, genetic alterations were discovered to be the cause for cancer on the molecular level. In 2000, Hanahan and Weinberg formulated the hallmarks of cancer (Hanahan and Weinberg, 2000), which describe the six major capabilities that cells acquire during the malignant transformation process. Those hallmarks include sustaining proliferative signaling, evading growth suppressors, enabling replicative immortality, activating invasion and metastasis, inducing angiogenesis and resisting cell death. In 2011, deregulation of cellular energetics and avoiding immune destruction were added as two new emerging hallmarks and tumor-promoting inflammation and genome instability and mutation were added as two 'enabling characteristics' (Hanahan and Weinberg, 2011).

1.1 Human papillomavirus and associated diseases

Papillomaviruses (PVs) cause epithelial infections in most mammals and birds, and are highly species-specific (de Villiers et al., 2004). PVs were first identified in warts of cottontail rabbits (Shope and

Hurst, 1933) and in 1935, Francis Peyton Rous discovered that the cottontail rabbit papillomavirus (CRPV) induces malignant transformation and tumors in the skin of infected rabbits (Rous and Beard, 1935). In the 1970s, the first connection between cervical cancer and HPV was postulated by Harald zur Hausen (zur Hausen et al., 1975; zur Hausen, 1977), which could be later confirmed biologically (Gissmann and zur Hausen, 1980; Gissmann et al., 1982a; Gissmann et al., 1982b) and epidemiologically (Munoz et al., 2006). Since the first isolation of HPV16 in 1983 (Durst et al., 1983), HPV has been investigated intensively finally leading to the development of prophylactic vaccines that have been introduced in more than 40 national vaccination programs worldwide (Poljak, 2012).

HPV types can be subdivided into low-risk and high-risk types. Low-risk HPV types mainly cause benign ano-genital and skin warts whereas high-risk types are associated with ano-genital cancer, such as cervical, vaginal, penile and anal cancers (Chow et al., 2010), and head and neck cancers including their precursor lesions (Pim and Banks, 2010). HPV-associated squamous cell carcinomas (SCCs) of the head and neck (HNSCC) are mainly found in the oropharynx, especially at the base of the tongue and the tonsils (Gillison et al., 2000; Chow et al., 2010; Lajer and von Buchwald, 2010). Other sites in the head and neck region can also be infected by HPVs, e.g. the eye conjunctiva, the nasal sinuses and ear canals.

The high-risk types HPV16, 18, 31, 33, 35, 45, 52 and 58 account for most of all ano-genital cancers and especially cervical carcinomas. HPV16 and 18 together cause approximately 70% of all cervical cancers, and in virtually all other cervical cancers DNA from other high-risk HPV types can be detected (Munoz et al., 2006).

Depending on the site of infection, cervical, vulval, vaginal and anal intraepithelial neoplasias are distinguished (CIN, VIN, VAIN and AIN, respectively). Persisting infection with high-risk HPV can progress to intraepithelial neoplasia grade I, such as CIN1 in the cervix. Most squamous intraepithelial lesions are cleared within 6 to 12 months after infection, however a small number of lesions persist (2% over 5 years) and can develop to moderate dysplasia (CIN2) or severe dysplasia (CIN3), which is the immediate precursor of cervical cancer (zur Hausen, 2002; Longworth and Laimins, 2004). It has been shown that even CIN3 lesions can regress spontaneously in some cases and are thus considered to be a dynamic disease (Zehbe et al., 1998). However, a high viral load of especially HPV16 and 18 has been shown to elevate the risk to develop CIN3 (Schlecht et al., 2001).

The general time frame between the initial HPV infection and CIN3 development was estimated to be 7 to 15 years. If the primary infection has occurred in the late teens or early twenties, as seen mostly, CIN3 diagnosis peaks around 25-30 years of age (Bosch and de Sanjose, 2003). For some cohort studies it was documented, however, that there is a much faster development of CIN2-3 among women infected with HPV16 or 18 (Winer et al., 2005).

HPV is the most common sexually transmitted agent worldwide and the associated risk of cancer development is a major health burden. The virus is strictly tissue-tropic, infecting only squamous epithelia of cutaneous and mucosal surfaces in humans. At highest risk for malignant transformation are the so-called transformation zones between the squamous and columnar epithelium. Such zones are found in the larynx, nasal sinuses, urethra, cervix and anal/rectal junctions. HPV is mainly transmitted during sexual intercourse or other contact of affected surfaces. Therefore, the majority of the sexually active population, up to 95%, are or will become infected once in their lifetime (Evander et al., 1995; Woodman et al., 2007). Of all the women who acquire a genital HPV infection, half of them are infected within three years of their first sexual contact (Collins et al., 2002). The infection is usually transient and resolves spontaneously within 6 to 18 months in 95% of all cases (Crosbie et al., 2013). Thus, HPV infections are very common amongst young women at ages 20 to 24, and the prevalence in this age group ranges from 20 and 40% depending on the geographical region (Richardson et al., 2003; Cuschieri et al., 2004; Dunne et al., 2007). The incidence of HPV infections declines with age because infections are often cleared and controlled by the host's immune system (Doorbar, 2006; Stanley, 2008). Despite the high prevalence and the transforming potential of HPV infections, only a minority of women infected with oncogenic HPV types develop cervical intraepithelial neoplasia (CIN) and cervical cancer (Doorbar, 2006). Cervical cancer is mainly slow-growing and symptoms are not always present, but premalignant and malignant stages can be detected with a regular Papanicolau test (Pap test, a gynecological screening test).

Globally, HPVs accounted for approximately 528,000 new cases and more than 265,000 death cases in women in 2012 (WHO, 2014) and it is estimated that about 5.2% of all cancers worldwide are associated with HPV infection (Parkin, 2006; Frazer et al., 2011). In developing countries, where more than 90% of cases occur, cervical cancer is still the second leading cause of death among women (van Bogaert, 2013) (Fig.1).

In different studies, the prevalence of HPV in cervical cancer varies between 87 and 99%. Additionally, HPVs have already been associated with 85% of anal squamous cell cancers (Daling et al., 2004), 40-50% of penile cancers (Parkin, 2006), 33-60% of oropharyngeal cancers and 23% of oral cancers (Mork et al., 2001; Kreimer et al., 2005). Genital HPV types are also accountable for a number of benign clinical conditions, such as genital warts, which are important health burdens as well.

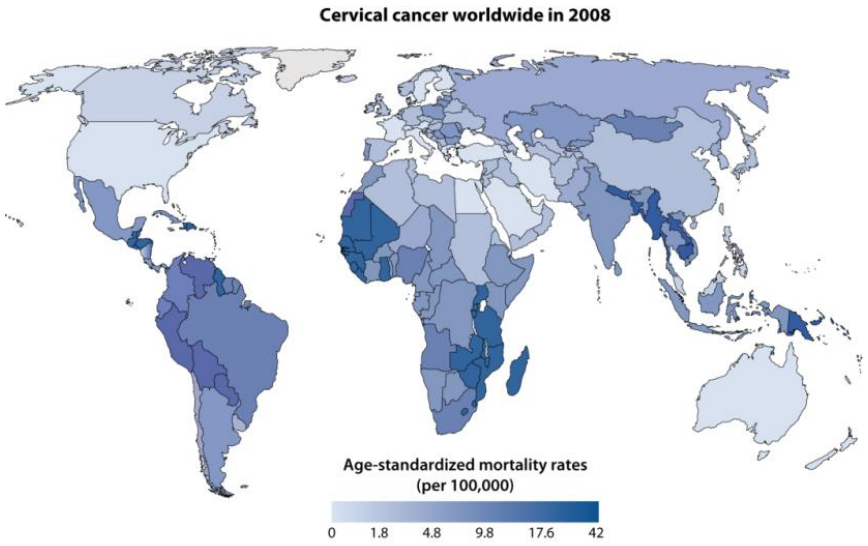

Figure 1 I Global cervical cancer distribution in 2008. Age-standardized mortality rates are depicted in blue. The highest mortality rates occur in less developed countries. This figure is adapted from (Frazer et al., 2011).

1.1.1 HPV classification and distribution

To date, 170 to 180 different HPV genotypes were identified based on the coding sequence of the major capsid protein L1 (de Villiers, 2013). By comparing the L1 gene, the family of *Papillomaviridae* has been classified into genera, species (clades) and types. The genera, which are described by Greek letters, include species that are phylogenetically related but often biologically quite diverse. There are five different genera including the α, β, γ, μ and ν genus (de Villiers et al., 2004; Bernard, 2005). The latter four primarily infect cutaneous sites. The clinically most significant and largest genus is that of the alpha papillomaviruses, which can be further subdivided into mucosal and cutaneous species according to the site of infection. Mucosal species are divided into high-risk and low-risk types depending on their capacity of causing malignant transformation of cells. Critical determinants distinguishing these two groups of viruses are biological and biochemical differences between the E7 proteins (Munger et al., 1991). Alpha papillomaviruses are grouped into 15 species, which are named α1 to α15 (Doorbar, 2006). HPV16, for example, belongs to the α9 species and HPV18 to the α7 species. Those two are the most common representatives of their species. Within each species, different types are differentiated based on the most conserved gene L1. A type is defined by a minimal difference of 10% in the open reading frame (ORF) of its L1 gene compared to any other characterized HPV type of the same species (Burk et al., 2009). Furthermore, types are classified into subtypes and variants and are subdivided into variant lineages and sublineages (Burk et al., 2011; Smith et al., 2011; Burk et al., 2013). If the nucleotide sequence of the L1 gene differs less than 10% but more than 2% from that of a described HPV type, a subtype is defined. Only a few HPV types (HPV34, 44, 54, 68, 82) comprise subtypes, and it is questionable if "subtype" is a useful designation, because so far no differences of biological importance have been described for subtypes (Burk et al., 2009).

A variant of a respective HPV type is defined by showing less than 2% differences in the nucleotide sequence of the L1 open reading frame. To classify further, whole genome sequences are compared. By this, variant lineages and sublineages can be distinguished, where variant lineages are defined by whole genome sequences with a nucleotide difference of 1 to 10% compared to other sequences of the same type (Burk et al., 2011). In case of HPV16, a maximum pair wise difference of 2.3% was confirmed (Smith et al., 2011) and thus this type can be divided into lineages. Here, the four major intratypic variant lineages are called European (E), Asian-American (AA), African-1 (Af-1) and African-2 (Af-2). Within such variant lineages, sublineages are defined by 0.5 to 1% nucleotide difference in whole genomes. For HPV16, the European variant lineage is comprised of the sublineages European Prototype 1 and 2 (E-1, E-2) and European Asian (E-A). Asian-American 1 and 2 (AA1, AA2) and North American (NA1) are sublineages of the Asian-American variant lineage. The HPV16 reference sequence (NC_001526) belongs to the European Prototype 1 sublineage (Burk et al., 2011; Smith et al., 2011).

The distinct classification system of papillomaviruses is presented exemplarily for HPV16 in Figure 2.

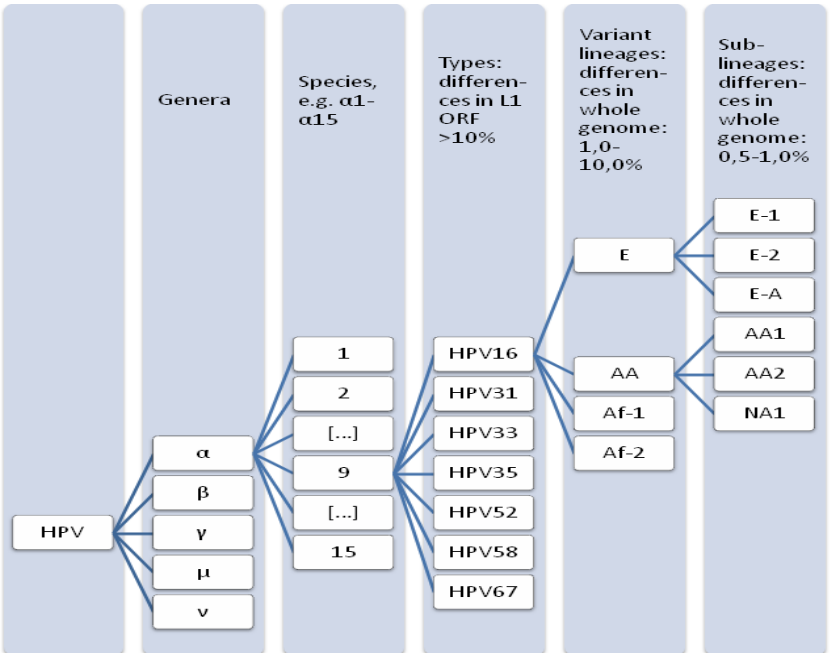

Figure 2 I HPV classification demonstrated by HPV16. HPVs are classified into genera, species, types and variants. The latter can be further subdivided into variant lineages and sublineages depending on their whole genome differences. All five genera (α-ν) are listed. At lower levels of the classification, only HPV16 relevant groups are listed. E: European, AA: Asian-American, Af-1: African-1, Af-2: African-2, E-1: European Prototype 1, E-2: European Prototype 1, E-A: European Asian, AA1: Asian-American 1, AA2: Asian-American 2, NA1: North American. This figure is taken from (Dickmann, 2012).

Variants are described by specifying the exchanged nucleotide and its position in comparison to the closest related variant lineage (Burk et al., 2011). The variant lineage to which the variant belongs is stated, followed by the initial nucleotide, the position of exchange and new base. For example, a variant with a nucleotide sequence that is identical to the European Prototype 1 apart from nucleotide 350 (T in the European Prototype 1) that is exchanged by a G, would thus be called E-1-T350G.

Variants can also be described by the amino acid changes that are caused by the nucleotide exchange. In this case, the position within the respective protein is designated. The T350G nucleotide exchange results in an amino acid exchange from leucine to valine at position 83 of the Early (E)-6 protein and is referred to as L83V.

Related variants often correlate with the distribution of major ethic groups, which might explain the endemic nature of HPV variants due to adaption of variants to respective hosts over time (Tabora et al., 2010). The variants are distributed all over the world, despite clustering in specific regions. Thus, the European variant lineage is for example not restricted to Europe (Tu et al., 2006).

1.1.2 The HPV genome and its organization

PVs contain double-stranded circular DNA, are non-enveloped and have a conserved icosahedral capsid structure. The capsid is composed of 72 capsomers consisting of the structural proteins, which are named late (L)-1 and L2 protein (Modis et al., 2002). L1 represents approximately 80% of the capsid and is thus called the major structural protein of the virus, whereas the minor L2 protein accounts for the remainder and is found mostly internally (Frazer et al., 2011). A model of the virus capsid structure is depicted in Figure 3.

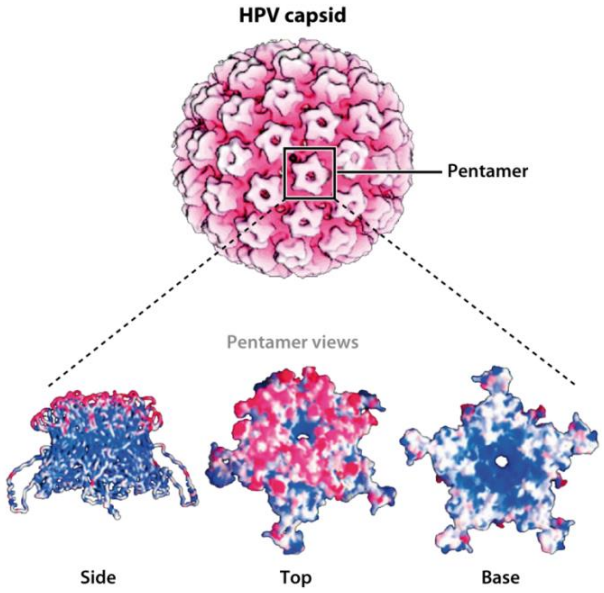

Figure 3 I Structure of the papillomavirus capsid. The capsid is assembled from 72 pentamers of the L1 protein in a icosahedral symmetry. Genotypic variations are depicted in pink and mostly affect the external surface whereas the internal structure (blue) is largely conserved. This figure is adapted from (Frazer et al., 2011).

The virus measures about 55nm in diameter (Hagensee et al., 1993). It has a genome of between 7400 and 8200 base pairs (bp), in case of HPV16 7908 bps, which encode for eight ORFs (Chen et al., 2005; Doorbar, 2006). The HPV genes are divided into early (E) and late (L) genes depending on their time point of expression during the viral life cycle as shown in Figure 4.

The whole HPV16 genome can be divided into three regions. The smallest region is the noncoding upstream regulatory region (URR) that contains binding sites for cellular and viral transcription and

replication factors (e.g. AP1, E1 and E2). The second largest segment are the two late ORFs that comprise the genetic sequence of the major capsid protein L1 and the minor capsid protein L2 and thus are transcribed in the latest phase of the viral life cycle. The largest region are the early ORFs that code for the six early proteins E6, E7, E1, E2, E4 and E5, which are transcribed throughout the course of infection. To fit all relevant information into the relatively small genome of approximately 8 kb, the sequences of some gene products overlap (Fig. 4). They are separated after transcription by mRNA splicing. For instance, the E2 sequence also contains the genetic information for the E4 protein (Doorbar, 2006).

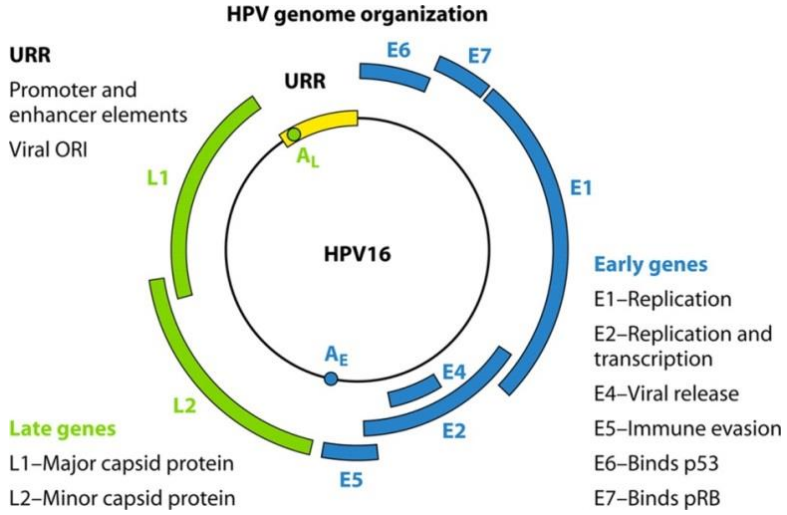

Figure 4 I Genomic organization of HPV16. The circular genome with eight open reading frames (ORFs) marked in blue and green encodes for six early proteins which are involved in viral replication and transcription (E1 and E2), release and immune evasion (E4 and E5) and transformation (E6 and E7). The two late proteins L1 and L2 form the viral capsid. Control of early gene transcription and replication is conferred by the upstream regulatory region (URR). It contains the viral origin of replication (ORI) and the late polyadenylation signal (AL). The corresponding polyadenylation signal for early genes is located between E5 and L2. This figure is taken from (Stanley, 2012).

1.1.3 Viral life cycle and viral proteins

In general, PVs are adapted perfectly to their natural host tissues, the squamous epithelia of mucosa and skin, where the rapidly cycling and dividing, nondifferentiated basal keratinocytes set the stage for the viral life cycle (Doorbar, 2005). High-risk HPVs show a special tropism for the so called transformation zone, which consists of the basal cell layers at the metaplastic epithelial site of the cervix. This area is a ring of mucosa where squamous epithelium of the ectocervix replaces the glandular epithelium of the endocervix (Schiffman et al., 2007). Cells close to this area have a higher susceptibility for persistent infections (Chow et al., 2010; Doorbar et al., 2012). Other sites of the body that are prone to HPV associated cancers show strong similarities in terms of intersecting epithelium, like the uneven reticulated epithelium lining the base of the tongue and the crypts of the palatine tonsils (Boscolo-Rizzo et al., 2013). These sites are susceptible to HPV-mediated HNSCCs.

Initially, virions infect cells of the basal layer of the epithelium as displayed in Figure 5. This requires (micro-) trauma or epithelial wounding in the stratified epithelium to permit access to basal cells. The subsequent healing processes have also been suggested to play a role as active cell division is

necessary for establishing an infection (Pyeon et al., 2009; Schiller et al., 2010). Binding of HPV to the surface of the epithelium or the basement membrane occurs by interaction of the major capsid protein L1 of the virion with heparan sulfate proteoglycans (Johnson et al., 2009; Kines et al., 2009; Abban and Meneses, 2010; Horvath et al., 2010). The internalization of the virus and transfer of its genome to the nucleus is propagated by changes in the capsid structure (Doorbar, 2005; Horvath et al., 2010; Schiller et al., 2010). To date, many different studies tried to elucidate the mechanism of infection, however the exact details of endocytosis still remain elusive. Endocytosis of HPV16 viruses has been shown not to depend on clathrin, caveolin, or dynamin. It might occur via a so far uncharacterized endocytotic pathway that could be supported by tetraspanins and actin (Spoden et al., 2008; Schelhaas et al., 2012). Moreover, it is possible that various internalization and entry pathways exist that might use different cell surface molecules (Raff et al., 2013) and that this process is also dependent on the virus type (Doorbar et al., 2012). In contrast to other virions, for HPV the process takes several hours (Horvath et al., 2010).

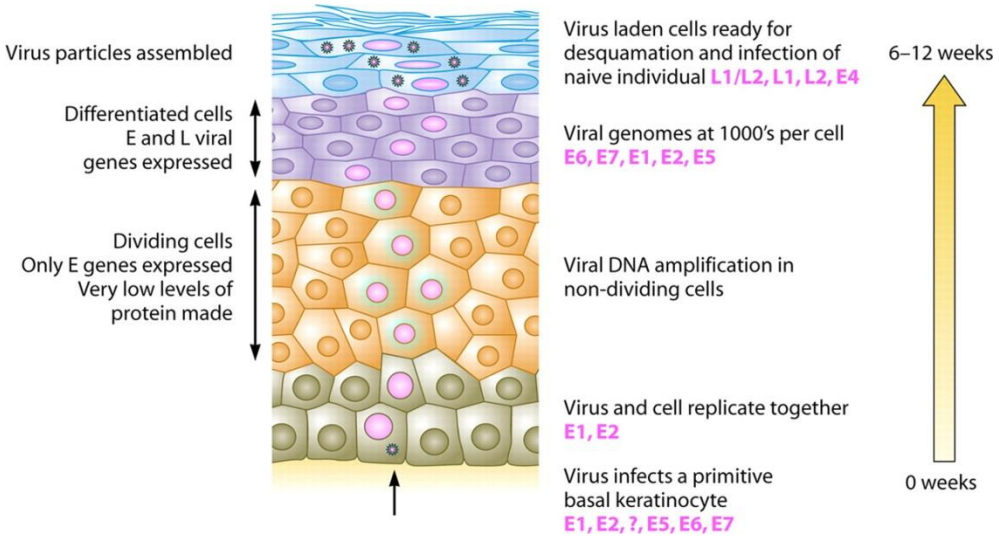

Figure 5 I HPV viral life cycle from infection of basal keratinocytes to virion release. After infection, the virus replicates and maintains its genome in dividing cells. Upon cell differentiation into mature keratinocytes, viral gene amplification is increased. Finally, virions assemble and are released via shedding. Proteins are depicted in pink. This figure is taken from (Stanley, 2012).

After internalization, the virus is trafficked across early and late endosomal compartments, is uncoated and final entry of the viral genome to the nucleus is achieved by a complex of the L2 protein and DNA (Sapp and Bienkowska-Haba, 2009; Bergant Marusic et al., 2012; Schelhaas et al., 2012). The HPV genome is maintained as an episome, a closed DNA element, which is able to replicate extrachromosomally within the host cell. Soon after infection, the virus replicates up to 50 to 100 copies separate from the cell cycle but dependent on the cellular DNA synthesis machinery, as well as the viral helicase E1 and the transcription factor E2 (Doorbar et al., 2012). Specifically, E2 is a DNA binding protein that forms a complex with E1 to initiate episome replication in the S-phase (Doorbar, 2006). The E5 protein helps to create a favorable environment by e.g. enhancement of epidermal growth factor (EGF)-signaling and mitogen-activated protein (MAP)-kinase activity. Upon host cell

division, viral episomes are distributed to daughter cells. The initially infected cell in the basal cell layer maintains the viral episome in a low copy number. The cells expand laterally, daughter cells move towards the surface and start to differentiate. Since viral replication depends on the host cell's DNA replication machinery, no replication would occur once the cell enters cell cycle arrest. In uninfected keratinocytes, this takes place as the cell undergoes terminal differentiation. In infected cells however, this step is prevented by expression of the E6 and E7 genes. The E7 protein associates with the retinoblastoma protein (pRB) and thus disrupts the binding of pRB to the transcription factor E2F. This way, S-phase entry is blocked, because E2F induces the activation of several genes, like cyclin A and E that promote S-phase (zur Hausen, 2002; Doorbar, 2006; Lehoux et al., 2009). However, cell cycle promotion by E7 also leads to increased p53 levels that would result in apoptosis. To suppress apoptosis, the E6 protein binds to an ubiquitin ligase, which then marks p53 for proteasomal degradation (Ganguly and Parihar, 2009). Their potential to stimulate cell cycle progression and block tumor suppressors makes these two oncoproteins essential for the malignant phenotype. Viral replication is kept active throughout the whole differentiation process at a low level.

When reaching the late stage of keratinocyte development, L1, L2 and E4 proteins are expressed. Here, in terminally differentiated cells, viral genomes are packed into self-assembling capsids consisting of L1 proteins and interspersed L2. Mature keratinocytes undergo their natural shedding process and meanwhile, with the help of the E4 protein, virions are released (Narisawa-Saito and Kiyono, 2007; Stanley et al., 2007; Stanley, 2008). These virions can infect more exposed basal keratinocytes of the same individual or can be transmitted to a naïve host. The whole viral life cycle takes up to 6 to 12 weeks which is remarkably long for a virus (Stanley, 2012). A detailed description of functions of all HPV proteins is given in section 1.1.3.1 and section 1.1.3.2.

In case of HPV high-risk types, the viral genome eventually can integrate into the host cell's DNA. In contrast to benign and low-grade lesions, where HPV DNA is mostly found extrachromosomally, in premalignant lesions (CIN 2/3) HPV DNA is integrated into the chromosome. Therefore, lesions can progress to microinvasive and invasive cancer (Doorbar, 2006). In case of integration, the episome is mostly opened within the E2 ORF and thereby functional expression of E2 is prevented. Since E2 represses expression of both oncogenes E6 and E7, loss of E2 leads to a deregulated expression of E6 and E7 and increases the proliferative capacity (zur Hausen, 2002; IARC, 2007). Preferential sites of integration have been described including the region in and around the human telomerase reverse transcriptase gene (hTERT). Increased hTERT expression induces telomerase activity which finally leads to the immortalization of infected cells. Hence, is has been suggested that changed expression of genes adjacent to the integration site may contribute to cancer development as well (Doorbar, 2006; IARC, 2007).

1.1.3.1 The early proteins E1, E2, E4, E5 and the oncoproteins E6 and E7

As outlined above, after infection of dividing basal cells, the viral genome is established as a stable episome with a low copy number. The viral proteins E1 and E2 are responsible for regulating early transcription and additionally serve for maintenance of the viral episome in the basal layer. The E1 protein is a DNA helicase. The E2 protein plays a crucial role in the beginning of the viral life cycle, as it initiates viral DNA replication directly after entry into the host cell (Zheng and Baker, 2006). E2 recognizes four palindromic motifs in the non-coding region of the viral genome (Dell et al., 2003). Upon E2 binding, E1 binds to the viral origin of replication (Amador-Molina et al., 2013). E2 eventually dissociates, letting E1 form a hexameric ring. E2 binds to the viral DNA via multiple binding sites in the long control region (LCR), which on the one hand leads to gene replication as described above and on the other hand might also activate expression of the late genes (Johansson et al., 2012). Moreover, E2 is controlling the expression of the two oncogenes E6 and E7 in lower epithelial layers. While high levels of E2 repress the expression of E6 and E7, lower levels enhance their transcription. An additional function of E2 is to cause cell cycle arrest at the G_2 phase and thus inhibition of cell proliferation. E2 is also important for correct segregation during mitosis as it anchors the viral episomes to cellular chromosomes. Besides, E2 is thought to be involved in virus assembly during productive infection in upper epithelial layers. During viral DNA integration into the host cell's genome, the E2 gene is often disrupted leading to loss of E2, which causes increased expression of E6 and E7 as already metioned above (Doorbar, 2006).

The E4 protein is expressed in terminally differentiated keratinocytes (Zheng and Baker, 2006). It accumulates at the epithelial surface and is believed to support viral release by disrupting the keratin network (Doorbar, 2006).

The transmembrane E5 protein is mostly found in the endoplasmic reticulum (ER) and plays an important role in maintaining the environment in favor of cellular replication in the upper epithelial layers. E5 binds to vacuolar proton ATPases leading to delayed endosomal acidification, which in turn causes recycling of growth factor receptors to the cell surface rather than their being degraded by the endosome (Doorbar, 2006). By this, E5 is enhancing EGF receptor activity. The subsequent increase in EGF-mediated receptor signaling promotes cellular replication (Frazer et al., 2011). E5 also prevents apoptosis due to DNA damage but is not considered of special importance in late stages of HPV-mediated carcinogenesis because it may be lost during integration of viral DNA (Doorbar, 2006).

The two oncoproteins E6 and E7 are mainly responsible for the malignant transformation of infected cells in high-risk HPV types, such as HPV16 (zur Hausen, 2002; Ganguly and Parihar, 2009). As mentioned above, the virus is in need of the cellular replication machinery in cells that stopped dividing. To solve this problem, the E6 and E7 proteins reactivate cellular DNA synthesis, inhibit apoptosis and delay differentiation. Thus, cell growth becomes largely uncontrolled, which leads to the

development of neoplasias and eventually cancer. The p97 promoter directs the expression of the E6 and E7 proteins (Kammer et al., 2000), which consist of 158 and 98aa, and have a weight of approximately 19 and 11kDa, respectively. The E7 protein keeps the cell in a proliferating state to ensure viral replication as mentioned before. To this end, E7 binds to pRb which in turn releases and thereby activates the transcription factor E2F. E2F is enhancing gene transcription that is needed for G1/S-phase transition. In uninfected cells, pRb is associated with E2F and regulates cell cycle arrest and G1/S-phase transition depending on its phosphorylation status. Cyclin dependent kinases (CDK) such as cyclinD/Cdk4/6 phosphorylate pRb, E2F dissociates and gene expression to promote G1/S-phase transition is activated. In infected cells, E7 binds directly to pRb and thus leads to the same events (reviewed in (Longworth and Laimins, 2004; Doorbar, 2006). In addition, this process is further regulated by a negative feedback loop as E2F mediates transcription of p16 and $p14^{Arf}$. While p16 regulates the levels of active cyclin kinases, which are absent in infected cells (McLaughlin-Drubin et al., 2011), $p14^{Arf}$ increases the levels of p53. More specifically, $p14^{Arf}$ is encoded by the alternative reading frame of the *CDKN2A* gene and usually regulates the activity of the MDM (murine double minute) ubiquitin ligase. This ligase maintains p53 at a low level that is not sufficient to trigger cell cycle arrest and/or apoptosis. An increased level of $p14^{Arf}$ leads to the inhibition of MDM function and thus elevates the level of p53 (Piette et al., 1997; Busch et al., 2010). E7 also supports proteasome-mediated degradation of pRb. The different potentials of low and high-risk E7 to immortalize seem to depend rather on their ability to degrade pRb than to bind to pRb (Doorbar, 2006). Additionally, E7 also associates with other proteins involved in cell proliferation, it activates cyclin A and E genes, which are required for S-phase progression. Moreover, it blocks CDK inhibitors p21 (WAF1) and p27 (KIP1), interacts with the AP1 transcription complex and with enzymes that mediate histone acetylation (Antinore et al., 1996; Doorbar, 2006). Finally, E7 promotes genomic instability by activation of the ataxia telangiectasia mutated (ATM)- ataxia telangiectasia and Rad3-related (ATR) pathway and induction of abnormal centrosome synthesis by interaction with CDK2 and γ-tubulin (Moody and Laimins, 2010).

The function of the E7 protein is complemented by the E6 protein. E6 counteracts apoptosis by interaction with p53 and other pro-apoptotic proteins. p53 is polyubiquinated and degraded by the proteasome upon interaction with the cellular E3-ubiquitin E6-associated protein (E6-AP). This prevents apoptosis in response to E7-mediated cell cycle entry in the upper epithelial layers (Doorbar, 2006). External and internal apoptotic signaling is inhibited through interaction with tumor necrosis factor α (TNFα), Fas-associated protein with Death Domain (FADD), caspase 8 and the pro-apoptotic proteins Bak and Bax. Moreover, E6 is activating transcription of hTERT, which is the catalytic subunit of the telomerase. Telomerase activity prevents cells from becoming senescent due to telomere shortening, and is thus an essential step for immortalization (Kiyono et al., 1998). The presence of E6 and E7 alone is not sufficient to cause the multi-step process of carcinogenesis, but in synergy they allow for secondary mutations, centrosome amplification and aneuploidy (Narisawa-Saito and Kiyono,

2007). These events can lead to accidental integration of HPV episomal DNA, which in turn is increasing expression of the E6 and E7 proteins and thus also increases cell growth. All those factors and the fact that E7-mediated apoptosis is prevented by E6 account for their synergistic effect (zur Hausen, 2002). Besides these well known functions of the two oncoproteins E6 and E7, a variety of other binding partners have been identified that have many different functions (Klingelhutz and Roman, 2012). Detailed mechanisms behind these functions still remain greatly elusive (Narisawa-Saito and Kiyono, 2007; Ganguly and Parihar, 2009; Klingelhutz and Roman, 2012).

1.1.3.2 The late proteins L1 and L2

The capsid of HPV is composed of the two structural late proteins, L1 and L2, which are key players in mediating infectivity. The primary structural element of the capsid is the major capsid protein L1, which can form pentamers (Hagensee et al., 1993). These pentamers have the ability to self-assemble into capsids as depicted in Figure 3. In case of HPV16, the L1 protein consists of 503aa and has a molecular weight of 56kDa. The minor capsid protein L2 has a size of 473aa and a molecular weight of 51kDa. It was found to be located in the central internal cavity of the L1 pentamer (Buck et al., 2008). Moreover, it was shown to interact with the viral genome and is essential for the encapsidation process of the viral genome (Stauffer et al., 1998). The L2 protein has furthermore been suggested to play a role in infection and immune escape mechanisms of HPV (Fahey et al., 2009). Natural virus capsids consist of 72 L1 pentamers that comprise 360 L1 molecules and approximately 30 L2 molecules (Baker et al., 1991). The rim of the L1 pocket is variable whereas the L1 side chains lining the axial cavity are highly conserved between different HPV types (Chen et al., 2000). The capsomers are stabilized by formation of intercapsomeric disulfide bridges between neighboring capsomers (Sapp et al., 1998; Sapp and Bienkowska-Haba, 2009). The non-covalent interaction of L2 with the L1 capsomers is based on a hydrophobic C-terminal L1 binding domain of L2 and an additional L1 binding domain at the N-terminus of the L2 sequence (Volpers et al., 1995; Okun et al., 2001; Finnen et al., 2003). L2 incorporation enhances the formation of infectious viruses. Moreover, it has been postulated that there exists an L2 network within the viral capsid (Buck et al., 2008).

1.2 The immune system

The human body is constantly exposed to numerous different pathogens, including viruses, bacteria, parasites and fungi. To be able to prevent or combat infections of the body, a system of organs, cellular and soluble components, has evolved – the immune system. In 1796, Edward Jenner, an English physician, tested his hypothesis that healthy individuals inoculated with cowpox could be protected from severe infections with smallpox and proved this to be true. Thus the term “vaccination”, coming from Variolae Vacciniae (cow pox), was born and today, Edward Jenner is regarded to be the ‘father of immunology’ (Murphy, 2007).

The bone marrow, spleen, thymus, lymph nodes, tonsils and the mucosa- and gut-associated lymphoid tissues are organs of the immune system, which are classified into primary and secondary lymphoid organs. All cells of the immune system develop from specialized hematopoietic stem cells in the bone marrow, a primary lymphoid organ. T cells further develop in the thymus. These cells migrate towards secondary lymphoid tissue for further maturation or circulate in the blood or lymph for detection of pathogenic or malignant threats to the body. To be able to discriminate self and non-self or malignant tissues, immune cells possess a distinct set of receptors (Murphy, 2007).

1.2.1 The innate and adaptive immune system

The human immune system is classically subdivided into the innate and adaptive arm. However, the innate and adaptive immune system branches are in close contact through signaling mechanisms. They differ in response kinetics, their cellular subsets and the mechanisms of pathogen recognition.

Innate immunity shows an array of first line defense mechanisms against invading pathogens that are immediately available and display low specificity. Cells of the innate immune system express germline encoded receptors that are non-clonally distributed, and are specific for surface repeating structural patterns that are shared by many microorganisms. Thereby, upon recognition of bacteria or viruses, for instance, an immune reaction is instantly initiated without the need for prior sensitization. These functions are carried out by the most important cell types of the innate branch: macrophages, monocytes, dendritic cells (DCs), granulocytes and natural killer (NK) cells.

Patterns that are recognized by innate immune cell receptors, are called pathogen-associated molecular patterns (PAMPs) and are recognized by pattern recognition receptors (PRR). For example. Toll-like receptors (TLRs), initiate different signaling pathways that lead to the transcription of genes for inflammatory cytokines like type I interferons (IFNs). PAMPs, which are promiscuously expressed on many pathogens, confer self/non-self discrimination capabilities. For instance, double-stranded RNA, that is often exposed upon viral infection, is recognized by TLR3, bacterial lipopolysaccharide (LPS) by TLR4, flagellin by TLR5 and unmethylated CpG by TLR9.

DCs are specialized in capturing antigens by phagocytosis and macropinocytosis and subsequent presentation of these antigens to T cells. Therefore, DCs act as a link between the innate and adaptive sides of the immune system. The adaptive immune system is composed of B and T lymphocytes. These cells express non-germline receptors with unique specificity and are able to recognize virtually every foreign antigen. During their development, B and T cells recombine their receptor genes randomly, a process known as V(D)J recombination. The whole process of expression of one single functional receptor can create up to 10^{14}-10^{18} specificities on the way, which get depleted of self-reactive receptors, a process known as clonal deletion, leading to central tolerance.

Upon recognition of their specific antigen, naïve B and T lymphocytes differentiate to effector cells and undergo clonal expansion and massive proliferation. B cells differentiate into plasma cells that

produce antibodies and thus mediate humoral immunity. T cells mediate adaptive immunity by developing into different subsets of effector cells that produce cytokines and display cytotoxic effector functions. $CD4^+$ T cells recognize antigens originating from extracellular proteins that are presented by major histocompatibility complex (MHC) II molecules and can differentiate into T helper (T_H) cells, e.g. T_H1 or T_H2 depending on the cytokine milieu during activation. $CD8^+$ T cells are specialized in recognition of antigens that are presented on MHC I molecules. They play a pivotal role in anti-tumor immunity. Upon elimination of a pathogen, most effector cells are eliminated, but some lymphocytes persist and constitute a pool of immunological memory cells. Upon a subsequent encounter with the same antigen, these cells mount a more rapid and effective immune response and can provide their host with life-long protection (Murphy, 2007).

Since the field of immunology is extremely complex and this work is focused on the investigation of T cell epitopes for therapeutic vaccine development, only components of the immune system that are involved in generation of antigen-specific immune responses are described in greater detail.

1.2.2 The major histocompatibility complex

Major histocompatibility complex (MHC) molecules were first discovered as the major determinants of histocompatibility in transplantation. In humans MHC molecules are called human leukocyte antigen (HLA) molecules. MHC molecules are surface proteins that form complexes with peptides inside the cell and are then transported to the cell surface for antigen presentation, where they can be recognized by T cells. There exist two major classes of MHC molecules, class I proteins are presenting peptides from the cytosol, mainly with a length of 8 to 11aa, while class II proteins present peptides from intracellular vesicles of variable length between 9 and 25aa. While MHC class I molecules (MHC I) are found on virtually all nucleated cells, MHC class II molecules (MHC II) are mainly expressed on specialized antigen-presenting cells (APCs) such as B lymphocytes, macrophages and DCs (Rammensee, 1995; Villadangos, 2001; Gromme and Neefjes, 2002).

Peptide presentation by MHC I is crucial for the detection of intracellular pathogens, including viruses, by cytotoxic T lymphocytes (CTLs) that can subsequently kill these cells. MHC I complexes consist of a transmembrane α-chain with three extracellular Ig domains (α1-α3) that have a mass of approximately 44kDa and a soluble β_2-microglobulin chain, which weights 13kDa and is non-covalently associated (Fig. 6). The interface of the α_1 and α_2 domains forms a closed peptide binding cleft in which the peptide ligand is bound in an elongated conformation (Fremont et al., 1992; Madden et al., 1993). The binding is stabilized on both ends of the peptide via intermolecular interactions by H-bonds and ionic interactions, which are independent of the peptide's sequence. These interactions limit the length of bound peptides to 8 to 11aa.

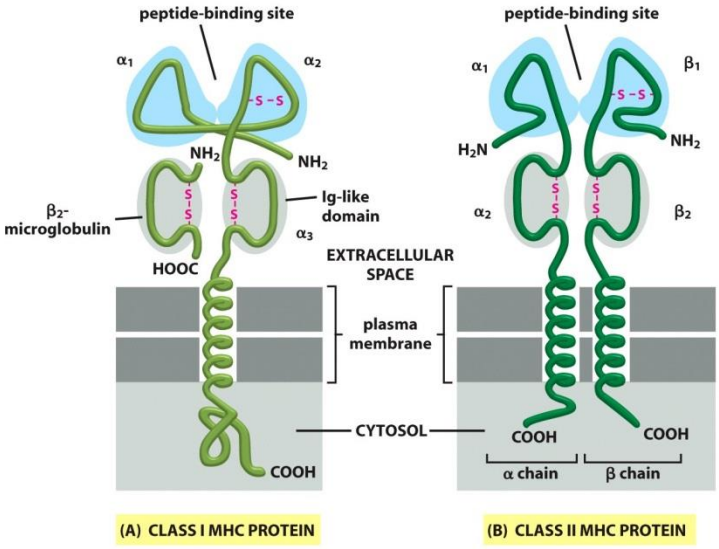

Figure 6 I Schematic structure of MHC class I and MHC class II molecules. A The MHC class I molecule consists of an α-chain with three extracellular domains and a non-covalently associated polypeptide chain, β_2-microglobulin. The β_2-microglobulin chain is invariant, while especially α_1 and α_2 are highly polymorphic (blue shading). **B** In MHC class II molecules both chains are polymorph, mainly in the α_1 and β_1 domains (blue shading). Both proteins possess peptide binding sites that present peptides to T cells. This figure is taken from (Alberts, 2007).

The generation of MHC I peptides involves a complex process starting in the cytosol, followed by translocation of peptide intermediates into the endoplasmatic reticulum (ER), and trimming of the peptides that will be subsequently transported as a MHC/peptide complex via the Golgi apperatus to the cell surface (Fig. 7). Cytoplasmic proteins are degraded by the proteasome into peptides (Yewdell and Bennink, 2001). C-terminal cleavage of peptide bonds is facilitated by the three catalytical beta subunits 5-7 (Tanaka, 2009). Proteasomal products have usually a size of 2 to 25aa (Nussbaum et al., 1998; Kisselev et al., 1999) and therefore, the majority are too long or short for MHC I binding. Longer peptides are digested at the N-terminus by various cytosolic aminopeptidases (Stoltze et al., 2000; Reits et al., 2004). Subsequently, these peptides are translocated into the ER by the transporter associated with antigen processing (TAP) complex. The TAP heterodimer consist of TAP1 and TAP2 that actively translocate peptides (Momburg et al., 1994; Koopmann et al., 1996). Within the peptide-loading complex (PLC) which consists of the transporter TAP, the chaperones tapasin, thiol oxidoreductase ERp57, calreticulin and the MHC I molecule, a peptide is loaded into the binding pocket of the MHC I molecule. In detail, tapasin binds to TAP and is linked to a cysteine residue at the active site of ERp57 (Peaper et al., 2005), leading to recruitment of MHC class I molecules and calreticulin to the PLC (Wearsch and Cresswell, 2007). The PLC receives the peptides translocated by TAP and induces MHC loading. Final trimming of peptides is mediated by endoplasmatic reticulum-associated aminopeptidase/endoplasmatic reticulum aminopeptidase 1 (ERAAP/ERAP1) and ERAP2 (Wearsch and Cresswell, 2008). Components, which are involved in these processes are named together the antigen-processing machinery (APM). Eventually, the peptide/MHC I complex is transported via the Golgi apparatus to finally reach the cell surface where it is exposed to the T cell receptor (TCR) of $CD8^+$ T cells (Neefjes et al., 2011).

Of note is the so-called immunoproteasome that has a different composition of subunits, which are formed under the influence of IFNγ or TNF (Kloetzel and Ossendorp, 2004). Here, three catalytic subunits are replaced, which leads to an increased proteolytic activity and throughput (Sorokin et al., 2009; Kruger and Kloetzel, 2012). Moreover, it results in a change of the epitope repertoire presented, suggesting an altered cleavage specificity (Van den Eynde and Morel, 2001; Kloetzel and Ossendorp, 2004).

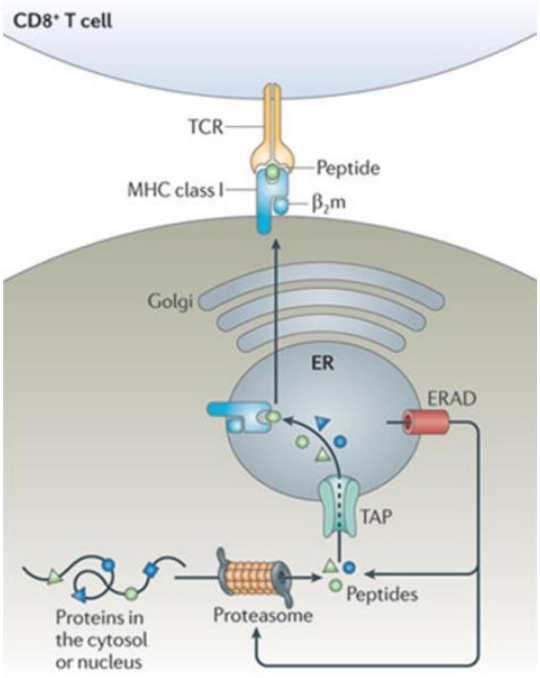

Figure 7 I Antigen presentation via the classical MHC class I pathway. Proteins are degraded into smaller peptide fragments via the proteasome and translocated into the endoplasmatic reticulum (ER) by the transporter associated with antigen processing (TAP). The peptide loading complex is formed and peptides are loaded onto MHC class I molecules. The MHC I/peptide complex is transported via the Golgi apperatus to the cell surface, where peptides are presented to $CD8^+$ T cells. This figure is taken from (Neefjes et al., 2011).

Besides the classical MHC I pathway, some APCs can also present peptides from exogenous antigens on their MHC I molecules. Since in the canonical model, these peptides would be expected to be presented by MHC II, the process has been named ‘cross-presentation’ (Bevan, 2006; Kurts et al., 2010). Antigens escape from early endosomes into the cytosol through the Sec61b transporter and are then processed in the same way as intracellular antigens (Amigorena and Savina, 2010).

The MHC II complex consists of two transmembrane chains, α and β, of approximately 30kDa with two Ig domains each with the peptide binding site in between α_1 and β_1 as depicted in Figure 6 (Dessen et al., 1997). In comparison to MHC I, the binding cleft of MHC II is open and can accommodate peptides of various lengths up to 25aa. Peptides that are presented by MHC II are usually derived from phago- or pinocytosed extracellular proteins that are digested in the phagolysosome by acidic proteases and cathepsins. Peptides can also be derived from pathogens that replicate within intracellular vesicles. The MHC class II complex reaches the endosomal compartment from the ER together with the invariant chain (Ii), which is blocking the peptide binding cleft

(Weenink and Gautam, 1997). Ii is degraded and the left over fragment class II-associated Ii peptide (CLIP), now occupying the binding groove. Consecutively, MHC II molecules like HLA-DM and HLA-DO (Dengjel et al., 2005), bind and stabilize the MHC II/CLIP complex and catalyze the exchange of CLIP with peptides. At the plasma membrane, MHC II presents these peptides to $CD4^+$ T cells (Fig. 8).

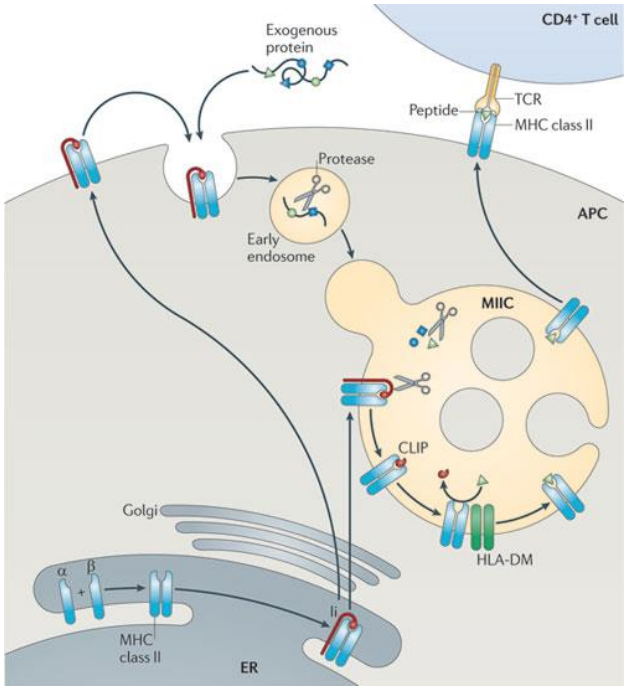

Figure 8 I Antigen presentation via the classical MHC class II pathway. MHC class II complexes including the invariant chain (Ii) arrive from the ER via the Golgi complex to the endosomal compartment termed the MHC class II compartment (MIIC) where Ii is degraded to CLIP, which occupies the MHC class II peptide cleft. CLIP is exchanged for an antigenic peptide from exogenous proteins, the MHC class II/peptide complex is eventually transported to the plasma membrane and recognized by $CD4^+$ T cells. This figure is taken from (Neefjes et al., 2011).

The MHC complex is a large gene cluster, which is located on chromosome 6 in humans and contains more than 200 genes coding for HLA molecules. The genes encoding for the β_2-microglobluin and the invariant chain, however, are located outside the MHC locus on chromosome 15. MHC molecules need to bind and present a multitude of different peptides, ideally all possible ones. In contrast to TCRs, the required variability is not achieved by somatic recombination, but by polygeny and polymorphism of the MHC genes. There are three loci for the MHC I heavy chain in the human genome, HLA-A, HLA-B and HLA-C, with approximately 9,500 alleles being known. To date (March 2015), these alleles include 2,995 for HLA-A, 3,760 for HLA-B, 2,553 for HLA-C (EMBL-EBI). The gene encoding for β_2-microglobulin is nonpolymorphic. For MHC II molecules there are also at least three functional loci each for the α- and the β-chains, with in total 3,104 known functional alleles (EMBL-EBI). The facts that each individual is heterozygous for the whole MHC locus and that the MHC haplotypes are codominant, increase the diversity between individuals of the same species as well.

The peptide binding cleft of each allele is different and has a unique specificity for certain amino acids in defined positions. There are so-called key-peptide interaction sites inside the MHC molecule's binding groove which preferentially bind to certain amino acid residues inside the peptide. Thus, they determine parts of the amino acid sequence of peptides which are presented by the respective MHCI molecule. Since these interactions also strengthen the binding of the peptide to the peptide binding pocket, the peptide residues involved are referred to as anchor residues. Considering anchor positions and length preferences of certain HLA alleles, peptide motifs were described by Rammensee and colleagues for different alleles (Falk et al., 1991; Rammensee et al., 1993). By eluting peptides from MHC complexes, sequences of these peptides were consequently identified via mass spectrometry. On the basis of these gathered sequence findings, Rammensee and colleagues developed an algorithm for the prediction of short peptides derived from protein sequences that are potentially presented by a given MHC molecule. This algorithm is called SYFPEITHI (Rammensee et al., 1999) and will be described in the context of other T cell epitope prediction servers in section 1.3.1 in greater detail.

1.2.3 Dendritic cells

Dendritic cells (DCs) are APCs, which can prime naïve T lymphocytes. Myeloid and lymphoid progenitors in the bone marrow give rise to DCs that migrate via the blood stream to secondary lymph organs and other tissues throughout the body. DCs can be subdivided into plasmocytoid DCs and conventional DCs, which are differentiating into further subsets.

Immature DCs ingest antigens by receptor mediated phagocytosis and micropinocytosis, leading to the uptake of surrounding fluids. Phagocytosis is mediated by receptors such as Fc receptors, C-type lectins and dectin-1. DCs also express TLRs which recognize PAMPs and other danger signals. Through extensive antigen sampling, DCs can present virtually all kinds of antigens derived from various sources such as parasites, fungi, bacteria, viruses and tumors. The antigen-presenting pathways, described in section 1.2.2, are initiated. Upon TLR-triggering, antigens are more efficiently processed and chemokine receptor expression patterns are altered, leading to migration of DCs to lymphoid tissues. They migrate via the CCR7-CCL21-axis to lymph nodes and mature meanwhile. Maturation terminates the uptake of antigens and increases the expression of high levels of MHC class I and II molecules that present epitopes from processed pathogens. Moreover, mature DCs attract naïve T lymphocytes by secretion of chemokines and express the costimulatory molecules CD70, CD80 and CD86 (Murphy, 2007).

In virus-infected and tumor cells, the antigens need to be cross-presented to prime naïve $CD8^+$ T cells to become fully activated cytotoxic T lymphocytes (CTLs). Cross-priming describes the initiation of a $CD8^+$ T cell response which is not produced solely by the APC itself and is depicted in Figure 9 (Kurts et al., 2010). Here, conventional tissue DCs transmit antigens from the affected peripheral tissue to resident ($CD8\alpha^+$) DCs in lymph nodes and other secondary lymphoid organs (Allan et al., 2006). TLRs of DCs are required to receive signals from PAMPs to enable cross-presentation. Antigen-specific

$CD4^+$ T_H cells are recruited and alter the DCs into a transient phase that leads to programming CTLs for effector functions and memory formation. This process is accomplished by interaction of CD40 on the DC and CD40L on the T_H cell (Smith et al., 2004). The so-called licensed, cross-presenting DCs start to program naïve $CD8^+$ T cells which have been shown to be attracted to the DCs likely by CCR5-ligands. Besides TCR-MHC I binding and CD28-CD80/CD86 interaction, CD27 on the T cell side and CD70 on the DC side need to interact (Keller et al., 2009). Interleukin 2 (IL-2) has been reported to be essential during priming for CTL survival (Williams et al., 2006b). In humans, CD141 positive DCs seem to cross-present most efficiently (Haniffa et al., 2012).

In conclusion, DCs are crucial for anti-tumor immune responses as they can cross-present antigens and prime CTLs. Melief and colleagues have suggested that this process also takes place after anti-cancer vaccination with synthetic peptides. Subcutaneously injected antigens are engulfed by tissue resident DCs, that migrate to draining lymph nodes of the vaccination site, where the antigen is cross-presented (Melief and van der Burg, 2008).

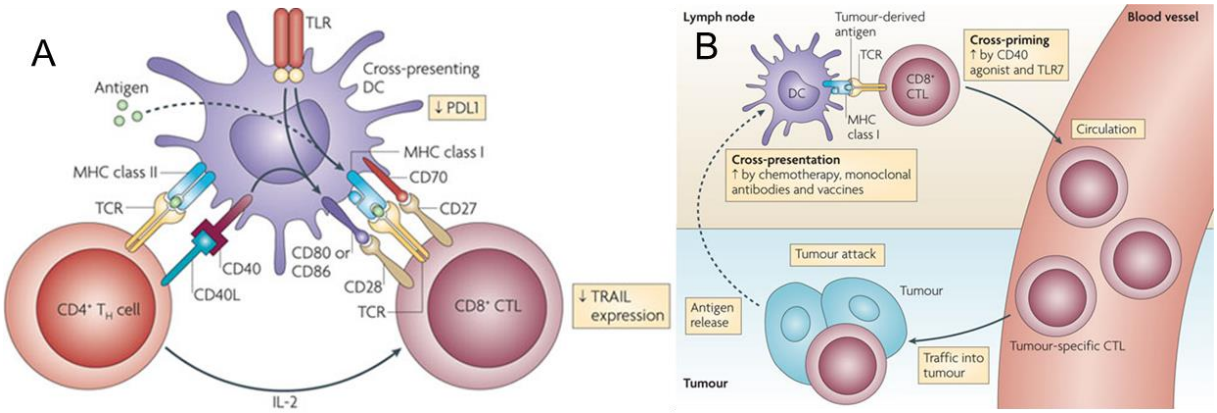

Figure 9 I Mechanism of classical cross-priming and its role in anti-tumor immunity. A Dendritic cells (DCs) present antigens via MHC class II to $CD4^+$ T helper cells (T_H) and cross-present antigens via MHC class I to $CD8^+$ cytotoxic T cells (CTLs). DCs upregulate costimulatory molecules like CD70, CD80 and CD86 while downregulating inhibitory molecules like programmed cell death ligand 1 (PD-L1). **B** Tumor-antigens are released either by the tumor or introduced through vaccination and are cross-presented by DCs to CTLs. This process requires costimulation (e.g. by CD40) or danger signals (e.g. by TLRs). This figure is adapted from (Kurts et al., 2010).

1.2.4 T lymphocytes

T lymphocytes are mediators of cellular immunity. They express highly variable TCRs on their surface, which are able to recognize specific non-self peptides presented on MHC class I or II molecules. While most T cells have α:β receptors, consisting of an α- and β-chain, a minority with greatly reduced receptor variability carries γ:δ receptors (Chien and Konigshofer, 2007). The α:β T cell subset express either CD4 or CD8 on their surface. These two proteins act as coreceptors mediating the recognition of MHC class I (CD8) or MHC class II (CD4) molecules (Bierer et al., 1989). $CD8^+$ T cells are also referred to as cytotoxic T lymphocytes (CTLs), due to their task to kill infected cells which are presenting peptides that are non-self on their surface. $CD4^+$ T cells can be

further subdivided (see section 1.2.4.1). When $CD4^+$ T cells are activated, they are responsible for activating macrophages and trigger antibody secretion by B cells. Moreover, T_H cells can also help to activate CTLs.

1.2.4.1 The T cell response and T cell subsets

After leaving the thymus, naïve T cells circulate through the blood and lymphoid system, entering the latter via the lymph nodes by high endothelial venules. High endothelial venules express ligands, CC chemokine 21 and peripheral node addressin (PNAd), that interact with CC chemokine receptor 7 (CCR7) and L-selectin CD62L on T cells and mediate migration (von Andrian and Mackay, 2000). In the lymph node, T cells encounter APCs, e.g. DCs, and T cells bind transiently to DCs via adhesion molecule interaction of LFA-1 and CD2 on the T cells side and ICAM-1, ICAM-2 and CD58 on the DC side, and screen for their cognate antigen (Grakoui et al., 1999). The fate of a T cell is determined as soon as they meet their cognate antigen-MHC complex on a DC. If such an interaction is not given, T cells remain naïve, leave the lymph node and reenter the blood stream via the thoracic duct. Apart from signaling through the TCR, further costimulatory signals are necessary for the T cell to be activated, undergo clonal proliferation and differentiate into effector cells. However, signaling through the TCR alone indicates recognition of a self-antigen and induces anergy or apoptosis (Guerder et al., 1994). The secondary signal is provided by the interaction between the costimulatory molecules CD28 and CD27 on T cells and CD80 and CD70 on activated DCs. Signaling through CD28 leads to the secretion of IL-2, which is an autocrine proliferation factor for T cells (Appleman et al., 2000; Zhou et al., 2002). Simultaneously, expression of the α-chain of the IL-2 receptor is induced, leading to the formation of the high affinity trimeric αβγ receptor, which increases the effect of IL-2. Additionally, other costimulatory signals are transmitted through the two TNF receptor family members 4-1BB (CD137) and OX40 (CD134) on T cells and their ligands 4-1BBL and OX40L (OX40 ligand or TNF receptor-associated factor 2 (TRAF2)) on the APC (Croft, 2003), or ICOS (CD278) and its ligand ICOSL (ICOS ligand (B7-H2)) (Dong et al., 2001; Carreno and Collins, 2002). Physical contact between the APC and the T cell is also reinforced by several cell adhesion molecule pairs like ICAM-1/LFA-1 or DC-SIGN/ICAM-3, thus forming a so-called ‘immunological synapse’ (Grakoui et al., 1999; Bromley et al., 2001). Next to the activating costimulatory signals, several inhibitory receptors are expressed on T cells as well, which can downmodulate or inhibit complete activation. The two most prominent representatives are cytotoxic T lymphocyte antigen 4 (CTLA-4, CD125) and programmed cell death 1 (PD-1). Negative costimulatory signals have been shown to be important to prevent excessive immune responses and maintain self-tolerance (Greenwald et al., 2005).

$CD4^+$ T cells differentiate into three major classes of T_H cells, T_H1, T_H2 or the more recently identified T_H17 T cells. All subsets differ in their cytokine secretion pattern and by this also in the target cells that they activate. T_H1 cells produce mostly IFNγ and control cell-mediated immunity by activating macrophages and CTLs (Stout and Bottomly, 1989; Andreasen et al., 2000). T_H2 cells produce IL-4,

IL-5 and IL-13 and direct the immune response towards humoral immunity by activation of B cells and their antibody production (Croft and Swain, 1991b; Croft and Swain, 1991a; Parker, 1993). T_H17 cells secrete IL-17A, IL-17F, IL-21, IL-22 and IL-23 (Tato and O'Shea, 2006), which are important in activation of neutrophils and immunity against parasites (Fallon et al., 2006). Naïve $CD4^+$ T cells differentiate into the respective subtype depending on the cytokine milieu prevailing during their priming. While development of the T_H1 phenotype is induced by IL-12 and IFNγ, IL-4 leads to development of T_H2 $CD4^+$ T cells (Mosmann and Coffman, 1989; O'Garra and Arai, 2000). Of note, T_H1 and T_H2 cells have been shown to inhibit the activation of each other, therefore committing the local immune response to either one of the two pathways (Jankovic et al., 2001). T_H17 cells are induced early during an immune response in the presence of transforming growth factor β (TGF-β) and IL-6 (Veldhoen et al., 2006)

Moreover, other suppressive and regulatory $CD4^+$ T cell populations are known. Amongst those are regulatory T cells (T_{reg}). While natural T_{regs} develop in the thymus in between positive and negative selection (Klein et al., 2014), induced T_{regs} develop in the periphery. Both T_{reg} types can suppress $CD4^+$ as well as $CD8^+$ T cells, and are crucial for the maintenance of self-tolerance (Sakaguchi et al., 1995). Expression of CD25 and especially the master transcription factor forkhead box P3 (FoxP3) are characteristic markers for T_{regs} (Fontenot and Rudensky, 2005).

After priming, naïve $CD8^+$ T cells differentiate into effector cytotoxic T cells, produce IFNγ, TNFα and lytic granules containing enzymes such as perforin and granzymes. Effector T cells leave secondary lymphoid organs and migrate into tissues to kill infected and altered cells. Of note, effector CTLs can kill cells expressing the MHC/peptide complex they recognize without further stimulatory signals being needed. CTLs express CD95L, which is capable of inducing apoptosis by binding to its receptor on target cells (Russell and Ley, 2002). Upon activation, CTLs produce effector molecules and store them in modified lysosomes, so-called cytotoxic granules (Henkart, 1994), from which they can be quickly released after contact with the cognate epitope. The glycoprotein CD107a (LAMP-1: lysosomal associated membrane protein-1) in the membranes of these granules is a marker for degranulation and can give information about the cytolytic activity of CTLs (Aktas et al., 2009). Cytotoxic granules include the aforementioned perforin, which disintegrates the plasma membrane of a target cell (Tschopp et al., 1986), and granzymes, which are serine proteases. These can enter target cells and induce an apoptotic cascade through activation of caspase 3 (Heusel et al., 1994). Additionally, cytokines like IFNγ and TNFα are secreted, which increase for example the density of MHC molecules on target cells (Slifka and Whitton, 2000).

After the ‘effector phase’ and clearance of an infection, a contraction phase occurs and approximately 90 to 95% of the effector T cells undergo apoptosis, while the remaining activated T cells constitute the immunological memory T cell pool (Murali-Krishna et al., 1998). Upon reinfection with the same pathogen, memory T cells show a higher sensitivity to antigen stimulation, are less dependent on

costimulatory signals and display effector functions more efficiently and rapidly than naïve T cells (Veiga-Fernandes et al., 2000). These memory T cells show a differential expression of cell surface markers namely no CD45RA expression in comparison to naïve T cells which are positive for CD45RA. The expression of CCR7 in combination with the CD45RO tyrosine phosphatase, another isoform of CD45RA, allows to subdivide central memory T cells (T_{CM}) ($CD45RO^-CCR7^+$) and effector memory T cells (T_{EM}) ($CD45RO^-CCR7^-$). T_{CM} cells show a similar homing behavior as naïve T cells and circulate in the blood and lymphoid system, while T_{EM} are found in the periphery more frequently (Sallusto et al., 1999). The latter ones display more rapid effector functions, have cytolytic abilities and produce IFNγ. T_{CM}, however, produce IL-2, have a higher proliferative capacity and undergo less cell divisions. Furthermore, they are also able to differentiate into effector cells upon secondary stimulation (Masopust et al., 2001). Another subset is referred to as T_{SCM} (stem cell memory), which are similar to T_{EM} but express CD45RA (Faint et al., 2001; Gattinoni et al., 2011). T_{SCM} express large amounts of perforin (Sallusto et al., 1999) and it has been suggested that they are derived from T_{CM} cells upon homeostatic proliferation in the absence of antigens (Geginat et al., 2003). T_{SCM} have self-renewing potential and are highly proliferative. Besides, they are considered to be multipotent, being able to further differentiate into other (memory) T cell subsets. Of note, this subset is discussed as a valuable new tool for adoptive T cell therapies in the field of cancer immunotherapy (Gattinoni et al., 2012).

The expression of other cell surface markers such as the homing receptor CD62L, costimulatory receptors CD28 and CD27 and the IL-7 receptor α-chain (CD127) are also used to differentiate T cell subsets. In most tissues, a prominent population of long-lived $CD8^+$ T cells, tissue-resident memory cells (T_{RM}), which is distinct from the T_{EM} cell populations and does not recirculate, exist. They are residing in tissues of potential reinfection, such as the intestinal, genital and respiratory mucosa and the skin. Here, T_{RM}s coordinate the initial response to pathogens, providing an important function by directly recognizing antigen, recruiting circulating memory cells and reducing the amount of infected cells (Schenkel et al., 2013).

It has been suggested that determination of differentiation into memory T cells occurs early during infection (Marzo et al., 2005). For the generation of $CD8^+$ memory T cells, $CD4^+$ T cell help has been shown to be essential (Shedlock and Shen, 2003). Later on, however, $CD8^+$ memory T cells, do not require help of $CD4^+$ T cells for a recall response.

1.2.5 Tumor immunology

Besides fighting pathogenic invaders, the immune system has also evolved strategies to distinguish altered self from normal self and is thus able to initiate an immune reaction against tumor cells. However, tumor immunity is regarded as a double-edged sword, because on the one hand, inflammation can serve as the driving force to develop cancer and on the other hand, immune effector functions are crucial for tumor control (Schreiber et al., 2011). This ambivalence was recently also

integrated into the hallmarks of cancer by Weinberg and Hanahan as described in section 1. While one emerging hallmark is the avoidance of immune destruction, one of the enabling characteristic of cancer is promotion through inflammation (Hanahan and Weinberg, 2011).

In 1909, more than 100 years ago, Paul Ehrlich introduced the idea of immune cells that control cancer growth. About 50 years later in 1957, Burnet and Thomas proved this hypothesis to be true by observations in mice, giving rise to the concept of immunosurveillance (Burnet, 1957). Another 50 years later, Schreiber and colleagues summarized all these findings by formulating the immunoediting hypothesis (Dunn et al., 2004; Schreiber et al., 2011). In this hypothesis, they describe the cancer-immune cell crosstalk through several phases, that explain how immune cells can either benefit or harm patients with tumors (Dunn et al., 2002; Ikeda et al., 2002). This is illustrated in Figure 10.

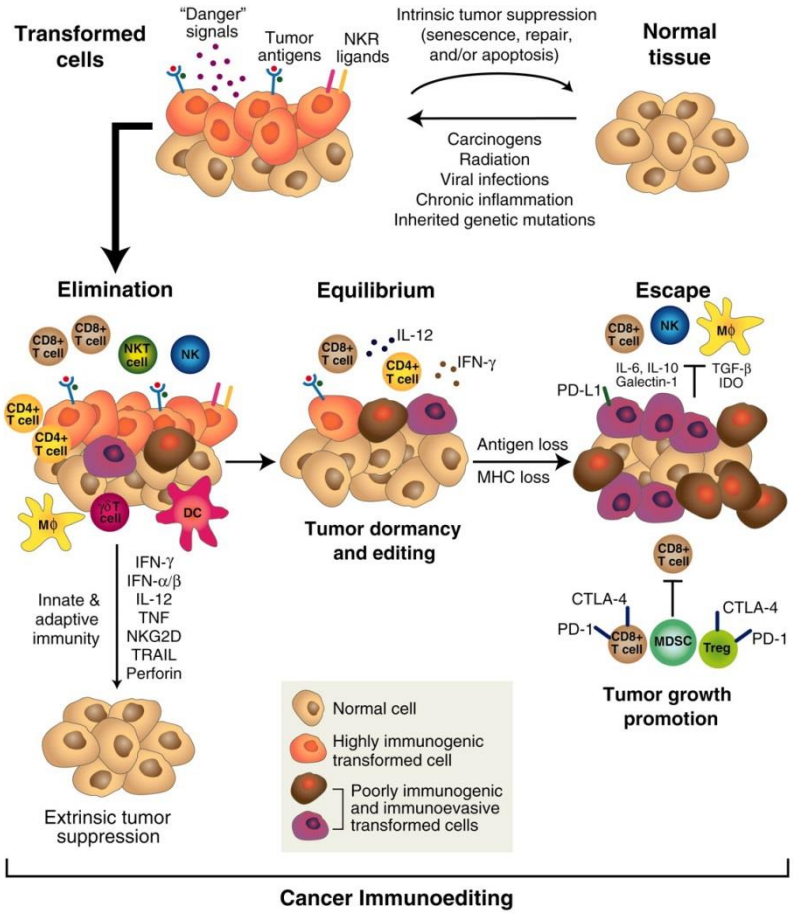

Figure 10 I The three E's of cancer immunoediting. This scheme displays the interplay between the immune system and tumor cells at various stages of tumor development. During the elimination and equilibrium stage, the immune system can eliminate and control tumor outgrowth. Entering the escape phase, the tumor has acquired strategies for immune escape and actively suppresses immune effector functions. This figure is taken from (Schreiber et al., 2011)

Transformation of normal cells to malignant cancer cells can be caused by multiple factors, such as exposure to carcinogens or viral infections resulting in mutations. Even after overcoming intrinsic tumor suppression, such as DNA repair, cellular senescence and apoptosis, transformed cells can still be detected by the immune system. Developing tumor tissue presents tumor antigens, expresses

danger-associated molecular patterns (DAMPs) and sends danger signals by secretion of cytokines, such as e.g. type I IFNs.

During cancer immunoediting the immune system recognizes and eliminates malignant cells. However, tumor cells can escape the immune system and sustain a pool of malignant cells. Cancer immunoediting is divided into three distinct phases, which are named the three capital "E"s, being comprised of an elimination, equilibrium and escape phase. In the first phase, the elimination phase, innate and adaptive immunity try to prevent tumor outgrowth by detection and elimination of transformed cells. T cells recognize the presentation of tumor-antigens by MHC molecules. Especially CTLs kill tumor cells by exploiting cytotoxic capabilities such as the secretion of cytotoxic granules and CD95L expression. Expression of markers by the tumor cell, such as the natural-killer group 2, member D (NKG2D) ligand can lead to activation of NK and γδ T cells (Cerwenka and Lanier, 2001). NK and T cells in turn secrete IFNγ, which can inhibit tumor cell proliferation and angiogenesis and induce apoptosis (Bromberg et al., 1996; Kumar et al., 1997; Qin and Blankenstein, 2000). On NK cells, TNF-related apoptosis-inducing ligand (TRAIL) is expressed on the cell surface and perforin dependent mechanisms are used to eliminate cells (Smyth et al., 2001). In addition, activated macrophages can kill tumor cells via reactive oxygen species (ROS) (Liou and Storz, 2010). Danger signals, like type I IFN, IL-1, TNFα, high mobility group box 1 (HMGB1) or hyaluronan fragments from damaged tissue contribute to recruitment of immune cells. Tissue resident sentinel DCs get activated by cytokines such as IFNγ or by tumor-infiltrating NK cells themselves (Sims et al., 2010). Additionally, the micromilieu is enriched for heat shock proteins (Hsps) and apoptotic cell fragments that constitute an large pool of tumor antigens (Haug et al., 2005; Berg et al., 2006). DCs that have engulfed tumor antigens migrate to the draining lymph node to induce specific anti-tumor T cell responses. In addition to an initial $CD8^+$ T cell response, $CD4^+$ T_H cells are also induced which subsequently help to activate CTLs via cross-presentation (Kurts et al., 2010).

However, rare tumor cells manage to survive the elimination phase, enter the equilibrium phase. Herein, $CD4^+$ and $CD8^+$ cells as well as the cytokines IFNγ and IL-12 seem to counterbalance immunosuppressive mechanisms and keep tumor cells in dormancy (Aguirre-Ghiso, 2007; Koebel et al., 2007). Immunoediting of the tumor cells takes place in the equilibrium phase, possibly due to the selection pressure of the immune system that enables survival of tumor cells with immunoevasive features. These variants of the tumor cells are more aggressive compared to the original tumor. Eventually, they cannot be killed by immune cells anymore and form new colonies of cancer cells.

In the last phase of immunoediting, tumor cells escape from immune control leading to tumor progression and clinical manifestation. The intrinsic mechanisms and mutations that finally lead to the escape stage are loss of immunodominant antigens, loss of MHC I and II molecules and defects in the APM (Khong and Restifo, 2002). Furthermore, tumor cells take advantage of various possibilities to

keep the microenvironment in an immunosuppressive state. Secretion of immunosuppressive cytokines leads to strong tumor-protective functions. These include IL-10, vascular endothelial growth factor (VEGF), TGF-β and indoleamine 2,3-dioxygenase (IDO) (Gabrilovich et al., 1996; Gorelik and Flavell, 2002; Uyttenhove et al., 2003). Moreover, tumor cells specifically recruit immunosuppressive immune cells such as T_{regs} and myeloid-derived suppressor cells (MDSCs). T_{regs} produce immunosuppressive cytokines such as TGF-β or IL-10 upon stimulation with their respective cognate peptide. High expression levels of CD25 are proposed to consume the IL-2 from the environment and by this limit effector T cell proliferation (Pandiyan et al., 2007). Further, T_{regs} express inhibitory molecules such as CTLA-4 and PD-1 (Vignali et al., 2008). MDSCs are a heterogeneous population of immature myeloid cells and exhibit various functions that suppress the functions of immune cells (Schlecker et al., 2012). Special mechanisms that lead to the immune escape of HPV-transformed cells are discussed in the next subchapter.

1.2.6 HPV and immune evasion

More than 95% of incident infections with HPV are cleared by the immune system within 6 to 18 months (Crosbie et al., 2013). For clearance, the HPV-infected cells need to be recognized by the host's immune cells. Regressing warts, for example, show a marked infiltration of macrophages and $CD4^+$ and $CD8^+$ T cells to the site of infection (Nicholls et al., 2001). $CD8^+$ T cell-mediated immune responses have been reported to be crucial for clearance of HPV16 (Stanley, 2012). Protective HPV immunity against reinfection is achieved by neutralizing antibodies in the serum, which are mainly directed against the viral capsid protein L1. However, antibody titers were found to be rather low after natural HPV infection and only occur in some patients (Stanley, 2006a).

In general, HPVs are very successful pathogens because they are able to cause chronic infections but rarely kill their host. Through this strategy, HPV is able to produce large amounts of infectious virions for transmission to naïve new hosts (Stanley, 2008). Comparable to other infections, in HPV-infected cells, both innate and adaptive immunity are invoked to eliminate the infected cell by various mechanisms. However, HPV and many other viruses have evolved numerous strategies to escape from host immune responses (O'Brien and Saveria Campo, 2002; Doorbar, 2006; Grabowska and Riemer, 2012). First of all, the HPV life cycle itself is an immune evasion mechanism, which delays virus detection by the host's immune system. The life cycle is non-lytic, neither tissue nor cell damage occurs and no pro-inflammatory signals are induced that could activate innate or adaptive immunity. Another strategy that HPV has evolved to avoid detection, is to stay outside the basement membrane and thereby maintain a very low profile. The virus is directly infecting basal skin cells from the outside, at a very low viral copy number and without a blood born infection phase. The expression of the oncogenes E6 and E7 is highly controlled by the repressor function of E2. Thus the viral early proteins are expressed at levels below those required for an effective host immune response (Doorbar, 2006; Kanodia et al., 2007; Stanley, 2008). Higher expression levels of viral proteins only occur in

upper layers of the epithelium. At this stage, also immunogenic particles like the capsid proteins L1and L2 are expressed. However, the keratinocytes are already in the last differentiation compartment and are soon shed from the surface of the epithelium (Stanley, 2012).

Regarding innate immune responses to viral infection, many mechanisms are affected by HPV. Usually, cells express TLRs which sense PAMPs and then elicit a response against the infection. TLR9, that senses CpG DNA patterns, has been shown to be downregulated in HPV-positive carcinomas (Hansen and Bouvier, 2009). Moreover, the two oncoproteins E6 and E7 counteract TLR signaling by directly interacting with different components of the IFN signaling pathways and these inhibit IFN synthesis (Kanodia et al., 2007; Stanley, 2008). The E7 protein of high-risk HPVs inhibits the activation of the IFNβ promotor by blocking the transcription factor interferon regulatory factor 1 (IRF-1), thereby inhibiting the transcription of the chemotactic ligand CCL2 and TAP1. Besides, E7 also interferes with IFNα signaling by preventing the translocation of IRF-9 to the nucleus. Hence, it inhibits the formation of the interferon-stimulated gene factor 3 (ISGF-3) complex, that binds to interferon-specific response elements (ISREs) which leads to activation of interferon-responsive genes. High-risk HPV E6 proteins are preventing transcriptional activation of IFNα by binding to the transcription activator IRF-3. The E6 protein additionally interferes with IFNα signaling by preventing the tyrosine kinase 2 (TYK2) to bind to the cytoplasmic side of the IFN receptor. This impairs phosphorylation of several signal transducers and activators of transcription (STATs) leading to impaired janus kinase (JAK)-STAT signaling (reviewed in Grabowska and Riemer, 2012).

In addition to TLRs, the innate immune system also includes nucleotide binding domain, leucine-rich repeat gene family receptors (NLR-receptors) which are expressed on keratinocytes. These receptors sense PAMPs, as well as DAMPs, and induce secretion of IL-1β and IL-18 and proinflammatory signaling. IL-1β and IL-18 activate macrophages and resident APCs and attract effector T cells, forming a bridge to the adaptive side of the immune system. IL-6 is also constitutively expressed by keratinocytes (Stanley, 2012). High-risk HPVs seem to be able to counteract expression and secretion of this cytokine. It has been reported that in HPV16 infected cells, many proinflammatory and chemotactic cytokines are downregulated, including IL-1β and IL-6. In case of IL-1β, this might be mediated by proteasomal degradation of pro-IL-1β through E6-AP and p53 (Niebler et al., 2013).

HPVs have also evolved to successfully escape from adaptive immune responses. Upon viral infection, APCs usually sense the virus in the periphery. Since HPV exclusively infects stratified squamous epithelia, Langerhans cells specialized epithelial DCs , act as APCs (Drijkoningen et al., 1988) (Miyagi et al., 2001). Langerhans cells have been reported to be decreased in low-grade HPV lesions and are even more markedly absent in high-grade lesions. Thus, the number of cells recognizing infection and presenting antigens is reduced, which may facilitate the establishment and persistence of local HPV infection (Leong et al., 2010). Langerhans cells normally take up antigens and mature during migration to the lymph node where they eventually prime naïve T cells (Mota et al.,

1999). However, in high-grade lesions, Langerhans cells were shown to exhibit an early failure of activation compared to normal tissue and low-grade lesions. Being not fully activated when presenting antigens to naïve T cells, Langerhans cells are believed to induce tolerance rather than the inflammatory response needed to induce a cytotoxic $CD8^+$ T cell response (Stanley, 2012).

On the keratinocyte side, HPV-positive cells have a downregulated MHC I surface expression in comparison to uninfected cells (Ashrafi et al., 2005; Kanodia et al., 2007). The downregulation of MHC molecules on the surface is mainly attributed to the E5 protein, which interferes with the trafficking of MHC I/peptide complexes via the Golgi network. E5 influences the pH of the Golgi network and thus reduces MHC I stability. Moreover, it directly interacts with the MHC I/peptide complex, leading to accumulation of the MHC I/peptide complex within the Golgi network (Ashrafi et al., 2005; Campo et al., 2010). In addition, reduced protein levels of various components of the APM were reported in cervical cancer lesions and HPV-positive cell lines (Seliger et al., 2000; Manning et al., 2008; Hasim et al., 2012). Dysregulation of the APM results in downregulation of MHC I/peptide complexes and protects infected cells from immune attack.

Taken together, in more than 95% of HPV infections the immune system successfully clears the virus, particularly via local antigen-specific $CD8^+$ and $CD4^+$ T cell responses (Stanley, 2012). However, if the immune system fails to clear the infection, the described immune evasion mechanisms allow establishment of a persistent infection, which might lead to CIN2/CIN3 and eventually cancer. The expression of cytokines, chemokines and signaling receptors that are necessary for proficient cytotoxic T cell responses are more and more reduced during progressing neoplastic transformation and associated genetic instability. This leads to a balance shift from an effective cytotoxic T cell response to increased immune suppression that is mediated by regulatory T cells (Stanley, 2012).

1.3 Cancer immunotherapy

At the end of 2013, the journal Science announced ‘Cancer Immunotherapy’ as the breakthrough of the year. The ability of immune cells and immune-modulatory drugs to substantially help in controlling tumor growth in cancer patients, which was shown in convincing clinical trials, were recognized by the scientific community. In Figure 11, several important milestones of cancer immunotherapy are displayed that include the translation of basic scientific findings from “bench to bedside”.

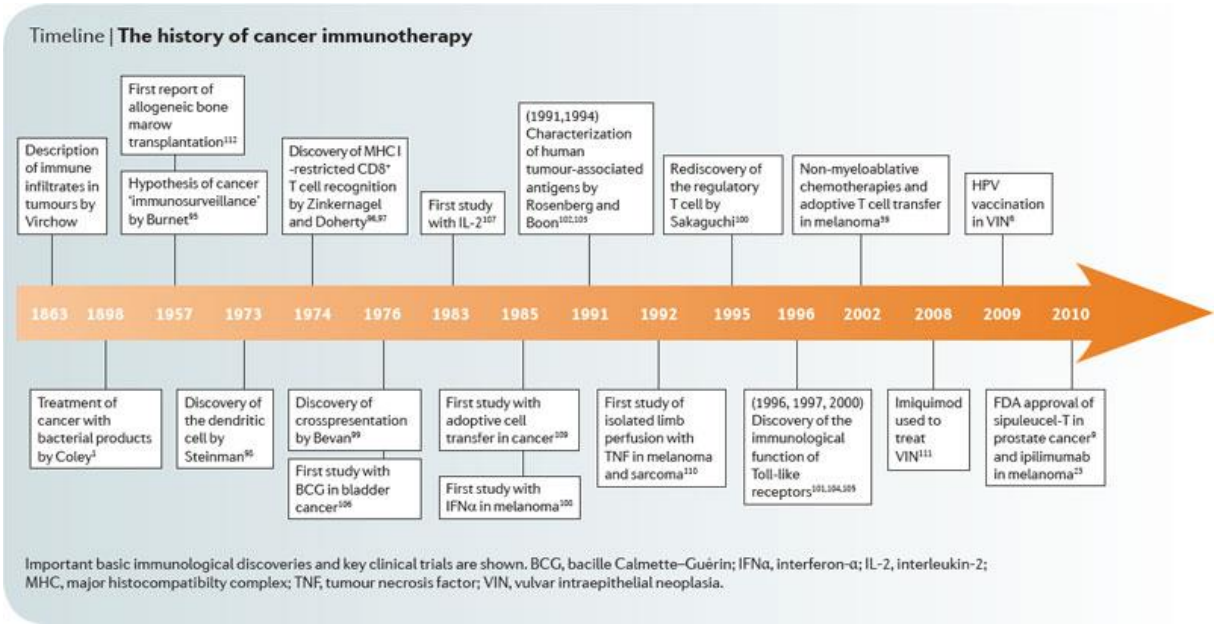

Figure 11 I Timeline of the most important breakthroughs in cancer immunotherapy. Important immunological discoveries and clinical trials that form the basis of today's cancer immunotherapy are displayed. This figure is taken from (Lesterhuis et al., 2011).

The overall concept of cancer immunotherapy is based on the aforementioned immunosurveillance mechanisms, which are hypothesized to prevent development of tumors from transformed cells on the one side, and immune escape of transformed cells on the other side. Thus, immunotherapy aims to manipulate the patient's immune system to enhance anti-tumor immunity and disable immune escape by the tumor (Fig. 12). First hints towards natural tumor immunity were observed after transplantation, that is accompanied by therapeutic immunosuppression, leading to an increased risk for patients to develop tumors (Vial and Descotes, 2003).

Direct evidence for the immune system controlling tumor growth was provided in the 1990s with IFNγ$^{-/-}$ or IFNγ receptor (IFN-γR)$^{-/-}$ mice that showed defective tumor rejection compared to immunocompetent wild type (wt) mice upon carcinogen challenge or injection of tumor cell lines. Additionally, tumors of immunodeficient mice that were implanted to immunocompetent wt mice, were completely rejected, implying that the immune system is not only capable of preventing tumor growth but also of eliminating established tumors, which were not grown under immunosurveillance. (Vesely et al., 2011).

Cancer immunotherapy comprises two different strategies to support the immune system for targeted cancer treatment. While passive immunotherapies specifically target tumor cells and perform anti-tumor effects on their own, active immunotherapy stimulates the host's immune system to generate anti-tumor cellular and humoral responses. In both cases, treatment can be directed at tumor antigens, which can be subdivided into highly tumor specific antigens (TSAs) and tumor associated antigens (TAA). The first class comprises for instance peptides of oncoviral proteins like HPV16 E6 and E7. The subset of cancer testis antigens is not strictly tumor specific, as those are also expressed on male

germline cells and trophoblastic cells. However, these cells do not express MHC molecules and therefore cannot present antigens. Cancer testis antigenes include the melanoma antigen (MAGE) family and the New York Esophageal Squamous Cell Carcinoma-1 (NY-ESO-1) (van der Bruggen et al., 1991; Ressing et al., 1995; Gnjatic et al., 2006). TAAs show a lower tumor specificity and include for example the overexpressed growth factor HER2/neu in breast and other epithelial tumors (Fisk et al., 1995) and the unglycosylated mucin. MUC-1, which is expressed on most adenocarcinomas, like breast and pancreatic cancers (Vlad et al., 2004). These antigens, however are also expressed in some normal tissues.

Antibody therapies belong to the most successful treatments of cancer by passive immunotherapy. The Her2/neu blocking antibody transtuzumab (Herceptin) was already approved in the 1990s for treatment of Her2/neu overexpressing breast cancer in combination with standard chemotherapy and significantly improved survival of patients (Piccart-Gebhart et al., 2005; Romond et al., 2005).

Checkpoint inhibitors build the newest group of immunotherapy strategies. The most famous examples include blocking of the inhibitory receptors CTLA-4 and PD-1 on T cells. Blocking these two receptors with antibodies can efficiently activate the whole T cell pool. Importantly, impilimumab, a CTLA-4 blocking antibody, has been shown in a large randomised trial to prolong overall survival of metastatic melanoma patients (Hodi et al., 2010) and was subsequently approved for treatment of melanoma by the US Food and Drug Administration (FDA) in 2011.

Infiltration of lymphocytes into the tumor was shown to be associated with a better prognosis in many different tumor entities, including HPV-driven tumors (Vanky et al., 1986; Zhang et al., 2003; Ward et al., 2014). During adoptive T cell transfer (ACT), autologous or allogenic effector T cells are activated *in vitro* and transferred to the patient. Various approaches have been developed through the last two decades and most of them employ T cells that are partly genetically engineered (Restifo et al., 2012). One of the first studies, published in 2002, showed that isolated and reinfused tumor infiltrating lymphocytes (TILs) of melanoma patients result in cancer regression (Dudley et al., 2002). Based on these findings, more targeted strategies were developed such as an ACT therapy with engineered T cells expressing tumor-antigen specific high affinity TCRs (Rosenberg, 2011). Moreover, genetically engineered T cells can express chimeric antigen receptors (CARs) (reviewed in Tey, 2014), which are not restricted to MHC molecules as they contain antigen-recognition domains of antibodies combined with intracellular signaling moieties of T cells. A CD19 B cell antigen CAR approach developed by June and colleagues led to complete remission of chronic lymphocytic leukemia (CLL) (Porter et al., 2011) and pediatric acute lymphoid leukemia (ALL) (Grupp et al., 2013). However, off target toxicity, which represents a problem when tumor-antigens are also expressed in normal tissue, has been shown to be fatal in ACT therapy. Cancer patients that were treated with an anti-MAGE-A3 TCR showed fatal neurologic toxicity attributed to cross-reactivity of the TCR with MAGE-12 (Morgan et al., 2013).

Cytokines such as IL-2, IFNα and GM-CSF have also been used in cancer immunotherapy. IL-2 was approved for treatment of renal cancer and metastatic melanoma despite low response rates (Rosenberg et al., 1985; Atkins et al., 1999; Smith et al., 2008). Toxic side effects, however, were severe, even leading to organ failure (Rosenberg et al., 1989). Importantly, besides the desired unspecific activation of T cells, IL-2 can induce T_{regs} when being injected systemically. Local administration of IL-2 and TNFα were reported to be beneficial in sarcoma and melanoma (Grunhagen et al., 2006; Weide et al., 2010).

Vaccination approaches, belonging to the active cancer immunotherapy strategies, are generally considered to be safe and cost-efficient. However, initially they are far less effective than passive immunotherapy approches. For a robust immune response, APCs, mostly DCs, need to take up tumor antigens, process them and present them by HLA molecules to naïve $CD4^+$ and $CD8^+$ T cells. These need to differentiate into effector T cells as described in detail in section 1.2.4.1. Antigen presentation can be achieved through DC-, protein- and peptide-based vaccines.

The DC-based vaccine Sipuleucel-T (Provenge™) was the first active cancer vaccine to be approved by the FDA. It induces T cell responses against the prostate carcinoma antigen prostatic acid phosphatase (PAP) (Kantoff et al., 2010). Protein vaccines include numerous $CD8^+$ and $CD4^+$ T cell epitopes. Vaccination with such a vaccine induce weak, variable antigen-specific $CD8^+$ T cells responses and mainly $CD4^+$ T cell responses, which are mainly immunodominant. The poor efficiency of vaccine antigen uptake, processing and presentation by APCs limits the magnitude of resulting immune responses. Peptide vaccines, on the other hand, induce more specific T cell responses in comparison. The NY-ESO-1 antigen was targeted by both, protein and peptide vaccines in various studies (Karbach et al., 2011; Sabbatini et al., 2012). More clinical studies, including protein and peptide vaccination for HPV treatment, will be discussed in section 1.3.2.

Possible options for the peptide vaccination approach are long and short synthetic peptides. Long synthetic peptides, presenting a defined sequence of a protein, may contain several $CD8^+$ and $CD4^+$ T cell epitopes. As proteins, these long peptides also require optimal uptake, processing and HLA loading of T cell epitopes by APCs to give rise to effective immune responses. Long synthetic peptide vaccines mainly result in good $CD4^+$ T cell responses and rather poor $CD8^+$ T cell responses, suggesting a failure of efficient processing and cross-presentation. Short synthetic peptides generally contain one exact, immunodominant $CD8^+$ T cell epitope that binds directly to a HLA molecule on APCs. Phagocytosis, processing and entry into the cross-presentation pathway is not required. Hence, short peptide vaccines induce very robust specific $CD8^+$ T cell responses but lack the ability to trigger a $CD4^+$ T_H cell response. Moreover, short specific peptides are HLA-restricted, combination of various different HLA-specific precise $CD8^+$ T cell epitopes into one vaccine can solve this shortcoming. Long peptides are not HLA-restricted. Thus, prior HLA typing of patients is not required.

Van der Burg and van Hall have published "Seven hallmarks of peptide vaccination" in analogy to Hanahan's and Weinberg's hallmarks of cancer (van Hall and van der Burg, 2012) that include factors which need to be considered for peptide vaccination. These include peptide length, APC targeting, $CD4^+$ T cell help, epitope breadth, peptide dose, bio distribution and supply of danger signals.

As described in section 1.2.5, $CD4^+$ T cell help (T_H1) is important for the priming of naïve $CD8^+$ T cells by DCs. Indeed, the addition of T_H cell epitopes to peptide vaccines improves protective T cell responses (Zwaveling et al., 2002; Bijker et al., 2007). Moreover, it was observed, that T_H cells also seem to provide help to CTLs in the tumor microenvironment and thus enhance CTL recruitment and their cytolytic functions (Bos and Sherman, 2010). Consequently, the inclusion of T_H cell epitopes increases a vaccine's efficiency. This can be achieved by either adding common agonistic sequences to the peptide vaccine, such as as known sequence, the pan HLA-DR-binding epitope (PADRE), or specific antigen-derived peptides (van Hall and van der Burg, 2012).

Equally important as the antigen is the mode of delivery. Especially for peptide vaccines, appropriate adjuvants are crucial. These are compounds that enhance the magnitude, breadth, quality and longevity of specific immune responses to antigens. Since the 1920s, adjuvants are commonly used for vaccinations. At that time an aluminium salt, also known as alum, was discovered and shown to improve diphtheria vaccination results (Park and Schroder, 1932). Adjuvants can be categorized into two main subsets, delivery systems and immune potentiators (Brito et al., 2013). While immune potentiators directly activate the immune system, delivery systems target the vaccine to immune cells, prolong their activity and enhance antigen uptake (Pashine et al., 2005). An example for immune potentiators are synthetic TLR ligands, such as polyinosinic-polycytidylic acid (poly I:C) and monophosphoryl lipid A (MPLA), which is e.g. a component of the prophylactic vaccine Cervarix™ together with aluminium hydroxide (Keam and Harper, 2008). Commonly used delivery systems for peptide-vaccines are water-in-oil emulsions such as Montanide (Brito et al., 2013). Especially Montanide ISA 51 (Aucouturier et al., 2002) has been widely used for clinical trials. It forms depots from which antigens are slowly released, which is thought to improve antigen uptake by DCs (Bijker et al., 2007).

Apart from activating the immune system, additional hurdles need to be overcome in cancer immunotherapy. These are the local immunosuppressive milieu at the tumor site and targeting of activated T cells to the tumor. Immunosupressive cell populations such as T_{regs} should be inhibited, leading to elevated antigen-specific responses. This was achieved in colorectal cancer patients by T_{reg} depletion (Clarke et al., 2006). This strategy, however, brought along the risk of autoreactive immune responses (Kim et al., 2007).

In summary, cancer immunotherapy has the aim to generate potent anti-tumor immune responses. To this end, DC priming for efficient antigen-presentation to T cells is very important, in addition to

enhancement of T cell functions, migration to the tumor site and inhibition of immunosuppression (Fig. 12).

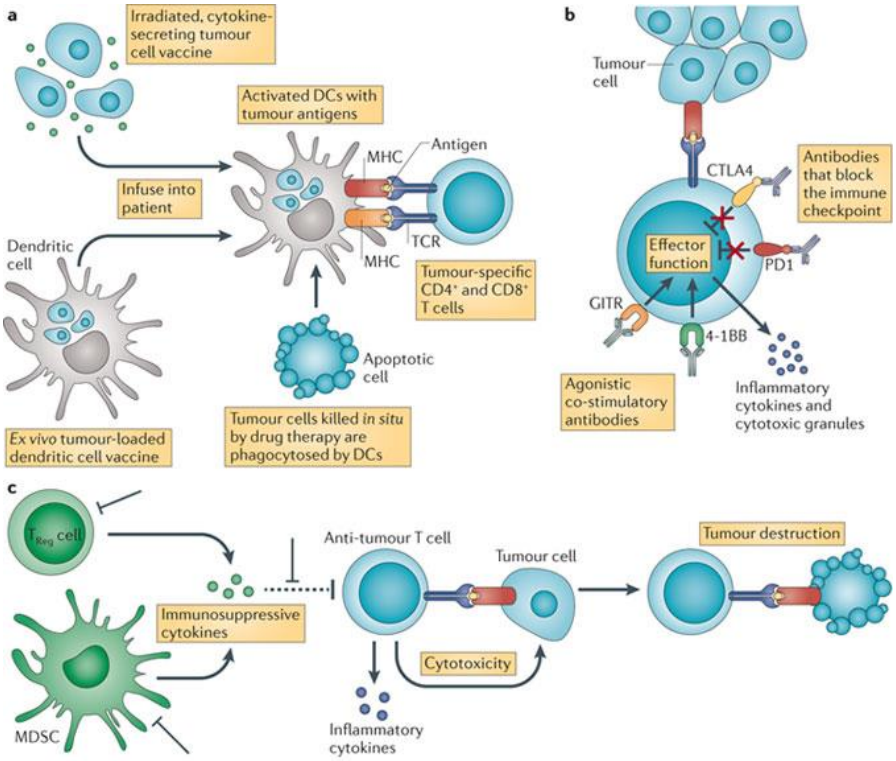

Figure 12 I Generation of an effective anti-tumor immune response and its multiple steps. a Priming of DCs with tumor-antigens can be accomplished by various means, including injection of whole irradiated tumor cells, or reinfusion of *ex vivo* antigen-loaded autologous DCs. Chemotherapy and targeted therapy can kill tumor cells which are then phagocytosed by DCs. **b** T cell function can be improved by costimulation or blocking of inhibitory signals with respective antibodies. **c** Immunosuppressive T_{regs} and myeloid-derived suppressor cells (MDSCs) have an inhibitory effect of immune responses by secretion of cytokines. Depletion of immunosuppressive cell or inhibition of cytokine secretion can increase effective anti-tumor T cell responses. This figure is adapted from (Vanneman and Dranoff, 2012).

1.3.1 T cell epitope predictions

Identification of the precise tumor-derived T cell epitopes is crucial for development of a short peptide vaccine to evoke efficient T cell immune responses. Since the experimental testing of binding affinity of peptides to MHC molecules in general is not economical in terms of time and cost, various computational approaches have been developed. These computational predictions of MHC I binding capacities have been used for many years now and are permanently updated (De Groot et al., 2001; Sylvester-Hvid et al., 2004; Sette and Rappuoli, 2010; Lund et al., 2011). For this study, different prediction servers were chosen to exploit the individual strengths of each server since they are based on different algorithms and training data sets.

In 1994, Parker and his group developed the first HLA peptide prediction server Bioinformatics and Molecular Analysis Section (BIMAS) (Parker et al., 1994), which is based on the predicted half-time of dissociation from HLA I molecules and some mouse MHC I. A few years later, Rammensee and colleagues developed a prediction server called SYFPEITHI (Rammensee et al., 1999), which is based

on allele-specific amino acid motifs and includes peptide predictions for MHC I as well as MHC II. The name SYFPEITHI is taken from the first MHC-eluted peptide that was directly sequenced (Falk et al., 1991).

A more recent group of servers, the NetMHC servers are hosted by the Center for Biological Sequence Analysis by the Technical University of Denmark and were developed by groups around Lund and Nielsen. These servers are based on different methods, such as artificial neural networks (ann) (NetMHC, (Nielsen et al., 2003)) that can be pan-specific (NetMHCpan, (Lundegaard et al., 2008a; Lundegaard et al., 2008b; Stranzl et al., 2010)) or matrix-based relying on receptor-pocket similarities between MHC molecules (PickPocket). They were also combined in one single server, NetMHCcons (Karosiene et al., 2012). Moreover, they developed a specific CTL prediction server, NetCTL, which integrates prediction of peptide MHC class I binding, proteasomal C-terminal cleavage and TAP transport efficiency (Larsen et al., 2005; Larsen et al., 2007). The MHC peptide binding is predicted using neural networks trained as described for the NetMHC server (Nielsen et al., 2003), TAP transport efficiency prediction uses a weight matrix based method (Peters et al., 2003) and proteasome cleavage events are predicted by NetChop neural networks trained on C-terminals of known CTL epitopes (Nielsen et al., 2005).

The Immune Epitope Database Analysis Resource (IEDB) website provides a collection of computational tools for the prediction and analysis of immune epitopes. Here, the tool for peptide binding to MHC class I molecules offers various prediction methods to the user, including some of the already described NetMHC methods, NetMHCpan, NetMHCcons and PickPocket. Besides, an artificial neural network-based algorithm (IEDBann) (Nielsen et al., 2003) and three matrix-based algorithms, average relative binding (IEDBarb) (Bui et al., 2005), the stabilized matrix method (IEDBsmm) (Peters and Sette, 2005) and SMM with a Peptide:MHC Binding Energy Covariance matrix (IEDBsmmpmbec) (Sidney et al., 2008) are available. CombLib, another method, stands for Scoring Matrices derived from Combinatorial Peptide Libraries (Sidney et al., 2008). IEDBrecommended combines the results of the Consensus method consisting of ANN, SMM, and CombLib if any corresponding predictor is available for the MHC molecule. Otherwise, NetMHCpan is used. Some of these mentioned algorithms, however, are only included in older versions of available tools.

Most prediction servers offer predictions for various MHC alleles, sometimes also including other species than human and mouse, and often allow for predictions for HLA supertypes. HLA supertypes consist of different HLA class I molecule types which share high similarities in binding peptides and were thus grouped into nine HLA supertype families (Sette and Sidney, 1999). Each supertype can be described by a supermotif reflecting the general main anchor motif recognized by molecules within the corresponding supertype. For instance, alleles of the HLA-A2 supertype share specificity for peptides with aliphatic hydrophobic residues at the C-terminus and at position 2 of the peptide. HLA-A3

supertype molecules, on the other hand, bind peptides with small or aliphatic residues in position 2 and basic residues at the C-terminus. Later on, the supertype concept was adapted and three more family clusters were added, resulting in twelve HLA supertypes (Lund et al., 2004). Moreover, HLA supertypes each have representative HLA alleles, presenting the most common ones of the respective supertype. The three HLA supertypes, which are investigated in this study, are HLA-A3 with the major allele HLA-A*03:01, HLA-A11 with the major allele HLA-A*11:01 and HLA-A24 with HLA-A*24:02 as the representative allele. While HLA-A24 is widely spread amongst Asian populations, reaching 58.6% in the Japanese population, up to 37.5% in Caucasians harbor HLA-A3 and HLA-A11 alleles (Sette and Sidney, 1999). In Germany, 28.6% carry the HLA-A*03:01 allele, while 10% are positive for HLA-A*11:01 and 18.1% for HLA-A*24:02. All three together thus cover a high percentage of the world's population (Gonzalez-Galarza et al., 2015).

1.3.2 HPV vaccines

In spite of relatively low serum antibody titers, it has been reported that HPV-seropositive animals are protected against further viral challenge (Kreider and Bartlett, 1981). A few years later, it was shown that passively transferred serum immunoglobulins from immunized to naïve animals conferred protection from infection (Suzich et al., 1995). HPV L1 virus-like particle (VLP) vaccines are subunit vaccines consisting only of the major viral capsid protein L1, which self-assemble into VLPs, which have been shown to be highly immunogenic. They induce circulating, neutralizing antibodies that offer protection against infection with HPV and were reported to have a good safety profile (Stanley, 2006b). These studies were the basis to develop prophylactic vaccines against several human high-risk HPV types based on L1 VLPs, of which the first two were approved in 2006.

Various vaccination strategies, including prophylactic and therapeutic approaches, are utilized to combat HPV-mediated malignancies. Currently used prophylactic HPV vaccines are administered to prevent uninfected individuals from acquiring a HPV infection. Therapeutic vaccination, in contrast, aims to support the patient's immune system to clear persistent HPV infection. Various stages of disease progression need to be taken into consideration, starting with low-grade lesions via high-grade lesions up to invasive cancer (Kanodia et al., 2008).

1.3.2.1 Prophylactic vaccines

To date, three prophylactic HPV vaccines have been licensed in the US by the FDA and two in Europe by the European Medicines Agency (EMA). All three vaccines are based on recombinant L1 proteins that spontaneously self-assemble into pentameric capsomeres congregating to form non-infectious VLPs. One single VLP consists of the repeated structure of 72 capsomers (360xL1) making it highly immunogenic and resembling native viruses (Frazer et al., 2011). Strong humoral and cell-mediated responses are induced by VLPs. Intramuscular injection ensures that VLPs quickly reach the lymph nodes. Here, they are recognized by the immune system by binding to the cell surface of monocytes, macrophages and DCs, which results in their acute activation and production of inflammatory

cytokines (Lenz et al., 2003). Those DCs initiate an immune cascade that results in T cell dependent B cell responses. These events are followed by generation of high levels of L1-specific neutralizing antibodies and immune memory (Stanley, 2008). Systemic vaccination was shown to induce markedly higher antibody titers against L1 of the respective HPV type than a natural local infection (Stanley et al., 2012).

The vaccines are HPV type-specific, since the genotypic variances between HPV types originate from the surface-exposed parts of the L1 capsid protein. The neutralizing antibodies generated by HPV L1 VLP vaccines thus only mediate protection against the corresponding virus type. Hence, to confer protection against multiple HPV types, respective type-specific L1 VLPs need to be included into the vaccine. Nonetheless, some evidence for cross-protection against HPV types other than those incorporated in the vaccines was reported (Frazer, 2010). However, it is not completely clear how and to what extent cross-protection against other types exist. In some immunized individuals, cross-protection against HPV31, 33, 45, 51 and 58 was reported (Malagon et al., 2012; Szarewski, 2012).

The bivalent vaccine Cervarix™ is produced by GlaxoSmithKline and combines VLPs of HPV16 and HPV18. VLPs are produced in a recombinant baculovirus expression vector system, that uses *Trichoplusia ni* Hi-5 insect cells. The formulation of the vaccine includes the AS04 adjuvant, consisting of 500µg aluminium hydroxide and 50µg 3-desacylatedmonophosphoryl lipid A (MPLA) (Harper et al., 2004).

The quadrivalent vaccine Gardasil™ was developed by Merck and includes HPV16 and 18 VLPs, but also additional VLPs from the low-risk HPV types 6 and 11, protecting against genital warts. It is produced in *Saccharomyces cerevisiae* by using recombinant DNA techniques. Aluminium hydroxyphosphate sulphate is used as an adjuvant here (Villa et al., 2005).

Both vaccines were found to be safe, immunogenic and efficient in various randomized controlled trials and confer protection against CIN induced by the respective HPV types (Stanley, 2006a). Various studies have been conducted to follow up Cervarix™ vaccination. High and sustained immune responses were detected in women aged 15-55 years. Antibody levels were several-fold higher than following natural infection, for at least 4 years after the first vaccine dose (Schwarz et al., 2011). In young girls and boys aged 10-14 or 12-15 years, the antibody levels were reported to be even higher for HPV16 and HPV18 antibodies (Medina et al., 2010). In the age group of 15-25 year old women, antibody levels remain high up to 8.4 years. Efficacy against incident infections was also sustained (95-97%), as well as against infections persisting for 12 months (100%), cytological abnormalities and histopathological lesions (CIN2+ 100%) that are caused by HPV 16 and/or 18 (GlaxoSmithKline Vaccine HPV Study Group et al., 2009). In a final report of the large PATRICIA (PApilloma TRIal against Cancer In young Adults) trial, immunogenicity and high efficacy against persistent infection and high-grade CIN were confirmed (Apter et al., 2015).

Gardasil™ was demonstrated to be highly immunogenic by inducing antibody levels that are 27-145-fold higher than HPV antibody levels detected in naturally HPV infected women. All vaccinated individuals seroconverted after the third dose (Villa et al., 2005). Combined final data from the FUTURE (Females United to Unilaterally Reduce Endo/Ectocervical Disease) I and FUTURE II studies included 17,622 women in the age group of 15-26 years. The vaccine efficacy against lesions related to HPV6, 11, 16 and 18 was 96% for CIN1, 100% for both VIN1 and VAIN1, and 99% for condylomata acuminata (Future I/II Study Group et al., 2010).

Recently, in December 2014, a new nonavalent prophylactic HPV vaccine from Merck was approved by the FDA. Gardasil™9 is an enhancement of the quadrivalent Gardasil and includes VLPs of nine HPV types, HPV6, 11, 16, 18, 31, 33, 45, 52 and 58. Thus it covers a broader range of high-risk HPV types than the original Gardasil. The new vaccine has been evaluated in five clinical studies including 14,204 16-26 year old females and was shown to be safe and add additional value regarding efficacy against HPV types 31, 33, 45, 52, and 58 in comparison to the first-generation vaccine (Joura et al., 2015). The EMA is currently assessing Gardasil™ 9 for European approval and Merck confirmed applications in other jurisdictions such as Australia.

The full impact of all prophylactic HPV vaccinations on cervical cancer prevention is not assessable yet, because routine vaccination is conducted for less than nine years and the development of cervical cancer can take much longer.

Vaccination programs are not completely successful everywhere, since not all people receive the recommended booster doses and vaccination coverage in populations in the US and Europe are lower than for other vaccinations (Bonanni et al., 2015). In Australia however, the national HPV immunization program started in 2007 and has resulted in high coverage with more than 70% for three doses (Garland, 2014). In contrast to developed countries, in developing countries, vaccination is often not accessible due to high cost and other social factors, which leads to a low percentage of vaccination in the population (van Bogaert, 2013).

The available described HPV vaccines, Cervarix™ and both Gardasil™ types, are strictly prophylactic und thus do not treat pre-existing infections or prevent progression of existing HPV-induced lesions (Kanodia et al., 2008). Hence, novel therapeutic strategies to control and treat existing HPV infections and associated malignancies are still needed.

1.3.2.2 Therapeutic Vaccines

A therapeutic vaccine against HPV that can support the immune system to clear a persistent HPV-infection would be an attractive option. Additionally it would need to overcome the viral evasion mechanisms and immunosuppressed situation at the site of infection (Frazer et al., 2011). Thus, HPV therapeutic vaccines should aim to evoke strong cellular immune responses, especially T cell-mediated

immune responses, against naturally processed and presented HPV antigens in HPV-infected cells (Kanodia et al., 2008).

HPV-associated tumors represent an ideal scenario for cancer vaccine development. In contrast to most other tumor entities, one can target immunologically foreign viral antigens and thus does not need to worry about breaking tolerance and potential subsequent autoimmunity. Furthermore, approximately 95% of HPV-infected people clear the infection (Crosbie et al., 2013), proving that elimination of HPV by the immune system is possible. Moreover a sufficient time window is given as it takes approximately 7 to 15 years from initial HPV infection to development of invasive cancer (Bosch and de Sanjose, 2003). Despite the availability of the prophylactic vaccines, development of a therapeutic vaccine is still desirable as a large proportion of the worldwide population is already infected and cannot be protected with prophylactic vaccination anymore (Frazer et al., 2011). Especially in developing countries, there is insufficient vaccine coverage due to economical and socio-cultural factors. The situation is worsend by the fact that in these countries screening and detection of pre-cancerous lesions is also limited. If detected in time, HPV-induced premalignant lesions are commonly removed surgically, which can lead to impaired function of the affected tissue, possibly resulting in premature births in case of the cervix. In conclusion, therapeutic HPV vaccination as a non-invasive treatment strategy is a goal worth pursuing.

The aim of therapeutic tumor vaccination is to stimulate the patient's own immune response to be able to recognize and eliminate cancer cells that express the targeted tumor antigens (Kanodia et al., 2008). All cells of HPV-induced lesions and tumors constantly express the two oncoproteins E6 and E7, as they are crucial for induction and maintenance of the malignant phenotype. Besides, E6 and E7 are viral proteins and therefore result in presentation of foreign viral epitopes on infected cells. Moreover, as HPV is replicating using the host's cellular replication machinery, mutation rates are extremely low in HPV proteins. This renders it unlikely that HPV16 escapes an immune response by mutating (Frazer et al., 2011). As T cell-mediated immunity is one of the most important factors to clear HPV infections and HPV-associated lesions, effective therapeutic vaccines should generate strong E6/E7-specific T cell-mediated immune responses to the early proteins E6 and E7 (zur Hausen, 2002; Tan et al., 2012). To reduce potential oncogenicity, the E6 and E7 oncogenes have been mutated in many studies to abrogate p53 and pRb binding. Next to E6 and E7, some attempts have also been made in targeting E2 and E5, as those two proteins are essential for immune escape and carcinogenic progression (Ganguly, 2012; Xue et al., 2012). Most HPV therapeutic vaccine studies have been designed with antigens from the most abundant HPV type, HPV16.

In the past two decades, major efforts have been made in terms of development of therapeutic HPV vaccines. A multitude of approaches was tested, including DNA-based, live vector-based, cell-based and protein- and peptide-based vaccines (Stern et al., 2012; Khallouf et al., 2014).

DNA-based vaccines are considered to be an attractive therapeutic approach, because they are safe, easily produced, show stable expression of the encoded antigen and can include adjuvant functions (Hemmi et al., 2000; Shirota and Klinman, 2014). A DNA vaccine based on the HLA-A2-restricted HPV16 E7/83-95 peptide called ZYC101 (Klencke et al., 2002) was tested in phase I and II trials with 15 patient with CIN2 and CIN3 lesions, and induced HPV-specific T cell responses in eleven and complete histological regression in five patients (Sheets et al., 2003). This DNA plasmid was formulated within biodegradable polymer microparticles. The next generation of this vaccine, including HPV16 and HPV18 E6 and E7-derived CTL epitopes, achieved regression of lesions in an even higher number of subjects, however the effect was not statistically significant (Garcia et al., 2004). An DNA vaccine targeting the HPV16 E7 oncoprotein, pNGVL4a-Sig/E7(detox)-HSP70, encodes a mutated form of HPV16 E7 with an abolished pRb binding site, denoted E7 (detox) in combination with a viral vector and has shown immune responses as well as clinical regression in CIN2/3 patients (Maldonado et al., 2014). More clinical trials taking advantage of the very same plasmid accompanied with other factors are ongoing for CIN1/3 and HNSCC (Bagarazzi et al., 2012) (NIH, NCT01493154 and NCT00988559).

Bacterial and viral vectors are also used as therapeutic strategies. A live-attenuated vaccine based on E7-secreting *Listeria monocytogenes* (Lovaxin-C, Lm-LLO-E7) was shown to reduce tumor load in some patients, however with severe adverse events in 40% of patients (Radulovic et al., 2009). Viral vectors show advantage as they can be attenuated easily and especially recombinant ones are fast to be developed and induce strong immune responses (Rollier et al., 2011). A disadvantage is, however, potential pre-existing immunity. This can be overcome by using viruses that infect other species. Preclinical studies have been conducted with recombinant adenoviral vectors, based on adenovirus type 5 and expressing HPV16 E6 and E7 (Lee et al., 2008). The first viral based HPV vaccine is called TA-HPV and based on recombinant vaccinia virus, encoding E6 and E7 fusion proteins of HPV16 and 18, where E7 is mutated (Borysiewicz et al., 1996). It has been used in various studies (Borysiewicz et al., 1996; Kaufmann et al., 2002; Baldwin et al., 2003) and was reported to lead to HPV16-specific immune responses and partial regression in some high-grade VIN patients (Davidson et al., 2003). TA-HPV was also applied in DNA prime/viral vector boost regimes as described above (Maldonado et al., 2014) and protein prime/viral vector boost regimes (Davidson et al., 2004; Smyth et al., 2004; Fiander et al., 2006), where vaccination with TA-CIN, a fusion protein of HPV16 E6, E7 and L2, and the TLR-agonist imiquimod resulted in complete histological regression of VIN2/3 in 63% of patients (Frazer et al., 2004).

Treatment with autologous DCs, was investigated with DCs being loaded with recombinant HPV16 E7 protein, and partial $CD4^+$ and $CD8^+$ T cell responses were seen in some patients with cervical cancer (Santin et al., 2006; Santin et al., 2008).

In comparison to whole protein formulations and other vaccination strategies, synthetic peptides show advantages concerning safety and production. The synthetic peptides can be subdivided into two categories, epitope-specific short peptides and synthetic long peptide (SLP) (Kanodia et al., 2008; Su et al., 2010). Short peptides only consist of a single CTL epitope, while SLPs combine CTL and $CD4^+$ T_H epitopes. Taking specific T cell epitopes as targets for a HPV peptide vaccine has the potential to precisely trigger epitope-specific T cell-mediated immune responses. However, to this end, short synthetic peptide needs to be administered in combination with adjuvants, which are described below.

Past preclinical studies have shown significant success for a peptide vaccination using 15-25aa long, overlapping E6/E7-derived peptides that cover the whole sequence of these two proteins(Melief and van der Burg, 2008). These peptides are processed by APCs for epitope presentation on HLA I and II molecules, and hence, prior HLA typing of patients is not required. Based on promising preclinical results, various clinical studies were initiated by Melief and colleagues which showed induction of HPV-specific $CD4^+$ and $CD8^+$ T cell responses (Bouvard et al., 2009). Moreover, complete regression was observed in 43% of VIN3 patients that received the HPV16 SLP vaccine (Kenter et al., 2009). A subsequent clinical trial with cervical cancer patients however did not succeed in tumor regression (van Poelgeest et al., 2013). In order to enhance the effect of the safe and highly immunogenic HPV16 SLP vaccines, different strategies are pursued, including combination with for instance chemotherapy to overcome local immunosuppression and other regulatory mechanisms (Van de Wall et al., 2014; van der Sluis et al., 2015).

In preclinical studies in mice, a mixture of HPV16 peptides E7/11-20, E7/82-90, E7/86-93 and E6/29-38 and a new adjuvant system (VacciMax® liposomes) has been reported to induce robust CTL responses and eradication of TC-1 tumors, which are HPV16 E6 and E7 positive. An E7-derived peptide with Hsp110 was also shown to evoke broad anti-TC-1 responses (Steller et al., 1998; Ressing et al., 2000). Various epitope-specific peptides, including E7/11-20, E7/12-20 and E7/86-93, were also tested in clinical trials either alone or together with different adjuvants. These studies ultimately reported partial responses in 50% of high-grade CIN and VIN patients (Muderspach et al., 2000). Promising clinical responses in CIN2/3 patients were achieved by vaccination with the HPV16 E7/86-93 peptide delivered by proteoliposomes (Solares et al., 2011). Ongoing phase I studies are combining HPV16 peptides with GM-CSF and Montanide ISA 51 (NIH, NCT00257738) or are taking advantage of novel adjuvants like Candin® (NIH, NCT01653249).

Linear short peptides representing precise epitopes with a length of 8-11aa have been shown to incduce strong cytotoxic responses, however, these peptides are HLA-restricted and necessitate HLA typing of patients. A therapeutic vaccine that is applicable to everyone without prior HLA typing needs to contain epitopes for all HLA-types. This issue is facilitated by the exploitation of HLA supertypes, that include groups of HLA molecules that share peptide-binding specificity (Sette and Sidney, 1999). Definition of epitopes for the five major HLA class I supertypes allows > 95%

population coverage (Sette and Sidney, 1999; Middleton et al., 2003; Lund et al., 2004). Nonetheless, slight variations even between closely related alleles might occur, leading to exclusion of some peptides or HLA types (Macdonald et al., 2003; Peters et al., 2006; Zhang et al., 2007).

These matters are addressed in this study by determining T cell epitopes for specific HLA molecules and supertypes. To this end, HPV16 E6 and E7 epitopes were assessed by a broad bioinformatics approach, which included the application of various T cell epitope prediction servers and algorithms which are described in detail in section 1.3.1. Actual HLA-peptide binding was verified *in vitro*.

In silico predictions and *in vitro* HLA-peptide binding assays can successfully narrow down the number of vaccine candidates but do not verify that those peptides are naturally processed and presented on infected kerationcytes of patients. Thus, direct identification of physically present epitopes needs to be conducted. Mass spectrometry (MS) techniques have been shown to be feasible to identify such epitopes on tumors (reviewed in Haen and Rammensee, 2013) and these techniques have been established and are refined in our laboratory. This approach was explored in studies by Riemer and colleagues (Riemer et al., 2010) for HLA-A*02:01-restricted peptides and led to the detection of HPV16 E7/11-19 as a naturally processed and presented peptide.

1.4 Objectives of this study

As outlined above, despite the introduction of prophylactic vaccines, HPV-mediated malignancies are still a major global health problem. Existing treatment options rely mainly on early detection and can have serious sequelae, such as premature births. Thus, a non-invasive treatment, harnessing the patient's own immune system, is an attractive option.

Moreover, HPV-mediated cancers represent an ideal scenario to develop a therapeutic cancer vaccine. Most people infected with HPV clear the infection, or even intraepithelial precursor lesions of cancer, proving that immune-mediated elimination of the virus is possible. HPV-mediated tumors also pose the opportunity to target immunologically foreign tumor-specific antigens. The viral oncoproteins E6 and E7 are expressed in all stages of HPV-mediated carcinogenesis and are essential for induction and maintenance of the malignant phenotype. Therefore, they are ideal targets for immunotherapeutic approaches.

For development of therapeutic vaccines, but also for other immunotherapies such as adoptive transfer of T cells with transgenic T cell receptors or chimeric antigen receptors (CARs), the precise identification of the viral epitopes that are naturally processed and presented on the target cell surface is crucial. Validated epitopes can also facilitate immunomonitoring, as only immune responses targeted against these epitopes need to be analyzed.

The aim of this study was, therefore, to identify and immunologically validate HPV16 E6 and E7-derived T cell epitopes. To date, HPV T cell epitopes have mostly been determined for the most prevalent HLA-type HLA-A2. The objective of this thesis was to describe epitopes for the highly prevalent HLA supertypes HLA-A3, HLA-A11 and HLA-A24.

To do so, the following experiments and analyses were performed:

1) Prospective T cell epitopes from the HPV16 E6 and E7 proteins for the above mentioned HLA supertypes were predicted *in silico*.
2) The actual peptide-HLA binding was tested in *in vitro* cellular binding assays.
3) Immunogenicity of identified peptides was assessed by screening memory responses and establishing T cell lines from healthy donors.
4) Functional assays, such as ELISpot and cytotoxicity assays, were conducted to determine the best vaccine candidates.

2. Material and Methods

2.1 Materials

2.1.1 Chemicals and biological reagents

Product	Company
1-Step™ NBT/BCIP	Thermo Scientific, Rockfort, IL, USA
2-Mercaptoethanol	Roth, Karlsruhe
51-Chromium radionuclide ($Na_2{}^{51}CrO_4$-solution (5 mCi, 185 MBq))	Perkin Elmer, Waltham, MA, USA
6x Orange DNA Loading Dye	Thermo Fisher Scientific Ldt., Loughborogh, UK
Acetic acid (100%)	Merck Millipore, Billerica, MA, USA
Agarose NEEO Ultra-Qualität Roti®garose	Roth, Karlsruhe
Albumin, from bovine serum albumin (BSA)	Sigma-Aldrich, Taufkirchen
Ammonium chloride (NH_4Cl)	Roth, Karlsruhe
Avidin-Horseradish Peroxidase	BioLegend, San Diego, CA, USA
Beta2-($ß_2$) microglobulin	MP Biomedicals, Illkirch, France BD Biosciences, Franklin Lakes, NJ, USA
Brilliant Blue G	Sigma-Aldrich, Taufkirchen
Calcium chloride ($CaCl_2$)	Sigma-Aldrich, Taufkirchen
CEF-Class I Peptide Pool “Classic”	Cellular Technology Limited, Shaker Heights, OH, USA
CHAPS	AppliChem, Darmstadt
Citric acid	AppliChem, Darmstadt
cOmplete Mini Protease Inhibitor Cocktail	Roche, Basel, Switzerland
Concanavalin A (ConA) from *C.ensiformis*	Sigma-Aldrich, Steinheim
Deoxynucleoside Triphosphate	Roche, Mannheim
Dimethyl sulfoxide (DMSO)	Sigma-Aldrich, Taufkirchen
Deoxynucleoside Triphosphate	Roche, Mannheim
Distilled water DNase/RNase free	Life Technologies, Brown Deer, WI, USA
Ethanol (absolute)	Sigma-Aldrich, Taufkirchen
Ethidium bromide	Roth, Karlsruhe
Ethylenediaminetetraacetic acid (EDTA)	Sigma-Aldrich, Taufkirchen
Gelatine	Roth, Karlsruhe
Glycine	Sigma-Aldrich, Taufkirchen
Hydrogen chloride (HCl)	VWR International, Fontenay-sous-Bois, France
Isopropanol	Sigma-Aldrich, Taufkirchen
Laemmli sample buffer (2x)	Biorad, Hercules, CA, USA
Magnesium chloride ($MgCl_2$)	Roche, Branchburg, NJ,

	USA
Methanol	Sigma-Aldrich, Taufkirchen
Milk powder	Roth, Karlsruhe
OneComp eBeads	eBioscience, San Diego, CA, USA
Oriole™ Fluorescent Gel Stain	Biorad, Hercules, CA, USA
Phenylmethanesulfonyl uoride (PMSF)	Roth, Karlsruhe
Phytohemagglutinin (PHA) from *Ph. vulgaris*	Sigma-Aldrich, Steinheim
Pierce ECL Western Blotting Substrate	Thermo Fisher Scientific, Waltham, MA, USA
Ponceau red solution	Serva, Heidelberg
Potassium bicarbonate ($KHCO_3$)	Roth, Karlsruhe
Potassium chloride (KCl)	Roth, Karlsruhe
Potassium dihydrogen phosphate (KH_2PO_4)	Roth, Karlsruhe
Protease inhibitor cocktail, cOmplete mini	Roche, Mannheim
Recombinant human IL-2 standard	BioLegend, San Diego, CA, USA
Sodium acetate ($C_2H_3NaO_2$)	Roth, Karlsruhe
Sodium azide (NaN_3)	AppliChem, Darmstadt
Sodium bicarbonate ($NaHCO_3$)	Sigma-Aldrich, Taufkirchen
Sodium chloride (NaCl)	Sigma-Aldrich, Taufkirchen
Sodium dihydrogen dibasic phosphate (NaH_2PO_4 2 H_2O)	Sigma-Aldrich, Taufkirchen
Sodium dodecyl sulfate (SDS) ultrapure	Roth, Karlsruhe
Sodium hydroxide (NaOH)	Sigma-Aldrich, Taufkirchen
Streptavidin-Alkaline Phosphatase	Mabtech, Nacka Strand, Sweden
TMB Substrate Set	BioLegend, San Diego, CA, USA
TMB Stop Solution	BioLegend, San Diego, CA, USA
Trizmabase	Sigma-Aldrich, Taufkirchen
Triton-x100	AppliChem, Darmstadt
Tween20 (=Polysorbat 20)	MP Biomedicals, Illkirch, France

2.1.2 Buffers and solutions

Name	**Ingredients**
10x PBS	1.37M NaCl 27mM KCl 100mM Na_2PO_4 (anhydrous) 20mM KH_2PO_4 pH 7.2 adjusted with NaOH or HCl
10x SDS-PAGE running buffer	30.3g Tris 144g Glycine 10g SDS ad. 1L ddH_2O
2x CHAPS buffer	1.2% (w/v) CHAPS dissolved in 1xPBS

2x CHAPS lysis buffer	5.25mL 2xCHAPS buffer 100mM PMSF 1 cOmplete Mini PIC tablet
50x TAE	484g Tris 41g $C_2H_3NaO_2$ 37g EDTA pH 7.8 adjusted with acetic acid ad. 2L ddH_2O
ACK lysis buffer	0.829g NH_4Cl 0.1g $KHCO_3$ 0.38mg EDTA pH 7.2-7.4 adjusted with NaOH or HCl ad. 100mL ddH_2O
Blocking buffer (WB)	1x PBS 5% (w/v)milk powder
Blocking buffer (FACS)	1x PBS 10% (v/v) FCS
Carbonate Coating buffer (ELISA)	8.4g $NaHCO_3$ 3.56g Na_2CO_3 pH 9.5 adjusted with NaOH or HCl ad. 1L ddH_2O
Coomassie Briliant Blue	25mL CH_3COOH 125mL MeOH 0.25g Brilliant blue G ad. 250ml ddH_2O
Coomassie destain	CH_3COOH:MeOH:ddH_2O (1:2:8)
dNTP mix	10mM each dATP, dCTP, dGTP, dTTP
Elution buffer	50% 0.263M (v/v)citric acid 50% 0.123M (v/v) Na_2HPO_4 pH 2.9 or 2.1: adjusted with HCl
FACS buffer	1x PBS 2% FCS 0.1% (v/v)NaN_3
MACS buffer	1x PBS 0.5% (v/v)FCS 2mM EDTA
PMSF stock	100mM PMSF dissolved in 100% ethanol
Transfer buffer	9g Tris 43.2g Glycine 20% (v/v) Methanol ad. 3L ddH_2O
Tween PBS (TPBS)	1xPBS 0.05% (v/v)Tween20 or 0.1% (v/v)Tween20

2.1.3 Consumables

Product	**Company**
Aluminium foil	CeDo GmbH, Mönchengladbach
Any kD™ Precast Gel	Biorad, Hercules, CA, USA
Blood collection tubes (NH, 170 I.U.)	BD, Plymouth, UK

Blood collection set (Safty-lok™)	BD, Franklin Lakes, NJ, USA
Cell culture dish (100mm x 20mm)	TPP, Trasadingen, Switzerland
Cell culture flask (25cm^2)	TPP, Trasadingen, Switzerland
Cell culture flask (75cm^2)	TPP, Trasadingen, Switzerland
Cell culture plate "CytoOne" (6-well)	Starlab, Hamburg
Cell culture plate (12-well)	Corning, Corning, NY, USA
Cell culture plate (24-well)	Corning, Corning, NY, USA
Cell culture plate (96-well) - U bottom (Microtest) - V bottom - Flat bottom, black (OptiPlate™)	 BD, Franklin Lakes, NJ, USA Greiner Bio-One, Frieckenhausen Perkin Elmer, Maltham, MA, USA
Cell scraper	Sarstedt, Newton, NC, USA
Cell strainer (40µM, 70µM)	BD, Corning, NY, USA
Cling film	CeDo GmbH, Mönchengladbach
Costar™, high binding plates	Thermo Fisher Scientific, Rochester, NY, USA
Cryogenic vials (Nalgene)	Thermo Fisher Scientific, Rochester, NY, USA
FACS tubes (5mL Polystrene round-bottom tube)	BD, Franklin Lakes, NJ, USA
Falcon tube (15mL and 50mL)	Nerbe Plus, Winsen
Leucosep™	Greiner Bio-One, Frieckenhausen
Filter (Millex®-GS, pore size 0.22µm)	Merck Milipore, Cork, Ireland
GammaBind™ Plus Sepharose™ beads	GE Healthcare, München
Gloves	Microflex, Reno, NV, USA
Kimwipes lite 200	Kimberly-Clark, Irving, TX, USA
Luma plate ™-96	Perkin Elmer, Waltham, MA, USA
MACS Seperation Column LS	Miltenyi Biotec, Bergisch Gladbach
MultiScreen®-HA, 96-well filtration plate	Merck Milipore, Cork, Ireland
Mini-PROTEAN®TGX™ gels, Any kD™, various combs	Biorad, Hercules, CA, USA
Parafilm	Bemis, Neeah, WI, USA
PVDF Transfer Membrane	Thermo Scientific, Rockford, IL, USA
Pipette tips, with and without filter	Starlab, Hamburg
Reaction tubes (0.2mL, 0.5mL, 1.5mL and 2mL)	Starlab, Hamburg
Scalpel	Feather, Osaka, Japan
Serological pipette (2mL)	BD, Franklin Lakes, NJ, USA
Syringe (20mL BD Plastipak Luer-Lok™)	BD, Drogheda, Ireland
Syringe (2mL Injekt®)	Braun, Melsungen
Vacuum filter (bottle top, pore size 0.22µM)	Corning, Corning, NY, USA
Western Blotting Filter Paper	Thermo Scientific, Rockford, IL, USA

2.1.4 Kits

Name	Company
$CD8^+$ T Cell Isolation Kit, human	Miltenyi Biotec, Bergisch Gladbach
$CD14^+$mircobeads, human	Miltenyi Biotec, Bergisch Gladbach
QIAamp DNA Mini Kit	Qiagen, Hilden

2.1.5 Markers and ladders

Name	Company
GeneRuler™ Ladder Mix, 100 bp -10000 bp	Thermo Fisher Scientific Ldt., Loughborogh, UK
Precision Plus Protein™ Standards Kaleidoscope ™, 10-250kDa	Biorad, Hercules, CA, USA
Precision Plus Protein™ Unstained Standards, 10-250kDa	Biorad, Hercules, CA, USA

2.1.6 Enzymes

Enzyme	Company
AmpliTaq Gold®DNA Polymerase	Roche, Branchburg, NJ, USA
REDTaq® ReadyMix™ PCR Reaction Mix	Sigma-Aldrich, Steinheim

2.1.7 Equipment

Equipment	Name	Company
Analytical balance		Ohaus, Nänikon, Switzerland
Cell counter	Countess® Automated Cell Counter	Invitrogen, Carlsbad, CA, USA
Cell freezing device	Mr. Frosty	Bel-Art Products, Wayne, NJ, USA
Centrifuge	Biofuge Pico, Fresco Centrifuge 5417R, 5418 Multifuge® 16R	Heraeus, Hanau Eppendorf, Hamburg Heraeus, Hanau
Centrifuge rotor	TX-400 M-20	Heraeus, Hanau Heraeus, Hanau
Chemiluminescence camera	Fusion-SL chemiluminescence-camera	Vilber Lourmat, Eberhardzell
Documentation agarose gels	Gel Jet Imager 2006 Printer P39D	Intas, Göttingen Mitsubishi, Electric, Tokio
Documentation gels	Gel Doc ™ EZ Imager	Biorad, Hercules, CA, USA
Electrophoresis chamber for agarose gels	Owl Easycast B2	Owl Seperation Systems, Portsmouth, NH, USA
Electrophoresis chamber for SDS-PAGE	Mini-PROTEAN® Tetra Cell	Biorad, Hercules, CA, USA
ELISpot plate reader	AID ELISpot reader	Autoimmun Diagnostika, Strassberg
Flow cytometer	FACS Canto II™	BD Biosciences, Franklin Lakes, NJ, USA
Freezer (-20° C)	Medline	Liebherr, Biberach an der Riss

		Bosch, Stuttgart
Freezer (-80° C)	U725 Innova	New Brunswick, Nürtingen
Glasware	Duran Fisherbrand	Schott, Mainz Thermo Fisher Scientific, Waltham, MA, USA
Ice machine	Hoshizaki Cube Star	Hoshizaki, Tokio, Japan
Incubator	Heracell 150i C200	Thermo Fisher Scientific, Waltham, MA, USA Labotec Göttingen,
Irradiator	Gammacell 1000	Atomic Energy of Canada Limited, Ottawa, Canada
Laminar flow hood	SterilGard® Class II laminar flow hood	The Baker Company, Sanford, USA
Light microscope	Wilovert Standard 30 microscope	Hund Wetzlar, Wetzlar
Liquid nitrogen tank	Locator 8 plus	Barnstead/Thermolyne, Dubuque, IA, USA
Luma plate reader	TopCount NXT™	Perkin Elmer, Waltham, MA, USA
Magnet for MACS	Quadro MACS	Miltenyi Biotec, Bergisch Gladbach
Magnetic stirrer	Combimag RCO MR-Hei-Standard	IKA-Werke GmbH, Staufen Heidolph Instruments, Schwabach
Microwave		Sharp, Osaka, Japan
Multilable plate reader	Victor^3	Perkin Elmer, Waltham, MA, USA
Nano Drop	ND-1000	peqLab Biotechnologies, Erlangen
Neubauer cell counting chamber	Profondeur	Brand, Wertheim
PCR cycler	C1000 Touch™ Thermal Cycler	Biorad, Hercules, CA, USA
pH Meter	766	Knick, Berlin
Pipette-Boy	pipetus®-akku	Hirschmann Labortechnik, Eberstadt
Pipettes	Pipetman® Gilson P2, P20, P200, P1000 FinnPipette F2	Gilson, Bad Camberg Thermo Scientific, Rockford, IL, USA
Pipettes glass		Hirschmann Labortechnik, Eberstadt
Power supply	EPS500-400, EPS3500 MP 250V	Pharmacia, Uppsala, Sweden MS Major Science, Saratoga, CA, USA
Pump	N86KT.18	KNF Neuberger, Freiburg
Refrigerator (4°C)	Medline	Liebherr, Biberach an der Riss Bosch, Stuttgart
Rolling shaker	CATMR5	Zipperer, Staufen
Rotator		NeoLab, Heidelberg
Scale	Kern EG 4200-2NM	Kern & Sohn, Balingen
Surgical tweezer and scissors		Dimeda, Tuttlingen
Thermomixer	Thermomixer compact	Eppendorf, Hamburg

Vortexer	Vortex-Genie 2	Scientific Industries, Bohemia, NY, USA
Water bath		GFL, Burgwedel
WB transfer chamber	Mini Trans-Blot® Cell	Biorad, Hercules, CA, USA

2.1.8 Eukaryotic cell lines

Name	Description	HPV-status	Source	Culture medium	Reference
866	human, cervical, adherent	HPV16 positive	Kindly provided by Peter L Stern, University of Manchester, Manchester, UK	F-medium	(Brady et al., 2000)
879	human, cervical, adherent	HPV16 positive	Kindly provided by Peter L Stern, University of Manchester, Manchester, UK	F-medium	(Brady et al., 2000)
915	human, cervical, adherent	HPV16 positive	Kindly provided by Peter L Stern, University of Manchester, Manchester, UK	F-medium	(Brady et al., 2000)
93VU147T	human, HNSCC, adherent	HPV16 positive	Kindly provided by Renske Steenbergen, University Medical Center Amsterdam, Netherlands	complete DMEM	(Steenbergen et al., 1995)
C66#3	human, cervical, HPV-transfected, adherent	HPV16 positive	Kindly provided by John H Lee, Sanford Health Center, Sioux Falls, SD, USA	E-medium	(Lee et al., 2004)
C66#7	human, cervical, HPV-transfected, adherent	HPV16 positive	Kindly provided by John H Lee, Sanford Health Center, Sioux Falls, SD, USA	E-medium	(Lee et al., 2004)
CaSki	human, cervical, adherent	HPV16 positive	Kindly provided by Felix Hoppe-Seyler, F065, DKFZ	complete DMEM	(Pattillo et al., 1977)
FK16A	human, foreskin keratinocytes, adherent	HPV16 positive	Kindly provided by Renske Steenbergen, University Medical Center Amsterdam, Netherlands	complete K-SFM	(de Wilde et al., 2008)
Goercke	human, cervical, adherent	HPV16 positive	Kindly provided by Andreas Kaufmann,	M10 medium	

			Charité, Berlin		
HPK 1A	human, foreskin keratinocytes, adherent	HPV16 positive	Kindly provided by Elisabeth Schwarz, F030, DKFZ	complete DMEM	(Henderson et al., 1991)
Marqu	human, cervical, adherent	HPV16 positive	Kindly provided by Andreas Kaufmann, Charité, Berlin	DMEM + 15% (v/v) FCS + 1% (v/v) HEPES	
MRI-H-196	human, cervical, adherent	HPV16 positive	Kindly provided by Elisabeth Schwarz, F030, DKFZ	complete DMEM	(Schmitt and Pawlita, 2011)
SCC090	human, HNSCC, adherent	HPV16 positive	Kindly provided by Susanne Gollins, University of Pittsburgh, Pittsburgh, PA, USA	M10 medium	(Ragin et al., 2004)
SCC152	human, HNSCC, metastasis of SCC90, adherent	HPV16 positive	Kindly provided by Susanne Gollins, University of Pittsburgh, Pittsburgh, PA, USA	M10 medium	(Ragin et al., 2004)
SCC154	human, HNSCC,	HPV16 positive	Kindly provided by Susanne Gollins, University of Pittsburgh, Pittsburgh , PA, USA	M10 medium	(White et al., 2007)
SiHa	human, cervical, adherent	HPV16 positive	Kindly provided by Felix Hoppe-Seyler, F065, DKFZ	complete DMEM	(Friedl et al., 1970)
SNU 1000	human, cervical, adherent	HPV16 positive	Korean Cell Line Bank, Seoul, South Korea	complete RPMI-H	(Ku et al., 1997)
SNU 1005	human, cervical, adherent	HPV16 positive	Korean Cell Line Bank, Seoul, South Korea	complete RPMI-H	(Ku et al., 1997)
SNU 1299	human, cervical, adherent	HPV16 positive	Korean Cell Line Bank, Seoul, South Korea	complete RPMI-H	(Ku et al., 1997)
SNU 17	human, cervical, adherent	HPV16 positive	Korean Cell Line Bank, Seoul, South Korea	complete RPMI-H	(Ku et al., 1997)
SNU 703	human, cervical, adherent	HPV16 positive	Korean Cell Line Bank,	complete RPMI-H	(Ku et al., 1997)

			Seoul, South Korea		
UD-SCC2	human, HNSCC, adherent	HPV16 positive	Kindly provided by Thomas Hoffmann, Uniklinikum Essen, Essen	complete RPMI-P + 1% (v/v) P/S	(Hoffmann et al., 2008)
UM-SCC-47	human, HNSCC, adherent	HPV16 positive	Kindly provided by Tom Carey, University of Michigan, Ann Arbor, MI, USA	complete DMEM	(Virolainen et al., 1984)
W12 20861	human, cervical, adherent	HPV16 positive	Kindly provided by Paul Lambert, University of Wisconsin, Madison, WI, USA	F-medium	(Jeon et al., 1995)
W12 20863	human, cervical, adherent	HPV16 positive	Kindly provided by Paul Lambert, University of Wisconsin, Madison, WI, USA	F-medium	(Jeon et al., 1995)
BSM	human, B-LCL, suspension	negative	IHWG Cell Bank, Seattle, WA, USA	complete RPMI-P	
EA	human, B-LCL, suspension	negative	IHWG Cell Bank, Seattle, WA, USA	complete RPMI-P	
FH8	human, B-LCL, suspension	negative	IHWG Cell Bank, Seattle, WA, USA	complete RPMI-P	
LKT3	human, B-LCL, suspension	negative	IHWG Cell Bank, Seattle, WA, USA	complete RPMI-P	
RiSH	human, B-LCL, EBV-immortalized, suspension	negative	generated in this studyfrom a healthy blood donor	RPMI + 10-20% (v/v) FCS	
WT100BIS	human, B-LCL, suspension	negative	IHWG Cell Bank, Seattle, WA, USA	complete RPMI-P	
3T3	mouse, fibroblasts, adherent	negative	Kindly provided by Paul Lambert, University of Wisconsin, Madison, WI, USA	complete DMEM	(Jainchill et al., 1969)
tCD40L NIH3T3	mouse, fibroblasts, transduced with human tCD40L	negative	Kindly provided by Derin Keskin, Harvard	tCD40L NIH 3T3 tCD40L WT	(Schultze et al., 1995)

	Medical School, Boston, MA, USA

2.1.9 Cell culture basal media and supplements

Product	Company
Dulbecco's Modified Eagle Medium (DMEM)	Sigma-Aldrich, Taufkirchen
Eagle's minimum essential medium (EMEM)	Sigma-Aldrich, Taufkirchen
Iscove's Modified Dulbecco's Medium (IMDM)	Life Technologies, Brown Deer, WI, USA
Ham's F12 Nutrient Mix	Invitrogen, Carlsbad, CA, USA
Keratinocyte serum-free medium (KSFM)	Invitrogen, Carlsbad, CA, USA
Minimum Essential Medium (MEM)	SAFC Biosciences, Nantes, France
RPMI 1640 (1x) with L-Glutamine	Sigma-Aldrich, Taufkirchen
2-mercaptoethanol	Life Technologies, Grand Island, NY, USA
Adenine	PAA Laboratories, Cölbe
Bovine pituitary extract (BPE)	Invitrogen, Carlsbad, CA, USA
Calcium chloride ($CaCl_2$)	Sigma-Aldrich, Steinheim
Cholera toxin	Sigma-Aldrich, Taufkirchen
Cyclosporin A	Sigma, St. Louis, MO, USA
Dimethylsulfoxide (DMSO)	Sigma-Aldrich, Steinheim
Epidermal growth factor (EGF)	Invitrogen, Carlsbad, CA, USA
Fetal Calf Serum (FCS)	Biowest, Nuaillé, France Sigma-Aldrich, Taufkirchen
Ficoll-Paque™ PLUS	GE Healthcare Bio-Sciences, Uppsala, Sweden
G-418 Sulfate	Cayman Chemical, Ann Arbor, MI, USA
Gentamycin	BioConcept, Allschwil, Switzerland
GM-CSF, recombinant human	R & D Systems, Minneapolis, MN, USA
Human serum, type AB	Life Technologies, Brown Deer, WI, USA
HEPES	Life Technologies, Grand Island, NY, USA
Hydrocortizone	Sigma-Aldrich, Taufkirchen
IL-1β, recombinant human	R & D Systems, Minneapolis, MN, USA
IL-2, recombinant human	PeproTech, Rocky Hill, NJ, USA
IL-4, recombinant human	R & D Systems, Minneapolis, MN, USA

IL-6, recombinant human	R & D Systems, Minneapolis, MN, USA
IL-7, recombinant human	R & D Systems, Minneapolis, MN, USA
Insulin, recombinant human	Sigma-Aldrich, Taufkirchen
Ionomycin	Sigma-Aldrich, Taufkirchen
L-Glutamine	Sigma-Aldrich, Taufkirchen
Lipopolysaccharide (LPS)	Invivogen, Toulouse, France
MEM Non-essential amino acid solution (MEM NEAA)	Invitrogen, Carlsbad, CA, USA
Paraformaldehyde (PFA)	Sigma-Aldrich, Taufkirchen
Penicillin/Streptomycin-Solution (P/S)	Sigma-Aldrich, Taufkirchen
Prostaglandin E_2 (PGE_2)	Cayman Chemical, Ann Arbor, MI, USA
Phorbol 12-myristate 13-acetate (PMA)	Sigma-Aldrich, Taufkirchen
Sodium bicarbonate ($NaHCO_3$)	Sigma-Aldrich, Taufkirchen
Sodium pyruvate ($C_3H_3NaO_3$)	PAA Laboratories, Cölbe
TNFα, recombinant human	R & D Systems, Minneapolis, MN, USA
Transferrin, recombinant human	Sigma-Aldrich, Taufkirchen
Tri-iodo-thyronine	Sigma-Aldrich, Taufkirchen
Trypsin-EDTA Solution	Sigma-Aldrich, Taufkirchen
Trypan Blue	Sigma-Aldrich, Taufkirchen

2.1.10 Cell culture media

All media were sterile filtered and stored at 4°C.

Name	**Ingredients**
B cell medium	IMDM 10% (v/v) human serum, AB, 2mM L-Glutamine, 50µg/mL human transferrin, 5µg/ mL human insulin, 15µg/mL Gentamycin
B-LCL medium	RPMI-1640 10%-20% (v/v) FCS
complete DMEM	DMEM 1% (v/v) P/S, 10% (v/v) FCS, 2mM L-Glutamine
complete K-SFM	K-SFM 1% (v/v) P/S, 10% (v/v) FCS, 5ng/mL EGF, 50µg/mL BPE
complete RPMI-P	RPMI-1640 15% (v/v) FCS, 1% 100mM sodium pyruvate
complete RPMI-H	RPMI-1640 1% (v/v) P/S, 10% (v/v) FCS, 25mM HEPES, 25mM $NaHCO_3$

DC medium	DMEM 1% (v/v) P/S, 10% (v/v) human serum, AB, 2mM L-Glutamine, 10mM HEPES
E-medium	DMEM 22.5% (v/v) Ham's F12. 10% (v/v) FCS. 1% (v/v) P/S, 0.5µg/mL hydrocortisone, 8.4ng/mL cholera toxin, 5µg/mL transferrin, 5µg/µL insulin, 1.36ng/mL tri-iodo-L-thyronine, 5µg/mL EGF
F-medium	Ham's F12 25% (v/v) DMEM, 5% (v/v) FCS, 1 % (v/v) P/S, 0.4mg/mL hydrocortisone, 0.5µg/mL cholera toxin, 5µg/mL insulin, 24.2µg/mL adenine, 0.1µg/mL EGF
M10 medium	EMEM 10 % (v/v) FCS, 1% (v/v) P/S, 2mM L-Glutamine, 1% (v/v) MEM NEAA
T cell medium	DMEM 1% (v/v) P/S. 10% (v/v) human serum, AB, 2mM L-Glutamine, 10mM HEPES, 0.1mM 2-mercaptoethanol
tCD40L NIH3T3 medium	Ham's F12/DMEM 10% (v/v) FCS, 2mM L-Glutamine, 10mM HEPES, 15µg/mL Gentamycin, 500µg/mL G418
tCD40L WT medium	Ham's F12/DMEM 10% (v/v) FCS, 2 mM L-Glutamine, 10mM HEPES, 15µg/mL Gentamycin
R10	RPMI-1640 1% (v/v) P/S, 10% (v/v) FCS, 2mM L-Glutamine, 10mM HEPES

2.1.11 Antibodies

2.1.11.1 Primary antibodies

Name	Clone	Description	Dilution	Company
anti-human CD4-PE	RPA-T4	Monoclonal, mouse IgG, PE-conjugated	FACS 1:20	BD Biosciences, San Diego, CA, USA
anti-human CD8-FITC	RPA-T8	Monoclonal, mouse IgG,FITC-conjugated	FACS 1:20	BD Biosciences, San Diego, CA, USA
anti-human CD14-FITC	M5E2	Monoclonal, mouse IgG,FITC-conjugated	FACS 1:20	BD Biosciences, San Diego, CA, USA
anti-human CD19-PE	LT19	Monoclonal, mouse IgG, PE-conjugated	FACS 1:20	Immunotools, Friesoythe Kindly provided by Alexandra Kurz, D030, DKFZ
anti-human CD19-Pacific blue	HIB19	Monoclonal, mouse IgG, Pacific blue-conjugated	FACS: 1:20	BioLegend, San Diego, CA, USA
anti-human CD80-PE	L307.4	Monoclonal, mouse IgG, PE-conjugated	FACS 1:20	BD Biosciences, San Diego, CA, USA

anti-human CD83-PE-Cy™7	HB15e	Monoclonal, mouse IgG, PE-Cy™7conjugated	FACS 1:20	BD Biosciences, San Diego, CA, USA
anti-human CD86-APC	2331	Monoclonal, mouse IgG, APC-conjugated	FACS 1:20	BD Biosciences, San Diego, CA, USA
anti-human HLA-DR-PerCP-Cy™5.5	G46-6	Monoclonal, mouse IgG, PerCP-Cy™5.5-conjugated	FACS 1:20	BD Biosciences, San Diego, CA, USA
anti-human HLA-A2	BB7.2	monoclonal, mouse IgG	WB 1:1000 FACS 1:100	BD Biosciences, San Diego, CA, USA
anti-human HLA-A2 FITC	BB7.2	monoclonal, mouse IgG, FITC-conjugated	FACS 1:20	BD Biosciences, San Diego, CA, USA
anti-human HLA-A3	GAP A3	monoclonal, mouse IgG	WB 1:1000 FACS 1:688	Kindly provided by Stefan Stevanović, University of Tübingen
anti-human HLA-A11	4i93	monoclonal, mouse IgG	WB 1:1000 FACS 1:100	Abcam, Cambridge, UK
anti-human HLA-A24	22E10	monoclonal, mouse IgG	WB 1:1000 FACS 1:200	MBL, Nagano, Japan
anti-human HLA-B7	BB7.1	monoclonal, mouse IgG	WB 1:1000 FACS 1:268	Abcam, Cambridge, UK
anti-human HLA-B13, B62, B15	4i109	monoclonal, mouse IgG	WB 1:1000 FACS 1:200	Abcam, Cambridge, UK
anti-human IFN-γ	1-D1K	monoclonal, mouse IgG, capture antibody	ELISpot 1:500	Mabtech, Nacka Strand, Sweden
anti-human IFN-γ biotin	7-B6-1	monoclonal, mouse IgG, biotinylated	ELISpot 1:2000	Mabtech, Nacka Strand, Sweden
anti-human IL-2	MQ1-17H12	monoclonal, rat IgG, LEAF™ purified, capture antibody	ELISA 4µg/mL	BioLegend, San Diego, CA, USA
anti-human IL-2 biotin	Poly5176	polyclonal, goat IgG, biotinylated	ELISA 1:2000	BioLegend, San Diego, CA, USA
anti-human MHC class I	EPR1394Y	monoclonal, rabbit IgG	WB 1:1500	Epitomics, Burlingame, CA, USA

2.1.11.2 Secondary antibodies

Name	Dilution	Company
goat-anti-rabbit IgG (H&L) Ab Peroxidase	WB 1:5000	Rockland, Gilbertsville, PA, USA
rabbit-anti-mouse IgG FITC	FACS 1:1500	DAKO, Glostrup, Denmark

2.1.12 Peptides

Peptides were synthesized with a purity of >95% and purchased from PSL GmbH (Heidelberg), SynBioSci (San Francisco, CA, USA) and the DKFZ Peptide Core Facility (Dr. Rüdiger Pipkorn, Dr. Stefan Eichmüller). Lyophilized peptides were dissolved in DMSO at 10mg/mL and stocked in small aliquots at -80°C.

2.1.12.1 Control peptides

HLA alleles for (potential) binding are indicated. FL: fluorescein

Name	Source	Region	aa sequence	HLA allele	Reference
HLA-A3 fl	consensus sequence		KVFPC(fl)ALINK	HLA-A3	(Sette et al., 1994)
HLA-A11 fl	consensus sequence		KVFPC(fl)ALINK	HLA-A11	(Sette et al., 1994)
HLA-A24 fl	HIV-1 Env gp41	583-591	RYLKC(fl)QQLL	HLA-A24	(Dai et al., 1992)
HLA-A2 control	HIV-1 Nef	137-145	LTFGWCFKL	HLA-A2	(Vaslin et al., 1994)
HLA-A3 control	consensus sequence		KVFPYALINK	HLA-A3	(Sette et al., 1994)
HLA-A11 control	HIV-1 Nef	73-82	QVPLRPMTYK	HLA-A11	(Koenig et al., 1990)
HLA-A24 control	HIV-1 Env gp41	583-591	RYLKDQQLL	HLA-A24	(Dai et al., 1992)
HLA-A24 EBV control	EBV BRLF1	28-37	DYCNVLNKEF	HLA-A24	(Pepperl et al., 1998)

2.1.12.2 HPV16 E6 and E7 peptides

Name	Origin	Region	aa sequence	HLA allele
HPV16 E6/18-26	HPV16 E6	18-26	KLPQLCTEL	HLA-A2
HPV16 E6/18-28	HPV16 E6	18-28	KLPQLCTELQT	HLA-A2
HPV16 E6/25-33	HPV16 E6	25-33	ELQTTIHDI	HLA-A2
HPV16 E6/28-38	HPV16 E6	28-38	TTIHDIILECV	HLA-A2
HPV16 E6/29-38	HPV16 E6	29-38	TIHDIILECV	HLA-A2
HPV16 E6/34-44	HPV16 E6	34-44	ILECVYCKQQL	HLA-A2
HPV16 E6/52-60	HPV16 E6	52-60	FAFRDLCIV	HLA-A2
HPV16 E7/7-15	HPV16 E7	7-15	TLHEYMLDL	HLA-A2
HPV16 E7/11-20	HPV16 E7	11-20	YMLDLQPETT	HLA-A2
HPV16 E7/11-19	HPV16 E7	11-19	YMLDLQPET	HLA-A2
HPV16 E7/11-21	HPV16 E7	11-21	YMLDLQPETTD	HLA-A2
HPV16 E7/11-18	HPV16 E7	11-18	YMLDLQPE	HLA-A2
HPV16 E7/12-20	HPV16 E7	12-20	MLDLQPETT	HLA-A2
HPV16 E7/12-19	HPV16 E7	12-19	MLDLQPET	HLA-A2
HPV16 E7/66-74	HPV16 E7	66-74	RLCVQSTHV	HLA-A2
HPV16 E7/76-86	HPV16 E7	76-86	IRTLEDLLMGT	HLA-A2
HPV16 E7/77-87	HPV16 E7	77-87	RTLEDLLMGTL	HLA-A2
HPV16 E7/77-86	HPV16 E7	77-86	RTLEDLLMGT	HLA-A2
HPV16 E7/78-86	HPV16 E7	78-86	TLEDLLMGT	HLA-A2
HPV16 E7/80-90	HPV16 E7	80-90	EDLLMGTLGIV	HLA-A2
HPV16 E7/81-90	HPV16 E7	81-90	DLLMGTLGIV	HLA-A2

HPV16 E7/81-91	HPV16 E7	81-91	DLLMGTLGIVC	HLA-A2
HPV16 E7/82-91	HPV16 E7	82-91	LLMGTLGIVC	HLA-A2
HPV16 E7/82-90	HPV16 E7	82-90	LLMGTLGIV	HLA-A2
HPV16 E7/82-92	HPV16 E7	82-92	LLMGTLGIVCP	HLA-A2
HPV16 E7/83-93	HPV16 E7	83-93	LMGTLGIVCPI	HLA-A2
HPV16 E7/84-93	HPV16 E7	84-93	MGTLGIVCPI	HLA-A2
HPV16 E7/85-93	HPV16 E7	85-93	GTLGIVCPI	HLA-A2
HPV16 E7/86-93	HPV16 E7	86-93	TLGIVCPI	HLA-A2
HPV16 E6/8-18	HPV16 E6	8-18	MFQDPQERPRK	HLA-A3
HPV16 E6/29-39	HPV16 E6	29-39	TIHDIILECVY	HLA-A3
HPV16 E6/32-41	HPV16 E6	32-41	DIILECVYCK	HLA-A3
HPV16 E6/33-41	HPV16 E6	33-41	IILECVYCK	HLA-A3
HPV16 E6/34-41	HPV16 E6	34-41	ILECVYCK	HLA-A3
HPV16 E6/37-46	HPV16 E6	37-46	CVYCKQQLLR	HLA-A3
HPV16 E6/37-47	HPV16 E6	37-47	CVYCKQQLLRR	HLA-A3
HPV16 E6/38-46	HPV16 E6	38-46	VYCKQQLLR	HLA-A3
HPV16 E6/43-50	HPV16 E6	43-50	QLRREVY	HLA-A3
HPV16 E6/43-52	HPV16 E6	43-52	QLLRREVYDF	HLA-A3
HPV16 E6/44-52	HPV16 E6	44-52	LLRREVYDF	HLA-A3
HPV16 E6/48-55	HPV16 E6	48-55	EVYDFAFR	HLA-A3
HPV16 E6/52-61	HPV16 E6	52-61	FAFRDLCIVY	HLA-A3
HPV16 E6/52-62	HPV16 E6	52-62	FAFRDLCIVYR	HLA-A3
HPV16 E6/53-62	HPV16 E6	53-62	AFRDLCIVYR	HLA-A3
HPV16 E6/58-67	HPV16 E6	58-67	CIVYRDGNPY	HLA-A3
HPV16 E6/59-67	HPV16 E6	59-67	IVYRDGNPY	HLA-A3
HPV16 E6/67-75	HPV16 E6	67-75	YAVCDKCLK	HLA-A3
HPV16 E6/68-75	HPV16 E6	68-75	AVCDKCLK	HLA-A3
HPV16 E6/68-76	HPV16 E6	68-76	AVCDKCLKF	HLA-A3
HPV16 E6/68-77	HPV16 E6	68-77	AVCDKCLKFY	HLA-A3
HPV16 E6/70-79	HPV16 E6	70-79	CDKCLKFYSK	HLA-A3
HPV16 E6/72-79	HPV16 E6	72-79	KCLKFYSK	HLA-A3
HPV16 E6/73-83	HPV16 E6	73-83	CLKFYSKISEY	HLA-A3
HPV16 E6/74-83	HPV16 E6	74-83	LKFYSKISEY	HLA-A3
HPV16 E6/75-83	HPV16 E6	75-83	KFYSKISEY	HLA-A3
HPV16 E6/75-84	HPV16 E6	75-84	KFYSKISEYR	HLA-A3
HPV16 E6/75-85	HPV16 E6	75-85	KFYSKISEYRH	HLA-A3
HPV16 E6/79-86	HPV16 E6	79-86	KISEYRHY	HLA-A3
HPV16 E6/79-88	HPV16 E6	79-88	KISEYRHYCY	HLA-A3
HPV16 E6/81-91	HPV16 E6	81-91	SEYRHYCYSLY	HLA-A3
HPV16 E6/84-91	HPV16 E6	84-91	RHYCYSLY	HLA-A3
HPV16 E6/89-97	HPV16 E6	89-97	SLYGTTLEQ	HLA-A3
HPV16 E6/89-98	HPV16 E6	89-98	SLYGTTLEQQ	HLA-A3
HPV16 E6/89-99	HPV16 E6	89-99	SLYGTTLEQQY	HLA-A3
HPV16 E6/92-101	HPV16 E6	92-101	GTTLEQQYNK	HLA-A3
HPV16 E6/93-101	HPV16 E6	93-101	TTLEQQYNK	HLA-A3
HPV16 E6/94-101	HPV16 E6	94-101	TLEQQYNK	HLA-A3
HPV16 E6/105-115	HPV16 E6	105-115	DLLIRCINCQK	HLA-A3
HPV16 E6/106-115	HPV16 E6	106-115	LLIRCINCQK	HLA-A3
HPV16 E6/107-115	HPV16 E6	107-115	LIRCINCQK	HLA-A3
HPV16 E6/113-122	HPV16 E6	113-122	CQKPLCPEEK	HLA-A3
HPV16 E6/116-124	HPV16 E6	116-124	PLCPEEKQR	HLA-A3
HPV16 E6/122-129	HPV16 E6	122-129	KQRHLDKK	HLA-A3
HPV16 E6/125-133	HPV16 E6	125-133	HLDKKQRFH	HLA-A3
HPV16 E6/129-136	HPV16 E6	129-136	KQRFHNIR	HLA-A3
HPV16 E6/129-138	HPV16 E6	129-138	KQRFHNIRGR	HLA-A3
HPV16 E6/134-142	HPV16 E6	134-142	NIRGRWTGR	HLA-A3

HPV16 E6/139-148	HPV16 E6	139-148	WTGRCMSCCR	HLA-A3
HPV16 E6/142-151	HPV16 E6	142-151	RCMSCCRSSR	HLA-A3
HPV16 E6/143-151	HPV16 E6	143-151	CMSCCRSSR	HLA-A3
HPV16 E6/143-153	HPV16 E6	143-153	CMSCCRSSRTR	HLA-A3
HPV16 E6/144-151	HPV16 E6	144-151	MSCCRSSR	HLA-A3
HPV16 E6/144-152	HPV16 E6	144-152	MSCCRSSRT	HLA-A3
HPV16 E6/144-153	HPV16 E6	144-153	MSCCRSSRTR	HLA-A3
HPV16 E6/144-154	HPV16 E6	144-154	MSCCRSSRTRR	HLA-A3
HPV16 E7/7-15	HPV16 E7	7-15	TLHEYMLDL	HLA-A3
HPV16 E7/49-57	HPV16 E7	49-57	RAHYNIVTF	HLA-A3
HPV16 E7/50-60	HPV16 E7	50-60	AHYNIVTFCCK	HLA-A3
HPV16 E7/51-60	HPV16 E7	51-60	HYNIVTFCCK	HLA-A3
HPV16 E7/52-60	HPV16 E7	53-60	YNIVTFCCK	HLA-A3
HPV16 E7/53-60	HPV16 E7	53-60	NIVTFCCK	HLA-A3
HPV16 E7/63-73	HPV16 E7	63-73	STLRLCVQSTH	HLA-A3
HPV16 E7/65-74	HPV16 E7	65-74	LRLCVQSTHV	HLA-A3
HPV16 E7/66-73	HPV16 E7	66-73	RLCVQSTH	HLA-A3
HPV16 E7/66-74	HPV16 E7	66-74	RLCVQSTHV	HLA-A3
HPV16 E7/82-91	HPV16 E7	82-91	LLMGTLGIVC	HLA-A3
HPV16 E7/87-97	HPV16 E7	87-97	LGIVCPICSQK	HLA-A3
HPV16 E7/88-97	HPV16 E7	88-97	GIVCPICSQK	HLA-A3
HPV16 E7/89-97	HPV16 E7	89-97	IVCPICSQK	HLA-A3
HPV16 E6/8-18	HPV16 E6	8-18	MFQDPQERPRK	HLA-A11
HPV16 E6/9-18	HPV16 E6	9-18	FQDPQERPRK	HLA-A11
HPV16 E6/18-25	HPV16 E6	18-25	KLPQLCTE	HLA-A11
HPV16 E6/27-36	HPV16 E6	27-36	QTTIHDIILE	HLA-A11
HPV16 E6/28-36	HPV16 E6	28-36	TTIHDIILE	HLA-A11
HPV16 E6/28-37	HPV16 E6	28-37	TTIHDIILEC	HLA-A11
HPV16 E6/29-37	HPV16 E6	29-37	TIHDIILEC	HLA-A11
HPV16 E6/29-39	HPV16 E6	29-39	TIHDIILECVY	HLA-A11
HPV16 E6/32-41	HPV16 E6	32-41	DIILECVYCK	HLA-A11
HPV16 E6/33-41	HPV16 E6	33-41	IILECVYCK	HLA-A11
HPV16 E6/34-41	HPV16 E6	34-41	ILECVYCK	HLA-A11
HPV16 E6/37-46	HPV16 E6	37-46	CVYCKQQLLR	HLA-A11
HPV16 E6/37-47	HPV16 E6	37-47	CVYCKQQLLRR	HLA-A11
HPV16 E6/38-46	HPV16 E6	38-46	VYCKQQLLR	HLA-A11
HPV16 E6/48-55	HPV16 E6	48-55	EVYDFAFR	HLA-A11
HPV16 E6/48-56	HPV16 E6	48-56	EVYDFAFRD	HLA-A11
HPV16 E6/52-62	HPV16 E6	52-62	FAFRDLCIVY	HLA-A11
HPV16 E6/52-62	HPV16 E6	52-62	FAFRDLCIVYR	HLA-A11
HPV16 E6/53-62	HPV16 E6	53-62	AFRDLCIVYR	HLA-A11
HPV16 E6/59-67	HPV16 E6	59-67	IVYRDGNPY	HLA-A11
HPV16 E6/63-73	HPV16 E6	63-73	DGNPYAVCDKC	HLA-A11
HPV16 E6/64-72	HPV16 E6	64-72	GNPYAVCDK	HLA-A11
HPV16 E6/67-75	HPV16 E6	67-75	YAVCDKCLK	HLA-A11
HPV16 E6/68-75	HPV16 E6	68-75	AVCDKCLK	HLA-A11
HPV16 E6/68-76	HPV16 E6	68-76	AVCDKCLKF	HLA-A11
HPV16 E6/68-77	HPV16 E6	68-77	AVCDKCLKFY	HLA-A11
HPV16 E6/68-78	HPV16 E6	68-78	AVCDKCLKFYS	HLA-A11
HPV16 E6/69-79	HPV16 E6	69-79	VCDKCLKFYSK	HLA-A11
HPV16 E6/70-79	HPV16 E6	70-79	CDKCLKFYSK	HLA-A11
HPV16 E6/71-79	HPV16 E6	71-79	DKCLKFYSK	HLA-A11
HPV16 E6/72-79	HPV16 E6	72-79	KCLKFYSK	HLA-A11
HPV16 E6/73-83	HPV16 E6	73-83	CLKFYSKISEY	HLA-A11
HPV16 E6/75-83	HPV16 E6	75-83	KFYSKISEY	HLA-A11
HPV16 E6/75-84	HPV16 E6	75-84	KFYSKISEYR	HLA-A11

HPV16 E6/75-85	HPV16 E6	75-85	KFYSKISEYRH	HLA-A11
HPV16 E6/77-84	HPV16 E6	77-84	YSKISEYR	HLA-A11
HPV16 E6/79-86	HPV16 E6	79-86	KISEYRHY	HLA-A11
HPV16 E6/79-88	HPV16 E6	79-88	KISEYRHYCY	HLA-A11
HPV16 E6/80-88	HPV16 E6	80-88	ISEYRHYCY	HLA-A11
HPV16 E6/81-89	HPV16 E6	81-89	SEYRHYCYS	HLA-A11
HPV16 E6/81-91	HPV16 E6	81-91	SEYRHYCYSLY	HLA-A11
HPV16 E6/84-91	HPV16 E6	84-91	RHYCYSLY	HLA-A11
HPV16 E6/88-97	HPV16 E6	88-97	YSLYGTTLEQ	HLA-A11
HPV16 E6/89-97	HPV16 E6	89-97	SLYGTTLEQ	HLA-A11
HPV16 E6/89-99	HPV16 E6	89-99	SLYGTTLEQQY	HLA-A11
HPV16 E6/91-101	HPV16 E6	91-101	YGTTLEQQYNK	HLA-A11
HPV16 E6/92-99	HPV16 E6	92-99	GTTLEQQY	HLA-A11
HPV16 E6/92-101	HPV16 E6	92-101	GTTLEQQYNK	HLA-A11
HPV16 E6/93-101	HPV16 E6	93-101	TTLEQQYNK	HLA-A11
HPV16 E6/94-101	HPV16 E6	94-101	TLEQQYNK	HLA-A11
HPV16 E6/101-109	HPV16 E6	101-109	KPLCDLLIR	HLA-A11
HPV16 E6/105-115	HPV16 E6	105-115	DLLIRCINCQK	HLA-A11
HPV16 E6/106-115	HPV16 E6	106-115	LLIRCINCQK	HLA-A11
HPV16 E6/107-115	HPV16 E6	107-115	LIRCINCQK	HLA-A11
HPV16 E6/113-122	HPV16 E6	113-122	CQKPLCPEEK	HLA-A11
HPV16 E6/116-124	HPV16 E6	116-124	PLCPEEKQR	HLA-A11
HPV16 E6/122-129	HPV16 E6	122-129	KQRHLDKK	HLA-A11
HPV16 E6/129-136	HPV16 E6	129-136	KQRFHNIR	HLA-A11
HPV16 E6/129-138	HPV16 E6	129-138	KQRFHNIRGR	HLA-A11
HPV16 E6/134-142	HPV16 E6	134-142	NIRGRWTGR	HLA-A11
HPV16 E6/139-148	HPV16 E6	139-148	WTGRCMSCCR	HLA-A11
HPV16 E6/140-148	HPV16 E6	140-148	TGRCMSCCR	HLA-A11
HPV16 E6/143-151	HPV16 E6	143-151	CMSCCRSSR	HLA-A11
HPV16 E6/143-153	HPV16 E6	143-153	CMSCCRSSRTR	HLA-A11
HPV16 E6/144-151	HPV16 E6	144-151	MSCCRSSR	HLA-A11
HPV16 E6/144-152	HPV16 E6	144-152	MSCCRSSRT	HLA-A11
HPV16 E6/144-153	HPV16 E6	144-153	MSCCRSSRTR	HLA-A11
HPV16 E6/144-154	HPV16 E6	144-154	MSCCRSSRTRR	HLA-A11
HPV16 E6/145-153	HPV16 E6	145-153	SCCRSSRTR	HLA-A11
HPV16 E7/18-25	HPV16 E7	18-26	ETTDLYCY	HLA-A11
HPV16 E7/18-26	HPV16 E7	18-26	ETTDLYCYE	HLA-A11
HPV16 E7/19-27	HPV16 E7	19-27	TTDLYCYEQ	HLA-A11
HPV16 E7/31-40	HPV16 E7	31-40	SSEEEDEIDG	HLA-A11
HPV16 E7/50-60	HPV16 E7	50-60	AHYNIVTFCCK	HLA-A11
HPV16 E7/51-60	HPV16 E7	51-60	HYNIVTFCCK	HLA-A11
HPV16 E7/52-60	HPV16 E7	52-60	YNIVTFCCK	HLA-A11
HPV16 E7/53-60	HPV16 E7	53-60	NIVTFCCK	HLA-A11
HPV16 E7/55-63	HPV16 E7	55-63	VTFCCKCDS	HLA-A11
HPV16 E7/63-71	HPV16 E7	63-71	STLRLCVQS	HLA-A11
HPV16 E7/63-73	HPV16 E7	63-73	STLRLCVQSTH	HLA-A11
HPV16 E7/68-77	HPV16 E7	68-77	CVQSTHVDIR	HLA-A11
HPV16 E7/71-80	HPV16 E7	71-80	STHVDIRTLE	HLA-A11
HPV16 E7/77-84	HPV16 E7	77-84	RTLEDLLM	HLA-A11
HPV16 E7/85-93	HPV16 E7	85-93	GTLGIVCPI	HLA-A11
HPV16 E7/87-97	HPV16 E7	87-97	LGIVCPICSQK	HLA-A11
HPV16 E7/88-97	HPV16 E7	88-97	GIVCPICSQK	HLA-A11
HPV16 E7/89-97	HPV16 E7	89-97	IVCPICSQK	HLA-A11
HPV16 E6/11-19	HPV16 E6	11-19	DPQERPRKL	HLA-A24
HPV16 E6/18-26	HPV16 E6	18-26	KLPQLCTEL	HLA-A24
HPV16 E6/26-34	HPV16 E6	26-34	LQTTIHDII	HLA-A24

HPV16 E6/35-44	HPV16 E6	35-44	LECVYCKQQL	HLA-A24
HPV16 E6/36-46	HPV16 E6	36-46	ECVYCKQQLLR	HLA-A24
HPV16 E6/38-45	HPV16 E6	38-45	VYCKQQLL	HLA-A24
HPV16 E6/38-46	HPV16 E6	38-46	VYCKQQLLR	HLA-A24
HPV16 E6/38-47	HPV16 E6	38-47	VYCKQQLLRR	HLA-A24
HPV16 E6/42-52	HPV16 E6	42-52	QQLLRREVYDF	HLA-A24
HPV16 E6/43-52	HPV16 E6	43-52	QLLRREVYDF	HLA-A24
HPV16 E6/44-52	HPV16 E6	44-52	LLRREVYDF	HLA-A24
HPV16 E6/44-54	HPV16 E6	44-54	LLRREVYDFAF	HLA-A24
HPV16 E6/45-54	HPV16 E6	45-54	LRREVYDFAF	HLA-A24
HPV16 E6/47-54	HPV16 E6	47-54	REVYDFAF	HLA-A24
HPV16 E6/47-57	HPV16 E6	47-57	REVYDFAFRDL	HLA-A24
HPV16 E6/48-57	HPV16 E6	48-57	EVYDFAFRDL	HLA-A24
HPV16 E6/48-58	HPV16 E6	48-58	EVYDFAFRDLC	HLA-A24
HPV16 E6/49-57	HPV16 E6	49-57	VYDFAFRDL	HLA-A24
HPV16 E6/49-59	HPV16 E6	49-59	VYDFAFRDLCI	HLA-A24
HPV16 E6/49-58	HPV16 E6	49-58	VYDFAFRDLC	HLA-A24
HPV16 E6/50-59	HPV16 E6	50-59	YDFAFRDLCI	HLA-A24
HPV16 E6/50-60	HPV16 E6	50-60	YDFAFRDLCIV	HLA-A24
HPV16 E6/51-59	HPV16 E6	51-59	DFAFRDLCI	HLA-A24
HPV16 E6/51-60	HPV16 E6	51-60	DFAFRDLCIV	HLA-A24
HPV16 E6/59-68	HPV16 E6	59-68	IVYRDGNPYA	HLA-A24
HPV16 E6/60-69	HPV16 E6	60-69	VYRDGNPYAV	HLA-A24
HPV16 E6/64-74	HPV16 E6	64-74	GNPYAVCDKCL	HLA-A24
HPV16 E6/65-74	HPV16 E6	65-74	NPYAVCDKCL	HLA-A24
HPV16 E6/66-74	HPV16 E6	66-74	PYAVCDKCL	HLA-A24
HPV16 E6/66-75	HPV16 E6	66-75	PYAVCDKCLK	HLA-A24
HPV16 E6/66-76	HPV16 E6	66-76	PYAVCDKCLKF	HLA-A24
HPV16 E6/67-76	HPV16 E6	67-76	YAVCDKCLKF	HLA-A24
HPV16 E6/72-80	HPV16 E6	72-80	KCLKFYSKI	HLA-A24
HPV16 E6/73-83	HPV16 E6	73-83	CLKFYSKISEY	HLA-A24
HPV16 E6/75-83	HPV16 E6	75-83	KFYSKISEY	HLA-A24
HPV16 E6/75-85	HPV16 E6	75-85	KFYSKISEYRH	HLA-A24
HPV16 E6/76-83	HPV16 E6	76-83	FYSKISEY	HLA-A24
HPV16 E6/76-84	HPV16 E6	76-84	FYSKISEYR	HLA-A24
HPV16 E6/76-85	HPV16 E6	76-85	FYSKISEYRH	HLA-A24
HPV16 E6/76-86	HPV16 E6	76-86	FYSKISEYRHY	HLA-A24
HPV16 E6/80-90	HPV16 E6	80-90	ISEYRHYCYSL	HLA-A24
HPV16 E6/81-90	HPV16 E6	81-90	SEYRHYCYSL	HLA-A24
HPV16 E6/81-91	HPV16 E6	81-91	SEYRHYCYSLY	HLA-A24
HPV16 E6/82-90	HPV16 E6	82-90	EYRHYCYSL	HLA-A24
HPV16 E6/82-91	HPV16 E6	82-91	EYRHYCYSLY	HLA-A24
HPV16 E6/85-94	HPV16 E6	85-94	HYCYSLYGTT	HLA-A24
HPV16 E6/85-95	HPV16 E6	85-95	HYCYSLYGTTL	HLA-A24
HPV16 E6/86-95	HPV16 E6	86-95	YCYSLYGTTL	HLA-A24
HPV16 E6/86-96	HPV16 E6	86-96	YCYSLYGTTLE	HLA-A24
HPV16 E6/87-94	HPV16 E6	87-94	CYSLYGTT	HLA-A24
HPV16 E6/87-95	HPV16 E6	87-95	CYSLYGTTL	HLA-A24
HPV16 E6/87-96	HPV16 E6	87-96	CYSLYGTTLE	HLA-A24
HPV16 E6/88-95	HPV16 E6	88-95	YSLYGTTL	HLA-A24
HPV16 E6/90-98	HPV16 E6	90-98	LYGTTLEQQ	HLA-A24
HPV16 E6/90-99	HPV16 E6	90-99	LYGTTLEQQY	HLA-A24
HPV16 E6/96-106	HPV16 E6	96-106	EQQYNKPLCDL	HLA-A24
HPV16 E6/97-106	HPV16 E6	97-106	QQYNKPLCDL	HLA-A24
HPV16 E6/98-106	HPV16 E6	98-106	QYNKPLCDL	HLA-A24
HPV16 E6/98-107	HPV16 E6	98-107	QYNKPLCDLL	HLA-A24

HPV16 E6/98-108	HPV16 E6	98-108	QYNKPLCDLLI	HLA-A24
HPV16 E6/109-117	HPV16 E6	109-117	RCINCQKPL	HLA-A24
HPV16 E6/124-132	HPV16 E6	124-132	RHLDKKQRF	HLA-A24
HPV16 E6/125-135	HPV16 E6	125-135	HLDKKQRFHNI	HLA-A24
HPV16 E6/126-135	HPV16 E6	126-135	LDKKQRFHNI	HLA-A24
HPV16 E6/127-135	HPV16 E6	127-135	DKKQRFHNI	HLA-A24
HPV16 E6/128-135	HPV16 E6	128-135	KKQRFHNI	HLA-A24
HPV16 E6/128-136	HPV16 E6	128-136	KKQRFHNIR	HLA-A24
HPV16 E6/128-137	HPV16 E6	128-137	KKQRFHNIRG	HLA-A24
HPV16 E6/128-138	HPV16 E6	128-138	KKQRFHNIRGR	HLA-A24
HPV16 E6/131-139	HPV16 E6	131-139	RFHNIRGRW	HLA-A24
HPV16 E6/138-146	HPV16 E6	138-146	RWTGRCMSC	HLA-A24
HPV16 E6/138-147	HPV16 E6	138-147	RWTGRCMSCC	HLA-A24
HPV16 E6/26-34var	HPV16 E6	26-34var	LQTTIHEII	HLA-A24
HPV16 E6/81-90var	HPV16 E6	81-90var	SEYRHYCYSV	HLA-A24
HPV16 E6/82-90var	HPV16 E6	82-90var	EYRHYCYSV	HLA-A24
HPV16 E6/82-91var	HPV16 E6	82-91var	EYRHYCYSVY	HLA-A24
HPV16 E6/85-93var	HPV16 E6	85-93var	HYCYSVYGT	HLA-A24
HPV16 E6/85-94var	HPV16 E6	85-94var	HYCYSVYGTT	HLA-A24
HPV16 E6/85-95var	HPV16 E6	85-95var	HYCYSVYGTTL	HLA-A24
HPV16 E6/87-94var	HPV16 E7	87-94var	CYSVYGTT	HLA-A24
HPV16 E6/87-95var	HPV16 E6	87-95var	CYSVYGTTL	HLA-A24
HPV16 E6/87-96var	HPV16 E6	87-96var	CYSVYGTTLE	HLA-A24
HPV16 E6/88-95var	HPV16 E6	88-95var	YSVYGTTL	HLA-A24
HPV16 E6/90-98var	HPV16 E6	90-98var	VYGTTLEQQ	HLA-A24
HPV16 E6/90-99var	HPV16 E6	90-99var	VYGTTLEQQY	HLA-A24
HPV16 E7/10-18	HPV16 E7	10-18	EYMLDLQPE	HLA-A24
HPV16 E7/10-19	HPV16 E7	10-19	EYMLDLQPET	HLA-A24
HPV16 E7/10-20	HPV16 E7	10-20	EYMLDLQPETT	HLA-A24
HPV16 E7/22-31	HPV16 E7	22-31	LYCYEQLNDS	HLA-A24
HPV16 E7/24-32	HPV16 E7	24-32	CYEQLNDSS	HLA-A24
HPV16 E7/24-33	HPV16 E7	24-33	CYEQLNDSSE	HLA-A24
HPV16 E7/48-57	HPV16 E7	48-57	DRAHYNIVTF	HLA-A24
HPV16 E7/49-57	HPV16 E7	49-57	RAHYNIVTF	HLA-A24
HPV16 E7/50-57	HPV16 E7	50-57	AHYNIVTF	HLA-A24
HPV16 E7/51-58	HPV16 E7	51-58	HYNIVTFC	HLA-A24
HPV16 E7/51-59	HPV16 E7	51-59	HYNIVTFCC	HLA-A24
HPV16 E7/51-60	HPV16 E7	51-60	HYNIVTFCCK	HLA-A24
HPV16 E7/56-65	HPV16 E7	56-65	TFCCKCDSTL	HLA-A24
HPV16 E7/56-66	HPV16 E7	56-66	TFCCKCDSTLR	HLA-A24
HPV16 E7/61-69	HPV16 E7	61-69	CDSTLRLCV	HLA-A24
HPV16 E7/67-76	HPV16 E7	67-76	LCVQSTHVDI	HLA-A24
HPV16 E7/67-77	HPV16 E7	67-77	LCVQSTHVDIR	HLA-A24
HPV16 E7/69-76	HPV16 E7	69-76	VQSTHVDI	HLA-A24
HPV16 E7/74-82	HPV16 E7	74-82	VDIRTLEDL	HLA-A24
HPV16 E7/74-83	HPV16 E7	74-83	VDIRTLEDLL	HLA-A24
HPV16 E7/77-87	HPV16 E7	77-87	RTLEDLLMGTL	HLA-A24
HPV16 E7/78-87	HPV16 E7	78-87	TLEDLLMGTL	HLA-A24
HPV16 E7/82-91	HPV16 E7	82-91	LLMGTLGIVC	HLA-A24
HPV16 E7/19-28var	HPV16 E7	19-28var	TTDLYCYEQF	HLA-A24
HPV16 E7/20-28var	HPV16 E7	20-28var	TDLYCYEQF	HLA-A24
HPV16 E7/21-28var	HPV16 E7	21-28var	DLYCYEQF	HLA-A24
HPV16 E7/22-30var	HPV16 E7	22-30var	LYCYEQFSD	HLA-A24
HPV16 E7/22-31var	HPV16 E7	22-31var	LYCYEQFSDS	HLA-A24
HPV16 E7/24-33var	HPV16 E7	24-33var	CYEQFSDSSE	HLA-A24
HPV16 E7/24-32var	HPV16 E7	24-32var	CYEQFSDSS	HLA-A24

HPV16 E6/15-23	HPV16 E6	15-23	RPRKLPQLC	HLA-B7
HPV16 E6/15-24	HPV16 E6	15-24	RPRKLPQLCT	HLA-B7
HPV16 E6/15-25	HPV16 E6	15-25	RPRKLPQLCTE	HLA-B7
HPV16 E6/19-26	HPV16 E6	19-26	LPQLCTEL	HLA-B7
HPV16 E6/44-54	HPV16 E6	44-54	LLRREVYDFAF	HLA-B7
HPV16 E6/59-69	HPV16 E6	59-69	IVYRDGNPYAV	HLA-B7
HPV16 E6/95-103	HPV16 E6	95-103	LEQQYNKPL	HLA-B7
HPV16 E6/101-108	HPV16 E6	101-108	KPLCDLLI	HLA-B7
HPV16 E6/101-111	HPV16 E6	101-111	KPLCDLLIRCI	HLA-B7
HPV16 E6/107-117	HPV16 E6	107-117	LIRCINCQKPL	HLA-B7
HPV16 E6/118-126	HPV16 E6	118-126	CPEEKQRHL	HLA-B7
HPV16 E6/134-144	HPV16 E6	134-144	NIRGRWTGRCM	HLA-B7
HPV16 E6/136-144	HPV16 E6	136-144	RGRWTGRCM	HLA-B7
HPV16 E6/148-158	HPV16 E6	148-158	RSSRTRRETQL	HLA-B7
HPV16 E6/149-158	HPV16 E6	149-158	SSRTRRETQL	HLA-B7
HPV16 E6/151-158	HPV16 E6	151-158	RTRRETQL	HLA-B7
HPV16 E7/5-12	HPV16 E7	5-12	TPTLHEYM	HLA-B7
HPV16 E7/5-13	HPV16 E7	5-13	TPTLHEYML	HLA-B7
HPV16 E7/49-57	HPV16 E7	49-57	RAHYNIVTF	HLA-B7
HPV16 E7/46-55	HPV16 E7	46-55	EPDRAHYNIV	HLA-B7
HPV16 E6/18-26	HPV16 E6	18-26	KLPQLCTEL	HLA-B15
HPV16 E6/41-50	HPV16 E6	41-50	KQQLLRREVY	HLA-B15
HPV16 E6/42-50	HPV16 E6	42-50	QQLLRREVY	HLA-B15
HPV16 E6/44-52	HPV16 E6	44-52	LLRREVYDF	HLA-B15
HPV16 E6/44-54	HPV16 E6	44-54	LLRREVYDFAF	HLA-B15
HPV16 E6/52-61	HPV16 E6	52-61	FAFRDLCIVY	HLA-B15
HPV16 E6/53-61	HPV16 E6	53-61	AFRDLCIVY	HLA-B15
HPV16 E6/57-67	HPV16 E6	57-67	LCIVYRDGNPY	HLA-B15
HPV16 E6/58-67	HPV16 E6	58-67	CIVYRDGNPY	HLA-B15
HPV16 E6/59-67	HPV16 E6	59-67	IVYRDGNPY	HLA-B15
HPV16 E6/68-77	HPV16 E6	68-77	AVCDKCLKFY	HLA-B15
HPV16 E6/73-83	HPV16 E6	73-83	CLKFYSKISEY	HLA-B15
HPV16 E6/74-83	HPV16 E6	74-83	LKFYSKISEY	HLA-B15
HPV16 E6/75-83	HPV16 E6	75-83	KFYSKISEY	HLA-B15
HPV16 E6/79-88	HPV16 E6	79-88	KISEYRHYCY	HLA-B15
HPV16 E6/81-91	HPV16 E6	81-91	SEYRHYCYSLY	HLA-B15
HPV16 E6/83-91	HPV16 E6	83-91	YRHYCYSLY	HLA-B15
HPV16 E6/84-91	HPV16 E6	84-91	RHYCYSLY	HLA-B15
HPV16 E6/89-99	HPV16 E6	89-99	SLYGTTLEQQY	HLA-B15
HPV16 E6/97-106	HPV16 E6	97-106	QQYNKPLCDL	HLA-B15
HPV16 E7/7-15	HPV16 E7	7-15	TLHEYMLDL	HLA-B15
HPV16 E7/15-23	HPV16 E7	15-23	LQPETTDLY	HLA-B15
HPV16 E7/15-25	HPV16 E7	15-25	LQPETTDLYCY	HLA-B15
HPV16 E7/42-52	HPV16 E7	42-52	AGQAEPDRAHY	HLA-B15
HPV16 E7/43-51	HPV16 E7	43-51	GQAEPDRAH	HLA-B15
HPV16 E7/43-52	HPV16 E7	43-52	GQAEPDRAHY	HLA-B15
HPV16 E7/49-57	HPV16 E7	49-57	RAHYNIVTF	HLA-B15
HPV16 E7/82-89	HPV16 E7	82-89	LLMGTLGI	HLA-B15
HPV16 E7/82-90	HPV16 E7	82-90	LLMGTLGIV	HLA-B15

2.1.13 Oligonucleotides

All oligonucleotides were used for sequencing and synthesized by Sigma-Aldrich, Steinbach. Lyophilized oligonucleotides were dissolved in ddH_2O at 100µM and stored in aliquots at -20°C.

2.1.13.1 Oligonucleotides for HPV16 E6 and E7 sequencing

Nucleotides in *italics* indicate T7 (forward) and T3 (reverse) sequencing primer sequences, respectively. Nucleotides in **bold** stand for actual PCR primer sequences.

Name	Sequence 5'-3'	T_m [C°]
E6_T7_for	*TAATACGACTCACTATAGGG***CGAAACCGGTTAGTATAA**	72.2
E6_T3_rev	*ATTAACCCTCACTAAAGGGA***GTATCTCCATGCATGATT**	74.6
E7_T7_for	*TAATACGACTCACTATAGGG***ATAATATAAGGGGTCGGTGG**	73.8
E7_T3_rev	*ATTAACCCTCACTAAAGGGA***CATTTTCGTTCTCGTCATCTG**	77.8

2.1.13.2 Oligonucleotides for HLA genotyping

Oligonucleotide sequences were taken from (Bunce, 2003).

Name	Sequence 5'-3'	T_m [C°]
HLA-f-402	AGGCCCACTCACAGACTC	60.5
HLA-r-249	CCTCCAGGTAGGCTCTCAA	62.0
HLA-f-296	GTGGATAGAGCAGGAGGGT	60.7
HLA-r-302	CCAAGAGCGCAGGTCCTCT	67.0
HLA-f-291	AGCGACGCCGCGAGCCA	76.6
HLA-r-299	CACTCCACGCACGTGCCA	71.4
HLA-f-290	ACGGAATGTGAAGGCCCAG	67.3
HLA-r-145	GAGCCACTCCACGCACTC	65.0
HLA-f-239	GGGTACCAGCAGGACGCT	65.4
HLA-r-167	GAGCCACTCCACGCACCG	70.8
HLA-f-208	ACCGAGAGAACCTGCGGAT	66.1
HLA-r-146	CCCTCCAGGTAGGCTCTCT	62.4
HLA-f-292	GGCCGGAGTATTGGGACGA	69,3
HLA-r-170	CCTCCAGGTAGGCTCTCTG	61.6
HLA-f-193	GGAGTATTGGGACCGGAAC	63.1
HLA-r-221	TACCAGCGCGCTCCAGCT	69.7
HLA-f-243	CGCGAGTCCGAGGATGGC	71.8
HLA-r-250	GCAGGTTCCGCAGGCTCT	68.1
HLA-f-280	CTACGTGGACGACACGCT	69.7
HLA-r-281	CTCGGTCAGTCTGTGCCTT	63.2
HLA-r-282	TCTCGGTAAGTCTGTGCCTT	61.5

2.1.14 Blood samples and buffy coats

Blood samples were taken from healthy donors after their written informed consent. Sampling and use of blood samples were in accordance with the Institutional Review Board at the Geramn Cancer Research Center (DKFZ) and the University of Heidelberg, Heidelberg, Germany. Blood buffy coats of anonymous, healthy donors were obtained from the German Red Cross (DRK) blood transfusion service Mannheim through the blood bank Institut für Klinische Transfusionsmedizin und Zelltherapie (IKTZ) Heidelberg.

2.1.15 Software

Name	Company/Source
AAcount.pl	Jan Winter, F130
Adobe Photoshop CS4	Adobe, San José, CA, USA
Adobe Illustrator CS4	Adobe, San José, CA, USA
AID EliSpot Evaluation System 5	Autoimmun Diagnostika, Strassberg
BD FACS Diva Software	BD Biosciences, San José, CA, USA
ExPASy ScanProsite	http://http://prosite.expasy.org/scanprosite/ access date: 20121025
EndNote X7.2	Thomas Reuters, Philadelphia, PA, USA
FlowJo 6.5	TreeStar, Ashland, OR, USA
Fusion	Vilber Lourmat, Eberhardzell
GENTle	Magnus Manske, University of Cologne, Cologne
Image Lab 3.0	Biorad, Hercules, CA, USA
MS Office 2010 (German version)	Microsoft Corperation, Redmond, WA, USA
Notepad++ 6.3	http://notepad-plus-plus.org/
PeptidePrediction.pI	Jan Winter, F130
PRISM® 5	GraphPad, La Jolla, CA, USA
ScanProsite_result.pI	Jan Winter, F130
SigmaPlot 12	Systat Software, San José, CA, USA
WebLogo 3 (Crooks et al., 2004)	http://weblogo.threeplusone.com/create.cgi access date: 20121024

2.2 Methods

2.2.1 *In silico* methods

As the experimental testing of binding affinity of peptides to MHC molecules is rather expensive and time-consuming, various computational approaches have been developed to predict MHC binding peptides. In theory, 941 peptides of the HPV16 E6 and E7 proteins with a length of 8-11 amino acids (aa) can be generated for each HLA allele and thus might be identified as potential T cell epitopes presented by HPV16-transformed cells. To cut down this number, different prediction servers were used to predict the binding affinities of all possible HPV16 E6 and E7 peptides to HLA-A3 (HLA-A*03:01), HLA-A11 (HLA-A*11:01) and HLA-A24 (HLA-A*24:02).

2.2.1.1 T cell epitope predictions

Peptide epitope prediction was performed using six prediction servers with ten algorithms in total. The NetMHC server is based on artificial neural networks and includes NetMHC 3.2 (Lundegaard et al., 2008a), NetMHCpan 2.4 (Nielsen et al., 2007) and NetMHCcons 1.0 (Karosiene et al., 2012), that combines the former two and a third algorithm, PickPocket. The Immune Epitope Database (IEDB) server includes two artificial neural network-based algorithms, IEDBann (Nielsen et al., 2003) and IEDBpan-specific ann (Hoof et al., 2009), as well as three matrix-based algorithms; IEDBarb (Bui et al., 2005), IEDBsmm (Peters and Sette, 2005) and IEDBsmmpmbec (Sidney et al., 2008). Those eight prediction methods all calculate a putative binding affinity given as IC_{50} [nM]. Two additional matrix-based servers, BIMAS (Parker et al., 1994) and SYFPEITHI (Rammensee et al., 1999), which display

the predicted peptide affinity as a score, were included as well. Since all prediction servers use different algorithms, are not trained with the same training databases and therefore yield different results, we took advantage of the high number of available servers and combined the results of the ten different prediction algorithms (Tab. 1).

Table 1 I Prediction servers used to predict binding peptides to designated HLA alleles. Algorithms: ANN: Artificial Neural Network, ARB: Average Relative Binding, SMM: Stabilized Matrix Method, SMMPMBEC: SMM with energy covariance matrix, AU: arbitrary units

Server	Algorithm	Scoring method	Peptide lengths predicted	Reference
netMHC 3.2	ANN	IC_{50}	8-11	(Lundegaard et al., 2008a)
NetMHCpan 2.4	pan-specific ANN	IC_{50}	8-11	(Nielsen et al., 2007)
NetMHCcons 1.0	NetMHC, PickPocket, NetMHCpan	IC_{50}	8-11	(Karosiene et al., 2012)
IEDB	ANN	IC_{50}	9+10	(Nielsen et al., 2003)
IEDB	ARB (Matrix)	IC_{50}	8-11	(Bui et al., 2005)
IEDB	SMM (Matrix)	IC_{50}	8-11	(Peters and Sette, 2005)
IEDB	SMMPMBEC (Matrix)	IC_{50}	8-11	(Sidney et al., 2008)
IEDB	Pan-specific ANN	IC_{50}	8-11	(Hoof et al., 2009)
SYFPEITHI	Matrix	Score (AU)	9+10	(Parker et al., 1994)
BIMAS	Matrix	Score (AU)	9+10	(Rammensee et al., 1999)

Whenever possible, the option to predict binding affinities for all possible peptides with 8, 9, 10 and 11 amino acids (8-11mers) was selected and standard settings recommended by the respective developers were chosen. HLA-A3 (HLA-A*03:01), HLA-A11 (HLA-A*11:01) and HLA-A24 (HLA-A*24:02) were selected as alleles individually. The protein sequences, HPV16 E6 and E7 (NC_001526), which were applied are shown in Table 2.

Table 2 I Amino acid sequences of HPV16 E6 and E7 proteins. Sequences were derived from the HPV16 reference sequence (NC_001526) and belong to the HPV16 variant European Prototype 1. The E6 protein is translated starting from the second methionine (M) at position 8.

Protein name	Amino acid sequence
HPV16 E6	MHQKRTAMFQDPQERPRKLPQLCTELQTTIHDIILECVYCKQQLLRREVYDFAFR DLCIVYRDGNPYAVCDKCLKFYSKISEYRHYCYSLYGTTLEQQYNKPLCDLLIRCI NCQKPLCPEEKQRHLDKKQRFHNIRGRWTGRCMSCCRSSRTRRETQL
HPV16 E7	MHGDTPTLHEYMLDLQPETTDLYCYEQLNDSSEEEDEIDGPAGQAEPDRAHYNI VTFCCKCDSTLRLCVQSTHVDIRTLEDLLMGTLGIVCPICSQKP

The output lists were combined into one file with binding affinities given as a score in arbitrary units (BIMAS and SYFPEITHI) or as IC_{50} values [nM] (all other servers). To this end, the PERL script PeptidePrediction.pl, which automatically combines all output files into one sortable file, was used (written by Jan Winter). The script only accepts tab-separated text files of the different prediction server results and all files had to be put into one folder. For NetMHC, NetMHCpan and NetMHCcons, the option "Save prediction to .xls file" had to be selected and the corresponding XLS files were renamed according to e.g. "netmhc%.txt". The script assumes certain standard values like the file name and the binding affinity threshold that is used by the prediction server. File name and binding affinity threshold for the respective server could be changed. For the other prediction servers, the results were copied directly from the website into Notepad++ and saved.

Depending on the number of peptide lengths that were available for one server, several files were created that were distinguishable by an additional number within the name, e.g. "netmhc1.txt", "netmhc2.txt" etc. The standard number of files and specifics are described in Table 3.

Table 3 I Naming system and specifies of output from prediction servers. Results of predictions were saved in tab-separated text files indicating the server name and number. % stands for the number (1, 2, 3 etc.) that describes the different outputs for various amino acid lengths for the same HLA allele and server.

Server	Standard file name	Standard # files	Standard threshold
NetMHC	netmhc%.txt	4	40000
NetMHCpan	netmhcpan%.txt	1	40000
NetMHCcons	netmhccons%.txt	1	40000
IEDB (all)	iedb%.txt	5	40000
SYFPEITHI	syf%.txt	1	0
BIMAS	bimas%.txt	2	0

Merging of data is achieved through comparing the information about the amino acid sequence, the starting position and the threshold for each predicted peptide and prediction server. This results in a tab-separated text file "PeptidePrediction.txt". The content of this file was then copied into a provided excel file "Peptide Prediction XX HLA.xlsx" to create a sortable excel sheet as shown in Table 4. Here, the peptides were sorted then by the average predicted IC_{50}-value calculated from all servers except BIMAS and SYFPEITHI. The *in vitro* binding affinities of all peptides with an average IC_{50} below 5000 or 7000nM were then tested in competition-based binding assay (section 2.2.3.1).

Table 4 I Final output of combined results from all peptide prediction servers. Results were combined by the PeptidePrediction.txt PERL script and pasted into a sortable excel sheet. A clipping of predictions of HPV16 E6 peptides binding to HLA-A*24:02 is shown exemplarily.

id	Position Sta	Regio	Leng	Sequenz	NetMHC Sco	NetMHC Pa	NetMHC con	IEDB - ann	IEDB - smm	IEDB - arb	IEDB - smmpmbec	IEDB - net	SYFPEITHI	BIMA
233	87	87 - 95	9	CYSLYGTTL	452,000	220,045	506,120	452,421	941,670	815,380	955,615	995,27	20,00	200,000
228	82	82 - 90	9	EYRHYCYSL	485,000	176,188	681,520	485,942	944,587	171,733	786,267	482,07	19,00	200,000
693	98	98 - 107	10	QYNKPLCDLL	641,000	320,498	1249,170	641,425	1843,395	320,666	966,079	1619,56	23,00	360,000
195	49	49 - 57	9	VYDFAFRDL	918,000	260,234	1242,430	918,266	1212,345	1477,972	1379,054	984,56	23,00	240,000
147	1	1 - 9	9	MHQKRTAMF	1302,000	452,602	628,400	1302,388	1435,462	627,973	1194,406	1550,96	12,00	
677	82	82 - 91	10	EYRHYCYSLY	1461,000	4160,745	4856,710	1461,167	1628,276	8155,474	1199,989	6262,79	11,00	5,000
655	60	60 - 69	10	VYRDGNPYAV	1524,000	1426,974	2403,860	1524,160	826,249	1845,831	636,616	2607,06	13,00	6,000
277	131	131 - 139	9	RFHNIRGRW	2617,000	287,708	1864,160	2617,660	1540,828	186,645	1763,666	598,54	6,00	

2.2.1.2 MHCcombine

Since it is very laborious to combine all different results even with the help of the PERL script PeptidePrediction.pl, we developed a web-based tool, *MHCcombine*, which combines the results of ten prediction servers directly into one file that can be opened in a sortable MS Excel® format. *MHCcombine* processes data directly from the respective servers and combines the outputs in the same manner as the PERL script. However, none of manual steps descriped above have to be performed by the user. This web-based tool was developed in context of this PhD thesis with the kind help of Jan Winter and Christine Zeller who programmed the tool.

2.2.1.3 Evaluation of prediction servers

By taking the reference sequence of HPV16 E6 and E7 proteins (NC_001526) and HLA-A3 (HLA-A*03:01), HLA-A11 (HLA-A*11:01), HLA-A24 (HLA-A*24:02) as examples, evaluation of the performance of the servers described in Table 1 was performed with *in vitro* data retrieved from competition-based binding assays (section 2.2.3.1). By this, we wanted to measure the ability of prediction servers to correctly classify our experimental results into binders or non-binders. Sensitivity is the proportion of experimentally measured binders, which were predicted as binders and is defined as true positive rate. The false positive rate describes the proportion of experimentally measured non-binders that were incorrectly predicted as binders. To this end, receiver operating characteristic (ROC) curves (Swets, 1988) were created. Plotting the rates of true positive predictions as a function of the rate of false positive predictions results in a ROC curve. The area under the curve (A_{ROC}) gives a measure of the prediction quality. The A_{ROC} of a prediction server is equivalent to the probability that the prediction server will rank a randomly chosen positive instance higher than a randomly chosen negative instance and is also equivalent to the Wilcoxon test of ranks (Hanley and McNeil, 1982).

All chosen NetMHC and IEDB prediction algorithms were included into this evaluation. The two servers BIMAS and SYFPEITHI were omitted due to unclear definition and discrimination of predicted binders and non-binders.

2.2.1.4 Peptide motif analysis

In order to identify HPV16 E6 and E7 peptides that were predicted with an average IC_{50} above a certain cutoff, but do bind to the desired HLA type nevertheless, amino acid distribution motifs were generated from the peptides identified as binders (positive motifs) and non-binders (negative motifs). By this, it was possible to screen peptides for potential motifs that either suggest binding due to defined positions of amino acids or exclude possible binding.

Generation of amino acid distribution motifs

Binding assay results (sections 3.1.2, 3.1.3 and 3.2) were processed with the AAcount.pl PERL script (written by Jan Winter) that creates matrices by counting the occurrence of amino acids at each position within a group of peptides. Those matrices can then be visualized with additional tools. To

this end, all HPV16 E6 and E7 peptides that were tested as binders (IC_{50} < 100µM) and non-binders (IC_{50} > 100µM) were combined into two tab-separated text-files containing the protein name, the amino acid position, the sequence and the experimental IC_{50} of the peptides (Tab. 5). AAcount.pl was applied on both files, creating a text-file output including a FASTA format summary of the peptides sorted by peptide length.

Table 5 I Tab-separated text file input for the PERL script AAcount.pl. Binding assay results were converted into a tab-separated format, starting with the protein, region, sequence and the IC_{50} value if applicable. A clipping of the file from tested HPV16 E6 peptides binding to HLA-A*24:02 is shown exemplarily.

Protein	Region	Sequence	IC_{50} (optinal)[µM]
E6	85-95	HYCYSLYGTTL	0,09536667
E6	49-57	VYDFAFRDL	0,10343333
E6	87-95	CYSLYGTTL	0,1191
E6	49-59	VYDFAFRDLCI	0,25856667
E6	66-76	PYAVCDKCLKF	0,2817
…	…	…	…

The FASTA output (Tab. 6) was then used to create sequence logos which visualize the amino acid occurrence at each position in a given set of peptides. To do so, the FASTA outputs for the different peptide lengths were copied to the input mask of the Weblogo 3 web service (Crooks et al., 2004), individually. Sequence logos (examples are displayed in section 3.1.3 Fig. 22 and 23), were created applying the settings listed in Table 7 and saved as .pdf files.

Table 6 I I FASTA format of predicted peptides used for creation of sequence logos with Weblogo3 and for ScanProsite. Peptides are written in the format: >region_length_protein_sequence. A clipping from the file for motif search of HPV16 E6 peptides binding to HLA-A*24:02 is shown exemplarily.

FASTA region length protein
>85-95_11_E6 HYCYSLYGTTL ← sequence
>49-57_9_E6 VYDFAFRDL
>87-95_9_E6 CYSLYGTTL
>49-59_11_E6 VYDFAFRDLCI
>66-76_11_E6 PYAVCDKCLKF
…

Table 7 I Settings applied for the creation of sequence logos with Weblogo 3 (Crooks et al., 2004).

Option	Input	Option	Input
Output format	PDV (vector)	Error bars	checked
Logo size	large	Title	Logo title
Stacks per line	40	Figure label	empty
Sequence type	protein	X-axis	position
Ignore lower case	checked	Y-axis	auto
Units	bits	Y-axis scale	auto
First position number	1	Y-axis tix spacing	1
Logo range	empty	Sequence end labels	unchecked
Composition	No adjustment	Version fineprint	checked
Scale stack widths	checked	Color scheme	Hydrophobicity

Motif search

To investigate possible additional binding peptides for HLA-A3 (HLA-A*03:01), HLA-A11 (HLA-A*11:01) and HLA-A24 (HLA-A*24:02), amino acid distribution results were used to search for motifs within the predicted peptide list that was created before. By searching for similar amino acid motifs, additional peptides might be found within the predicted list that were not considered due to thresholds that were applied before the selection peptides to be tested was made. The amino acid distribution was used to search for similar motifs with the ExPASy ScanProsite tool. To this end, binding motifs, that were compatible with the ScanProsite format, were created out of the amino acid distribution sequence logos and enriched by residue information described before by (Sette and Sidney, 1999) and (Rammensee et al., 1999).

For each peptide length, three positive and three negative motifs were generated. With the positive motifs, ScanProsite searches for existence of the amino acids at the defined positions, since they were found to facilitate binding to the respective HLA-type as proven by *in vitro* binding assays. With the negative motifs, in contrast, it searches for the absence of these amino acids at the defined positions in the peptides, since they were contained in peptides determined to not bind to the respective HLA-molecule. For each positive and negative motif, three sequences were created that account for a C- and N-terminal match or a C- or N-terminal match of the scanned peptide with the motif. The sequences inducing a C- and N-terminal match will only match with peptides of the same length as the motif. The C- or N-terminal sequences in contrast, allow longer or shorter peptides to match with this motif.

In addition to these motifs, ScanProsite requires a FASTA-formatted list of all peptides to be scanned for matches. Thus, the lists of predicted HPV16 E6 and E7 peptides were combined in a FASTA text-file and converted to the format shown in Tab. 6 using Notepad++.

Both, the motifs (section 3.1.3, Fig. 22 and 23) and the FASTA-formatted predicted peptide list (Tab. 6), were then copied to the web interface of ScanProsite. Here, all options were unticked and the output format was selected to ‘plain text tabular’. The results were copied and pasted to a new Notepad++ text-file. Since the tool handled a maximum of 30 peptides and eight motifs in one run at

the time of access, this step was repeated until all peptides were scanned for all motifs. The results were copied to the same text-file. Using the PERL Script ScanProsite_result.pl (written by Jan Winter), the file was then converted to an Excel file combining the motif matches of each peptide (Fig. 13). Results were analyzed for peptides matching with at least two positive motifs or with one positive and no matching with any negative motif. The binding affinities of these peptides were tested experimentally in competition-based binding assays (section 2.2.3.1).

Protein	Region	Length	Pattern	Sequence	Length
E6	85-95	11	2		11
			6	CYSLYGTTL	
			3	YSLYGTTL	

Figure 13 I ScanProsite result.pl output for one peptide. ScanProsite result.pl creates a list view and combines all matched motifs for one peptide. Within the result, the input information of the peptide is given (yellow), the matched motifs (blue), the matched sequence (green) and the peptide length (orange).

2.2.2 Molecular biological methods

2.2.2.1 DNA extraction

DNA extraction was conducted using the QIAamp DNA Mini Kit (Qiagen, Hilden). DNA binds specifically to the QIAamp silica-gel membrane while contaminants pass through and PCR inhibitors, such as divalent cations and proteins, are completely removed in wash steps. Pure DNA is then eluted in water. DNA extraction was performed according to the manufacturer's instruction. Briefly, cells were harvested as described under section 2.2.4, counted and up to $5x10^6$ cells were used. After isolation, the DNA concentration was measured by Nano Drop (section 2.2.2.4).

2.2.2.2 Polymerase Chain Reaction (PCR)

The polymerase chain reaction allows the amplification of DNA starting with a low concentrated template (Saiki et al., 1985; Mullis et al., 1986). As starter molecules, short synthetic oligonucleotides (primers) are used that bind specifically to the flanking 3' regions of the desired DNA-fragment. Using a heat stable polymerase, synthesis of the strand occurs in 5' to 3' direction. In this study, PCR was used on the one hand to amplify HPV16 E6 and E7 genes from cell lines for subsequent sequencing to determine their HPV16 variant and on the other hand to HLA genotype buffy coats that were used to generate peptide-specific short-term T cell lines (section 2.2.5.1).

The PCR reaction starts by heating up the DNA template to 95°C or 92°C, depending on the PCR program used, which denatures the double strands into single strands. Often an initial denaturation step is conducted before the first denaturation step. The sample is then cooled to a specific temperature, which allows the primers to anneal to the template. The melting temperature for primers was determined by software analysis and the PCR program adjusted accordingly. When the sample is heated up again to 72°C, the polymerase uses the primers as starting points to synthesize a new DNA

strand complementary to the DNA template strand. This cycle is repeated several times. After finishing the last cycle, a final elongation step follows in some cases, to ensure that all left single DNA strands are fully extended. Tables 8 and 10 show the compositions of the used PCR reactions for HPV16 variant sequencing and HLA genotyping, and Tables 9 and 11 the corresponding PCR programs.

Table 8 I Components for HPV16 E6 and E7 sequencing PCR.

Component	Stock concentration	Final concentration	Volume/sample [µL]
10x PCR buffer	10x	1x	5
dNTPs	10mM	200µM	4
$MgCl_2$ solution	25mM	2.5mM	5
Forward Primer	10µM	1µM	5
Reverse Primer	10µM	1µM	5
Template-DNA	40ng/µL	400ng	10
AmpliTaq Gold DNA Polymerase	5 U/µL	1.25 U/reaction	0.25
PCR grade ddH_2O	-	-	ad. up to 50µL
V_{total}			**50**

Table 9 I PCR cycles for HPV16 E6 and E7 sequencing PCR.

Step	Time [min]	Temperature [°C]	
Initial denaturation	15	95	
Denaturation	1	94	40x
Annealing	1	55	
Extension	2	72	
Final extension	10	72	
Final hold	∞	4	

Table 10 I Components for HLA genotyping PCR.

Component	Stock concentration	Final concentration	Volume/sample [µL]
REDTaq® ReadyMix™ PCR Reaction Mix	2x	1.08x	1.5
Forward Primer	10µM	1µM	2.5
Reverse Primer	10µM	1µM	2.5
Template-DNA	50µg/µL	50ng	1
PCR grade ddH_2O	-	-	ad. up to 25µL
V_{total}			**25**

Table 11 PCR cycles for HLA genotyping PCR.

Step	Time [min]	Temperature [°C]	
Initial denaturation	5	92	
Denaturation	1	92	30x
Annealing	2	65	
Extension	3	72	
Final hold	∞	4	

Denaturation, annealing and extension were repeated for 30 or 40 times, respectively. All PCR reactions were prepared on ice, mixed and put into the pre-heated PCR cycler (C1000 Touch™ Thermal Cycler; Biorad, Hercules, CA, USA). Primers were purchased from Sigma-Aldrich and primer sequences are listed in section 2.1.13.2. The exact used primer pairs for HLA-genotyping are displayed in Table 12. For controls, either DNA template or primers were substituted by PCR grade ddH_2O. DNA from cells with known HLA-type was used as a reference for HLA genotyping PCR. Optimized PCR conditions for HPV16 E6 and E7 sequencing were kindly provided by Tarik Gheit (WHO/IARC, Lyon). Successful PCR was verified by gel electrophoresis (section 2.2.2.3).

Table 12 I Overview of primer pairs for HLA genotyping PCR. Primers, the HLA types that are covered by the primer and the resulting product size are indicated (Bunce, 2003).

Primer names	Pair	HLA types	Product size
HLA-f-402 HLA-r-249	A2-1	A*0201, *0204, *0206, *0207, *0209, *0210, *0214, *0215N, *0216, *0217, *0218,*0220, *0221, *0224, *0225	521 bp
HLA-f-296 HLA-r-302	A2-2	A*0201, *0202, *0203, *0204, *0205, *0206, *0207, *0208, *0209, *0210, *0211,*0212, *0213, *0214, *0215N, *0216, *0217, *02172, *0218, *0219, *0220, *0221,*0222, *0225, *0226	489 bp
HLA-f-291 HLA-r-299	A3	A*0301, *0302, *0303N, *0304	628 bp
HLA-f-290 HLA-r-145	A11-1	A*1101, *1102, *1103, *2502, *6601	552 bp
HLA-f-239 HLA-r-167	A11-2	A*2501, *2502, *2601, *2603, *2605, *2607, *2608, *4301, *6601, *6602, *6603 (control for A11-1 and A11-3)	170 bp
HLA-f-290 HLA-r-167	A11-3	A*2501, *2502, *2601, *2603, *2605, *2607, *2608, *4301, *6601, *6602, *6603	552 bp
HLA-f-208 HLA-r-146	A24-1	A*2402, *2403, *2405, *2407, *2408, *2409N, *2410, *2411N, *2414	504 bp
HLA-f-292 HLA-r-170	A24-2	*2402, *2402102L, *2403, *2404, *2405, *2407, *2409N, *2410, *2411N, *2414	557 bp
HLA-f-193 HLA-r-221	B7	B*07021, *07022, *07023, *0703, *0704, *0705, *0706, *0707, *0708, *8101	1207 bp
HLA-f-243 HLA-r-250	B15	B*1501, *1502, *1504, *1505, *1506, *1507, *1508, *1511, *1512, *1514, *1515,*1519, *1520, *1521, *1525, *1526N, *1527, *1528, *1530, *1531, *1532, *1533,*1534, *1535, *1538, *1539	124 bp
HLA-f-280 HLA-r-281	B27-1	B*2701, *2702, *2703, *2704, *27052, *27053, *2706, *2707, *2708, *2709, *2710, *2711	149 bp
HLA-f-280 HLA-r-282	B27-2	B*2701, *2702, *2703, *2704, *27052, *27053, *2706, *2707, *2708, *2709, *2710, *2711	150 bp

2.2.2.3 Agarose gel electrophoresis

As nucleic acids are charged negatively due to their phosphate residues, they can be separated by agarose gel electrophoresis using an electric field (Sambrook and Gething, 1989). Shorter DNA fragments migrate faster and further than larger ones and therefore the DNA fragments undergo a characteristic separation. Detection is performed with the help of ethidium bromide, which interacts with nucleic acids and can be visualized by UV light. A 1% agarose gel was used which was supplemented with 0.5µg/mL ethidium bromide. Samples were mixed with 6x Orange DNA Loading

Dye (Thermo Fisher Scientific Ldt., Loughborogh, UK) before they were applied to the gel. GeneRuler™ DNA Ladder (Thermo Fisher Scientific Ldt., Loughborogh, UK) was used as a reference for the size of the DNA strands. Running of gels in 1x TAE buffer was conducted at 125V until bands were sufficiently separated. Afterwards, gels were documented using the INTAS UV System, Gel Jet Imager 2006.

2.2.2.4 Determination of DNA concentration

1µl of DNA sample was applied to the Nano Drop to measure the concentration and purity of the sample. Nucleic acids absorb light at different wavelengths. By using the Lambert-Beer law:

$$A = \varepsilon \times c \times d$$

(A: absorbance, ε: extinction coefficient; c: concentration; d: distance),

the absorbance can be related to the concentration of a sample. At a wavelength of 260nm, the extinction coefficient for ds DNA is 0.02 $(\mu g/mL)^{-1}$ cm^{-1}. Hence, an optical density (OD) of 1 corresponds to a concentration of 50µg/mL. In contrast, proteins show a maximum light absorption at 280nm. Thus the purity of nucleic acids can be determined by measuring the ratio of 260nm and 280nm with an optimal value between 1.8 and 1.95.

2.2.2.5 Sequencing of HPV 16 E6 and E7 genes

PCR products were sequenced by GATC Biotech, Konstanz. To this end, 20µL of unpurified PCR sample with a concentration of 100ng/µL DNA were sent for sequencing.

2.2.2.6 Analysis of HPV 16 E6 and E7 sequences

In order to characterize the HPV16 variants present in our cell line collection, 62 HPV16 whole genome sequences, representative of all known variants, provided by Robert D. Burk (Albert Einstein College of Medicine, New York, NY, USA) (Burk et al., 2011; Smith et al., 2011), were used as references. The sequences were grouped beforehand according to the variant lineages and sublineages they represent (European Prototype 1, European Prototype 2, European Asian, African-1, African-2, North American-1, Asian American-1, Asian American-2). Multiple sequence alignments within the groups were conducted by using the Clustal-W algorithm (match: 2, gap penalty: -2, gap extension penalty: -1) implemented in GENtle. By this, sequence differences within the E6 and E7 open reading frames (nucleotides 83-559 and 562-858, respectively) for each group were identified. The DNA sequences were then translated into protein sequences to reveal silent and non-silent mutations in comparison to the HPV16 reference sequence (NC_001526).

Sequences of the HPV16 E6 and E7 PCR samples obtained from GATC Biotech were aligned to the HPV16 reference sequence as described above. All nucleotide changes were listed and compared with variant lists to see if nucleotide exchanges would result in exchanges on protein level. In cases where novel nucleotide exchanges were detected, the sequence was translated into the protein sequence and

the respective codon was checked for silent and non-silent mutations. All HPV16-positive cell lines from our cell culture could be assigned to a specific HPV16 variant.

2.2.3 Biochemical Methods

2.2.3.1 Competition-based binding assays

Peptide binding affinity to selected HLA class I molecules was tested in competition-based cellular binding assays (Kessler et al., 2003; Kessler et al., 2004) based on the competition of HLA class I binding between a test peptide of interest and a fluorescein-labeled HLA class I binding reference peptide, which is a known strong binder to the HLA meolecule of interest. The binding affinity of the test peptide was determined by non-linear regression analysis as the concentration that inhibits 50% binding of the fluorescein-labeled reference peptide (IC_{50}).

Briefly, a 96-well plate was prepared containing serial dilutions in 1xPBS of a peptide with a high binding affinity (positive controls: HLA-A3: consensus sequence KVFPALINK (Sette et al., 1994); HLA-A11: HIV-1 Nef 73-82 QVPLRPMTYK (Koenig et al., 1990); HLA-A24: HIV-1 env pg41 583-591 RYLKDQQLL (Dai et al., 1992)), a peptide with a low binding affinity (negative control: HLA-A3/11: HPV16 E6/85-94 HYCYSLYGTTL; HLA-A24: HPV16 E6/93-101 TTLEQQYNK), a DMSO-only control (peptide diluent) and test peptides (dilutions from 600 – 4.6875µM in 1:2 steps in 1xPBS, 50µL per well). 25µL of each well were transferred to the same well of a second 96-well plate containing 25µL 900nM fluorescent reference peptide (HLA-A3/11: KVFP(fluorescein)ALINK; HLA-A24: RYLK(fluorescein)QQLL), in each well except for those of the DMSO-only control (25µL 1xPBS instead).

B-LCL cells with the desired HLA class I molecule were washed twice with 1xPBS and then stripped from natural bound peptides and β_2-microglobulin by using ice cold citric acid buffer (HLA-A3: pH 2.9; HLA-A11: pH 3.1; HLA-A24: pH 3.1) for 90sec. After stripping, the cells were instantly washed twice with ice-cold culture medium before they were finally dissolved in culture medium which contained 4µL/mL β_2-microglobulin (MP Biomedicals, Illkirch, France; BD Biosciences, Franklin Lakes, NJ, USA) to reconstitute the HLA class I complex. 100µL of the cell suspension containing $6x10^4$ cells were pipetted to each well of the 96-well plate resulting in a final concentration of control and test peptides from 100-0.78µM. The concentration of fluorescent reference peptide was 150nM. Plates were incubated o/n at 4°C in the dark, washed twice with 0.5% BSA in 1x PBS, resuspended in 80µL/well 1% PFA in 1xPBS and stored at 4°C in the dark until flow cytometric analysis.

Fluorescence was measured by flow cytometry (FACS Canto II™; BD Biosciences, Franklin Lakes, NJ, USA) and data processed as described in section 2.2.4.4. The binding of each test and positive-control peptide was calculated as the percent inhibition of Fl peptide binding relative to the minimal response (without Fl peptide; $MF_{background}$) and the maximal response (Fl peptide only; MF_{Fl}) using the following equation:

$$\text{Inhibition } (\%) = (1 - \frac{MF - MF_{background}}{MF_{Fl} - MF_{background}}) \times 100$$

Percent inhibition was plotted against the peptide concentration and a logistic 4-parametric non-linear regression curve was fitted to the data points using SigmaPlot software. From this regression analysis, the peptide concentration that inhibited binding of the fluorescent reference peptide by 50% (IC_{50}) was calculated for each peptide using the following equation:

$$y = a + \frac{b}{1 + (\frac{x}{c})^d}$$

(a-d: constants in equation),

where x represents the peptide concentration and y the corresponding inhibition (%). Peptides were ranked as strong binders (IC_{50} < 5µM), intermediate binders (IC_{50} 5-15µM) or weak binders (IC_{50} 15-100µM), as recommended for the used reference peptides (Kessler et al., 2003; Kessler et al., 2004). Peptides with an IC_{50} above 100µM were defined as non-binders. For confirmation and statistical significance, the assay was performed three times for binders and twice for non-binders.

2.2.3.2 Immunoprecipitation

To assess that the candidate peptides are truly presented on the surface of HPV16-transformed cells, HLA class I molecule/peptide complexes were isolated from these cells. Immunoprecipitations of various HLA-class I molecule/peptide complexes from different HPV16-transformed cells was carried out and analyzed for purity and enrichment by Oriole staining (section 2.2.3.5) and Western blot (section 2.2.3.6).

GammaBind™ Plus Sepharose™ beads (GE Healthcare, Munich) were prepared by taking 1mL of dry beads (equal to 2mL of beads in suspension) into a 2ml tube and centrifugation at 5000rpm for 3min at RT with a swinging rotor. The supernatant (SNT) was removed and 1mL of 10% acetic acid (pH 3.0) added, the beads were vortexed and centrifuged at 5000rpm for 3min at RT with a swinging rotor. The SNT was removed and the beads were washed five times with 1mL 1xPBS. Eventually, the SNT was removed and the beads were resuspended in 1mL 1xPBS with 0.02% sodium azide and stored at 4˚C.

Depending on growth properties, cells were seeded four to two days prior immunoprecipiation in 10cm Ø cell culture dishes. 50µL sepharose beads were washed three times with 500µL 1xCHAPS buffer and then coupled with 20µg of specific antibody directed against the desired HLA class I type in 500µL 1x CHAPS buffer for two to three hours at RT on a rotator. In the meantime, cells were washed twice with ice-cold 1xPBS, detached with a cell scraper and lysed in 1mL 2x CHAPS buffer. Cell lysates were pooled of different numbers of confluent 10cm Ø cell culture dishes, by transferring the lysate from one to the next dish without adding new CHAPS buffer. The lysate pools were then incubated for 10min on ice and vortexed every 3min before they were centrifuged for 30min at

14000rpm at 4°C. After centrifugation, an aliquot of the cleared lysate was taken for analysis. After incubation of beads with antibody, beads were centrifuged at 5000rpm for 3min with a swinging-rotor. The SNT was removed and beads were washed twice with 500µL 1xCHAPS buffer. Cleared lysate was incubated with the respective anti-HLA-class-I-antibody-coupled sepharose beads on a rotator at 4°C for 3hrs. As negative controls, CHAPS buffer was incubated with beads alone or beads coupled with antibody.

After incubation with cleared lysate, beads were washed twice with 500µL of ice-cold 1:1 diluted 2x CHAPS lysis buffer, once with ice-cold 1x CHAPS buffer and three times with ice-cold 10mM Tris-HCl (pH 8.0). Aliquots of the flow through and of the SNTs of all washing step were collected for analysis. HLA/peptide complexes on washed beads were then used for biochemical analysis or mass spectrometry (MS) analysis. Samples for MS were stored at -80°C. For SDS-PAGE, the beads were mixed with 20µL 10mM Tris-HCl (pH 8.0) and 20µL 2x Laemmli sample buffer (Biorad, Hercules, CA, USA).

2.2.3.3 Sodium Dodecyl Sulfate Polyacrylamide Gel Electrophoresis (SDS-PAGE)

SDS-PAGE (Laemmli, 1970) is a method for separating denatured proteins according to their molecular weight. In the process, one uses the negatively charged detergent SDS which is able to mask the different charges of the amino acid residues. All proteins are thus stretched, and these negatively charged polypeptides can be separated by an electric field in a polyacrylamide matrix. As proteins have a constant negative charge per mass unit, separation occurs exclusively by their molecular weight. Moreover, disulfide bridge formation is inhibited by adding 2-mercaptoethanol. The samples are commonly boiled at 95°C for 10min in 2x Laemmli buffer to enhance the denaturing effect of SDS.

The desired volume of sample was loaded onto an Any kD™ Precast Gel (Biorad, Hercules, CA, USA) that was put into an electrophoresis chamber for SDS-PAGE (Mini-PROTEAN® Tetra Cell; Biorad, Hercules, CA, USA). As a marker either Precision Plus Protein™ Standards Kaleidoscope ™, 10-250kDa (Biorad, Hercules, CA, USA) for Coomassie staining and Western blot or Precision Plus Protein™ Unstained Standards ™, 10-250kDa (Biorad, Hercules, CA, USA) for Oriole staining were used. The protein samples were run at 100V until loading pockets were empty and were subsequently run at 150V. Afterwards, the gels were either stained (sections 2.2.3.4 and 2.2.3.5) or used for Western blot analysis (section 2.2.3.6).

2.2.3.4 Coomassie stain

Protein gels were Coomassie-stained after electrophoresis (section 2.2.3.3) using Coomassie Brilliant Blue solution gently shaking o/n at RT. To reduce background staining, gels were destained for 30 to 60min in Coomassie destaining solution and subsequently washed with Milipore water. Gels were scanned for documentation.

2.2.3.5 Oriole stain

Oriole staining of protein gels was performed according to the manufacturer's instructions using Oriole™ Fluorescent Gel Stain (Biorad, Hercules, CA, USA). Briefly, gels were incubated for 90min in Oriole™ Fluorescent Gel Stain and put into Milipore water for documentation with the Gel Doc™ EZ Imager (Biorad, Hercules, CA, USA).

2.2.3.6 Western Blot

Western blot analysis is based on the principle that proteins bind to nitrocellulose or polyvinylidene fluoride (PDFV) membranes and can be detected by antibodies (Thorpe and Kricka, 1986). The electrical transfer of the proteins onto a PVDF membrane was performed using the tank transfer method. After SDS-PAGE (section 2.2.3.3), the PVDF Transfer Membrane (Thermo Scientific, Rockford, IL, USA) was activated shortly in 100% methanol and subsequently equilibrated together with the polyacrylamide gel and two Western Blotting Filter Papers (Thermo Scientific, Rockford, IL, USA) in transfer buffer for 1min. Western Blotting Filter Papers, the gel and the PVDF Transfer Membrane were assembled, occurring air bubbles removed, and the package placed into the transfer chamber (Mini Trans-Blot® Cell; Biorad, Hercules, CA, USA) according to the schematic diagram shown in Figure 14. Protein transfer was performed for 1.5hrs at 30V and 4°C. Successful transfer of proteins to the PVDF Transfer Membrane was monitored by Ponceau Red (Serva, Heidelberg) staining. To this end, the PVDF membrane was incubated for 30-60sec with Ponceau S solution. Afterwards the membrane was washed with ddH_2O to visualize red protein bands. For subsequent processing of the blot membranes, the Ponceau S stain was removed by incubation of the membrane in 1xPBS for several minutes.The blot was then blocked for 45min in 5% milk powder (blotting grade; Roth, Karlsruhe) in 1xPBS at RT.

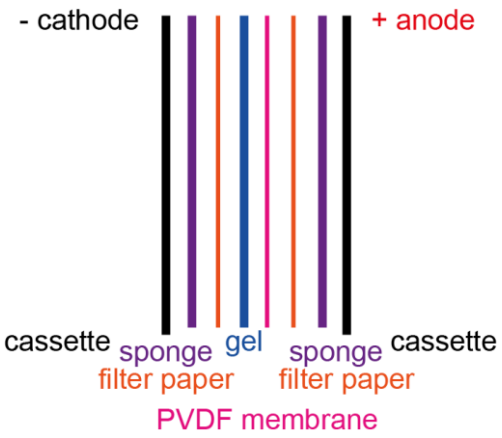

Figure 14 I Schematic presentation of the assembly of a Western Blot. The gel and PVDF membrane are placed into the cassette between two filter papers followed by a sponge on each side.

After blocking, the blot was incubated with the desired first antibody (diluted in 1.5% milk powder in 1xPBS) either o/n at 4°C or for 1hr at RT on a shaker. The antibody solution was then poured off and

the blot was washed three times for 5min with 1xTPBS with continuous shaking. Afterwards, the blot was incubated with the corresponding secondary antibody (diluted in 1.5% milk powder in 1xPBS) at RT for 45min. After incubation with the secondary antibody the blot was washed three times for 5min with 1xTPBS, covered with 750µL Pierce ECL Western Blotting Substrate (Thermo Fisher Scientific, Waltham, MA, USA) for 3min at RT and luminescence signals were recorded using a Fusion-SL chemiluminescence-camera (Vilber Lourmat, Eberhardzell).

2.2.4 Cell culture methods

Cell culture work was conducted under sterile conditions in a laminar flow hood. Prior to usage, equipment, material and solutions were sterilized or disinfected. Mycoplasma testing and cell authentification was performed upon arrival of newly acquired cell lines and at regular intervals to ensure mycoplasma negativity and cell authentiticy.

2.2.4.1 Thawing and freezing of cells

Frozen cells were stored in liquid nitrogen. In order to reduce extended exposure of cells to toxic concentrations of DMSO, handling of cells was done fast during freezing and thawing of cells.

50mL tubes were filled with 20mL of pre-warmed medium. Cryo vials were taken from the liquid nitrogen tank and thawed immediately at 37°C in a water bath. Cells were then directly transferred into the prepared tubes and resuspended. Cells were centrifuged at 1400rpm for 5min at RT and the SNT decanted. A second washing step was conducted and cells were resuspended in 7mL medium and seeded into a 25cm^2 flask. The next day or at least 12hrs after thawing, the medium was exchanged.

For freezing, the cell suspension was centrifuged at 1400rpm for 5min at 4°C, the SNT removed and the cell pellet was resuspended in the appropriate volume of freezing medium. Freezing medium was always freshly prepared by taking the pre-cooled usual medium of the respective cell line and adding 10% DMSO and 10% serum, either FCS or HS. Aliquots of 1mL with a cell concentration of up to 1x10^7 cells/mL were quickly transferred to 2mL cryo vials. Those were placed into a pre-cooled cell freezing device (Mr. Frosty; Bel-Art Products, Wayne, NJ, USA), which allows a consistent cool down of 1°C/min after being put into the -80°C freezer. Three days later, cryo vials were transferred to the liquid nitrogen tank for permanent storage.

2.2.4.2 Culturing and passaging of cells

All cell lines were cultured in an incubator at 37°C, 95% relative humidity and 5% CO_2 in either 25cm^2, 75cm^2 or 150cm^2 tissue culture flasks or cell culture plates from 6- up to 96-wells. Adherent cell flasks were kept horizontal while flasks for suspension cell lines were kept upright. Every second week at the latest, the cell culture flasks were exchanged.

In order to passage adherent confluent cells, medium was removed and cells were washed with 1xPBS. Cells were detached by incubation with trypsin-EDTA at 37°C until all cells detached upon

rocking of the flask. Trypsin-EDTA was inactivated by adding fresh, pre-warmed, serum-containing medium and cells separated by pipetting up and down. Cells were then transferred to 50mL tubes that were filled up with medium and centrifuged at 1400rpm for 5min at RT. The SNT was removed from the pellet by decanting and the cells were resuspended in fresh medium. They were either split at appropriate ratios (between 1:1 to 1:30) into fresh cell culture flasks or used for experiments. Cells were split whenever flasks reached between 80 to 100% confluency.

Suspension cells (e.g. B-LCLs) were resuspended every day by shaking to isolate cells from accumulations. The desired volume of cell suspension for splitting was transferred to 15 or 50mL tubes that were filled up with medium and centrifuged at 1400rpm for 5min at RT. Cells were then resuspended in the appropriate volume of medium.

W12 20861 and 20863 cells were grown on irradiated 3T3 fibroblast cells, serving as feeder cells. To this end, 3T3 cells were grown confluent, harvested by trypsination, washed with 1xPBS, irradiated at 50Gy (Gammacell 1000; Atomic Energy of Canada Limited, Ottawa, Canada) and washed again with 1xPBS. 10mL of cell suspension were then seeded at a concentration of $2x10^5$ cells/mL into a $75cm^2$ flask. The next day irradiated 3T3 cells were checked under the microscope for confluency and morphology and approximately $2x10^5$ W12 20861 or 20863 cells were placed on top. Flasks of irradiated feeder cells were freshly prepared as soon as W12 cells grew confluent.

Special cultivation methods for primary cells and other selected cell lines are described in section 2.2.5.1.

2.2.4.3 Counting of cells

For counting, the respective cell suspension was, if necessary, pre-diluted in 1xPBS and then mixed 1:1 with Trypan blue solution for live-dead discrimination. Cells were either counted manually with a Neubauer counting chamber (0.1mm depth) or counted automatically with the Countess® Automated Cell Counter (Invitrogen, Carlsbad, CA, USA). After manual counting with the Neubauer counting chamber, the total cell number was calculated using the following formula:

$$\text{total cell number} = \frac{\text{counted cells}}{\text{number of large squares}} \text{ x dilution factor x chamber factor (10000)}$$

2.2.4.4 Flow cytometry

For flow cytometry analysis, a FACS Canto II™ (BD Biosciences, Franklin Lakes, NJ, USA) was used provided either by the DKFZ FACS Core Facility or by the Devision of Translational Immunology (D015, Philipp Beckhove), DKFZ. The FACS Canto II™ of D015 is equipped with a high throughput (HTS) device, which enables automatic processing of samples from a 96-well plate. All solutions were applied ice-cold, incubation steps were carried out either on ice or at 4°C and cells were kept in 96-well plates or FACS tubes. Typically, between $6x10^4$ to $1x10^6$ cells were used for flow

cytometry analysis. Cells were usually washed with FACS buffer (section 2.1.2) once, centrifuged at 1400rpm for 5min at 4°C and blocked for 15min in 10% FCS in 1xPBS on ice. Subsequently, cells were resuspended in FACS buffer containing the appropriate dilutions of primary antibodies (section 2.1.11.1). After 30 to 60min incubation in the dark at 4°C, cells were washed twice with FACS buffer. If necessary, a second incubation step of 30min at 4°C in the dark with FACS buffer containing a suitable secondary fluorochrome-conjugated antibody (section 2.1.11.2) was performed. Cells were washed twice with FACS buffer and stored on ice in an appropriate volume of FACS buffer for immediate analysis by flow cytometry or resuspended in 1% PFA and stored at 4°C until analysis.

Autofluorescence of cells was determined by acquiring unstained cells. Voltages of lasers were adjusted based on single stainings. Gating was performed on living cells and adjusted to the desired subpopulations that were identified by distinctive markers. For each sample 10000 events or more were recorded in most cases. Final analysis was conducted with FlowJo 6.5 software (TreeStar, Ashland, OR, USA).

Whenever multi-color stainings with more than one fluorochrome were done, compensation needed to be performed. Compensation describes the process of determination, calculation and subsequent subtraction of spectral overlaps from one fluorescent detector channel in FACS Canto II™ to the other. The auto-compensation tool of the BD FACS Diva Software (BD Biosciences, San José, CA, USA) calculated and applied the compensation to all acquired samples of one experiment. To determine the spectral overlap from one channel to another, additional single color stainings for each color used in the experiment were conducted and acquired. For this purpose, beads were coated with the same antibodies used for staining of cells. For each antibody, the same concentration as used for the cells was diluted in 100µL FACS buffer. One droplet of previously shaken OneComp eBeads (eBioscience, San Diego, CA, USA) was added to the solution. Samples were tapped for resuspending the antibodies and then incubated in the dark for 20min on ice. After labeling, 1mL FACS buffer was added for washing and beads were centrifuged at 4500rpm at 4°C. SNT was discarded and beads were resuspended in 200µL FACS buffer. The bead controls were then acquired with the FACS Canto II™ for compensation.

Multi-color stainings

Multi-color stainings were performed for determining the percentage of B cells in B cell cultures that were either generated by immortalizing B cells with EBV or by co-culture of PBMCs with tCD40L-3T3 NIH feeder cells (section 2.2.5.1). Cells were stained with an antibody against CD19, a B cell marker, and antibodies against CD4 and CD8, markers for T cells, to discriminate between these cell populations.

In addition, different protocols for generation of DCs (section 2.2.5.1) were compared and monitored by multi-color stainings. To this end, cells were stained on day 0, day 3, and day 8 to follow their

development. A panel of antibodies against CD14, CD80, CD83, CD86 and HLA-DR was used to discriminate between monocytes, immature Mo-DCs and mature Mo-DCs, displaying the following phenotypes:

monocytes: $CD14^+$, $CD80^-$, $CD83^-$, $CD86^+$ and $HLA\text{-}DR^+$

immature monocyte-derived (Mo-)DCs: $CD14^-$, $CD80^+$, $CD83^-$, $CD86^+$ and $HLA\text{-}DR^+$

mature Mo-DCs: $CD14^-$, $CD80^-$, $CD83^+$, $CD86^+$ and $HLA\text{-}DR^+$

HLA staining

To estimate the expression level of HLA molecules on cell lines, cells were stained for their respective HLA type to be able to isolate high amounts of presented peptides in the subsequent immunoprecipitation (section 2.2.3.2). Here, cells were only stained for the known HLA type. In addition, PBMCs from buffy coats that were used to generate peptide-specific short-term T cell lines (section 2.2.5.1) were also stained with specific antibodies against various HLA supertypes to determine their HLA type. In this case, antibodies against all HLA supertypes analyzed in our laboratory, HLA-A2, HLA-3, HLA-A11, HLA-A24, HLA-B7 and HLA-B15 were included. For each HLA type, a positive control with cells with known HLA type was included as reference.

Briefly, cells were either detached with trypsin-EDTA or taken from suspensions, washed twice with 1xPBS, counted and at least $1x10^6$ cells were resuspended in 1mL 10% FCS in 1xPBS for blocking. Of this cell suspension 100µL ($1x10^5$ cells) were transferred to a well of a 96-well plate which was subsequently centrifuged at 1200rpm for 5min at 4°C. Unstained controls and controls for background fluorescence of the secondary antibody alone were included if necessary. After discarding the SNT, the cells of one well were incubated with 100µL solution of the desired antibody diluted in FACS buffer (section 2.1.11.1) for 30 to 60min at 4°C in the dark. In case of unstained controls, cells were incubated in FACS buffer without antibody. If a secondary antidody was necessary for detection, cells were washed twice with 150 µL/well FACS buffer before 100µL FACS buffer with the fluorochrome-conjugated secondary antibody (section 2.1.11.2) was added. Cells were incubated for 30min at 4°C in the dark. Afterwards, cells were washed twice with 150µL FACS buffer, resuspended in 100µL FACS buffer, stored on ice and analyzed with a flow cytometer.

2.2.4.5 Peripheral blood mononuclear cell (PBMC) isolation

Peripheral blood mononuclear cells (PBMCs) were either isolated from fresh blood donations or from buffy coats obtained from the DRK through the IKTZ (Heidelberg, Germany) by density gradient centrifugation. Prior to PBMC isolation, Ficoll-Paque™ PLUS (GE Healthcare Bio-Sciences, Uppsala, Sweden) and ACK lysis buffer (section 2.1.2) were brought to RT.

First, the blood or buffy coat was diluted 1:1 or 1:10, respectively, in 1xPBS to improve detection of cells after centrifugation. In case of fresh blood donations, special Leucosep tubes (Greiner Bio-One,

Frieckenhausen) containing a porous barrier were used for gradient separation. 15mL Ficoll-Paque™ PLUS were pipetted into each tube and spun down at 1400rpm for 1min at RT. The Ficoll-Paque™ PLUS was then located directly under the barrier. 30mL of diluted blood were then poured carefully directly on top of the barrier. If PBMCs were isolated from buffy coats, 50mL tubes were filled with 30mL each of the diluted buffy coat. About 15mL of Ficoll-Paque™ PLUS solution were added underneath the diluted buffy coat by using a 10mL glass pipette. To this end, the liquid was aspirated to fill the pipette up to the rim. Then the pipette was closed with a thumb and transferred to the 50mL tube, where the pipette was carefully placed into the tube to the tip of the bottom. The thumb was released to let the ficoll form a layer underneath the diluted buffy coat. As soon as the liquid surfaces inside the pipette and the tube were at the same level, the pipette was carefully lifted until its tip reached the layer boundary. When the surfaces were balanced again, the pipette was closed with the thumb and removed carefully from the tube.

Every step was conducted carefully not to disturb the layering of the gradient solution and the blood or buffy coat, respectively. The tubes containing the layered Ficoll-Paque™ PLUS and diluted blood or buffy coat were then centrifuged at 1400rpm for 10min at RT with the centrifuge break turned off to prevent disturbing the layers during deceleration. After careful removal of the tubes from the centrifuge, a clear layer pattern was observed. The Ficoll-Paque™ PLUS containing most of the erythrocytes was located at the bottom of the tube. Clear serum containing soluble blood components and small particles was located at the top of the tube. In between those two layers, an opaque layer containing the desired PBMCs was located. To isolate this layer, most of the serum, down to 1cm above the PBMCs, was aspirated and discarded. The PBMC containing layer was then carefully taken up by using a 5mL glass pipette. The cells were collected in 50mL tubes and the volume was filled to 50mL with 1xPBS. Cells were centrifuged at 1400rpm for 10min at RT. After removing the SNT by decanting, the cell pellet was loosened by grinding the tube on the margin of the sterile hood. As the cells still included erythrocytes, erythrocyte lysis had to be performed. Depending on the size of the pellet, 3 to 5mL of ACK lysis buffer were used to resuspend each cell pellet. The tubes were then shaken gently by inverting for 5min. Lysis was stopped by adding 1xPBS up to 50mL into each tube. Cells were then washed twice with 1xPBS. If cells were sticking to each other, cell suspensions were filtered using a 40µm cell strainer and pooled into a fresh 50mL tube. Eventually, cells were counted and stored on ice for subsequent experiments.

2.2.4.6 Magnetic-activated cell sorting (MACS)

Magnetic-activated cell sorting (MACS) is a method to separate various cell populations depending on their surface molecules (CD molecules). Cells are separated by incubation with magnetic nanoparticles coated with antibodies against a particular surface molecule. Cells that express this molecule attach to the magnetic nanoparticles and can be separated by a strong magnetic field. Thus, cells can be separated positively or negatively with respect to the particular surface molecule. The MACS

technology was used to purify $CD14^+$ monocytes with $CD14^+$ microbeads (Miltenyi Biotec, Bergisch Gladbach) from freshly prepared PBMCs (section 2.2.4.5) and to isolate $CD8^+$ T cells with the $CD8^+$ T Cell Isolation Kit (Miltenyi Biotec, Bergisch Gladbach) from bulk T cell cultures (section 2.2.5.1). All buffers were pre-cooled and cells kept on ice as long as possible. First, cells were counted, adjusted to up to $1x10^8$ cells per sample and washed with ice-cold MACS buffer. The procedures were carried out according to the manufacturer's instructions. Afterwards, cell numbers of purified cells were determined and adjusted to desired cell numbers in respective media.

2.2.5 T cell assays

2.2.5.1 Generation of peptide-specific T cell lines

Peptide-specific T cell lines were generated in order to show immunogenicity of candidate peptides, which were previously identified by competition-based binding assays (section 2.2.3.1). Additionally, peptides with confirmed immunogenicity were used to generate peptide-specific T cells that were tested for their cytolytic capability. To this end, DCs and B cells were matured and activated, which were then peptide-pulsed to serve as antigen-presenting cells (APCs) for stimulation of T cells. Different peptides and protocols, discriminating between short-term, semi long-term and long-term, were established and used to generate peptide-specific T cell lines.

Generation of monocyte-derived dendritic cells (Mo-DCs)

Mature, immunologically competent DCs are the most efficient APCs to stimulate T cells (Steinman, 1991; Banchereau and Steinman, 1998; Thery and Amigorena, 2001). DCs need to be differentiated, matured and activated for this purpose. This is achieved by cultivation with the cytokine IL-4 and the growth factor GM-CSF and final maturation with a cocktail of TNFα, IL-1β, IL-6, PGE_2 and LPS. Matured DCs can then be pulsed with the desired peptide.

$CD14^+$ monocytes were purified by MACS technology (section 2.2.4.6) with magnetic labelling and subsequent isolation. Cells were then resuspended at a concentration of $1x10^6$ cells/mL in DC medium, supplemented with 500U/mL IL-4 and 1000 U/mL GM-CSF and 2mL seeded into wells of a 6-well plate. On day 3 and day 6, 500µL DC medium supplemented with IL-4 and GM-CSF, that reached a final concentration of 500U/mL and 1000U/mL, respectively, were added per well.

A cocktail for final maturation of 1000U/mL TNFα (R & D Systems, Minneapolis, MN, USA), 10ng/mL IL-1β (R & D Systems, Minneapolis, MN, USA), 10ng/mL IL-6 (R & D Systems, Minneapolis, MN, USA), 1µM PGE_2 (1mg/mL) (Cayman Chemical, Ann Arbor, MI, USA) and 1µl/mL LPS (5mg/mL, $5x10^4$ EU/mL) (Invivogen, Toulouse, France) was added on day 6 and cells were incubated for additional 24 hours. On day 8, mature Mo-DCs showed a unique morphology with multiple long thread-like dendrites and were harvested by gentle scraping and pipetting up and down. Cells were then stored on ice for subsequent experiments.

Differentiation and maturation of $CD14^+$ monocytes was followed by flow cytometric analysis as described in section 2.2.4.4. (data not shown).

Generation of CD40-activated B cells

To generate CD40-B cells from naïve B cells , the following protocol was used. CD40-activated B cells (CD40-B cells) have been identified as an alternative source of immuno-stimulatory APCs to DCs for cancer immunotherapy studies (Schultze et al., 1997; Schultze et al., 2004; von Bergwelt-Baildon et al., 2006). Upon stimulation with IL-4 and CD40 ligand, CD40-B cells show a strong migratory capacity, an increased expression of HLA and costimulatory molecules and present antigens efficiently to T cells (Liebig et al., 2009).

Preparation of tCD40L NIH/3T3 feeder cells, an adherent murine fibroblast cell line, was always done one day before the initial PBMCs were ready or before reculturing of CD40-B cells (see schedule, Tab. 13). tCD40L NIH/3T3 feeder cells were never kept in culture for more than six weeks, never grown completely confluent und usually split every three days. Cells were harvested as described before (2.2.4.2) and adjusted to the desired cell number, which was needed to prepare tCD40L NIH/3T3 feeder 6-well plates. Left over tCD40L NIH/3T3 feeder cells were split in an appropriate dilution and kept in culture in tCD40L WT medium. tCD40L NIH/3T3 feeder cells for plating were irradiated at 98Gy (Gammacell 1000; Atomic Energy of Canada Limited, Ottawa, Canada) and washed twice with 1xPBS and centrifugation at 1400rpm for 5min at RT. Then, $2x10^5$ cells/mL and 2ml per well in tCD40L NIH3T3 medium were seeded into 6-well plates an incubated o/n at 37°C and 5% CO_2.

On day 0, PBMCs were obtained as described in 2.2.4.5. Cells were then resuspended in B cell medium at $2x10^6$ cells/mL. Cyclosporin A (Sigma, St. Louis, MO, USA) was added at 0.55ng/mL to prevent outgrowth of T cells and IL-4 at 50U/mL as growth factor. Cells were kept on ice until the tCD40L NIH/3T3 feeder cells plates were ready. Confluency and adherence of tCD40L NIH/3T3 feeder cells was confirmed and the medium aspirated with a 2mL pipette and the pump system. Now, 4ml/well of PBMC cell suspension were added carefully at the side of the well and incubated at 37°C and 5% CO_2. Cells were not disturbed for the first 96hrs.

For reculturing of PBMCs/CD40-B cells, the schedule shown in Table 13 was followed. Cells were harvested by vigorously pipetting up and down with a 5mL pipette. Production of air bubbles was avoided. Cells were collected in 50mL tubes, washed with 1xPBS and centrifuged at 1400rpm for 5min at RT. Now, the same procedure as for the initial culturing of PBMCs was conducted with the indicated number of cells.

Table 13 I Schedule for culturing of PBMCs/CD40-B cells and preparation of tCD40L plates.

Day	Task	Number of cells
day -1	preparation of tCD40L plates	
day 0	start of co-culture	
day 4	preparation of tCD40L plates	
day 5	reculture of PBMCs	$2x10^6$ PBMCs/ml
day 7	preparation of tCD40L plates	
day 8	reculture of CD40-B cells	$1.5x10^6$ PBMCs/ml
day 11	preparation of tCD40L plates	
day 12	reculture of CD40-B cells	$1x10^6$ B cells/ml
day 14	preparation of tCD40L plates	
day 15	reculture of CD40-B cells	$7.5x10^5$ B cells/ml
day 18	preparation of tCD40L plates	
day 19	reculture of CD40-B cells	$1x10^6$ B cells/ml
day 21	preparation of tCD40L plates	
day 22	reculture of CD40-B cells	$7.5x10^5$ B cells/ml
etc.		

If the viability of CD40-B cells was less than 70%, cells were subjected to Ficoll-Paque™ PLUS treatment (section 2.2.4.5) omitting the ACK lysis step, to remove dead cells. In addition, CD40-B cells were always ficolled before they were used as APCs. If there were still a lot of tCD40L NIH/3T3 cells contaminating the CD40-B cell population, a 20min adherence step was performed.

Quantity of $CD19^+$ cells in the culture was monitored regularly between day 8 and 22 by flow cytometry (section 2.2.4.4). CD40-B cells should be at least 85% $CD19^+$ on day 8 and 95% on day 12. This was always achieved (data not shown).

If not all activated CD40-B cells were used for stimulation of T cells or other experiments, they were cryopreserved for later use.

Generation of the Epstein-Barr Virus (EBV)-transformed B cell line "RiSH"

Since CD40-B cell were not always available in the amount that was needed for experiments, B cells from a regular HLA typed donor were immortalized with EBV to be always accessible for use.

The protocol used was slightly modified from (Tosato and Cohen, 2007). Briefly, 11mL EBV SNT (from B95.8 marmoset cells, titer: $1x10^7$, MOI: 2.5) were added to $6x10^7$ PBMCs (section 2.2.4.5) in 1ml RPMI with 20% FCS in a 50mL tube and incubated for 2hrs at RT on a roller. Cells were centrifuged at 1200rpm for 10mins at 4°C and seeded at $3x10^7$ cells/mL in RPMI with 20% FCS in 1mL per well into a 24-well plate. In order to prevent outgrowth of T cells and kill regulatory T cells that might prevent growth of EBV-B cells in EBV-seropositive donors, medium was supplemented with 1mg/mL cyclosporin A (Sigma, St. Louis, MO, USA). Morphology, viability and formation of cell clusters were monitored daily. Two days post infection, fresh medium was added and five day post infection the first clusters appeared that were then transferred in groups of at least five clusters to new wells of the 24-well plate. Transfer of cell clusters was done for four weeks every couple of days,

increasing the medium volume slowly from time to time. Cells were thus kept first in 24-well plates, then in 6-well plates and finally grown in 25cm^2 and 75cm^2 flasks. The purity of the B cell population was confirmed by FACS staining (section 2.2.4.4) before cyclosporine A treatment was stopped and cells were either used directly for experiments or cryopreserved. During cultivation, the percentage of FCS in the medium was slowly reduced from 20 to 10%. EBV SNT was kindly provided by Katharina Bernhardt, Division of Pathogenesis of Virus Associated Tumors (F100, Henri-Jacques Delecluse), DKFZ.

Peptide-pulsing of APCs

To prepare Mo-DCs and B cells for peptide-pulsing, cells needed to be washed with the respective serum-free DC or B cell medium, to avoid presentation of FCS peptides later one. Washing was performed once with centrifugation at 1400rpm for 5min at RT. DCs were then irradiated at 30Gy and B cells at 32Gy. Subsequently, washing was performed three times with centrifugation at 1400rpm for 5min at RT to remove toxic compounds formed during irradiation. Cells were then resuspended in the respective serum-free medium at a concentration of 1x10^6 cells/mL and transferred to 15mL tubes. The desired peptide or the corresponding volume of DMSO for negative controls was added at a concentration of 10µg/mL. After peptide addition, cell suspensions were immediately resuspended by pipetting up and down with a 1000µL pipette. The cell suspensions incubated with an unscrewed lid at 37°C and 5% CO_2 for 3-4hrs. The tube were tapped gently once every hour. Afterwards, cells were washed three times with the respective medium containing serum with centrifugation at 1400rpm for 5min at RT. After counting, cells were resuspended in the desired medium and stored on ice for subsequent experiments. If peptide-pulsed APCs were left over, they were cryopreserved for other experiments.

Peptide-specific short-term T cell lines

Peptide-specific short-term T cell lines were established to test the immunogenicity of previously identified peptide candidates in a high throughput manner. A timeline, displaying the work flow is shown in Fig. 15.

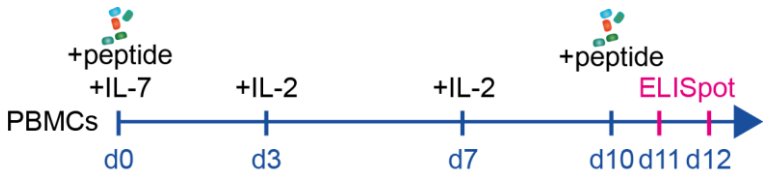

Figure 15 I Schematic work flow of generation of peptide-specific short-term T cell lines. PBMCs are seeded on day 0, stimulated with peptide and IL-7. IL-2 is added on day 3 and day 7, cells are restimulated on day 10 with peptides and ELISpot assays conducted subsequently starting on day 11.

PBMCs were prepared from buffy coats or blood (section 2.2.4.5) and resuspended at a concentration of 1x10^6 cells/mL in R10 medium that was supplemented with 10ng/mL IL-7 (R & D Systems, Minneapolis, MN, USA). In case of buffy coats, 5x10^6 cells were spared for DNA extraction for HLA

typing by PCR (section 2.2.2.2) and $1x10^6$ cells were used for HLA typing by flow cytometry (section 2.2.4.4). The remaining cells were distributed to 24-well plates in a volume of 1mL/well. Plates were incubated at 37°C and 5% CO_2 until HLA typing by FACS staining was accomplished. Depending on the determined or known HLA types and the number of available cells, HLA-matching peptides and controls were added to individual wells. Duplicates were done if possible. Peptides were added at a concentration of 10µg/mL. Background controls consisted of non-treated and DMSO-treated (peptide diluent) cells, 10µg/mL HLA-specific HIV peptide (only for HLA-A2 and HLA-24) served as negative control. Additionally 2µg/mL ConA (Sigma-Aldrich, Steinheim), 5µg/mL PHA (Sigma-Aldrich, Steinheim) and 2µg/mL CEF-Class I Peptide Pool "Classic" (Cellular Technology Limited, Shaker Heights, OH, USA) and/or 10µg/mL HLA-specific EBV peptide were used as positive controls. Cells were then incubated at 37°C and 5% CO_2. On day 3 and day 7, plates were centrifuged at 1400rpm, 500µL medium was carefully removed from each well by holding the plate at an 45° angle not to aspirate any cells, collected and frozen at -20°C for other experiments. 1mL R10 medium was added for washing per well. This washing step was repeated twice and then 500µL R10 medium supplemented with 40U/mL IL-2 (PeproTech, Rocky Hill, NJ, USA) were added to achieve a final concentration of 20U/mL IL-2 per well. On day 11, plates were centrifuged at 1400rpm for 5min at RT, the medium was carefully removed and cells were washed once with 1mL R10 medium per well. Cells were resuspended in 1mL R10 medium and restimulated with the same peptides as on day 0. Cells were once more incubated for 18-20hrs at 37°C and 5% CO_2. Subsequent steps for IFNγ ELISpot are described in section 2.2.5.3.

Peptide-specific long-term T cell lines

Peptide-specific long-term T cell lines for four selected peptides, HPV16 E6/87-95var, HPV16 E6/49-57, HPV16 E6/49-59 and HPV16 E7/56-65, were established from three HLA-A24 positive healthy donors (Fig. 16). Those four peptides were chosen because of a strong binding affinity to HLA-A24 *in silico* (sections 3.1.1, 3.1.3, 3.2), *in vitro* (sections 3.1.2, 3.2) and because they were shown to be immunogenic when screening for long-term T cell memory responses (section 3.4.2, Fig. 30-31).

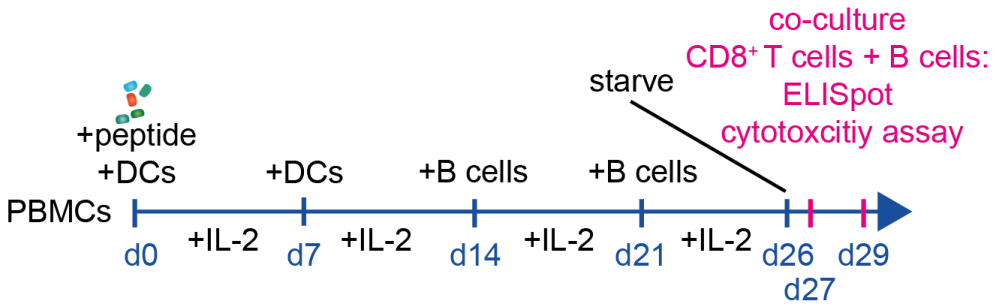

Figure 16 I Schematic work flow of generation of peptide-specific long-term T cell lines. PBMCs are seeded on day 0, stimulated with peptide and peptide-pulsed DCs. IL-2 is added five days after each stimulation. Cells are restimulated on day 7 with peptide-pulsed DCs and on day 14 and 21 with peptide-pulsed activated autologous B cells. On day 26, cells are starved and used for co-culture for various subsequent experiments on day 27.

Seven days prior to PBMC seeding, DCs were differentiated from donor monocytes and used as APCs as described above. Matured DCs were peptide-pulsed and plated together with freshly isolated PBMCs (section 2.2.4.5) from the same donor. Here, specifically, $1x10^7$ PBMCs and at least $5x10^4$ peptide-pulsed DCs, to reach a ratio of 1:200, were plated in 2mL T cell medium supplemented with 10ng/mL IL-7 in one well of a 24-well plate. If possible, a ratio of PBMCs to DCs of 1:50 was pipetted. In addition, the respective peptide was also added to the well at a concentration of 10µg/mL. On day 5 after stimulation, the plate was centrifuged at 1400rpm for 5min at RT and 1mL SNT was aspirated. 1mL T cell medium supplemented with 40U/mL IL-2 was added to reach a final IL-2 concentration of 20U/mL per well. Seven days after the first stimulation, PBMCs were restimulated with fresh peptide-pulsed DCs as before. This time, however, no peptide was added. Again, IL-2 was added five days later in the same manner as described before. This scheme was followed until day 26. On day 14 and 21, however, restimulation was performed with autologous activated peptide-pulsed B cells, which were generated by using the tCD40L/NIH-3T3 system. On day 26, cells were starved o/n in plain T cell medium without any cytokine supplements. To this end, cells were washed twice with 2mL of T cell medium and centrifuged at 1400rpm for 5min at RT before cells were resuspended in 2ml T cell medium.

As subsequent assays, IFNγ ELISpot (section 2.2.5.3) and cytotoxicity assays (section 2.2.5.5) were performed, to assess if the established T cell line was functionally active (IFNγ secretion) and had cytolytic activity against cells presenting the cognate peptide.

Peptide-specific semi long-term T cell lines

Peptide-specific semi long-term T cell lines were generated for the same purpose as long-term T cell lines. Here, only two stimulations with peptide-pulsed DCs were done, and the third and fourth stimulation with peptide-pulsed activated B cells were omitted. The IL-2 concentration, however, was increased from 20U/mL to 50U/mL and fresh IL-2 was added to the T cells every other day (Fig. 17).

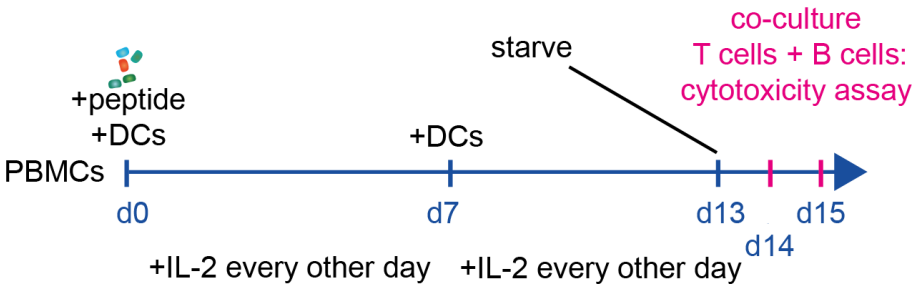

Figure 17 I Schematic work flow of generation of peptide-specific semi long-term T cell lines. PBMCs are seeded on day 0, stimulated with peptide and peptide-pulsed DCs. IL-2 is added every second day. Cells are restimulated on day 7 with peptide-pulsed DCs. On day 13, cells are starved and used for cytotoxicity assays on day 14.

2.2.5.2 T cell receptor sequencing

T cell receptor (TCR) sequencing of peptide-specific long-term $CD8^+$ T cell lines was kindly performed by Eliana Ruggiero, Division of Translational Oncology (G100, Christoph von Kalle), DKFZ. In short, cells were resuspended in a provided lysis buffer. RNA was extracted, purified and cDNA of the TCR α- and β-chain was reverse transcribed. Sequencing on an Illumina machine was carried out by using primers attaching to conserved flanking sequences. Thus, the quantity and variability of α- and β-chain TCRs in the T cell lines was determined.

2.2.5.3 Interferon (IFN)γ ELISpot assays

The interferon (IFN)γ ELISpot assay is widely used as a general screening method for the quantification of antigen-specific $CD8^+$ T cell responses. Two different approaches were followed to this end. In case of peptide-specific short-term T cell lines, PBMCs were incubated with peptides as described above. In case of peptide-specific long-term T cells lines, peptide-pulsed autologous B cells served as targets for $CD8^+$ T cells.

IFNγ ELISpot assays were performed, depending on whether short-term or long-term T cell lines were used, two days after the last peptide stimulation or seven days after the last stimulation with peptide-pulsed APCs, respectively (section 2.2.5.1). All steps on the first two days were carried out under sterile conditions in a flow hood. On day 1, 96-well MultiScreen®-HA plates (Merck Milipore, Cork, Ireland) were coated with 100 µL/well anti-human IFNγ capture antibody (Mabtech, Nacka Strand, Sweden) diluted 1:500 in 1xPBS. Plates were wrapped in cling foil and incubated at 4°C o/n. On day 2, capture antibody was removed by inverting the plate quickly and tapping it afterwards on a paper tissue. Plates were washed with 1xPBS three times in the same manner. Plates were then blocked with 200µL corresponding culture medium for 1-2hrs at 37°C and 5% CO_2. Either peptide-specific $CD8^+$ T cells, bulk T cell cultures or PBMCs (sections 2.2.5.1 and 2.2.4.5) and peptides or peptide-pulsed autologous B cells (section 2.2.5.1) were prepared during this incubation time. The blocking medium was removed and between 1 - $5x10^5$ cells/well of peptide-specific $CD8^+$ T cells, bulk T cell cultures or PBMCs were seeded in a volume of 50-100µL. In case of peptide stimulations, 1µL/mL DMSO was used as a background control and 10µg/mL HIV peptides as negative control, if applicable for the

respective HLA-type. Additionally, 2µg/mL ConA, 5µg/mL PHA and 2µg/mL CEF-Class I Peptide Pool "Classic" were used as positive controls. Peptide stimulation was already performed on day 0 and 10 of short-term T cell line generation (section 2.2.5.1). For co-culture of peptide-specific $CD8^+$ T cells between 2-4x10^4 cells/well of peptide-pulsed autologous B cells (section 2.2.5.1) were added in a volume of 50µL. 2ng/mL ConA was added to T cells as a positive control, and autologous B cells that were peptide-pulsed with a HLA-matching HIV peptide or DMSO were used as negative controls. Autologous B cells were also seeded alone as a background control. A typical loading scheme for co-culture of peptide-specific T cells and peptide pulsed autologous B cells is depicted in Figure 18, it was, however, adapted depending on the number of available cells and peptides tested.

T			**E6 87-95var**	**E6 49-57**		**E6 87-95var**	**E6 49-57**		**E6 87-95var**	**E6 49-57**		
B			*DMSO*	*DMSO*		*E6 87-95var*	*E6 49-57*		*HIV A24*	*HIV A24*		
	1	2	3	4	5	6	7	8	9	10	11	12
A												
B												
C												
D												
E			**E6 87-95var** ConA	**E6 49-57** ConA		*DMSO*	*HIV A24*	*E6 87-95var*	*E6 49-57*			
F			**E6 87-95var** ConA	**E6 49-57** ConA		*DMSO*	*HIV A24*	*E6 87-95var*	*E6 49-57*			
G			**E6 87-95var** ConA	**E6 49-57** ConA		*DMSO*	*HIV A24*	*E6 87-95var*	*E6 49-57*			
H												

Figure 18 I Plate loading scheme of IFNγ ELISpot. Co-culture wells of T cells with indicated peptide-specificy and indicated peptide pulsed-B cells are displayed in blue. Positive control wells with peptide-specific T cells stimulated with ConA are shown in green, while wells with peptide-pulsed B cells alone are depicted in yellow.

Triplicates were done if possible. After incubation for 16-24hrs at 37°C and 5% CO_2, cells were removed and plates were washed seven times with 0.05% Tween20 in 1xPBS (TPBS). 100µL of biotinylated anti-human IFNγ antibody (Mabtech, Nacka Strand, Sweden) diluted 1:1000 in 1xPBS were added per well and incubated for 2hrs at RT. After removing the detection antibody, plates were washed four times with 1xTPBS. Then, 100µL streptavidin-alkaline phosphatase (Mabtech, Nacka Strand, Sweden) diluted 1:1000 in 1xPBS were added per well and incubated for 90min at RT in the dark. Plates were subsequently washed four times with 1xTPBS. 100µL/well 1-Step™ NBT/BCIP substrate (Thermo Scientific, Rockfort, IL, USA) were added and incubated in the dark. The staining reaction was monitored for around 20-30min and stopped by rinsing the plates thoroughly with distilled water. Plates were left to dry for at least 2hrs in a flow hood or o/n on the bench. Spots were then quantified with an AID ELISpot reader (Autoimmun Diagnostika, Strassberg).

2.2.5.4 IL-2 Enzyme Linked Immunosorbent Assay (ELISA)

IL-2 Enzyme Linked Immunosorbent Assays (ELISAs) were performed with SNT from peptide or APC-stimulated T cells (section 2.2.5.1) to test the secretion of this pro-proliferation cytokine.

On day 1, 96-well Costar™ high binding plates (Thermo Fisher Scientific, Rochester, NY, USA) were coated with 100µL/well of 4µg/mL LEAF™ purified anti-human IL-2 capture antibody (BioLegend, San Diego, CA, USA) in carbonate coating buffer (pH 9.5, section 2.1.2). The plates were wrapped in cling foil and incubated at 4°C o/n. On day 2, capture antibody was removed by inverting the plate quickly and tapping it afterwards on a paper tissue. The plate was washed with 0.05% Tween20 in 1xPBS (TPBS) and blocked with 200µL/well 0.2% gelatine in 1xPBS for 1hr at 37°C and 5% CO_2. The blocking solution was removed and 100µL sample or standard (recombinant human IL-2 standard; BioLegend, San Diego, CA, USA) were added per well and incubated o/n at 4°C or for 3hrs at RT. The samples were removed and plates washed five times with TPBS. For detection, biotin anti-human IL-2 antibody (BioLegend, San Diego, CA, USA) was diluted 1:2000 in TPBS, 100µL/well were added and incubated for 1-2hrs at RT. Detection antibody solution was removed and the plate was washed five times with TPBS. Avidin-Horseradish Peroxidase (HRP) (BioLegend, San Diego, CA, USA) was diluted 1:1000 in TPBS and 100µL/well were added and incubated for 30min at RT. In the meantime, TMB substrate (BioLegend, San Diego, CA, USA) was prepared and pre-warmed to RT. The Avidin-HPR solution was removed and the plate was washed five times again with TPBS. 100µL/well of TMB substrate was added for color development and the plate was wrapped in aluminium foil. After 4 to 30min, the color reaction was stopped with TMB Stop solution (BioLegend, San Diego, CA, USA). The optical density (OD) was read for each well with a microplate reader, Victor^3 (Perkin Elmer, Waltham, MA, USA), set to 405nm.

2.2.5.5 Cytotoxicity assay

In vitro cytotoxicity assays were performed to assess the cytotoxic capacity of peptide-specific T cells by using the standard method based on chromium release. In this assay, target cells are pre-labeled by incubation with ^{51}Cr. These target cells are then incubated with effector cells, which will lyse the target cells. The amount of radioactivity that is released in the SNT, is taken as an indicator of the amount of lysis that has occurred.

Autologous peptide-pulsed B cells were taken as target cells, adjusted to $1x10^6$ cells and were centrifuged at 1400rpm for 5min at RT. Target cells were peptide-pulsed with the peptide that was used to generate the effector cells for 3hrs as described in section 2.2.5.1. As negative control, autologous B cells that were pulsed with HIV HLA-A24 peptide: RYLKDQQLL were used, which should not be recognized by HPV-specific T cells. The cell pellet was resuspended in 200µL medium and labeled with 100µL of $Na_2{}^{51}CrO_4$-solution (5 mCi, 185 MBq, Perkin-Elmer, Waltham, MA, USA) for 90min at 37°C and 5% CO_2.

Peptide-specific T cells, which were generated as describe before (2.2.5.1), were used as effector cells. They were adjusted to $2.5x10^6$ cells/mL for a 50:1 effector:target ratio or to less when fewer cells were available and were titrated in 1:1 dilution steps into the wells of a round bottom 96-well plate.

After three washing steps with medium at 1400rpm for 5min at RT, target cells were counted and adjusted to $5x10^4$ cells/mL. For co-culture, 100µL of labeled target cells were added to the serial dilution of effector cells. A typical loading scheme is depicted in Figure 19. In addition, target cells were added to wells to determine spontaneous lysis (assay medium) or maximum lysis (10% Triton-x100 in medium).

T			**E6 87-95var**	**E6 49-57**	**E6 87-95var**	**E6 49-57**	**E6 87-95var**	**E6 49-57**	**E6 87-95var**	**E6 49-57**		
B			*E6 87-95var*	*E6 49-57*	*HIV A24*	*HIV A24*	*E6 87-95var*	*E6 49-57*	*HIV A24*	*HIV A24*		
	1	2	3	4	5	6	7	8	9	10	11	12
A		50:1										
B		25:1										
C		12.5:1										
D		6.25:1										
E		1.5625:1										
F												
G												
H												

Figure 19 I Plate loading scheme for cytotoxicity assays. Co-culture wells of T cells with indicated peptide specificity and indicated peptide pulsed-B cells are displayed in blue. Ratios of effector to target cells are displayed on the left side. Maximum lysis control wells with target cells treated with Triton-x100 are shown in green, while control wells for spontaneous lysis, target cells in medium, are depicted in yellow.

Plates were spun down briefly at 300rpm and RT to bring the target and effector cells into close proximity. The plates were then incubated for 5hrs at 37°C and 5% CO_2. After centrifugation at 1400rpm for 5min at RT, 100µL of SNT were transferred to LumaPlates (Perkin Elmer, Waltham, MA, USA). After drying o/n under the hood, the plates were read with a γ-counter (TopCount NXT™; Perkin Elmer, Waltham, MA, USA). Specific cytotoxicity (lysis) was calculated with the following formula:

$$\%\ \text{specific lysis} = \left[\frac{\text{cpm (sample)} - \text{cpm (spontaneous lysis)}}{\text{cpm (maximum lysis)} - \text{cpm (spontaneous lysis)}}\right] \text{x } 100$$

3. Results

To date, three prophylactic vaccines are available that can protect from infection with the major cancer-causing HPV types (Harper et al., 2004; Villa et al., 2005; Joura et al., 2015). Still, a therapeutic vaccine is desirable that can clear already established infections and thus prevent the development of HPV-driven invasive cancer. The overall goal of our group is the development of a therapeutic vaccine that elicits T cell-mediated immune responses against HPV16-infected cells. This study aimed at the identification of specific T cell epitopes that can elicit $CD8^+$ T cell-mediated immune responses.

To this end, the strategy of reverse immunology, first described in 1994, was employed (Celis et al., 1994). Predictions of potential T cell binding peptides, 8mers to 11mers, derived from HPV16 E6 and E7 proteins were calculated using different web-based prediction servers. *In silico* predictions were performed for the representative alleles of the HLA-A3, HLA-A11 and HLA-A24 supertypes, HLA-A*03:01, HLA-A*11:01 and HLA-A*24:02, respectively (section 3.1.1). These three frequent HLA supertypes were selected because together they provide a high population coverage in all ethnic groups (Gonzalez-Galarza et al., 2015). Predicted peptides were ranked according to their IC_{50} or highest score. The actual binding affinity of best predicted peptides to the respective HLA molecules was tested in competition-based cellular binding assays (section 3.1.2) (Kessler et al., 2003; Kessler et al., 2004). To identify strongly binding peptides that are not well-predicted *in silico*, amino acid motifs of identified binding and non-binding peptides were created, the HPV16 E6 and E7-derived peptide repertoire was scanned for motif-matches *in silico* and resulting strong-matching tested peptides *in vitro* (section 3.1.3). Moreover, several HPV16 variants exist, that differ in their E6 and E7 protein sequences. These sequence differences might change the set of peptides presented on HPV16-transformed cells. Amino acid exchanges in various HPV16 variants were identified, predictions performed for the respective protein sequences and the binding affinities of predicted binders to HLA-A24 was tested *in vitro* (section 3.2). To identify HPV16 E6 and E7 peptides that are naturally processed and presented on the cell surface of HPV16-transformed cells, HPV16-positive cell lines were stained for expression levels of HLA molecules of interest and HLA/peptide complexes were isolated from these cell lines via immunoprecipitation (section 3.3). Peptides were eluted for subsequent mass spectrometry (MS) analysis. MS analysis is performed by Renata Blatnik, another PhD student in our laboratory. Immunogenicity of identified peptides was assessed by establishing T cell lines from PBMCs from HLA-matched blood donors (section 3.4). Functional assays such as ELISpot assays and cytotoxicity assays were conducted to determine the best vaccine candidates (section 3.5). Single steps of the workflow are depicted schematically in Figure 20.

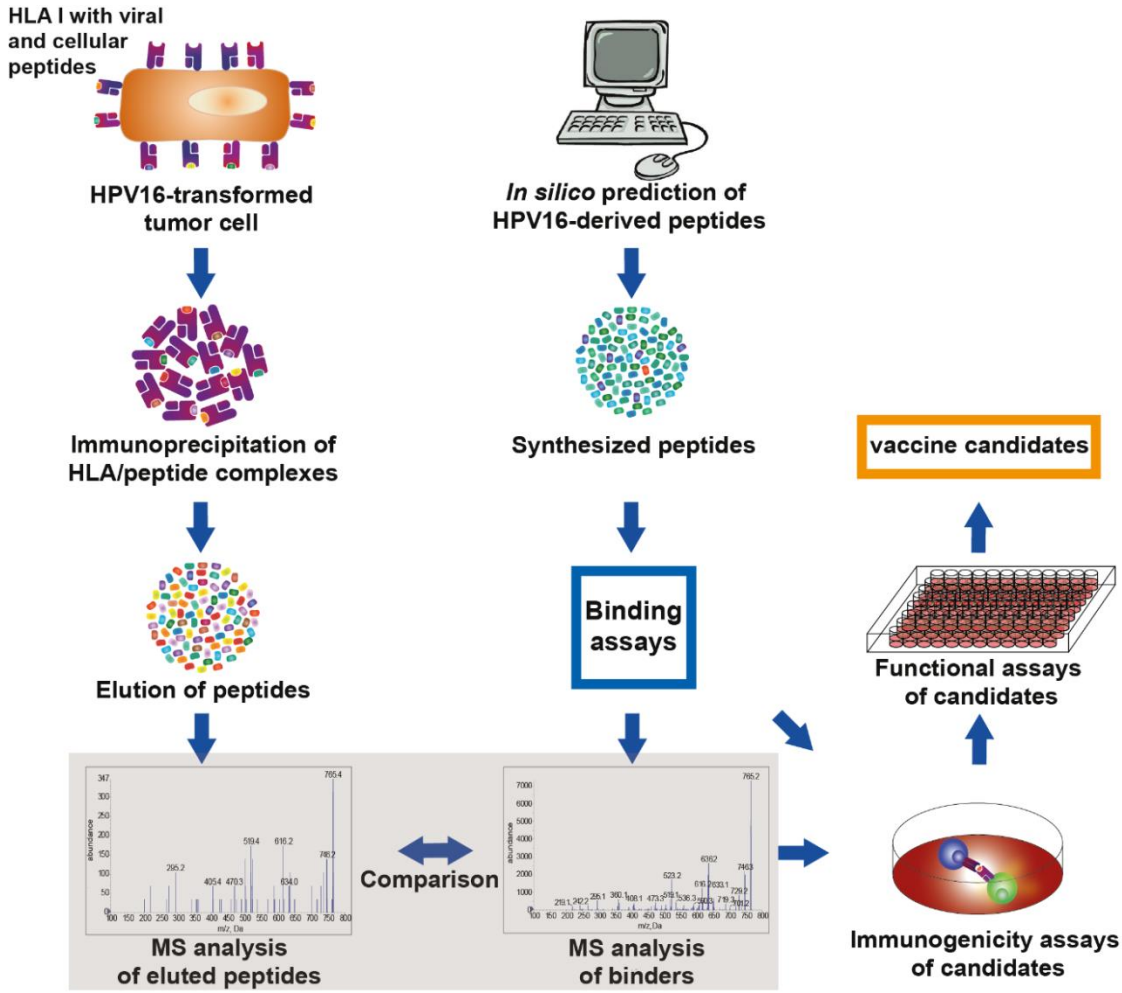

Figure 20 I Schematic overview of the experimental set up. The workflow of T cell epitope identification for a therapeutic HPV16 E6 and E7 vaccine is depicted. Grey shading indicates cooperation with another PhD project in our laboratory.

3.1 *In silico* predictions and *in vitro* binding affinity of HPV16 E6 and E7 peptides to HLA-A3, HLA-A11 and HLA-A24 molecules

In the first part of this study, T cell epitopes from the HPV16 E6 and E7 proteins of the HPV16 reference sequence (NC_001526) were identified. The E6 and E7 proteins were chosen for epitope predictions for multiple reasons. They are constantly expressed in all stages of HPV16-mediated carcinogenesis as they are crucial for induction and maintenance of the malignant phenotype. Being viral and thus resulting in presentation of foreign viral epitopes on infected cells, these antigens allow immunological distinction of infected cells from healthy tissue. Moreover, as HPV is replicated using the host's cellular replication machinery, mutation rates are very low in these viral proteins preventing immune escape (Frazer et al., 2011). Since 941 peptides with a length of 8 to 11 amino acids can be derived from the HPV E6 and E7 proteins, binding affinities were first predicted *in silico* to reduce the number of peptides to be tested *in vitro*. Predictions were performed with high throughput *in silico* approaches that estimated potential binding to chosen HLA types. Predicted strong binders were further tested experimentally for their actual binding affinity to the HLA types of interest in

competition-based cellular binding assays (Kessler et al., 2003; Kessler et al., 2004). The three HLA supertypes HLA-A3, HLA-A11 and HLA-A24 were selected because all three together cover a high percentage of the world's population (Gonzalez-Galarza et al., 2015). While HLA-A24 is widely spread amongst Asian populations, reaching 58.6% in the Japanese population, up to 37.5% in Caucasians harbor HLA-A3 and HLA-A11 alleles.

3.1.1 T cell epitope predictions reveal numerous potential HLA binding HPV16-derived peptides

Multiple prediction servers were chosen for T cell epitope predictions to exploit the individual strengths of each single server. Servers are based on different algorithms and trained with different data sets. A set of six different web-based prediction servers employing ten different algorithms was selected (Parker et al., 1994; Rammensee et al., 1999; Nielsen et al., 2003; Peters and Sette, 2005; Nielsen et al., 2007; Lundegaard et al., 2008a; Karosiene et al., 2012). To combine all results in a sortable excel sheet, the PERL script PeptidePrediction.pl, developed in our laboratory, was applied. Complete lists of E6 and E7 peptides that were predicted and tested for HLA-A3, HLA-A11 and HLA-A24 binding are displayed in Tables 14 and 15 and Tables 22-25 (Appendix). The results of all predictors giving an IC_{50} value as output were combined to an average IC_{50} value for each peptide to determine overall testing cutoffs. The thresholds for *in vitro* testing were lowered throughout the course of experimental binding affinity assessment, as a final stage where none of the predicted peptides was binding anymore, was not reached. Moreover, cutoffs were chosen individually for all servers to make sure not to exclude any peptides that were indicated to possibly bind by one individual server.

Of the 941 potential peptides, 69 peptides, 48 for the E6 protein and 21 for the E7 protein, were predicted to bind to HLA-A24 with an average IC_{50} below 7000nM. In case of HLA-A3 and HLA-A11, the chosen general cutoffs were 5000nM for the average IC_{50}. For HLA-A3, 55 E6 and 16 E7 peptides were predicted to be binders. In case of HLA-A11, 70 E6 and 19 E7 peptides were predicted to bind. For clarity reasons, only HLA-A24 results are shown in Tables 14 and 15. For HLA-A3 and HLA-A11, please refer to the Appendix (Tab. 22-25). Tables 14 and 15 display the binding affinities for each peptide color-coded according to their predicted and experimental binding strength to HLA-A24. Not all servers predicted peptides that were actually binding to HLA-A24 and *vice versa*, not all peptides that were *in silico* predicted to bind, did actually bind experimentally. This applies to many peptides that were predicted to be weak or intermediate binders. Of note, no peptides were predicted to strongly bind to HLA-A24 by the NetMHC and IEDB servers. In conclusion, none of the servers employed showed clear superior results in comparison to the others and thus the average IC_{50} of NetMHC and IEDB servers was selected as one cutoff among individual cutoffs for individual servers as indicated in Tables 14 and 15. Highlighted peptides in *Italic* were not predicted by prediction servers, but were added because they were identified as potential binders by the motif analysis mentioned above and described below (section 3.1.3). Dashes in the table indicate that prediction of

this peptide length was not supported by the respective server and empty cells that the predicted binding affinity was above the chosen cutoff which was selected during initial individual predictions (40000nM for all NetMHC and IEDB servers).

Table 14 I Predicted and experimental binding affinities to HLA-A24 for HPV16 E6 peptides. Peptides are sorted by the actual binding affinity as determined in the cellular binding assays. Binding affinities are color-coded according to their predicted and experimental binding strength. NetMHC and IEDB servers indicate binding affinities as IC50 [nM] and the average is displayed in the third column from the left. SYFPEITHI and BIMAS show scores as arbitrary units. Dashes indicate that the peptide length was not supported by the respective server and empty cells indicate that the chosen cutoff for the individual prediction server was exceeded. *Italic* highlighting indicates peptides that were determined to be potential binders by motif analysis. The code colors dark blue, blue and light blue indicate strong, intermediate and weak binders, repectively. Individual recommended ([a], [b], [c]) and self-determined ([d], [e], [f]) binding affinities: [a]: strong: < 5µM, intermediate: 5-15µM, weak: 15-100µM, non: > 100µM; [b]: strong: < 50nM, weak: 50-500nM, non: > 500nM; [c]: strong: < 50nM, intermediate: 50-500nM, weak: 500-5000nM, non: > 500nM; [d]: strong: < 50nM, intermediate: 50-500nM, weak: 500-7000nM, non: > 500nM [e]: strong: > 22, intermediate: 22-19, weak: 19-15, non: < 15; [f]: strong: > 240, intermediate: 240-100, weak: 100-10, non: < 100; exp: experimental

peptide	length	exp. IC50 [µM][a]	NetMHC[b]	NetMHC Pan[b]	NetMHC cons[b]	IEDB ann[c]	IEDB smm[c]	IEDB arb[c]	IEDB smmpmbec[c]	IEDB netmhcpan[c]	average IC50[d]	SYFPEITHI[e]	BIMAS[f]
E6/85-95	11	0,10	782	298,02	912,75	-	-	-	-	1196,26	797,26	-	-
E6/49-57	9	0,10	918	260,23	1242,43	918,27	1212,35	1477,97	1379,05	984,56	1049,11	23	240,00
E6/87-95	9	0,12	452	220,05	506,12	452,42	941,67	815,38	955,62	995,27	667,32	20	200,00
E6/49-59	11	0,26	359	187,47	456,69	-	-	-	-	344,70	336,97	-	-
E6/66-76	11	0,28	243	215,22	183,04	-	-	-	-	645,63	321,72	-	-
E6/82-90	9	0,32	485	176,19	681,52	485,94	944,59	171,73	786,27	482,07	526,66	19	200,00
E6/98-107	10	0,54	641	320,50	1249,17	641,43	1843,39	320,67	966,08	1619,56	950,22	23	360,00
E6/98-108	11	0,77	764	80,69	344,70	-	-	-	-	442,10	407,87	-	-
E6/18-26	9	0,83	13649	7391,50	10527,33	13649,07	12695,54	4273,52	10000,34	10757,62	10367,99	13	15,84
E6/60-69	10	1,06	1524	1426,97	2403,86	1524,16	826,25	1845,83	636,62	2607,06	1599,34	13	6,00
E6/67-76	10	1,09	12927	2914,05	6262,79	12927,77	2131,56	26477,50	3084,65	7446,48	9271,47	12	3,30
E6/26-34	9	1,42	9960	6885,20	8950,22	9960,87	5769,79	1095,70	5425,19	7446,48	6936,68	12	-
E6/66-74	9	1,97	2987	4994,68	4129,12	2987,78	2417,63	543,85	3322,73	6829,04	3526,48	20	20,00
E6/82-91	10	1,98	1461	4160,75	4856,71	1461,17	1628,28	8155,47	1199,99	6262,79	3648,27	11	5,00
E6/38-45	8	2,45	356	116,96	273,16	-	-	-	-	743,14	372,31	-	-
E6/98-106	9	2,97	6922	1904,71	4288,48	6922,10	3232,16	783,10	2867,38	5869,13	4098,63	21	300,00
E6/51-59	9	3,35	2918	2271,98	1746,99	2918,64	1001,55	1031,70	1285,49	6755,55	2491,24	17	5,00
E6/88-95	8	3,36	9862	4393,89	7092,61	-	-	-	-	8571,13	7479,91	-	-
E6/76-83	8	3,36	3094	807,68	2252,76	-	-	-	-	1062,03	1804,12	-	-
E6/44-54	11	3,84	6091	3709,41	5382,48	-	-	-	-	7287,08	5617,49	-	-
E6/49-58	10	4,30	22795	4425,62	7016,28	22795,33	968,71		403,99	8853,90	9608,41	14	5,00
E6/48-57	10	4,75	26316	24252,68	23192,26	26316,72		4692,18		29425,27	22365,85	12	5,76
E6/76-85	10	4,76	5504	4887,55	6755,55	5504,09	145,37	3597,79	365,53	7054,34	4226,78	11	
E6/87-96	10	6,87	8746	15398,63	15373,84	8746,03	193,67		259,91	23699,60	10345,38	12	
E6/90-99	10	7,08	16642	2598,01	4062,65	16642,41	2908,53		2089,47	3272,12	6887,88	10	7,20
E6/72-80	9	7,50	3451	3613,62	3167,62	3452,04	2154,86	195,40	1440,51	4989,87	2808,11	16	3,30
E6/35-44	10	8,13	33170	36581,43	31912,64	33170,33		28070,65		34986,78	32981,97	10	
E6/76-86	11	10,60	1928	1112,81	2766,91	-	-	-	-	1235,73	1760,86	-	-
E6/66-75	10	10,93	30424	23055,24	19932,31	30424,20	1332,71	6586,21	2313,76	33144,32	18401,59	12	
E6/50-59	10	11,01	23074	5886,57	10136,12	23074,37	6104,61	1919,25	6959,29	8119,76	10659,25	10	
E6/81-90	10	11,98	13783	7388,10	10246,39	13783,08	11149,56	984,55	7561,08	8208,09	9137,98	10	
E6/38-47	10	22,28	18572	13666,71	15967,20	18572,52	1649,24	14208,27	3299,59	27875,69	14226,40	13	
E6/47-54	8	23,27	6661	7472,81	8342,39	-	-	-	-	10527,33	8250,88	-	-
E6/131-139	9	23,93	2617	287,71	1864,16	2617,66	1540,83	186,64	1763,67	598,54	1434,53	6	
E6/128-136	9	28,64	28763	36595,66	30232,07	28763,13	-	18872,82	-	39837,46	30510,69	2	
E6/75-85	11	32,00	21556	13775,40	16493,98	-	-	-	-	17505,31	17332,67	-	-
E6/86-96	11	36,66	30341		33324,12	-	-	-	-		31832,56	-	-
E6/38-46	9	46,40	6475	11044,46	12183,00	6475,71	3256,63	535,81	2980,63	27875,69	8853,37	15	
E6/128-135	8	46,84	7821	12305,20	7609,38	-	-	-	-	8950,22	9171,45	-	-
E6/75-83	9	51,47	11252	2369,46	5470,55	11252,52	9147,96	32534,00	8892,20	4106,84	10628,19	9	
E6/127-135	9	55,95	18250	34674,63	22451,54	18250,31	9077,38	35918,49	10174,33		21256,67	11	
E6/125-135	11	60,80	17052	17963,69	18882,64	-	-	-	-	18478,42	18094,19	-	-
E6/42-52	11	non-binder	4683	1691,82	2707,68	-	-	-	-	6399,79	3870,57	-	-
E6/44-52	9	non-binder	4438	3493,93	3869,58	4438,46	2884,43	1062,40	2860,01	9654,43	4087,66	10	2,00
E6/124-132	9	non-binder	4281	6074,72	4551,43	4281,62	1692,30	2665,22	1624,08	7860,43	4128,85	14	
E6/76-84	9	non-binder	5695	2363,40	5651,03	5695,84	4421,74	365,41	4927,30	4242,33	4170,26	13	
E6/43-52	10	non-binder	8384	1224,53	1824,25	8384,65	1292,96	11225,05	1013,41	5382,48	4841,42	13	3,00
E6/45-54	10	non-binder	10952	12814,39	12790,86	10952,58	713,18	2356,75	520,03	14099,07	8149,86	12	
E6/87-94	8	non-binder	9504	4665,36	8758,62	-	-	-	-	11233,42	8540,35	-	-
E6/138-146	9	non-binder	13401	5789,73	4989,87	13401,90	5872,85	6220,18	3119,40	16404,99	8649,99	1	
E6/90-98	9	non-binder	7752	18535,08	16583,46	7752,90	1765,11	876,04	2961,56	13356,59	8697,84	11	

E6/86-95	10	non-binder	12452	8267,63	11355,63	12452,21	3691,83	3474,34	3363,25	15541,08	8824,75	10	4,00
E6/138-147	10	non-binder	15881	10125,40	5126,69	15881,56	1810,69	-	876,51	17888,25	9655,73	0	
E6/80-90	11	non-binder	10546	7767,88	10584,44	-	-	-	-	11986,87	10221,30	-	-
E6/85-94	10	non-binder	17108	10602,05	13212,86	17108,63	1331,30	-	1212,91	17505,31	11154,44	10	6,00
E6/81-91	11	non-binder	21935	22891,05	21852,38	-	-	-	-	17505,31	21045,94	-	-
E6/47-57	11	non-binder	20108	20194,14	20589,91	-	-	-	-	24218,04	21277,52	-	-
E6/109-117	9	non-binder	18214	27395,10	24614,30	18214,31	22120,02	13695,08	20203,06	32434,80	22111,33	12	12,00
E6/51-60	10	non-binder	28310	10539,62	10246,39	28310,34	28766,77	-	32185,40	17888,25	22320,97	6	
E6/50-60	11	non-binder	32878	19145,63	22573,33	-	-	-	-	23444,56	24510,38	-	-
E6/126-135	10	non-binder	33076	18647,54	17410,87	33076,26		27422,18		18082,85	24619,28	11	
E6/59-68	10	non-binder	36299	38750,49	34610,27	36299,58	1559,93		2854,29	37739,56	26873,30	0	
E6/73-83	11	non-binder	29213	25271,80	27278,95	-	-	-	-	26123,53	26971,82	-	-
E6/96-106	11	non-binder	24516	26529,74	23571,74	-	-	-	-	34237,82	27213,82	-	-
E6/97-106	10	non-binder	27905	19727,40	20589,91	27905,87	36383,71		36462,87	26123,53	27871,18	10	4,00
E6/11-19	9	non-binder	30651		36931,66	30651,36					32744,67	16	7,92
E6/64-74	11	non-binder	30188	34548,26	27278,95	-	-	-	-	39408,75	32855,99	-	-
E6/128-138	11	non-binder	33875		34237,82	-	-	-	-		34056,41	-	-
E6/36-46	11	non-binder	33136		35752,13	-	-	-	-		34444,07	-	-
E6/65-74	10	non-binder	33112	38780,96	34053,09	33112,06					34764,53	10	4,00
E6/48-58	11	non-binder	33954		31569,21	-	-	-	-	39408,75	34977,32	-	-
E6/128-137	10	non-binder	38406		34798,02	38406,26			35060,22		36667,63	1	

Table 15 I Predicted and experimental binding affinities to HLA-A24 for HPV16 E7 peptides. Peptides are sorted by the actual binding affinity as determined in the cellular binding assays. Binding affinities are color-coded according to their predicted and experimental binding strength. NetMHC and IEDB servers indicate binding affinities as IC50 [nM] and the average is displayed in the third column from the left. SYFPEITHI and BIMAS show scores as arbitrary units. Dashes indicate that the peptide length was not supported by the respective server and empty cells indicate that the chosen cutoff for the individual prediction server was exceeded. *Italic* highlighting indicates peptides that were determined to be potential binders by motif analysis. The code colors dark blue, blue and light blue indicate strong, intermediate and weak binders, repectively. Individual recommended ([a], [b], [c]) and self-determined ([d], [e], [f]) binding affinities: [a]: strong: < 5µM, intermediate: 5-15µM, weak: 15-100µM, non: > 100µM; [b]: strong: < 50nM, weak: 50-500nM, non: > 500nM; [c]: strong: < 50nM, intermediate: 50-500nM, weak: 500-5000nM, non: > 500nM; [d]: strong: < 50nM, intermediate: 50-500nM, weak: 500-7000nM, non: > 500nM [e]: strong: > 22, intermediate: 22-19, weak: 19-15, non: < 15; [f]: strong: > 240, intermediate: 240-100, weak: 100-10, non: < 100; exp: experimental

peptide	length	exp. IC50 [µM][a]	NetMHC[b]	NetMHC Pan[b]	NetMHC cons[b]	IEDB ann[c]	IEDB smm[c]	IEDB arb[c]	IEDB smmpmbec[c]	IEDB netmhcpan[c]	average IC50[d]	SYFPEITHI[e]	BIMAS[f]
E7/49-57	9	0,15	1271	142,84	430,30	1271,89	1198,42	443,07	1386,58	525,66	3984,13	10	4,00
E7/56-65	10	0,75	2929	3552,99	6095,65	2929,71	6023,37	2344,86	3845,98	4151,52	8160,61	17	20,00
E7/48-57	10	1,32	11267	9645,45	6719,10	11267,87	1231,09	776,14	933,70	23444,56	1372,49	11	
E7/50-57	8	2,28	1510	1087,00	1709,59	-	-	-	-	1183,39	5811,00	-	-
E7/51-59	9	6,06	7898	2017,39	2403,86	7898,36	1717,58	335,90	1020,71	5500,22	3599,00	12	10,50
E7/51-58	8	16,51	12750	3501,54	4989,87	-	-	-	-	9245,51	7621,73	-	-
E7/67-76	10	34,74	29517	27513,69	23318,07	29517,43				31060,99	28185,44	11	1,50
E7/69-76	8	84,61	8359	10090,02	8806,13	-	-	-	-	14252,45	10376,90	-	-
E7/77-87	11	non-binder	9445	3621,79	7903,07	-	-	-	-	6682,85	8210,00	-	-
E7/10-20	11	non-binder	6446	5280,10	7054,34	-	-	-	-	12790,86	6913,18	-	-
E7/10-19	10	non-binder	16393	8677,53	12584,95	16392,93	504,79		2343,86	21734,48	7892,83	10	9,90
E7/51-60	10	non-binder	22977	10339,78	11479,16	22977,83	2441,57	1745,32	3922,35	15710,15	11233,08	11	0,90
E7/10-18	9	non-binder	10809	21693,29	17130,58	10809,19	3910,09	471,81	4558,84	29425,27	11449,14	10	0,90
E7/22-31	10	non-binder	25185	23251,23	23828,16	25185,83	1738,60		2917,89	29108,61	12351,01	10	6,00
E7/74-82	9	non-binder	24247	21127,54	20926,80	24247,54	22409,06	8321,77	24756,05	25289,19	18745,05	15	0,60
E7/74-83	10	non-binder	33435	14130,72	16493,98	33435,71	25835,18	20063,15	16146,11	18082,85	10062,00	16	0,72
E7/56-66	11	non-binder	20559	20269,23	23067,13	-	-	-	-	25842,40	21415,62	-	-
E7/24-33	10	non-binder	26532	35350,60	32787,64	26532,87	885,03		748,67	38150,11	22202,84	10	0,75
E7/24-32	9	non-binder	25058	23098,35	26550,96	25058,49	21161,45	29406,78	30173,54	28795,36	22434,44	10	9,00
E7/82-91	10	non-binder	35937	36804,84	28485,48	35937,71	6989,67		2410,59	37739,56	22998,13	0	
E7/61-69	9	non-binder	34954	25374,15	27725,29	34954,43				31060,99	26162,87	0	
E7/78-87	10	non-binder	32729	29422,19	27426,93	32730,04	37061,59		27609,62	29745,37	26329,26	12	8,64
E7/67-77	11	non-binder	33264	38900,17	34986,78	-	-	-	-	-	30813,77	-	-

3.1.2 Competition-based cellular binding assays verify binding of HPV16 E6 and E7 peptides to designated HLA types

The binding affinity of predicted HLA-binding HPV16 E6 and E7 peptides from the HPV16 reference sequence was tested experimentally in competition-based cellular binding assays (Kessler et al., 2003;

Kessler et al., 2004). This assay is based on the competition of the peptide in question with a strongly binding, fluorescein-labeled reference peptide for binding to the binding cleft of the HLA molecule on B-LCL cells expressing the HLA type of interest. The higher the binding affinity of the test peptide, the more the reference peptide is prevented from binding to the HLA molecule, thus resulting in decreased fluorescence intensity measured by flow cytometry. By testing a dilution series of the test peptide, the concentration needed to inhibit 50% binding of the reference peptide (IC_{50}) could be determined. A low IC_{50} value indicates strong binding affinity.

In Figure 21, the individual results for HPV16 E6 and E7 peptides binding to HLA-A3, HLA-A11 and HLA-A24 are shown. Many binding peptides known from the literature could be confirmed and numerous novel binding peptides were identified. HPV16 peptides binding to HLA-A3 and HLA-A11 displayed strong (< 5µM), intermediate (5-15µM) and weak (15-100µM) binding affinities, while the majority of tested peptides for HLA-A24 showed strong binding affinity (< 5µM), which stands in contrast to the prediction results of the NetMHC and IEDB servers (Tab. 14 and 25). These predicted intermediate or weak binding affinity, if they predicted binding at all.

For HLA-A3, nine HPV16 E6 and E7 peptides have been previously reported to bind (Kast et al., 1994; Bourgault Villada et al., 2010). The peptides E6/106-115, E7/89-97, E6/33-41, E6/93-101, E6/125-133 and E6/75-83 were identified as binders by Kast and colleagues and E6/59-67 in addition by Bourgault and colleagues. E6/54-61, which was shown to bind by Bourgault and colleagues as well, did not meet the chosen criteria for testing in this study. A total of 71 peptides were tested for HLA-A3 binding. Binding of seven previously identified binders could be confirmed and eleven peptides were identified as novel binders (Fig. 21 A). Three peptides displayed strong binding affinity, while six peptides showed intermediate and nine peptides showed weak binding. 53 of the tested peptides did not bind to HLA-A3.

In case of HLA-A11 (Fig. 21 B), 70 peptides were tested for their actual binding. Ten reported binding peptides (Kast et al., 1994; Bourgault Villada et al., 2010) were confirmed and 23 novel binders were found. One previously identified binder, E6/88-97 could not be confirmed and another three peptides, E7/7-15, E6/42-52 and E6/54-61 were not included for experimental testing due to the selected cutoff. Binding peptides displayed a strong binding affinity in nine cases, intermediate binding for nine and weak binding for 15 peptides. 55 tested peptides were not binding to HLA-A11.

For HLA-A24 (Fig. 21 C and D), a total of 69 peptides were tested for their binding affinity. Eight HPV16 peptides have been described to bind in previous studies (Kast et al., 1994; Morishima et al., 2007; Bourgault Villada et al., 2010). Of those, E6/71-78 was not predicted within the chosen cutoff and thus excluded from *in vitro* testing in this study. While E7/61-69 and E6/44-52 could not be confirmed as binders, E6/49-57, E6/87-95, E6/26-34, E6/98-106 and E6/131-139 were identified to bind to HLA-A24. 35 peptides could be identified as novel binders. The binding peptides included 26

strong binding peptides, comprising the highest number of all binders, and six peptides with intermediate binding affinity. Nine peptides were identified as weak binders and 28 peptides classified as non-binders.

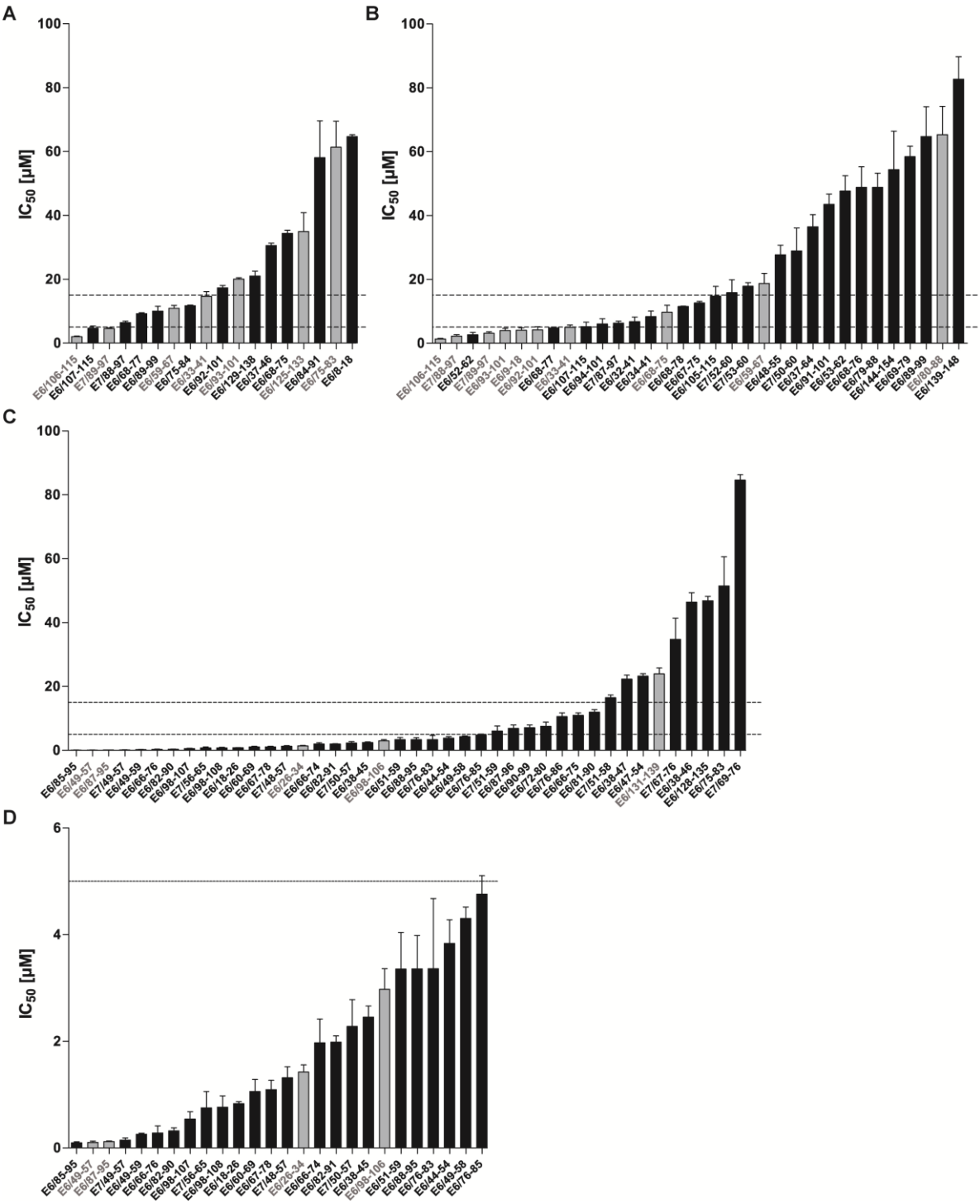

Figure 21 I Peptide binding affinity to HLA-A3, HLA-A11 and HLA-A24. Binding affinities of predicted peptides were tested in competition-based binding assays using B-LCL cells expressing the designated HLA types. Known binders are marked in grey. **A** Binding affinities of peptides binding to HLA-A3. **B** Binding affinities of peptides binding to HLA-A11. **C** Binding affinities of peptides binding to HLA-A24. **D** Close up of all HLA-A24 peptides with a binding affinity of < 5µM. Dashed lines indicate the ranges of binding affinity: strong (< 5µM), intermediate (5-15µM) and weak (15-100µM). Peptides with a binding affinity above 100µM were classified as non-binders and are not shown in this figure. Results are plotted as means ± SEM of three independent experiments.

3.1.3 Motif analysis identifies additional binding peptides

In order not to miss any peptide that lies outside the chosen cutoffs but might still bind to the designated HLA type, a peptide motif search was performed. To this end, amino acid patterns were generated of peptides identified as binders (positive motifs) and as non-binders (negative motifs). Peptide motifs generated for HLA-A24 are described as a paradigm for all HLA types investigated in this study.

In Figure 22, positive motif patterns are displayed for peptides with the lengths of 8 to 11 amino acids that bind to HLA-A24. All peptides, independent of their length, showed a predominance for tyrosine at position 2. Besides this, no clear predominace of other amino acids at designated positions could be seen in 8mer peptides. 9mers binding to HLA-A24 showed a predominance of leucine and isoleucin at position 9 in the peptide sequences. In 10mer binding peptides, leucine was often present at the last two positions of the sequences. In the sequences of 11mer binding peptides, aspartic acid was predominant at position 8 and isoleucine was often present at position 9. However, for motif patterns of 8mers and 11mers, it has to be considered that the input for motif generation was lower than for 9mers and 10mers.

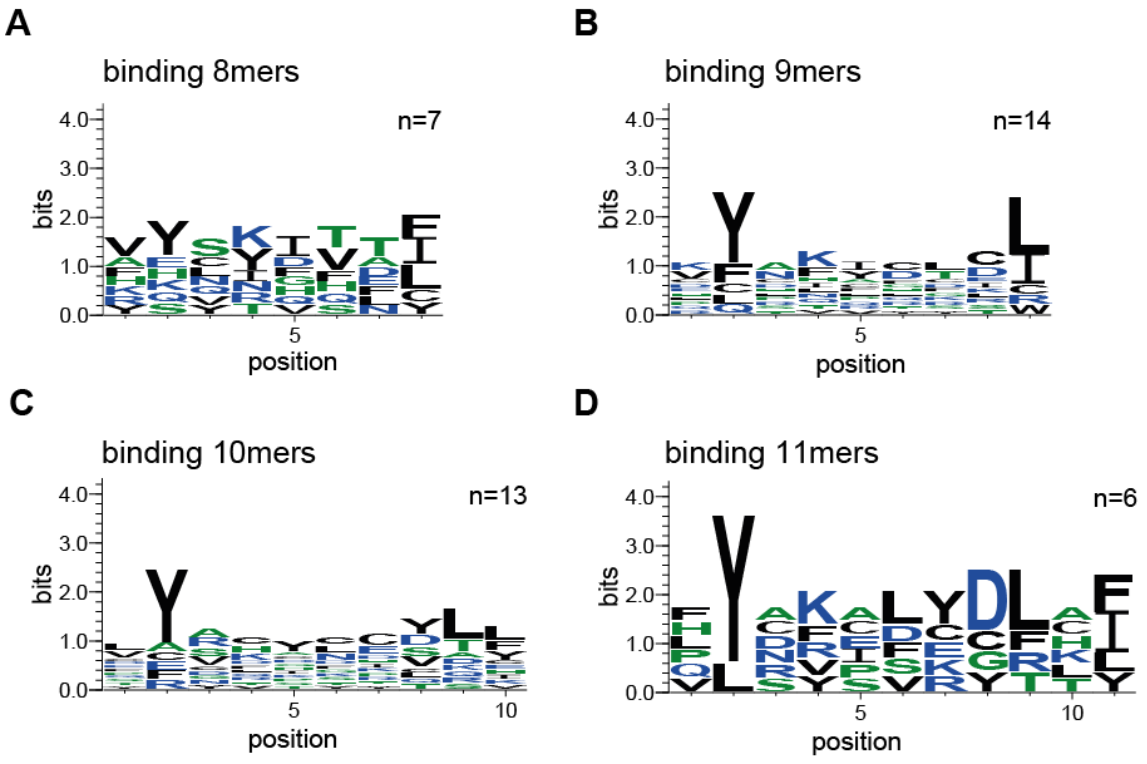

Figure 23 I Sequence logos of HPV16 E6 and E7 peptides binding to HLA-A24. Logos were created including all experimentally identified binding peptides (n) by using WebLogo 3. Sequence logos were generated separately for each peptide length. **A** The logo for 8mers. **B** The logo for 9mers. **C** The logo for 10mers. **D** The logo for 11mers. The larger an amino acid is depicted, the higher its frequency at a given position. The total bit height indicates the amino acid variation at one position. Lower bit height indicates less variation. Blue: hydrophilic amino acids, green: neutral amino acids, black: hydrophobic amino acids.

Figure 23 displays the sequence logos of peptides that were identified as non-binders. In case of motifs generated for 8mers and 11mers, no clear statement could be deducted due to the limited numbers of

identified non-binders. For 9mers, arginine and tyrosine were slightly predominant at position 1 and 2, respectively. At position 7 of 9mers, glutamic acid had a slightly higher frequency than other amino acids and at position nine leucine and phenylalanine were slightly predominant. Tyrosine was often present at position 2 in the sequences of 10mer peptides. However, as all tested peptides were originally predicted as binders by the prediction servers, that are based on the tyrosine predominance at position 2, being a common residue at this position for HLA-binding, this is likely to result from this preselection.

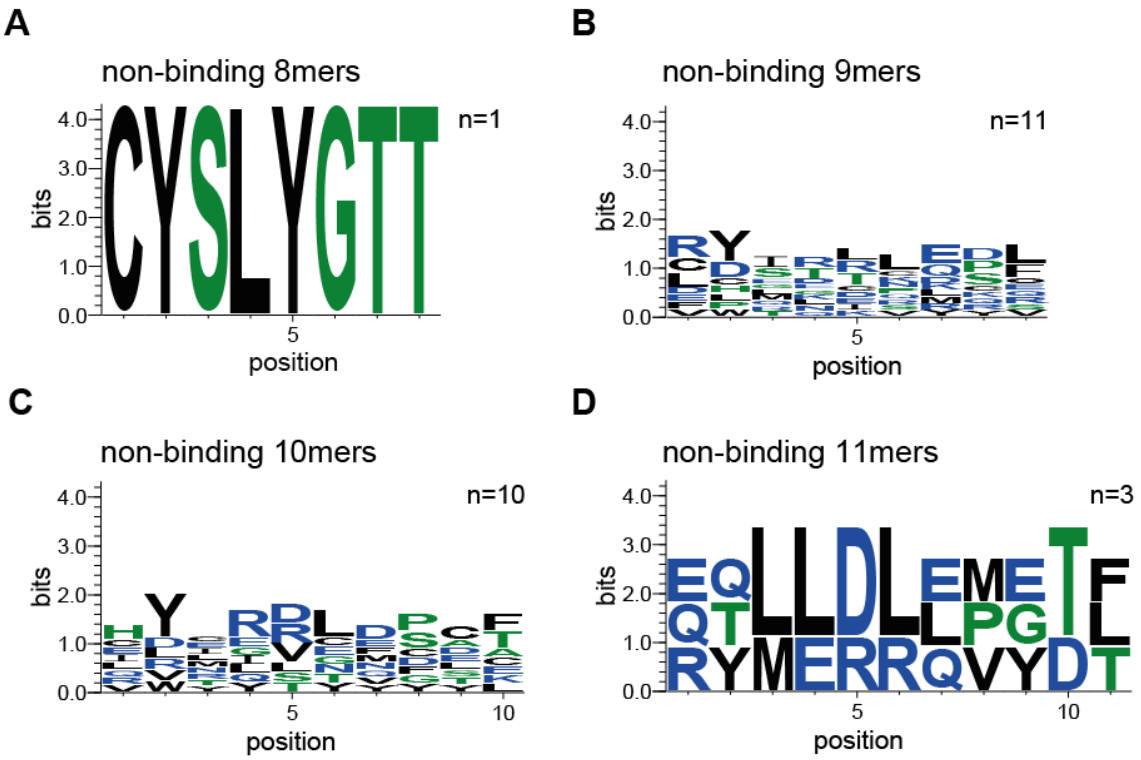

Figure 24 I Sequence logos of HPV16 E6 and E7 peptides not binding to HLA-A24. Logos were created including all experimentally identified non-binding peptides (n) by using WebLogo 3. Sequence logos were generated separately for each peptide length. **A** The logo for 8mers. **B** The logo for 9mers. **C** The logo for 10mers. **D** The logo for 11mers. The larger an amino acid is depicted, the higher its frequency at a given position. The total bit height indicates the amino acid variation at one position. Lower bit height indicates less variation. Blue: hydrophilic amino acids, green: neutral amino acids, black: hydrophobic amino acids.

From the sequence logos, peptide motifs were constructed and applied in a motif search including all non-tested HPV16 E6 and E7 peptides using the ExPASy ScanProsite tool. Results were analyzed for peptides matching with at least two positive motifs or with one positive and no matching with any negative motif. Peptides identified as potential binders by motif analysis are marked in *italic* in Tables 14 & 15 and Tables 22-25 (Appendix). For HLA-A3, three peptides were identified by motif search, E6/91-101, E6/91-103 and E6/52-61. Motif analysis for HLA-A11 resulted in seven potential additional binding peptides, namely E6/ 31-41, E6/65-75, E6/66-75, E7/63-43, E7/41-50, E7/42-50 and E7/68-75. Since the binding analysis of HLA-A24 had resulted in most novel binders, most strong binders and the most peptides suggested through motif analysis, we decided to focus this study on HLA-A24 from here on. Furthermore, of the three HLA types initially analyzed, HLA-A24 reached

amongst the highest frequencies in various ethnic populations as for example 58.6% in the Japanese population or 40.1% in the Chinese population and up to 23.9% in the Caucasion population (Sette and Sidney, 1999; Gonzalez-Galarza et al., 2015). For HLA-A24, 26 additional peptides were indicated as potential binders through motif analysis. In Figure 24, the results of the competition-based binding assays for HLA-A24 motif search-derived peptides are summarized. While one peptide, E6/48-57, showed strong HLA-A24 binding properties, two peptides, E6/35-44 and E6/50-59, displayed intermediate binding affinity to HLA-A24. Four peptides, E6/75-85, E6/86-96, E6/127-135 and E6/125-135 could be identified as weak binders. The remaining 18 peptides did not bind to HLA-A24.

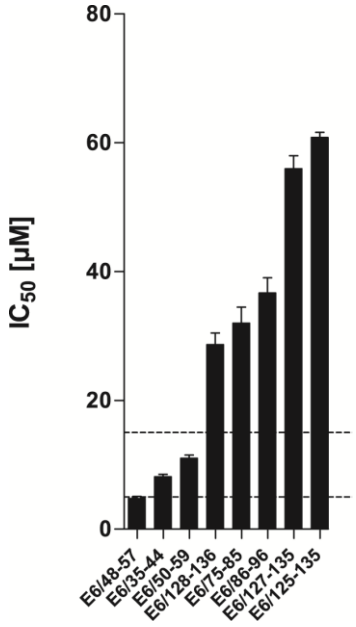

Figure 25 I Peptide binding affinity to HLA-A24 of peptides predicted by motif analysis. Binding affinities of peptides predicted by motif analysis were tested in competition-based binding assays using B-LCL cells expressing HLA-A24. Dashed lines indicate the ranges of binding affinity: strong (< 5µM), intermediate (5-15µM) and weak (15-100µM). Peptides with a binding affinity above 100µM were classified as non-binders and are not shown in this figure. Results are plotted as means ± SEM of three independent experiments.

3.1.4 Evaluation of prediction servers

Throughout the experimental validation of predicted binders and while setting new cutoffs for further testing of actual peptide binding (see section 3.1.1 and 3.1.2), it became obvious that not all servers were equally good at prediction binding affinities for all peptide lengths and for all three HLA types. In order to find the best prediction server for each peptide length and for each HLA type, evaluation of the performance of the prediction servers was performed by exploiting the large amount of generated experimental binding data in this study. To this end, receiver operating characteristic (ROC) curve analysis was performed and the area under the curve (A_{ROC}) was calculated, yielding a useful measure of prediction quality. The two servers BIMAS and SYFPEITHI were not included for performance evaluation due to unclear definition and discrimination of predicted binders and non-binders by the developers.

In Figure 25, individual ROC curves are shown for predictions of 8mer (A), 9mer (B), 10mer (C) and 11mer (D) peptides binding to HLA-A24. Corresponding ROC analyses for HLA-A3 and HLA-A11 are depicted in Figure 36 and Figure 37 in the Appendix. Here, sensitivity represents the proportion of experimentally measured binders, which were correctly predicted as binders. This is defined as the true positive rate. Experimentally measured non-binders that were incorrectly predicted as binders were defined as the false positive rate. Practically, this means that, as shown i.e. in Figure 25 C, if NetMHCpan (dark grey) predicts at a given sensitivity of 0.84, 84% of binders are predicted correctly as binding. At the same sensitivity, four out of ten peptides that are actual non-binders would be predicted as binders. In general, a prediction server that showed a high true positive rate and at this sensitivity a low false positive rate could be rated as a good predictor. Thus ROC curves at the upper left corner of the graph are favorable. Of note, only four prediction servers, the NetMHC family and IEDBpan supported the prediction of 8mers and 11mers.

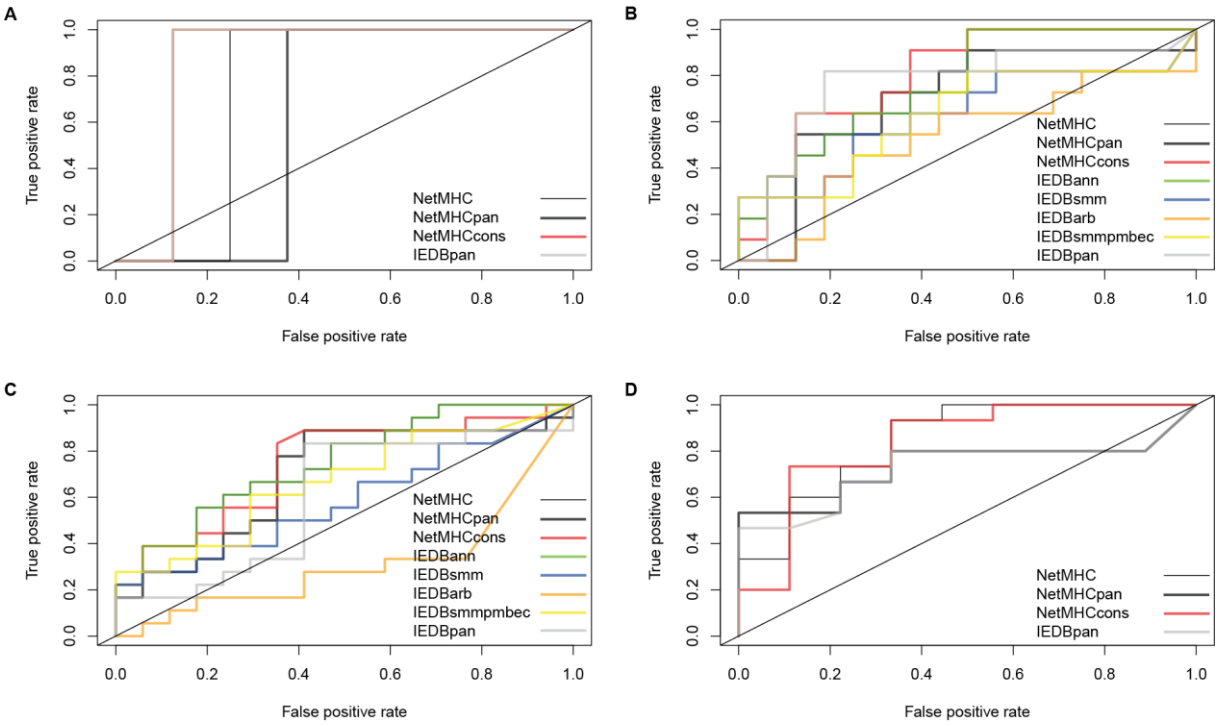

Figure 26 I Evaluation of prediction server performance for peptide predictions of 8mers, 9mers, 10mers and 11mers binding to HLA-A24 by ROC analysis. The rates of true positive predictions are plotted as a function of the rate of false positive predictions. **A** Analysis for 8mers (n=9). **B** Analysis of 9mers (n=27). **C** Analysis of 10mers (n=35). **D** Analysis of 11mers (n=24). Some curves are slightly overlayed.

Figure 26 summarizes the ROC analyses for predictions comprising all four peptide lengths combined for HLA-A3 (A), HLA-A11 (B) and HLA-A24 (C). Comparing the prediction capabilities of all servers combined for all peptide lengths for the three different HLA types, indicated that predictions for HLA-A3 (A) are more precise than for HLA-A11 and HLA-A24. This is also reflected by calculation of the area under the curve (A_{ROC}) (Tab. 16).

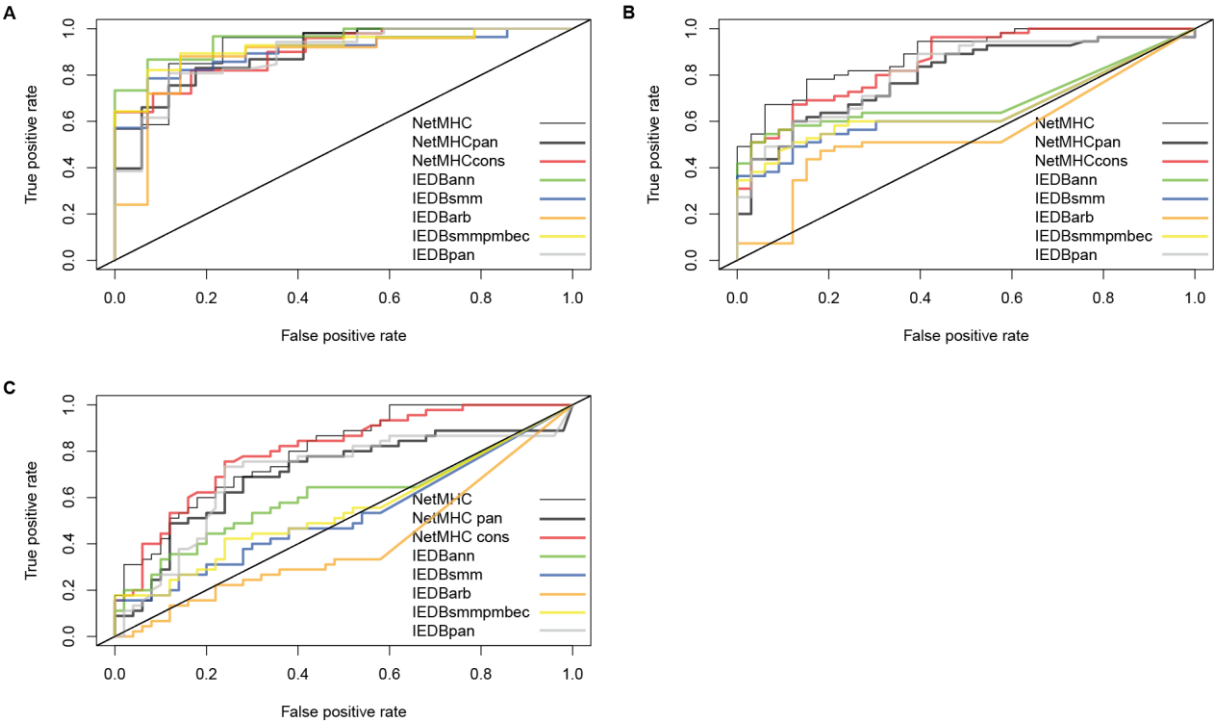

Figure 27 I Evaluation of prediction server performance for peptide predictions for HLA-A3, HLA-A11 and HLA-A24 by ROC analysis. The rates of true positive predictions are plotted as a function of the rate of false positive predictions. **A** Analysis for HLA-A3 (n=70). **B** Analysis for HLA-A11 (n=88). **C** Analysis for HLA-A24 (n=95). Some curves are slightly overlayed.

In Table 16, the A_{ROC} is given for each single ROC curve. The A_{ROC} is equal to the probability that a prediction server will rank a randomly chosen binding pepide higher than a randomly chosen non-binding peptide. Thus a higher A_{ROC} indicates a higher probability of a prediction server to identify true positive binders. Dashes in the table indicate that prediction for the designated peptide length is not supported by this predictor. Importantly, it has to be mentioned again, that not all prediction servers predict for all peptide lengths. Therefore, the overall (all lengths) performance cannot be compared between servers that only include 9mer and 10mers and those that support all lengths. Results for the overall performance for servers that do not support predictions for all lengths ar thus indicated in brackets in Table 16.

For HLA-A3, NetMHCpan was identified as the best prediction server for 8mers and 11mers based on the experimental data of this study. Moreover, for 11mers, NetMHC and IEDBpan displayed equally good prediction performance as NetMHCpan. 9mers could be best predicted by NetMHC, IEDBann and IEDBpan. In case of 10mers, NetMHCpan was found to be the best predictor. For prediction of 8mers binding to HLA-A11, NetMHCcons and IEDBpan showed the best prediction capabilities. For 9mers and 10mers, NetMHC and IEDBann scored best, and 11mers were best predicted by NetMHC. In case of HLA-A24, predictions by NetMHCcons and IEDBpan provided best performance for 8mers. For 9mers, NetMHCcons showed the best prediction capability and for 10mers NetMHC and IEDBann could be determined as the best predictors. NetMHC and NetMHCcons were shown to display the best performance for prediction of 11mers for HLA-A24. For all peptides lengths,

NetMHC could be determined as the best prediction server for HLA-A3 and for HLA-A11. For HLA-A24 both NetMHC and NetMHCcons were shown to be best predictors.

NetMHC and IEDBann are based on the same algorithms and similar training data sets, and therefore resulted in similar results for 9mers and 10mers. Taking all peptide lengths into consideration, NetMHC showed better performance since IEDBann does not support prediction of 8mers and 11mers. Additionally, NetMHCcons and IEDBpan do partially use the same training data sets, e.g. for predictions for 8mers binding to HLA-A3 and HLA-A24.

The predictive performance of the prediction servers was also assessed in accordance to criteria previously determined by Lin and colleagues (Lin et al., 2008). A_{ROC} values above 0.9 indicate excellent prediction capability, while values between 0.9 and 0.8 show intermediate prediction performance and values under 0.8 indicate poor predictive capability. For HLA-A3, excellent prediction performance was achieved by many servers – especially for 9mers and 10mers. For all lengths, predictors could be mainly classified as excellent and moderate. In case of HLA-A11, the overall prediction capabilities of prediction servers were a bit less accurate than for HLA-A3. Still, mostly excellent and moderate prediction performance was shown for prediction servers predicting 8mers, 9mers and 10mers. However, for 11mers, predictors displayed only moderate prediction performance. Some predictors reached the best possible prediction performance of 1.00 for predicting 11mers binding to HLA-A3 and for predicting 8mer binding to HLA-A11. This results should be regarded with caution as the sample size that was used as input in these cases is rather small (Fig. 36 and 37, Appendix). For HLA-A24, the overall performance of predictors was shown to be worse than for HLA-A3 and HLA-A11. This was already expected, as many peptides were experimentally shown to be strong binders albeit being predicted mostly as intermediate, weak or non-binding peptides (Tab. 14 and 15). NetMHC, NetMHCcons and IEDBpan showed moderate prediction performance for some lengths, otherwise all predictors displayed poor prediction capabilities for HLA-A24 (Tab. 16).

Table 16 I Predictor assessment for classification of binders and non-binders using the A_{ROC}. The values indicate excellent ($A_{ROC} > 0.9$), moderate ($0.8 < A_{ROC} < 0.9$) and poor ($A_{ROC} < 0.8$) prediction performance as classified by (Lin et al., 2008). Performance was determined for individual HLA type, for individual length, and for overall (all lengths) performance for each HLA type. The best performing predictors for each HLA type and length is indicated in **bold.** Dashes indicate that the peptide length was not supported by the respective server and brackets indicate that the overall (all lengths) performance only includes 9mer and 10mers.

	NetMHC	NetMHC pan	NetMHC cons	IEDB ann	IEDB smm	IEDB arb	IEDB smmpmbec	IEDB pan
HLA-A3								
8mers	0.64	**0.86**	0.82	-	-	-	-	0.82
9mers	**0.99**	0.97	0.94	**0.99**	0.82	0.84	0.84	**0.99**
10mers	0.95	**0.96**	0.95	0.95	0.89	0.68	0.91	0.91
11mers	**1.00**	**1.00**	0.92	-	-	-	-	**1.00**
all lengths	**0.92**	0.89	0.90	(0.95)	(0.90)	(0.88)	(0.92)	0.89
HLA-A11								
8mers	0.96	0.96	**1.00**	-	-	-	-	**1.00**
9mers	**0.96**	0.92	0.94	**0.96**	0.89	0.89	0.92	0.92
10mers	**0.91**	0.76	0.86	**0.91**	0.76	0.39	0.80	0.76
11mers	**0.65**	0.47	0.63	-	-	-	-	0.48
all lengths	**0.89**	0.80	0.86	(0.69)	(0.65)	(0.55)	(0.65)	0.81
HLA-A24								
8mers	0.75	0.63	**0.88**	-	-	-	-	**0.88**
9mers	0.77	0.70	**0.81**	0.77	0.63	0.53	0.63	0.77
10mers	**0.75**	0.69	0.74	**0.75**	0.58	0.31	0.67	0.60
11mers	**0.84**	0.74	**0.84**	-	-	-	-	0.73
all lengths	**0.80**	0.70	**0.80**	(0.60)	(0.52)	(0.40)	(0.55)	0.70

Overall, these results indicate that not all servers have the same capability to predict for all peptide lengths and for all HLA types. This result was already expected and has been partly observed in previous studies that evaluated predictor performance for 9mers and 10mers (Lin et al., 2008; Gowthaman et al., 2010; Zhang et al., 2011). In these evaluations, IEDBarb showed the least reliable prediction performance while NetMHC and NetMHCcons performed best for the given binding data input. Hence, the combination of various different prediction servers as employed in this study is of great importance if prediction of different lengths and for different HLA types is desired.

Although the applied prediction servers operated with a generally high accuracy for HLA-A3, these results, especially for HLA-A24, indeed indicate a risk of missing potential binding peptides. The lowering of individual cutoffs beneath the advised cutoffs by the developer of the prediction servers and the use of alternative prediction approaches, such as the motif search (see section 3.1.3), thus proved to be beneficial to minimize the loss of potential binding peptides. By combining multiple servers and alternative approaches, the probability to find potent HPV16 E6 and E7 derived peptides was significantly increased.

3.2 HPV16 variants and their HLA-binding E6 and E7 peptides

HPV16 includes different variants which are associated with but not restricted to different geographic regions (Tu et al., 2006; Tabora et al., 2010). For epitope identification as well as vaccine

development, it is important to include these distinct HPV16 variants. HPV16 variants harbored by 26 cell lines from our cell line collection were characterized. To this end, genomic DNA was isolated and the viral genes E6 and E7 were amplified by PCR. PCR products were verified by agarose gel electrophoresis (data not shown), sequenced by GATC Biotech and then aligned to the HPV16 reference sequence (NC_001526), belonging to the HPV16 variant European Prototype 1, to detect nucleotide and amino acid exchanges. In parallel, a multiple sequence alignment of 62 HPV16 sequences already assigned to a specific variant (Burk et al., 2011) was performed (Tab. 26, Appendix). HPV16 sequences harbored by the 26 tested cell lines were assigned to a variant based on the detected nucleotide exchanges. Table 17 shows the 26 cell lines carrying distinct HPV16 variants and their corresponding E6 and E7 amino acid exchanges. Different amino acid exchanges in the E6 and/or E7 proteins were found in cell lines carrying the same HPV variant sublineage. To be able to discriminate between them, the suffix -v1, -v2, -v3 etc. was assigned to the sublineage name.

Table 17 I HPV16 variants present in cell lines with their amino acid exchanges compared to the HPV16 reference sequence. Amino acid position is counted from the first methionine in E6. HLA-A24-positive cell lines are indicated in **bold**. E-1: European Prototype 1, E-2: European Prototype 2, E-A: European (Asian), AA: Asian-American, Af-2: African 2, v: variant

HPV16 variant	Amino acid exchanges in E6 and E7 compared to the HPV16 reference sequence	Cell lines harboring the variant
E-1-v1	reference prototype	879, 915, 93VU147T, **FK16A**, Goerke , HPK1A, Marqu
E-1-v2	E6 L90V	C66#3, C66#7, MRI-H-196, **W12 20861**, **W12 20863**
E-1-v3	E7 H51N	UD-SCC2
E-1-v4	E6 L90V, E6 E120D, E7 L28F	**SiHa**
E-2	E6 R17T, E6 L90V	CaSki, SCC090, SCC152
E-A-v1	E6 D32E, E7 N29S	SNU 17, SNU 703, **SNU 1005**
E-A-v2	E6 D32E, E6 I34R, E7 N29S	SNU 1000
E-A-v3	E6 D32E, E7 N29S, E7 S63F	SNU 902
AA	E6 Q21D, E6 H85Y, E6 L90V	SCC154, SNU 1299
Af-2-v1	E6 R17I, E6 Q21D, E6 H85Y, E7 N29S	866
Af-2-v2	E6 R17I, E6 Q21D, E6 E36Q, E6 A68G, E6 H85Y, E7 N29S	UM-SCC-47

A complete list of all cell lines, the exact nucleotide exchanges within the E6 and E7 open reading frames (ORFs), also including silent mutations, and the designated HPV16 variant is displayed in Table 27 (Appendix). Since transcription of the E6 protein starts at the second methionine of the E6 ORF (section 2.2.1.1, Tab. 2), the nomenclature for identification of HPV variants does not include the first 21 nucleotides or seven amino acids, respectively. For peptide prediction however, the first seven amino acids are included nevertheless, resulting in the change of position by seven. As an example, the nucleotide exchange T350G results in the amino acid change L83V in HPV variant terms and is named L90V in peptide prediction terms. In Table 17 we adhered to the peptide prediction nomenclature, while in Table 27 (Appendix) the positions of amino exchanges are shown according to the variant nomenclature. In total eighteen and eleven nucleotide exchanges were detected for the E6

and E7 ORFs, respectively. These nucleotide exchanges resulted in nine amino acid exchanges for the E6 protein and four exchanges for the E7 protein. The remaining nucleotide exchanges were silent.

Moreover, the HLA types of all HPV16 positive cell lines were determined in order to be able to correlate HLA type and potentially presented HPV16 E6 and E7 peptides for subsequent experiments. To this end, genomic DNA was extracted from the cell lines of our HPV16-positive cell line collection that were not HLA typed before or in cases were literature search resulted in contradicting descriptions. HLA genotyping in resolution of four digits was conducted by the DNA subgroup of the Department of Transplantation Immunology of the Institute of Immunology at the University of Heidelberg and is displayed in Table 27 (Appendix).

After testing the potential set of HLA-A3-, HLA-A11- and HLA-A24-binding E6 and E7 peptides derived from the prototype HPV16 sequence (section 3.1.2), this work was focused on HLA-A24 and the effects of amino acid exchanges in the E6 and E7 protein sequences were determined only for this HLA molecule. Binding affinities were predicted *in silico* in the same manner as done initially for the HPV16 reference sequence. As depicted in Table 18, peptides were filtered for those with an average predicted IC_{50} below 5000nM.

Table 18 I HPV16 E6 and E7 variant peptides predicted to bind to HLA-A24. Changes in comparison to the HPV 16 reference sequence are indictaed in the second and third column for E6 and E7, respectively. Amino acid sequences including the change are indicated in **bold** in the 4th and 5th column. The peptide names include "var " in the end, indicating that they are derived from a HPV16 variant. * No peptides were predicted to bind within a 5000nM average IC_{50} cutoff for E120D.

HPV16 variant	E6 aa changes	E7 aa changes	Potential HLA-A24 binders derived for E6 variants within a 5000nM average IC_{50} cutoff	Potential HLA-A24 binders derived for E7 variants within a 5000nM average IC_{50} cutoff
E-1v2	L90V		SEYRHYCYS**V** (E6/81-90var), EYRHYCYS**V** (E6/82-90var), EYRHYCYS**V**Y (E6/82-91var), HYCYS**V**YGT (E6/85-93var), HYCYS**V**YGTT (E6/85-94var), HYCYS**V**YGTTL (E6/85-95var), CYS**V**YGTT (E6/87-94var), CYS**V**YGTTL (E6/87-95var), CYS**V**YGTTLE (E6/87-96var), YS**V**YGTTL (E6/88-95var), **V**YGTTLEQQ (E6/90-98var), **V**YGTTLEQQY (E6/90-99var)	
E-1-v4	L90V, E120D	L28F	see E-1v1 *	TTDLYCYEQ**F** (E7/19-28var) TDLYCYEQ**F** (E7/20-28var), DTDLYCYEQ**F** (E7/21-28var)
E-A-v1	D32E	N29S	LQTTIH**E**II (E6/26-34var)	LYCYEQF**S**D (E7/22-30var), LYCYEQF**S**DS (E7/22-31var), CYEQF**S**DSS (E7/24-32var), CYEQF**S**DSSE (E7/24-33var)

Twenty HPV16 variant peptides predicted to bind to HLA-A24 were tested in competition-based binding assays (Fig. 28). Seven of these variant peptides were identified as binders. These include

three strong binders, E6/87-95var, E6/90-99var and E6/26-34var, and one intermediate binder, E6/82-90var. E7/21-28var, E6/87-96var and E6/88-95var were ranked as weak binders and the remaining thirteen peptides did not bind to HLA-A24. Of note, the respective HPV16 reference-derived peptides that were binding as well, scored twice an comparable binding affinity (E6/87-95 and E6/26-34), once a slightly lower binding affinity (E6/90-99) and in three cases a higher binding affinity (E6/82-90, E6/87-96 and E6/88-95). The counterpart of E7/21-28var was not included in testing due to prediction under the chosen cutoff.

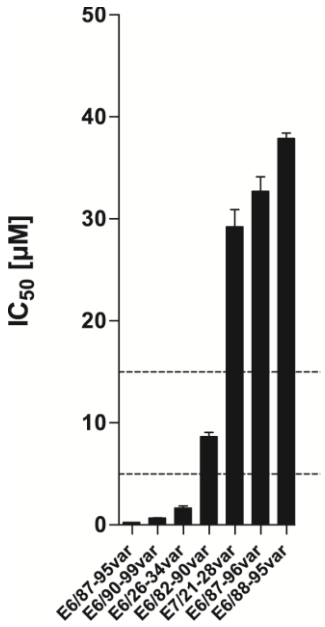

Figure 28 I Peptide binding affinity of predicted HPV16 variant peptides to HLA-A24. Binding affinities of predicted HPV16 variant peptides were tested in competition-based binding assays using using B-LCL cells expressing HLA-A24. Dashed lines indicate the ranges of binding affinity: strong (< 5µM), intermediate (5-15µM) and weak (15-100µM). Peptides with a binding affinity above 100µM were classified as non-binders and are not shown in this figure. Results are plotted as means ± SEM of three independent experiments.

Table 19 summerizes all *in silico* predicted binding peptides of this study, including sequences derived from the HPV16 E6 and E7 reference sequences and the HPV16 variants, and *in vitro* tested peptides for all three HLA types. In total, 74 were predicted for HLA-A3, 96 for HLA-A11 and 115 peptides for HLA-A24, including HPV16 E6 and E7 peptides based on prediction for the HPV16 reference type, peptides predicted by motif analysis and HPV16 variants, were predicted. Of those, 18 binders could be identified for HLA-A3, 33 for HLA-A11 and 56 for HLA-A24. Those binders can be further subdivided into confirmed known binders and novel binders, resulting in seven known binders for HLA-A3, ten for HLA-A11 and five for HLA-24. Novel binders comprise eleven for HLA-A3, 23 for HLA-A11 and 51 for HLA-A24. 167 tested peptides were found to be non-binders.

Table 19 I Predicted and tested HPV16 E6 and E7 peptides and their binding status to their respective HLA type.

HLA supertypes	possible epitopes	predicted peptides	tested peptides	actual binders	known binders	novel binders	non-binders
HLA-A3	all	74	71	18	7	11	53
HLA-A11	8mers to	96	88	33	10	23	55
HLA-A24	11mers	115	115	56	5	51	59
total	**941 +variants**	**285**	**274**	**107**	**22**	**85**	**167**

3.3 Immunoprecipitation of HLA/peptide complexes from HPV16-transformed cells

In order to identify naturally processed and presented HPV16 E6 and E7 T cell epitopes on HPV16-transformed cells, HLA/peptide complexes were isolated. First, HLA expression levels on HPV16-transformed cells were determined to evaluate the number of cells needed for immunoprecipitation of HLA/peptide complexes. After successful immunoprecipitation, peptides were eluted from HLA/peptide complexes for subsequent MS analysis. Purity and enrichment of HLA/peptide complexes are a prerequisite for MS analysis.

3.3.1 HLA expression levels

HLA expression levels were determined for all HLA-A3, HLA-A11 and HLA-A24 positive cell lines of our HPV16 positive cell line collection. Cells were stained with corresponding specific HLA antibodies and analyzed by flow cytometry. Expression levels were normalized to CaSki HLA-A*02:01 expression levels, as the cell number needed for immunoprecipitation was initially optimized for HLA-A2 and CaSki cells. Results are summarized in Figure 28. For HLA-A3 (A) all cell lines showed relatively high HLA expression levels compared to the reference. Expression levels for HLA-A11 (B) were lower than the reference. The cell line SiHa showed the highest HLA-A24 expression level (C), while levels for FKA16A were almost not detectable.

For HLA-A24, all cell lines were selected for isolation of HLA/peptide complexes and analysis of the E6 and E7 epitopes presented. For HLA-A3 and HLA-A11, cell lines with the highest expression levels, CaSki, MRI-H196 and 93VU147T (HLA-A3) and SNU 1000 (HLA-A11) were chosen.

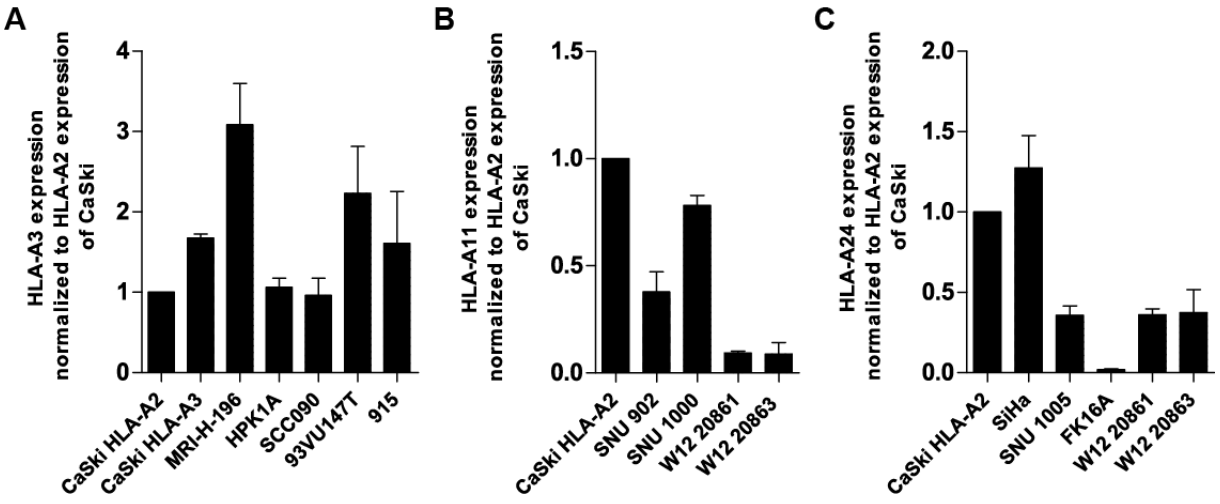

Figure 29 I HLA expression levels determined for HPV16 positive cell lines. Cells were stained with HLA type specific antibodies and the mean fluorescent intensity was analyzed by flow cytometry. Results are normalized to the reference cell line's (CaSki) HLA-A2 expression. **A** HLA expression levels for HLA-A3-positive cell lines. **B** HLA expression levels for HLA-A11-positive cells. **C** HLA expression levels for HLA-A24-positive cells. Results are plotted as means ± SEM of three independent experiments.

3.3.2 Immunoprecipitation

Various methods for immunprecipitation (IP) of HLA/peptide complexes were compared and optimized. The whole initial optimization procedure was performed with HLA-A2 positive CaSki cells, as they are fast growing and eventually were used for MS analysis optimization. Different parameters such as antibody concentrations and incubation times were tested and optimized. Furthermore, it was assessed whether sonication of cell lysates improved the yield of HLA/peptide complex isolation. Moreover, different lysis buffers such as the radioimmunoprecipitation assay (RIPA) buffer or a lysis buffer based on Triton-x 100 and NP40, were compared (Alcaraz et al., 1990; Riemer et al., 2010). This involved testing of various detergents such as Triton-x 100, NP40, SDS and CHAPS. The optimal cell number was determined for each cell line. To this end, cell numbers used in each single IP experiment were monitored and cell numbers needed for IP of a novel cell line were estimated based on HLA expression levels (Fig. 28). Purity and enrichment of HLA molecules was assessed by Coomassie or Oriole staining and Western Blot analysis. Eventually, the IP procedure was optimized to the current protocol described in section 2.2.3.2. In brief, 20µL dry sepharose beads were coupled with 20µg capture antibody and incubated for two to three hours at room temperature. For both, HLA-A2 positive CaSki and HLA-A24 positive SiHa cells, five confluent dishes containing approximately $5.5x10^7$ cells were used, cells scraped off and then lysed in 1mL of CHAPS buffer. After centrifugation of lysed cells, the remaining cleared lysate was incubated with washed sepharose beads coupled with capture antibodies for three hours at 4°C. Susequently, the supernatant (SNT) named the'flow through' of the beads, fluids from different washing steps and the sepharose beads containing the immunoprecipitate were collected for analysis. Figure 29 depicts representative Oriole

stained polyacrylamide gels and Western Blots of immunoprecipiated HLA-A24/peptide complexes from SiHa cells and HLA/A2 peptide complexes from CaSki cells which served as a reference.

In the IP fractions for both SiHa (IP SiHa) and CaSki (IP CaSki) cells, a distinct band could be detected by Western blot analysis with a pan anti-MHC class I antibody at approximately 44 kDa, which is the expected size of the HLA class I α-chain. This verified successful immmunoprecipitation of HLA-A24/peptide and HLA-A2/peptide complexes. Enrichment of HLA/peptide complexes was achieved for HLA-A24 and HLA-2, as the bands in the IP samples are clearly stronger than the bands in the cleared lysate. Some HLA/peptide complexes, however, did not bind to the capture antibodies as the 44kDa band was still detectable in the flow through, most probably due to oversaturation. Moreover, some HLA/peptide complexes were lost during the first washing steps indicated in the lanes of wash 1 and wash 2. No bands were detected in the last washing step, wash 6. Both IP samples also includeded other proteins apart from the immunoprecipitated HLA/peptide complexes, as other bands than the 44kDa band are detected by Oriole staining and also by Western blot analysis. Since peptides had to be eluted anyway from HLA/peptide complexes and purified by size exclusion in subsequent steps towards MS analysis, further purification was not nesseccary at this point. Bands at a size of 23kDa, that are detectable in the beads and capture antibody control and throughout all samples from the whole immmunoprecpitation procedure, represent the light chain of the antibody. This band is visible in Oriole stained gels and in the Western blots. On the other hand, the heavy chain of the antibody with a size of 50kDa was not detectable with the antibody used for HLA class I detection and thus is only visible in Oriole stained gels. The band detected at 100kDa in both IP samples with Western blot analysis likely represents antibody heavy chain dimers.

So far, no peptides defined as potential epitopes in the immunoprecipitated samples could be detected by MS analysis. The MS method is currently being optimized and future analysis will reveal whether potential peptides are actually presented on the cells transformed by HPV16.

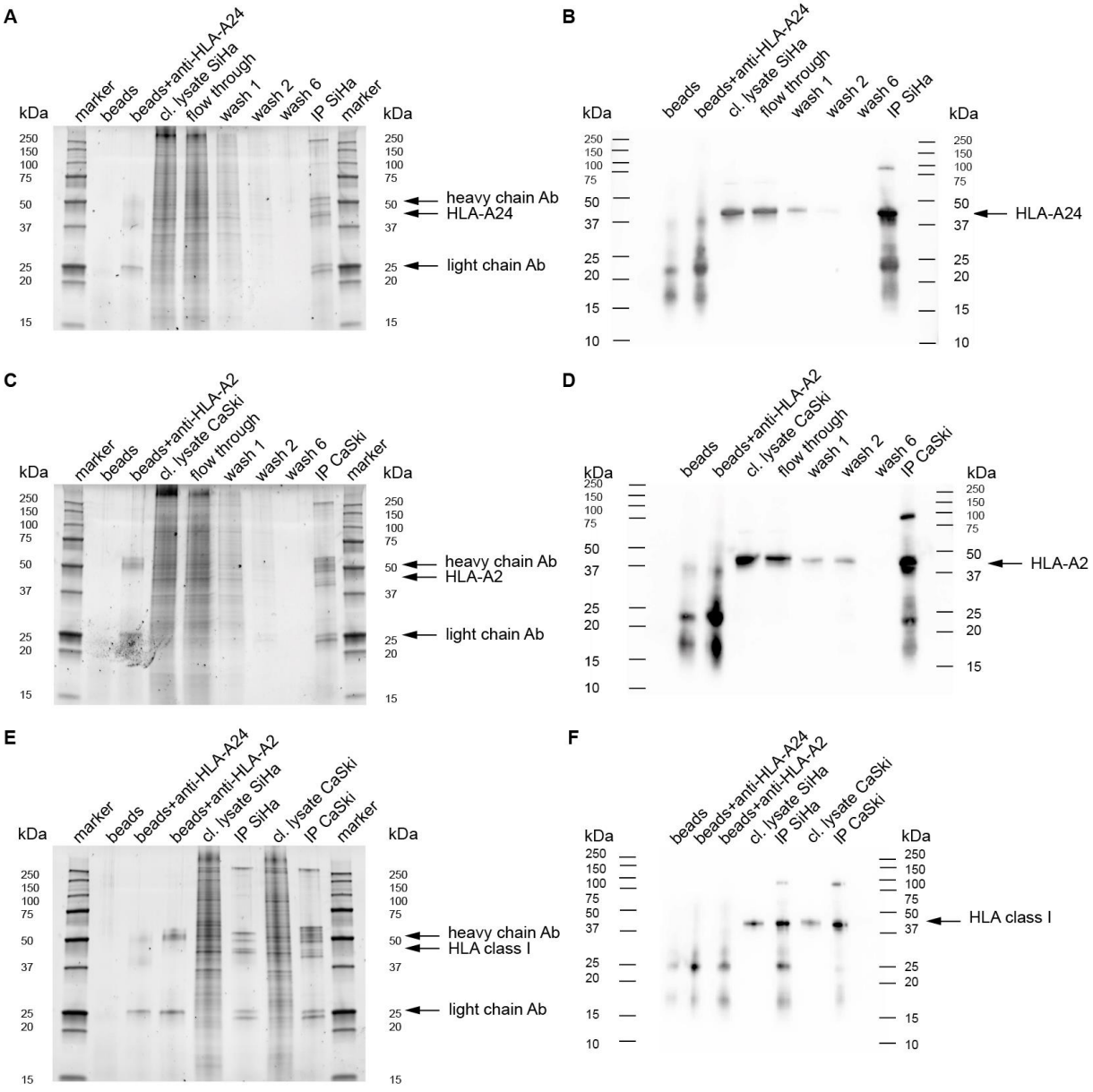

Figure 30 I Immunoprecipitation of HLA/peptide complexes from SiHa and CaSki cells. After cell scraping, cells were lysed and centrifuged. The cleared lysate (cl. lysate) was incubated with beads coupled to capture antibody for three hours at 4°C. Subsequently, samples were centrifuged, the supernatant (flow through) collected and beads washed (wash 1-6). As controls, uncoupled beads and beads coupled with respective capture antibody, either anti-HLA-A2 or anti-HLA-A24, were incubated with buffer instead of cleared lysate in the same manner as IP samples. Controls are always loaded in the first lanes. **A**, **C, E** Oriole staining of polyacrylamide gels. Prescision Plus Protein™ Unstained Standard (BioRad) was used as a marker. **B**, **D**, **F** Western blot analysis of immunoprecipitated HLA-A24 and HLA-A2 performed with an rabbit-anti-human MHC class I specific monoclonal antibody (anti-MHC class I). Detection of primary antibody was done with a secondary HRP-conjugated goat-anti rabbit antibody and ECL detection. Prescision Plus Protein™ Kaleidoscope (BioRad) was used as a marker. Equal protein amounts where loaded in each lane. Arrows indicate HLA class I moleules, either HLA-A24 or HLA-A2, heavy chains of antibody (Ab) and light chains of antibody.

3.4 Evaluation of peptide immunogenicity by establishing short-term T cell lines

In order to assess the immunogenicity of binding peptides, we established peptide-specific short-term T cell lines. In order to test the high number of all binding peptides for the HLA types investigated in this of the study (Tables 14 and 15 for HLA-A24, Tables 22-25 for HLA-A3 and HLA-A11, and section 2.1.12.2 for HLA-A2, HLA-B7 and HLA-B15), a large number of PBMCs was needed. To

obtain such a large number, buffy coats of healthy donors were used. Buffy coats are a by product of blood donations for erythrocytes and contain concentrated white blood cells. They were easily obtained from our local blood bank. Buffy coat donations were HLA typed by FACS staining, which provided a fast first test on day 1. For validation, HLA genotyping was performed by PCR. Since blood donors are required to be over 18 years in Germany, a contact with a high-risk HPV type can be assumed to be likely but not taken for granted (Evander et al., 1995; Woodman et al., 2007). For the generation of peptide-specific short-term T cell lines, peripheral blood mononuclear cells (PBMCs) were isolated from the buffy coats, stimulated *ex vivo* with the identified binding HLA-matching peptides and kept in culture for twelve days. In this setting, stimulation with HPV16 E6 and E7-derived peptides is likely to trigger T cell memory responses in individuals, who were previously transiently infected by HPV16. IFNγ ELISpot assays were conducted to test peptide immunogenicity.

3.4.1 HLA typing of buffy coat cells

The HLA typing results of all twelve buffy coat donors using FACS staining and HLA genotyping PCR are displayed in Table 20. The data determined by FACS staining for buffy coats 2 and 6 suggested, that these donors carry more than two alleles on the A locus. Since this is impossible, validation of the HLA types with a more accurate method was required. For validation, HLA genotyping with two digits precision was performed with primer sets specific for each probed HLA type (Bunce, 2003) (section 2.2.2.2 Tab. 12).

The false positive results seen in FACS stainings can be explained by cross-reactivity of HLA-A3 with the anti-HLA-A11 antibody, according to the product's data sheet. Thus all buffy coats with HLA-A3 were also characterized as HLA-A11 positive by FACS. HLA genotyping could, however, confirm whether a donor was truly positive for HLA-A11. For buffy coat eight, HLA-A11 could not be confirmed by PCR, possibly because the HLA-A11 subtype was not covered by the primer pairs. Here, we assumed that the buffy coat was HLA-A11 positive anyway because it was not HLA-A3 positive, eliminating the possibility of a cross-reaction with this molecule.

The false positive results in HLA-A24 FACS stainings may be due to cross-reactivity of the anti-HLA-A24 antibody with HLA-B27. This cross-reaction was reported by the manufacturer MBL and led to 20% false postive results in their studies with samples of Japanese origin. HLA-B27 has an allele frequency of 8.5% in the German population (Gonzalez-Galarza et al., 2015) and therefore it is possible that the false positive buffy coats were truly positive for HLA-B27. Recognition by the antibody was tested positive using a HLA-B27 positive cell line and HLA genotyping confirmed which buffy coats were really positive for HLA-A24. The results of HLA-B7 typing by FACS staining could not be validated by HLA-B7 specific PCR reactions due to a lack of specific primers for this genotype. Determined HLA types for each buffy coat are shaded in grey in Table 20. The prevalence of HLA types that were determined for the twelve buffy coat donations in the study, fits quite well to

the reported prevalence for HLA types in the German population as indicated in the last row of Table 20.

Table 20 I HLA typing for twelve buffy coats by FACS staining and HLA genotyping PCR. Buffy coats were first tested for their HLA type by staining with a panel of HLA-specific antibodies and subsequent FACS analysis. The results are shown on the left side of the dash. HLA genotyping PCR results are indicated on the right side. Grey highlighting indicates the determined HLA types. The prevalence of each HLA type is shown for the German population (Gonzalez-Galarza et al., 2015). * HLA-B7 primers were not specific for this genotype.

Buffy coat	**HLA type:**					
	HLA-A2	**HLA-A3**	**HLA-A11**	**HLA-A24**	**HLA-B7 ***	**HLA-B15**
1	+/+	-/-	+/+	-/-	-/	-/-
2	+/+	+/+	+/-	+/-	-/	-/-
3	-/-	-/-	-/-	+/+	-/	-/-
4	-/-	+/+	+/-	+/-	+/	-/-
5	-/-	-/-	-/-	+/-	+/	-/-
6	-/-	-/-	+/+	+/+	+/	-/-
7	+/+	-/-	+/-	-/-	-/	-/-
8	-/-	+/+	+/-	-/-	-/	-/-
9	-/-	-/-	-/-	+/-	-/	+/+
10	+/+	-/-	-/-	+/-	-/	-/-
11	+/+	+/+	+/-	-/-	-/	+/+
12	+/+	-/-	-/-	-/-	-/	+/+
prevalence in this sample set (%)	**50**	**33.3**	**25**	**16.7**	**25**	**25**
prevalence in Germany (%)	**49.9**	**28.6**	**10.0**	**18.1**	**24.5**	**15.3**

3.4.2 IFNγ ELISpot assays

Isolated PBMCs were stimulated with peptides according to their HLA type and cultured for twelve days. IFNγ ELISpot assays were performed. As an example, the results of HLA-A24-restricted peptides tested with cells from buffy coat donor 3, are displayed in Figure 30. A peptide-specific T cell response was considered positive only when the mean spot number for a given peptide was at least twofold higher than the mean spot number of the negative control (DMSO) (upper dashed lines). For this donor, five E6 peptides, E6/85-95, E6/66-76, E6/67-76, E6/82-91, and E6/50-59 and two E7 peptides, E7/56-65, and E7/51-59, could be identified to elicit IFNγ responses.

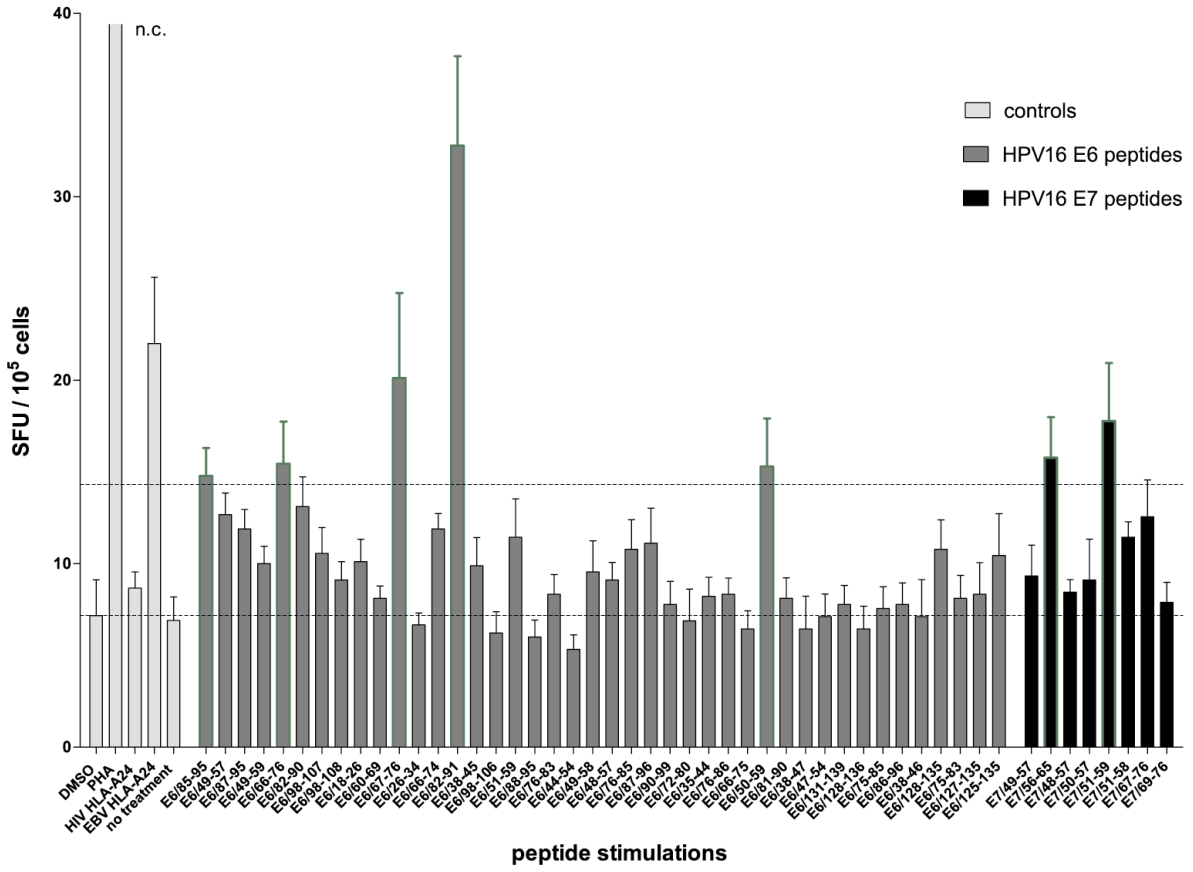

Figure 31 I Immunogenicity screening of HPV16 E6 and E7 epitopes by IFNγ ELISpot assay. ELISpot analysis of peptide-specific IFNγ responses to HPV16 E6 and E7 peptides with cells from a HLA-A24-positive buffy coat (donor 3). Light grey indicates controls. DMSO (peptide diluent), no treatment and a HIV HLA-A24-restricted peptide were used as negative controls and PHA and an EBV HLA-A24-restricted peptide were used as positive controls. Dark grey shows all HPV16 E6 HLA-A24-binding peptides and black all HPV16 E6 HLA-A24-binding peptides that were tested for immunogenicity. Results are plotted as means ± SEM of at least three replicates. A peptide-specific T cell response was considered positive when the mean spot number for a given peptide was at least twofold higher than the mean spot number of the DMSO negative control (lower dashed line). upper dashed line: threshold, bars lined in green: peptides displaying positive responses, SFU: spot forming units, n.c.: not countable

A graphic summary of all immunogenic peptides is displayed in Figure 31. The peptides are sorted by their position in the viral proteins E6 (A) and E7 (B) and color-coded for their immunogenicity according to how many donors have reacted to the respective peptide. Due to the FACS typing difficulties mentioned above, several peptides were tested with non-matching donors. If the assays resulted in IFNγ responses, it can be safely assumed that this was caused by cross-reactive binding of the peptide to another HLA type. These results are marked with an asterisk in Figure 31.

HLA-A2 was the most frequent HLA type amongst all donors and several HLA-A2-restricted peptides were shown to be immunogenic in more than three donors. One region (20-30aa) for the E6 protein and two regions (10-20aa and 74-92aa) for the E7 protein contained these immunogenic peptides. Also for HLA-A3 and HLA-A11, immunogenic regions around 67-78aa and 90-115aa for E6 and at 85-95aa for E7 could be identified. For the HLA types HLA-A24, HLA-B7 and HLA-B15 further data is neccesary to draw clear conclusions. In case of HLA-A24-restricted peptides, various cross-reactions

with other HLA types could be observed. One peptide, E6/85-95, was, however, tested to be immunogenic in both HLA-A24 positive donors.

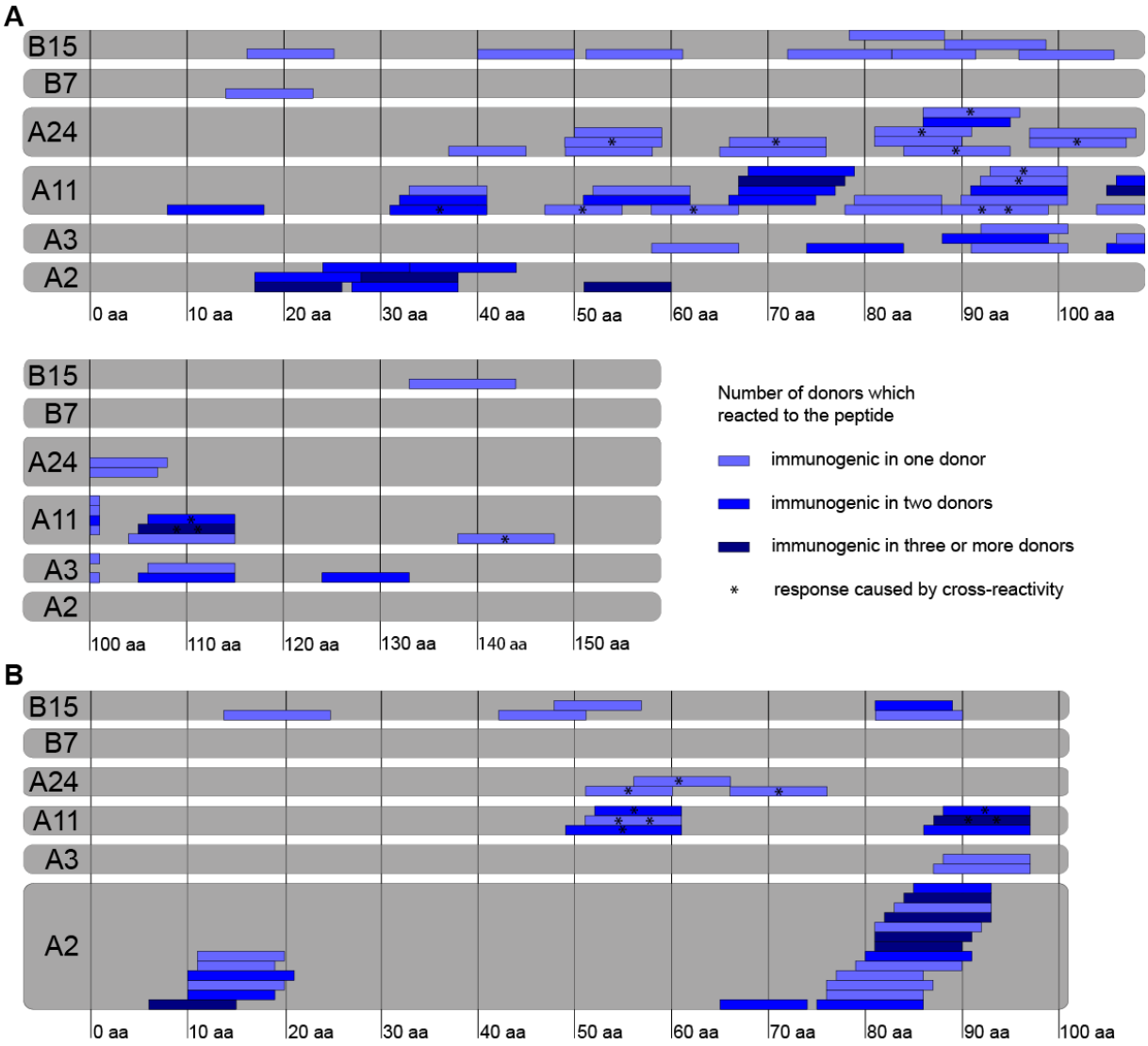

Figure 32 I Immunogenicity testing results of HPV16 E6 and E7 peptides in twelve donors. All peptides are sorted by their position in the viral protein, E6 (**A**) and E7 (**B**), and color coded by the frequency of the IFNγ responses across different donors. Peptides that were tested and did not show immunogenicity are not depicted.

Several facts complicate the interpretation of this data set. First, even though the peptides were chosen because of certain HLA alleles being present, it remains elusive whether the observed responses were associated only with these particular HLA molecules or with one of the other HLA molecules present on the cells. Testing of immunogenicity in a total of twelve buffy coat donors only gives hints towards potential general immunogenicity of a peptide related to a specific HLA type. In order to find significant correlations between the peptide and the HLA type, the number of tested donors would have to be increased. Moreover, the medical history and especially the HPV status of the donors is unknown. Even if T cell memory responses are assumed to occur, due to the high percentage of the world population that acquire a transient infection with a high-risk HPV type in their lifetime (Evander et al., 1995; Woodman et al., 2007), the immune system of every individual reacts differently. Thus, a

peptide might elicit memory IFNγ responses in one healthy donor, but not in another, even if both individuals carry the same HLA type and have been transiently infected with the same HPV16 variant.

3.5 Functional analysis of peptide candidates using peptide-specific HLA-A24-positive T cell lines

To further characterize the potential of peptides to be candidates for a therapeutic HPV16 vaccine, various functional assays were performd. IL-2 secretion was assessed in supernatants from peptide-specific short-term T cell lines. IFNγ secretion and cytolytic activity of peptide-specific long-term T cell lines were tested in response to autologous peptide-presenting B cells. Additionally, the clonality of peptide- specific T cell lines was assessed by TCR sequencing. Four candidate peptides were selected for these experiments based on their binding to HLA-A24 (sections 3.1.2 and 3.2) and the immunogenicity screening in short-term peptide-specific T cell lines (section 3.4.2): E6/87-95var, E6/49-57, E6/49-59 and E7/56-65. In case of E6/87-95, the variant peptide was chosen to be able to test cytolytic activity on the HLA-A24 positive cell line SiHa, which harbors the HPV16 variant European Prototype 1 variant 4, with an amino acid exchange of leucine to valine at position 90 in the E6 protein. Moreover, these four peptides also showed promising *in silico* results, indicating at least weak binding, when tested for CTL prediction with the prediction server NetCTL (Larsen et al., 2007). This prediction server – next to peptide-HLA binding – also takes TAP transport efficiency and proteasomal C-terminal cleavage prediction into account. This server was not included in our initial predictions as its results are impossible to be combined with other predictive tools. Therefore, we only used it for post-hoc assessment of promising candidates.

Experiments were performed with PBMCs from HLA-A24 positive blood donors. Donor 1 was a 24 year old male and donors 2 and 3 were 24 and 37 year old females, respectively. No history of persistent infection with HPV was known for any donor. Donor characteristics and HLA types are given in Table 28 (Appendix).

3.5.1 IL-2 secretion upon peptide stimulation

Enzyme Linked Immunosorbent Assays (ELISAs) were performed with supernatants (SNT) from peptide-stimulated PBMCs (section 2.2.5.1) to monitor the secretion of the pro-proliferation cytokine IL-2. IL-2 secretion was assessed on day 3 and day 7 in peptide-specific short-term T cell lines. To this end, SNT was collected before washing and addition of exogenous IL-2.

Figure 32 shows IL-2 levels of PBMCs from donor 3 stimulated with peptides as indicated, compared to the negative control DMSO. IL-2 levels were elevated significantly on day seven in PBMCs stimulated with E6/87-95var, E6/49-57 and E7/56-65. Of note, exogenous IL-2 was added on day 3 after taking the sample. The effect of this exogenous IL-2 on IL-2 levels on day seven can be neglected since levels are compared to the negative control, which was treated with the same

concentration of exogenous IL-2 and did not show an increase of the measured IL-2 from day 3 to day 7. At this point, it remained elusive, which cells contained in the PBMC culture specifically produced IL-2. It can be assumed, however, that the secreted IL-2 is mainly derived from activated $CD4^+$ and $CD8^+$ T cells (Boyman and Sprent, 2012). Additionally, NKT cells have also been reported to secrete IL-2, albeit to a lesser extent (Jiang et al., 2005).

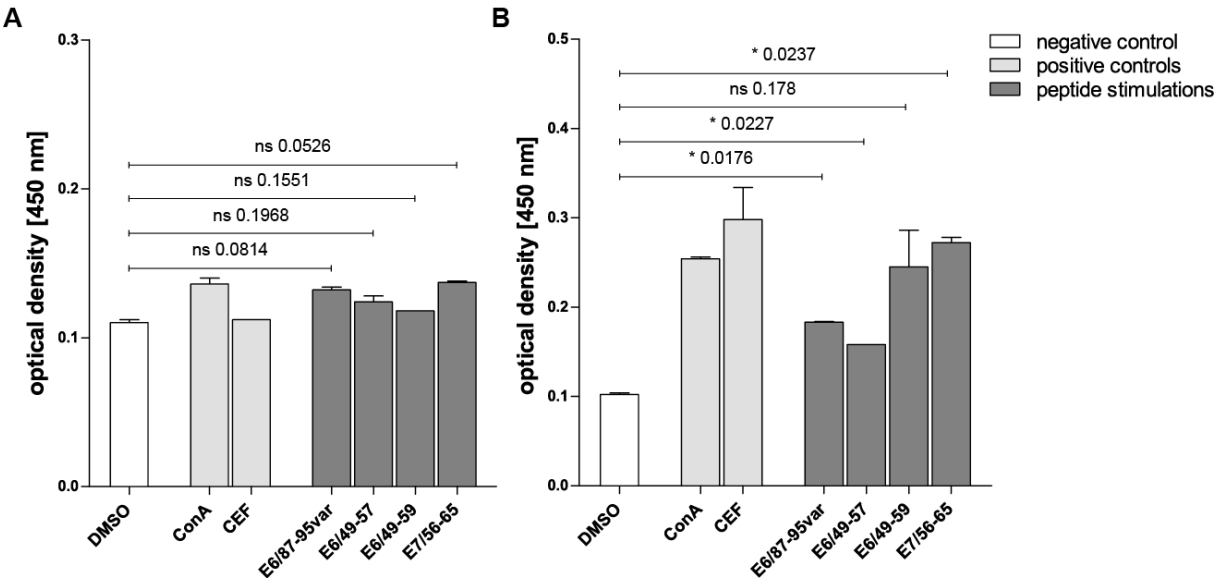

Figure 33 I IL-2 secretion of PBMCs after stimulation with HPV16 E6 and E7 peptides. PBMCs of donor 3 were seeded on day 0 and stimulated with peptides and IL-7. IL-2 was added on day 3 and day 7. DMSO was used as negative control and ConA and the CEF peptide pool were used as positive controls. IL-2 levels in SNT collected prior to exogenous IL-2 addition on day 3 (**A**) and day 7 (**B**) were measured by ELISA. Results are plotted as means ± SEM of duplicates. * $p < 0.05$, ns: not significant (unpaired student's t test)

3.5.2 Clonality of T cell receptors of peptide-specific long-term $CD8^+$ T cell lines

To assess the clonality of $CD8^+$ T cell in peptide-specific T cell lines, the T cell receptor (TCR) α- and β-chains were sequenced in collaboration with Eliana Ruggiero of the Division of Translational Oncology (G100, Christoph von Kalle), DKFZ. To this end, RNA was extracted from $CD8^+$ T cells of peptide-specific long-term T cell lines (section 2..2.5.1) and cDNA of the TCR α- and β-chain was reverse transcribed. Sequencing on an Illumina machine was carried out by using primers attaching to conserved flanking sequences. Of all four peptide-specific T cell lines, results could only be obtained for TCR sequencing of E6/49-75-specific $CD8^+$ T cells for both the α- and β-chain and for the α-chain of E6/87-95var-specific $CD8^+$ T cells of donor 3. Different regions of the variable domains of the TCRs were analyzed including the variable region (V), the diversity region (D) and the complementary determining region 3 (CDR3). CDR3 includes some of the V, all of the D and the joining (J) regions. It is the most variable amongst all CDRs and recognizes antigens presented by MHC I and MHC II molecules (Murphy, 2007). The findings of CDR3 sequencing are displayed in Figure 33. The ten sequences that were retrieved most often for each peptide-specific $CD8^+$ T cell line are color-coded according to their retrieval frequency, and the respective CDR3 sequences are

displayed on the right side. These results indicated high polyclonality of E6/49-75-specific $CD8^+$ T cells for both chains. However, E6/87-95var-specific $CD8^+$ T cells were basically monoclonal for the α-chain. Thus, putative E6/49-75-specific $CD8^+$ T cells were not a specific "cell line" and therefore a new E6/49-75-specific T cell line was generated for subsequent experiments.

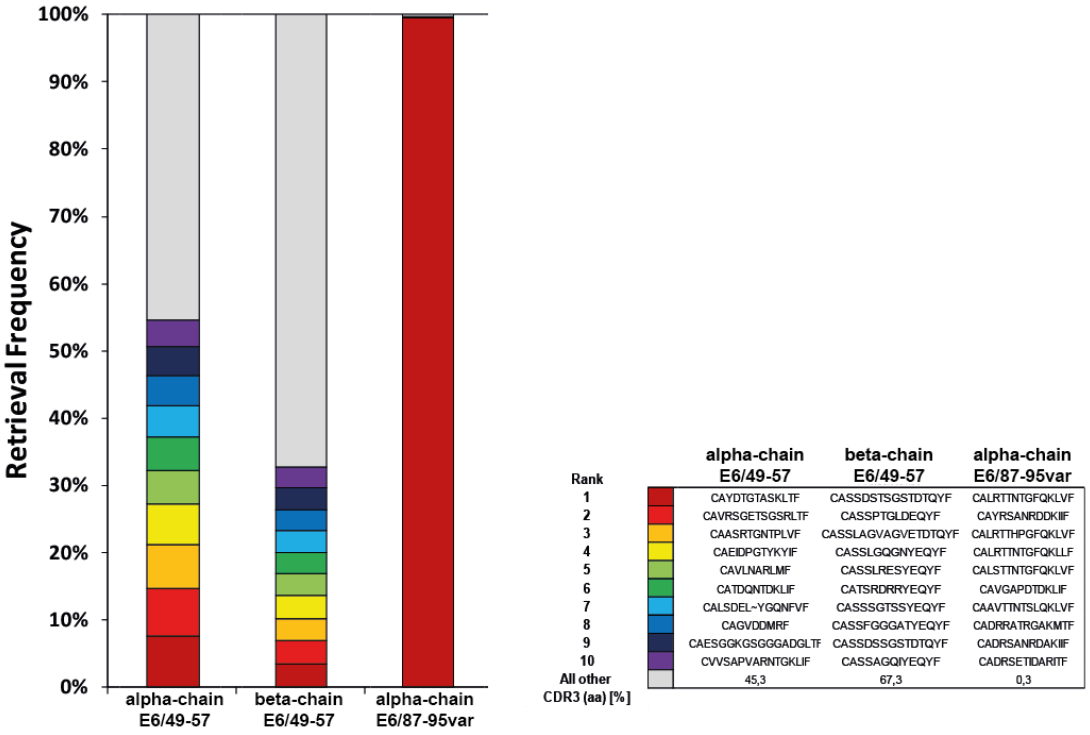

Figure 34 I CDR3 sequencing of peptide-specific $CD8^+$ T cells indicates poly- and monoclonal cultures. The TCRs of peptide-specific $CD8^+$ T cell were sequenced after four weeks of culture including four stimulations with antigen-presenting cells (APCs) presenting the respective peptide. Retrieval frequencies of CDR3 sequences are presented color-coded on the left. The ten sequences that were retrieved most often are shown on the right. The percentages of all other CDR3 sequences are indicated.

Table 21 gives an overview of all sequencing results comprising the numbers of overall TCR sequences and V, J and CDR3 sequences. For the E6/87-95var alpha chain, a total of 24,631 TCR sequences resulted in 13 sequences for the V region, 14 for the J region and 81 sequences for the CDR3 region. Of note, it is not known which α-chain belongs to which β-chain. The method is currently still under development and aims at an assignment of these two chains to each other. TCR sequencing does not allow to conclude any peptide sequences recognized on binding HLA/peptides complexes.

Table 21 I TCR sequencing of peptide-specific T cell lines. The number of identified TCR sequences, V region sequences, J region sequences and CDR3 sequences are shown.

	E6/49-57 alpha chain	**E6/49-57 beta chain**	**E6/87-95var alpha chain**
TCR sequences	85055	40855	24631
V	42	43	14
J	45	13	13
CDR3	597	2387	81

3.5.3 IFNγ secretion by peptide-specific long-term CD8$^+$ T cells upon co-culture with autologous peptide-pulsed B cells

Additionally to the immunogenicity screening of peptides in peptide-specific short-term T cell lines, IFNγ secretion was monitored in peptide-specific long-term CD8$^+$ T cell lines upon co-culture with autologous peptide-pulsed B cells. To this end, eleven long-term peptide-specific T cell lines from the three HLA-A*24:02 positive donors were generated (section 2.2.5.1) by four weekly stimulations of PBMCs with antigen-presenting cells (APC) pulsed with one of the four candidate peptides described above. Subsequently, untouched CD8$^+$ T cells were isolated by negative selection using MACS technology (> 95% CD8$^+$ T cell purity) as described in section 2.2.4.6. For the IFNγ ELISpot assay 1x10^5 peptide-specific CD8$^+$ T cells were co-cultured with 2x10^4 auotologous B cells presenting the respective peptide or control peptides. Figure 34 shows the results of IFNγ ELISpot assays for co-culture of E6/87-95var-, E6/49-47-, E6/49-59- and E7/56-65-specific CD8$^+$ T cells with their respective peptide-presenting B cell targets. CD8$^+$ T cell responses were considered positive only when the mean spot number was at least twofold higher than the mean spot number of the negative control (peptide-specific CD8$^+$ T cells co-cultured with DMSO-pulsed B cells). In (A) the spot counts for E6/49-57-specific CD8$^+$ T cells from donor 2 co-cultured with peptide presenting autologous B cells and controls are displayed exemplarily. E6/49-57-specific CD8$^+$ T cells exhibited significant IFNγ secretion upon recognizing their cognate peptide. Representative IFNγ ELISpot wells of data shown in (A) are displayed in (B). In (C) the stimulation indices for all tested peptide-specific CD8$^+$ T cell lines are summerized. The stimulation indices are defined as the ratio between the number of spots per 1x10^5 peptide-specific CD8$^+$ T cells co-cultured with epitope-pulsed B cells and those detected in control wells, where peptide-specific CD8$^+$ T cells were co-cultured with DMSO-pulsed B cells. Positive CD8$^+$ T cell responses are indicated by green lines, while red lines mean that the CD8$^+$ T cell responses were considered negative. All assays were performed in duplicates with the exception of cells from donor 1 and E7/56-65-specific CD8$^+$ T cells from donor 2, which were only carried out in single wells, due to the low numbers of CD8$^+$ T cells. E6/87-95var- and E6/49-59-specific CD8$^+$ T cell lines of donor 1 were shown to be positive for IFNγ secretion. In case of donor 2, E6/87-95var- and E6/49-57-specific CD8$^+$ T cell lines showed significant IFNγ secretion. Positive IFNγ responses could be observed for all four peptide-specific CD8$^+$ T cell lines co-cultured with respective peptide-pulsed autologous B cells from donor 3. Thus all four tested candidate peptides were capable of inducing CTL specific responses in some donors and only one peptide in all three donors. Differences in strength of immune reactions between different donors were expected.

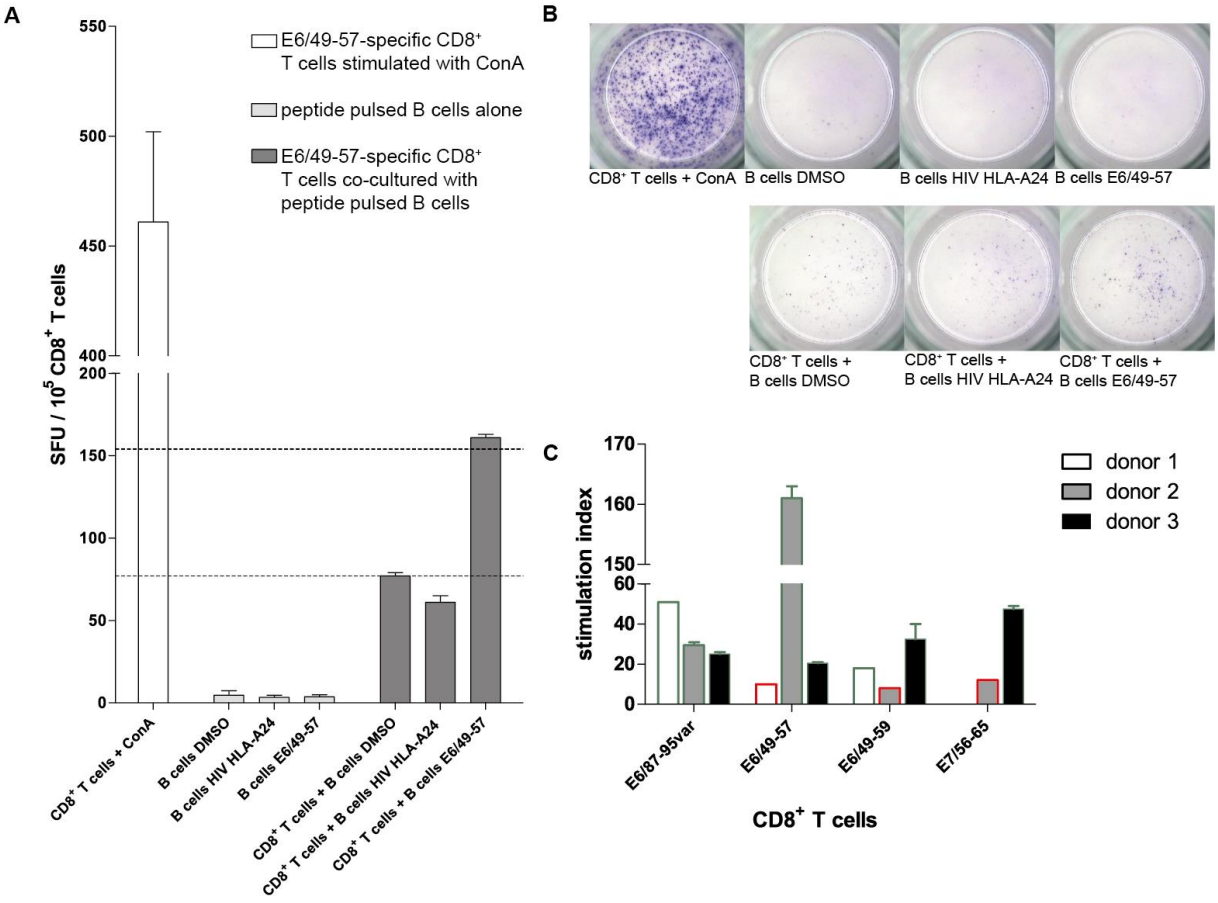

Figure 35 I IFNγ secretion of peptide-specific CD8$^+$ T cells upon co-culture with autologous B cells presenting the respective peptide. ELISpot analysis of peptide-specific CD8$^+$ T cell IFNγ responses to their cognate peptide presented on autologous B cell in three HLA-A*24:02 positive donors. Eleven peptide-specific CD8$^+$ T cell lines were generated by peptide-specific long-term T cell culture including four stimulations with APCs pulsed with the desired peptide over a time period of four weeks. CD8$^+$ T cell responses were considered positive only when the mean spot number was at least twofold higher than the mean spot number of the negative control (peptide-specific CD8$^+$ T cells co-cultured with DMSO-pulsed B cells). **A** Spot counts for E6/49-57-specific CD8$^+$ T cells from donor 2 co-cultured with peptide presenting autologous B cells and controls. E6/49-57-specific CD8$^+$ T cells stimulated with ConA were used as positive control. Autologous B cells (without T cells) pulsed with either DMSO, a HIV HLA-A24-restricted peptide or E6/49-57 are are shown as background controls. E6/49-57-specific CD8$^+$ T cells were co-cultured with autologous B cells pulsed with DMSO and a HIV HLA-A24-restricted peptide as negative controls. Results are plotted as means ± SEM of duplicates. SFU: spot forming units. **B** IFNγ ELISpot wells corresponding to the results shown in **A**. **C** Summary of the results of all eleven peptide-specific CD8$^+$ T cell lines co-cultured with respective autologous B cells presenting the cognate peptide. Green lines of bars indicate IFNγ reponses that were considered to be positive, while red lines of bars indicate negative results. The stimulation index was calculated as the ratio between the number of spots per 1x10^5 peptide-specific CD8$^+$ T cells stimulated with autologous B cells presenting their cognate peptide and those detected in control wells were peptide-specific CD8$^+$ T cells were co-cultured with autologous DMSO-pulsed B cells. Results are plotted as means ± SEM of dupliactes in all cases, except data from donor 1 and the E7/56-65-specific CD$^+$ T cells of donor 2, which are derived from single wells.

3.5.4 Cytotolytic activity of E6/56-65-specific T cells

Cytotoxicity assays were performed to assess if established peptide-specific T cell lines display cytolytic activity against cells presenting their cognate peptide. To this end, semi long-term peptide-specific T cells were generated by two stimulations of PBMCs of HLA-A24 positive donor 3 with peptide-pulsed autologous DCs in an interval of seven days (section 2.2.5.1). On day 13, cells were starved from cytokines overnight and on the next day the cytotoxicity assay was conducted. The classical chromium release method (section 2.2.5.5) was used as it is still the gold standard for

cytotoxicity assays and very sensitive. Autologous peptide-pulsed B cells were taken as target cells and labeled with radioactive $Na_2{}^{51}CrO_4$-solution. Labeled target cells were then co-cultured with peptide-specific T cells and SNTs harvested for analysis after 5 hours. Due to the small population size of $CD8^+$ T cells (15%) as determined by FACS analysis, bulk T cells were used. Thus it is also possible that the cytotoxic effect might have been due to $CD4^+$ T cells, as for those a cytolytic phenotype has been described (Mumberg et al., 1999; Corthay et al., 2005; Perez-Diez et al., 2007). However, as the peptides used to generate the T cell lines were HLA class I-restricted, the majority of the observed effects can safely be attributed to $CD8^+$ T cells.

Figure 35 summarizes the result of the cytotoxicity assay. Cytotoxicity, measured as percentage of specific lysis of autologous B cells presenting E7/56-65 was ranging between 99% and 40% (upper curve with dots). In comparison, no cytotoxicity was detected for target cells presenting the unrelated HIV HLA-A24 control peptide (lower curve with squares).

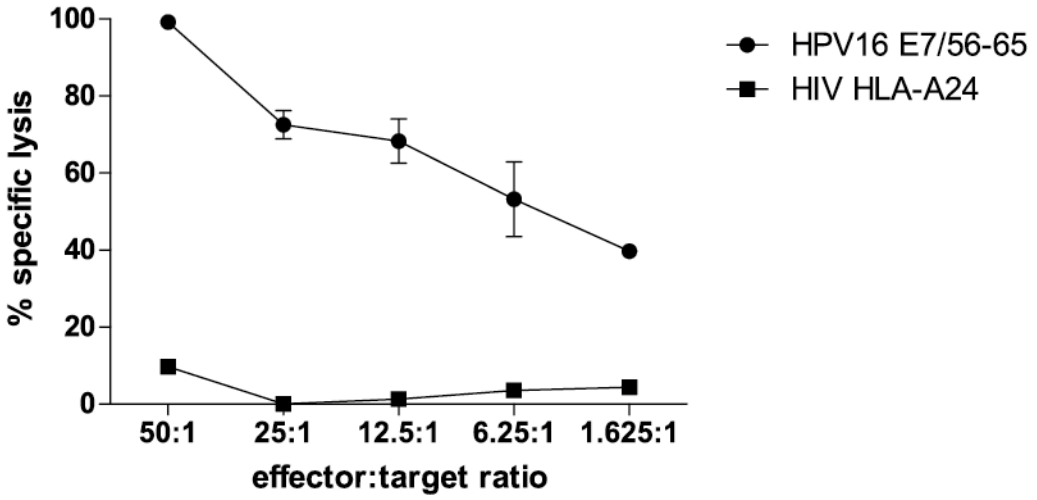

Figure 36 I HPV16 E7/56-65-specific cytolytic activity. Cr^{51} release cytotoxicity assay with E7/56-65-specific effector T cells and autologous B cells presenting either E7/56-65 or the negative control peptide HIV HLA-A24. Target cells were labeled with $Na_2{}^{51}CrO_4$-solution and incubated together with effector cells in indicated ratios for 5hrs. Results are plotted as means ± SEM of duplicates.

These results give a first hint that the E7/56-65 peptide might present a potent HPV16 vaccine candidate. However, results need to be reproduced and should be tested with cells from other donors and with cancer cells as target cells that naturally present the respective peptides.

4. Discussion

Today, cervical cancer is the third most common cancer worldwide (Schiffman et al., 2007; Scarinci et al., 2010). Annualy, approximately half a million women are diagnosed with this form of cancer (Ferlay et al., 2012) and more than 90% of cervical cancer cases occur in developing countries (van Bogaert, 2013). Human papillomavirus (HPV)16 accounts for the majority of cervical cancer cases and is found in approximately 50% of all HPV-induced cervical carcinomas (Munoz et al., 2006). Additionally, in the past decade oropharyngeal head and neck squamous cell carcinoma (HNSCC) cases have been shown to increase and HPV16 and other high-risk HPVs were reported to be associated with HNSCC (Gillison et al., 2000; Howlader et al., 2013; Michaud et al., 2014). The identification of HPV as a causative agent for cervical carcinomas (zur Hausen, 1977) has led to the development of effective prophylactic vaccines against HPV-mediated malignancies (Lowy et al., 2008; Joura et al., 2015). These vaccines prevent infections with the most prevalent high-risk HPV types but, however, cannot clear persistent HPV infections and thus have no therapeutic effect on individuals already infected with HPV (Hildesheim et al., 2007). Moreover, due to the long period between infection and tumor development, a large proportion of the global population is already HPV-infected (Frazer et al., 2011). Especially in developing countries, preventive medical health care such as detection of HPV-induced pre-malignant lesions is limited and vaccination with available prophylactic vaccines problematic due to socio-cultural factors and high costs of vaccination. Existing therapeutic modalities for HPV-induced premalignant lesions and tumors are surgical and can impair functions of the affected tissue, leading e.g. to premature births. Thus, there is a great need for novel and non-invasive therapeutic treatment options that include therapeutic vaccines (Conesa-Zamora, 2013).

Throughout the last decades, immunotherapy with all its tools has evolved as a promising treatment approach for various malignant diseases. Recent blockbusters, such as the anti-CTLA-4 antibody (Hodi et al., 2010) or CD19-targeting chimeric antigen receptors (CARs) (Grupp et al., 2013) eventually raised the awareness of the usefulness of immunotherapy in clinical cancer treatment. Both, the development of monoclonal antibodies and engineered T cells took years with steady improvements. The same holds true for peptide vaccination, for which the first clinical trial was conducted soon after the first tumor antigens were discovered (Hu et al., 1996).

To date, two main approaches comprise the concept of peptide vaccination, synthetic long peptides (SLPs) and synthetic short peptides (SSPs). The overall goal of peptide vaccination is to evoke a targeted immune response. To this end, antigen-presenting cells (APCs), mostly dendritic cells (DCs), need to present antigens by human leukocyte antigen (HLA) molecules to naïve $CD4^+$ and $CD8^+$ T cells. It is an ongoing discussion in the field of peptide vaccination, which approach, long or short synthetic peptides, is more suitable in terms of induction of effective T cell immune responses. SLPs

need to be taken up by APCs, processed intracellularly and loaded on HLA molecules for presentation of T cell epitopes. They evoke good $CD4^+$ T cell responses and in comparison lower $CD8^+$ T cell responses (Melief and van der Burg, 2008). In case of SSPs, APCs present only precise $CD8^+$ T epitopes, which can elicit much more specific $CD8^+$ T cell responses than SLPs. However, peptide vaccination with SSPs has been shown to be less effective in generating long-term memory responses and can even lead to tolerance due to presentation of $CD8^+$ T cell epitopes by non-professional APCs (Bijker et al., 2008). Thus, other components included into the vaccine formulation besides the pure peptide(s), such as adjuvants, need to be taken into consideration to determine if short peptides are superior to long peptides or the other way around. These issues are addressed in detail in section 4.6.

Nevertheless, regardless of the length of peptides used for vaccination, it is important to know which target epitopes are present on the cancer cell. Therefore, this study focused on the identification of HPV16 E6 and E7 $CD8^+$ T cell epitopes for the HLA-A3, HLA-A11 and HLA-A24 supertypes. The identified epitopes could be potentially used in a therapeutic vaccine setting or for other approaches such as immunomonitoring.

The E6 and E7 oncoproteins of high-risk HPVs present ideal targets for immunotherapeutical approaches, as they are foreign to the body, have been shown to be crucial for carcinogenesis and are constantly expressed in infected cells (Kanodia et al., 2008; Frazer et al., 2011). Consequently, these two oncoproteins are the most frequently targeted HPV antigens for therapeutic vaccine design. Pioneering work with HPV16 SLPs was carried out by Cornelis Melief and his team and by other groups in Leiden, The Netherlands (Melief and van der Burg, 2008). They have developed therapeutic SLP vaccines consisting of overlapping peptides, 27-35 amino acids in length, of the complete sequence of HPV16 E6 and E7. These peptides were found to facilitate simultaneous priming of T cells against multiple dominant and subdominant $CD4^+$ and $CD8^+$ T cell epitopes, evoking a broad T cell response (Welters et al., 2010). They were thoroughly tested in experimental models, reviewed in (Melief and van der Burg, 2008). Partial success could be demonstrated in clinical studies (Kenter et al., 2008; Kenter et al., 2009; de Vos van Steenwijk et al., 2012; van Poelgeest et al., 2013; de Vos van Steenwijk et al., 2014).

Rammensee and colleagues from Tübingen, Germany, pursue a slightly different approach for cancer immunotherapy. They identify naturally processed and presented HLA-associated peptides directly from primary tumor cells. Tumor-associated peptides are then selected by differential gene expression analysis and data mining. In the last step, selected candidates are validated from immunogenicity by monitoring T cell responses with cells from healthy volunteers (Stevanovic, 2002; Singh-Jasuja et al., 2004). This approach has led to the development of IMA901, the first therapeutic vaccine for renal cell cancer (RCC), which prolonged the survival of patients in a phase II trial in combination with chemotherapy (Walter et al., 2012).

The work of our laboratory and this study is partly based on a similar approach as employed by Rammensee and colleagues. Within the scope of the presented work, potential HPV16 E6 and E7 $CD8^+$ T cell epitopes were investigated. First, potential HLA class I-restricted T cell epitopes for three different HLA supertypes were predicted *in silico* by several prediction servers. *In silico* predictions were refined and eventually the actual binding of the best predicted binders was determind experimentally. Subsequently, the immunogenicity of binding peptides was assessed in healthy HLA-matched donors by screening for memory T cell responses. Furthermore, four promising peptide candidates were used to generate peptide-specific long-term T cell lines to further determine their potential as vaccine candidates in functional assays. For the direct identification of naturally processed and presented HPV16 E6 and E7 $CD8^+$ T cell epitopes on HPV16-transformed cells, our group is using a highly sensitive mass spectrometry (MS) approach. Identified $CD8^+$ T cell epitopes do not only represent candidates for peptide vaccines but are also useful for the development of other immunotherapies. Validated epitopes can be used for the development of adoptive T cell transfer with transgenic T cell receptors (TCRs) or CARs and additionally for immunomonitoring purposes.

4.1 Identification of HLA-A3, HLA-A11 and HLA-A24-binding HPV16 E6 and E7 peptides

In the past, epitope identification has been carried out mostly by analyzing the specificities of single T cell lines or clones. A more recent and widely applied strategy is called the "reverse immunology" approach, which involves pre-screening of proteomes by computational algorithms which are followed by experimental validation of selected peptides (Celis et al., 1994; Mora et al., 2006; De Groot et al., 2008; Larsen et al., 2010). This strategy was followed in this study and to this end, a total of ten predictors were employed to predict potential HPV16 E6 and E7-derived T cell epitopes that are restricted by either HLA-A3, HLA-A11 or HLA-A24 (section 3.1). After adjusting the threshold for experimental testing of the predicted peptides throughout the course of experimental testing, 69 peptides were predicted to bind to HLA-A24. In case of HLA-A3 and HLA-A11, 71 and 79 were predicted to bind to the respective HLA type. Many peptides could be verified to bind to the respective HLA type by cellular competition-based binding assays (Fig. 21, Tab. 14 and 15, Tab. 22-25, Appendix). 18 peptides could be shown to bind to HLA-A3 including seven peptides that were previously shown to be binders by other groups (Kast et al., 1994; Bourgault Villada et al., 2010). In case of HLA-A11, ten reported binding peptides (Kast et al., 1994; Bourgault Villada et al., 2010) could be confirmed and 23 novel binders were found. For HLA-A24, a total of 41 peptides were shown to bind including five peptides that have been reported to bind before (Kast et al., 1994; Morishima et al., 2007; Bourgault Villada et al., 2010).

As expected, some of the peptide repertoire binding to HLA-A3 did also bind to HLA-A11 (Fig. 21 A and B). This can be explained by great similarities of these two HLA supertypes in terms of their binding clefts (Sette and Sidney, 1999). No correlation could be observed, however, comparing

peptides binding to HLA-A3 and HLA-A11 with peptides binding to HLA-A24. Peptide sequence motifs binding to HLA-A24 are functionally quite distant from peptide sequence motifs binding to HLA-A3 or HLA-A11 (Thomsen et al., 2013). This highlights the necessity to define the epitope set for each HLA type individually, since a non-binding peptide for one HLA type might be strongly binding to another HLA type and *vice versa* (Paul et al., 2013).

Due to the magnitude of binding data generated in this study, it was possible to conduct an evaluation of the performance of individual prediction servers. The best predictors for each HLA allele in combination with either all peptide lengths or single peptide lengths are discussed in section 4.2.

After using conventional available T cell epitope prediction servers to identify potential HLA-specific HPV16 E6 and E7-derived peptides, the prediction approach was expanded to check if any binding peptides were missed. To this end, amino acid sequence motifs of all tested peptides that were binding (positive motifs) and not binding (negative motifs) to either HLA-A3, HLA-A11 or HLA-A24 were generated (section 3.1.3, Fig. 22 and 23). For HLA-A24, amino acid sequence motifs have been described with distinct anchor residues at position 2 and at the C-terminus. Tyrosin and phenylalanine were reported to be prefered residues at position 2 and phenylalanine, leucine and isoleucine at the C-terminus of the sequence (Kubo et al., 1994; Maier et al., 1994; Sette and Sidney, 1999). In line with these findings, HLA-A24 binding peptides of this study showed tyrosine predominately at position 2 and leucine and isoleucine at the C-terminal end of the peptide (Fig. 22). Phenylalanine was often present at the C-terminus of 8mers and 11mers (Fig 22 A and D).

Interestingly, tyrosine was also predominant on position 2 of 9mers and 10mers that were not binding. This is most likely due to the fact that all tested peptdies were predicted to be binders in the first place and all servers are trained with sequences of binding data which often included a tyrosine at position 2. Since not all predicted peptides were binding, this indicates that this residue alone is not sufficient for peptide binding and other residues are important as well.

The generated peptide motifs were used to screen non-tested peptides that were predicted with a low binding affinity but might bind nevertheless. Peptides with amino acid motifs similar to those of identified binding peptides and different to those of non-binding peptides were assumed to possibly bind to the respective HLA allele. For HLA-A3 and HLA-A11, three and seven potential peptides were identified by this approach, respectively. As HLA-A24 resulted in the highest number of novel and strong binders (Fig. 21 D) and is highly prevalent especially in Asian populations (Gonzalez-Galarza et al., 2015), this study was focused subsequently on this HLA type. For this reason, all 26 peptides that could be identified as potential binders to HLA-A24 by employing the motif search, were tested *in vitro* for their binding affinity (Fig. 24 and Tab. 14 and 15). Four peptides showed weak binding affininity to HLA-A24, two peptides were identified as intermediate binders and one peptide as a strong binder. These results indicate that this specific motif search based on known binders and

non-binders from the very same protein, is a valid and important supplement to the conventional prediction. Even a further decrease of the set cutoff would have failed to identify these peptides, as they were predicted badly by most servers, as for example E6/75-85 (Tab. 14). Moreover, in a study that determined the HLA-A*11:01-restricted HIV epitome, it was shown that weak binders were indeed strongly immunogenic (Yaciuk et al., 2014). Similar observations were made by Rosenberg and colleagues when they unraveled which T cell epitopes are actually good targets for a personalized treatment with adoptive transfer of tumor infiltrating lymphocytes (TILs) (Robbins et al., 2013). Here, only the 16th and 23rd best predicted peptide was acutally shown to be immunogenic (AACR meeting on Tumor Immunology and Immunotherapy, Dec 2015, Orlando, FL, USA). This implies that even very weak binders should not be omitted when searching for potential immungenicity of CD8$^+$ T cell epitopes.

In this study, potential CD8$^+$ T cell epitopes were considered only within a length of 8 to 11 amino acids. Other studies indicate that not only canonical peptides can be presented by HLA class I molecules, but also peptides with non-canonical lengths. MS-profiling by Escobar and colleagues revealed N-terminal extended peptide motifs (Escobar et al., 2008). They observed that some peptides longer than 11 amino acids represented N-terminal-extended peptides that contained an appropriate HLA-B35 peptide motif. In another recent study, the structures of two 15mers bound to HLA-A*02:01 could be solved and additionally it was shown that both HLA/peptides complexes were successfully recognized by T cells (Hassan et al., 2015). Moreover, it was reported that HLA-A*11:01 binds peptides containing unusal anchor residues. These epitopes were identified via deep ligand sequencing employing MS analysis and could be shown to be immunogenic by IFNγ ELISpot assays as well (Yaciuk et al., 2014). Taken together, this data suggests a paradigm change, indicating that longer epitopes can be presented by HLA class I molecules and may play a role in T cell immunity. In addition Calis and colleagues were able to demonstrate that the sequence positions 4 to 6 of a presented peptide enhance TCR-HLA/peptide interaction and are thus also important for immunogenicity (Calis et al., 2013). Since at the beginning of this study and still today, the best binding has been attributed to canonical peptides, we decided to focus on 8mers to 11mers.

Next to the HPV16 reference sequence which belongs to the European Prototype 1, several HPV16 variants exist, that bear amino acid differences in their protein sequences compared to the HPV16 reference sequence. As those variants needed to be taken into consideration for potential CD8$^+$ T cell epitope identification, 26 HPV16-positive cell lines from our cell line collection were tested for their HPV16 variant (section 3.2). To this end, genomic DNA was extracted and the viral genes E6 and E7 were amplified by PCR. The PCR products were sequenced and aligned to the HPV16 reference sequence in order to detect nucleotide exchanges. In parallel, a multiple sequence alignment of 62 HPV sequences already assigned to a specific variant was performed (Tab. 26, Appendix), showing the distinct nucleotide exchanges that are specfic for each variant. All 26 cell lines were then assigned

to a variant and mutations that resulted in amino acid exchanges were identified (Tab. 16 and Tab. 27, Appendix). A total of 13 amino acid exchanges could be detected in the E6 and E7 sequence variants present in our cell line collection. Potential binding of HPV16 variant T cell epitopes was predicted to HLA-A24 in the same manner as done initially for the HPV16 reference sequence. After setting an internal cutoff of 5000nM for binding, a total of 20 variant peptides were tested *in vitro* for their binding to HLA-A24 (Tab. 18). Seven of these variant peptides were shown to be binders (Fig. 27). The respective HPV16 reference-derived peptides that were binding as well, scored twice a comparable binding affinity, once a slightly lower binding affinity and in three cases a higher binding affinity. These observations are attributed to the different strength of binding affinity to the binding cleft of the HLA-A24 molecule by the distinct amino acids. Especially if a change occurs at an anchor residue position of the peptide sequence or the charge or polarity of the peptide is changed drastically, this may lead to stronger binding affinity or could abolish binding completely. The results presented here indicate that cells infected with different HPV16 variants likely present different E6 and E7 T cell epitopes. Some T cell epitopes might be more immunogenic than others, raising the question whether clinical outcomes are different in patients that are infected with different HPV16 variants. It was indeed reported, that depending on the patient cohort that was analyzed, different variants were correlated with different outcomes (Zehbe et al., 1998; Tu et al., 2006; Xi et al., 2007; Zuna et al., 2011). However, no clear correlation could be identified for specific HPV16 variants and increased or decreased risk of disease progression.

4.2 Performance evaluation of prediction servers

After having identified the HPV16 E6 and E7 T cell epitope sets which truly bind either to HLA-A3, HLA-A11 or HLA-A24, we decided to exploit the large amount of data that was generated and proceeded to assess the performance of the servers used for binding affinity predictions (section 3.1).

In a first step, the performance of all used prediction servers was roughly estimated step by step in the course of setting cutoffs for testing of binding affinity (section 3.1.1). To do so, the binding affinity of experimentally tested and predicted binding affinities of each peptide was color-coded according to our internal or to the server-specific category of strong, intermediate or weak binders. The cutoffs for *in vitro* testing were elevated throughout the course of experimental binding affinity assessment as a final stage where none of the predicted peptides was binding anymore was not reached. Moreover, cutoffs were chosen individually for all servers not to exclude any peptides that were indicated to possibly bind by only one individual server. Final color-coded lists of all predicted and tested peptides are displayed in Tables 14 & 15 and Tables 22-25 (Appendix). Not all peptides that were predicted to be binders were actually shown to bind to the respective HLA molecule *in vitro*. The server comparison also revealed that it was important to combine the results of multiple predictors, because some binding peptides would have been missed if only the results of individual servers would have been considered. For example E6/67-76, a 10mer strongly binding to HLA-A24, was only predicted to

be a weak binder by IEDBsmm and IEDBsmmpmbec and not predicted to bind by all other servers. Moreover, it has to be noted that not all prediction servers are capable of predicting binding of 8mers and 11mers. IEDBann, IEDBsmm, IEDBarb, IEDBsmmpmbec, SYFPEITHI and BIMAS only predict 9mers and 10mers.

In a second step, after the experimental testing of binding affinities was finalized, the performance of all prediction servers of the NetMHC and IEBD families was evaluated by receiver operating characteristic (ROC) analysis and calculation of the area under the curve (A_{ROC}) (section 3.1.4). The two servers BIMAS and SYFPEITHI were omitted in this evaluation due to unclear definition and discrimination of predicted binders and non-binders. A high degree of variability in the prediction efficacy for the three different alleles by the same predictors was observed, despite employing the same threshold levels. ROC analysis revealed that predictions for peptides binding to HLA-A3 (Fig. 26 A), if all four peptide lengths were taken into consideration, were more precise than predictions for HLA-A11 (Fig. 26 B). Binding predictions to HLA-A24 were shown to be worse than for HLA-A3 and HLA-A11 (Fig. 26 C). As the performance of a prediction server is depending on training data sets, the performance largely depends on the quality of these data sets. For some alleles, the availability of published data may be greater than for others (Gowthaman et al., 2010). That leads to imbalances in the prediction efficacy among the alleles and could explain why predictions for peptide binding to HLA-A3 and HLA-A11 were more accurate than for HLA-A24, as less binding data for the latter HLA type is available to train servers.

A large A_{ROC} is correlated to the probability that a prediction server will rank a randomly chosen binding pepide higher than a randomly chosen non-binding peptide and thus gives a useful measure of prediction quality. Individiual results for each HLA type and each peptide length, as well as for all peptide lengths for one HLA type, indicated different predictors to be the respective best choice for specific prediction tasks (Tab. 16). Considering all four peptide lengths, NetMHCcons was determined to be the best prediction server for HLA-A3 and HLA-A24. NetMHC was identified as the best prediction server for HLA-A11. For individual lengths and HLA types, all members of the NetMHC family, IEDBann and IEDBpan were ranked to be superior from case to case. For HLA-A3, excellent prediction performance was achieved by many prediction servers, especially for 9mers and 10mers and overall lengths in accordance to criteria previously determined by (Lin et al., 2008). In case of HLA-A11, mostly excellent and moderate prediction performance was shown for prediction servers predicting 8mers, 9mers and 10mers. For HLA-A24, the overall performance of predictors was shown to be worse than for HLA-A3 and HLA-A11. Here, NetMHC, NetMHCcons and IEDBpan showed moderate prediction performance for some lengths, otherwise all predictors displayed poor prediction performance. For 11mers binding to HLA-A11 and HLA-24, predictors displayed only moderate and mainly poor prediction performance. In summary, IEDBarb showed the least reliable prediction

performance while NetMHC and NetMHCcons performed best for the given binding data input in this evaluation.

In the past, assessments of *in silico* predicton servers have been performed by different groups. In general, these groups found, as we did in this study, that some of the predictors were highly accurate while others need improvement (Peters et al., 2006; Lin et al., 2008; Gowthaman et al., 2010; Zhang et al., 2011). In comparison to our study, predictors were previously only investigated for their prediction performance for 9 and 10mers. In these evaluations, mostly an extended set of available prediction servers that included partly the same prediction servers as in this study, were used. In line with our results (Tab. 16), one study rated NetMHCcons, together with NetMHC and NetMHCpan to be the best predictors (Zhang et al., 2011). Gowthaman and collegues reported IEDBann to be the best prediction server for HLA-A3. This is in line with our findings, where IEDBann was also amongst the best prediction server for 9mers and 10mers. For HLA-A11, NetMHC was rated to be the best predictor by us and rated third best, after NetMHCpan and IEDBann, by Gowthaman and colleagues. NetMHCcons, that was ranked as the best prediction server for HLA-A24 by us, was not considered by Gowthaman and collegues (Gowthaman et al., 2010). They described IEDBarb to be the best predictor for this HLA type. In contrast, this server was rated to be the worst predictor for HLA-A24 amongst the tested prediction servers in our study. This illustrates the importance of evaluation of prediction servers with different binding data sets.

It is important to note that some prediction methods such as the IEDBann method have their own limitations as they completetly rely on the training data set. Moreover, matrix-based methods, such as IEDBarb, IEDBsmm and IEDBsmmpmbec, depend on independent contributions of amino acids in the peptides, therefore ignoring their neighboring residues (Gowthaman et al., 2010). These drawbacks of individual prediction serveres need to be taken into consideration when selecting prediction servers to be used for a given task. It also has to be noted that some prediction servers are constantly improved by the developers and trained with newly available training data sets, as for example the NetMHC server family.

As a single predictor was not shown to be superior for all HLA types and peptides in this study, users should select the predictors individually, depending on the desired HLA allele and peptide length to get the best possible results.

4.3 Direct identification of $CD8^+$ T cell epitopes

In order to identify suitable peptides for the design of a therapeutic vaccine, natural processing and presentation of identified $CD8^+$ T cell epitopes on target cells should be confirmed. Indirect confirmation of CTL epitopes is feasible by immunonological methods, such as functional T cell assays that detect $CD8^+$ T cell specific responses triggered by cells displaying the epitope in question. This approach was pursued in this study and the results are discussed in the following sections.

However, a direct approach that identifies truly presented CTL epitopes is also desirable. To this end, a highly sensitive nano-UPLC-ESI-MS^3 multiple-reaction monitoring MS approach is being established in our laboratory (PhD project of Renata Blatnik) that identifies T cell epitopes presented by HLA molecules on HPV16-transformed cells. As a part of this study, sample preparation for subsequent MS analysis was established and optimized (section 3.3). First, suitable cell lines for immunoprecipitation (IP) of HLA/peptide complexes were determined by screening all HPV16-positive cell lines of our cell line collection, which were postitive for HLA-A3, HLA-A11 or HLA-A24, for HLA expression levels (section 3.3.1). 13 different cell lines were tested for their HLA expression levels (Fig. 28). For HLA-A3, all cell lines showed relatively high HLA expression levels compared to the HLA-A2 expression of the cell line CaSki, which was taken as a reference as it was used as the model cell line for optimization of the IP methodology (Fig. 28 A). Expression levels for HLA-A11 were lower than the levels of HLA-A2 on CaSki cells (Fig. 28 B). In case of HLA-A24-positive cell lines, SiHa displayed the highest HLA-A24 expression level, while levels for FKA16A were almost not detectable (Fig. 28 C). Consequently, cell lines with the highest HLA expression levels, CaSki, MRI-H196 and 93VU147T for HLA-A3 and SNU 1000 for HLA-A11 were selected for IP. In case of HLA-A24, all cell lines available, SiHa, SNU 1005, FK16A, W12 20861 and W12 20863 were selected, as this study became focused on the identification of HLA-A24-restricted $CD8^+$ T cell epitopes.

Figure 29 (section 3.3.2) displays Oriole protein staining and Western blot analysis of IPs of HLA/peptide complexes from SiHa and CaSki cells. Both, HLA-A2/peptide and HLA-A24/peptide complexes were successfully immunoprecipitated from cell lines carrying the respective HLA alleles. Purification and enrichment of HLA/peptide complexes was successfully achieved as shown by the presence of strong bands indicating the HLA class I α-chains at 44kDa in both Oriole stainings (A, C, E) and by Western blot analysis (B, D, F). Some HLA/peptide complexes, however, were lost in the flow through, which could indicate oversaturation of the capture antibodies. Thus, purity and enrichment of HLA/peptide complexes which are a prerequisite for MS analysis could be achieved. Since the MS technology is still being optimized, future analysis will reveal which E6 and E7 T cell epitopes are presented on the surface of HPV16-positive cells.

4.4 Immunogenicity of candidate peptides in short-term T cell lines

As the majority of the adult population has been transiently infected with a high-risk HPV type and therefore potentially with HPV16 (Evander et al., 1995; Woodman et al., 2007), buffy coats from blood donations of twelve healthy, anonymous donors were used to screen for peptide-specific memory T cell responses to determine the immunogenic potential of single peptides (section 3.4). Since $CD8^+$ T cell epitope screening was conducted without any knowledge of previous infection, this raises the possibility that some donors never had contact with HPV16. Additonally, every individual displays immune responses with a different strength and therefore one peptide might be considered to

be immunogenic in one healthy donor, but not in another, even if both individuals have been transiently infected with the same HPV16 type.

The prerequisite to be able to test the immunogenicity of HLA-specific peptides with anonymous blood donations was the successful determination of the donors' HLA types (section 3.4.1). HLA typing was only partly successful with FACS staining for six diefferent HLA supertypes (Tab. 20), as it resulted in false positive results in several cases due to cross-reactivity of antibodies. Specifically, the anti-HLA-A11 antibody showed cross-reactivity with HLA-A3, while the anti-HLA-A24 antibody cross-reacted with HLA-B27. Both cross-reactions were reported in the respective product's data sheet. Thus, we decided to subsequently HLA genotype the buffy coat cells by PCR in two digit resolution (Tab. 20). HLA genotyping could successfully confirm HLA-A11 and HLA-A24 positivity. However, buffy coats that were tested positive for HLA-B7 by FACS staining could not all be validated by PCR, as the used primers did not cover all HLA-B7 subtypes (Tab. 20 and Tab. 12). The reported prevalence for HLA types in the German population fits to our HLA typing results, even in this small sample of twelve donors.

IFNγ ELISpot analysis of peptide-specific short-term T cell lines generated from the buffy coats resulted in the identification of several immunogenic HPV16 E6 and E7 peptides (section, 3.4.2, Fig. 30 and 31). For instance, five peptides were shown to be immunogenic when tested with cells of the HLA-A24 positive donor 3 (Fig. 30). As depicted in Figure 31 A and B, multiple immunogenic peptides were identified for different HLA types. Peptides were often grouped in certain regions. Therefore, it seemed as if E6 and E7 harbor multiple immunogenic stretches within their aa sequence, where numerous HLA class I epitopes were located in close proximity. This was also shown for other proteins than E6 and E7, such as the well-known tumor antigens HER-2/neu (Disis et al., 2002) or NY-ESO-1 (Zeng et al., 2002). Identified immunogenic stretches also represent attractive regions for synthetic long peptides (SLPs).

Some obstacles complicate the interpretation of the obtained data. Even though the peptides were chosen because of certain HLA alleles being present, it remains elusive whether the observed T cell responses were only associated with these particular HLA molecules or with one of the other HLA molecules present on the used cells. Additionally, while immunogenicity of a peptide is confirmed by a positive response in one donor, a negative response in one or more donors does not necessarily mean that this peptide is not immunogenic. It simply might not be recognized by long-term memory T cells of this donor or the evoked immune response might be too low. The sample size of only twelve buffy coat donors restricts significance of the results and therefore only gives hints towards general immunogenicity of a peptide related to a specific HLA type. One possiblility to ensure that the immunogenicity of peptides is indeed HLA-specific, would be to mismatch donors in addition to HLA-matched donors and then demonstrate significance stastically. To this end, the group of tested donors would need to be increased. Moreover, it has to be taken into consideration that different

variants of HPV16 exist and thus the potential peptide repertoire that might have been encountered previously can differ in donors that carry the same HLA type but were infected with different variants.

In conclusion, the obtained data could show immunogenicity of several HLA-A2, HLA-A3, HLA-11, HLA-A24, HLA-B7 and HLA-B15-restricted HPV16 E6 and E7 peptides. However, cross-reactions with other HLA alleles cannot be excluded.

4.5 Functional analysis of peptide candidates

Four HLA-A24-restricted peptides, E6/87-95var, E6/49-57, E6/49-59 and E7/56-65 were selected for further functional characterization based on their binding to HLA-A24 (section 3.1.2 and 3.2) and their immunogenicity shown in peptide-specific short-term T cell lines (section 3.4.2). To this end, IL-2 secretion was tested in PBMCs upon peptide stimulation (section 3.5.1). Furthermore, eleven peptide-specific long-term T cell lines were generated from three different HLA-A24 positive donors, partly analyzed for their clonality (section 3.5.2) and co-cultured with autologous B cells pulsed with the respective peptide. The T cells were then studied for IFNγ secretion (section 3.5.3). Peptide-specific semi long-term T cell lines were tested for their cytolytic potential (section 3.5.4) in order to validate the peptides as CTL epitopes.

In previous studies, five HLA-A24-restricted CTL epitopes have already been described. These include one of the peptides that was also selected in this study to be tested for its potential as a CTL epitope, E6/49-57 (Morishima et al., 2007). Moreover, E6/75-83 and E6/91-100 were shown to elicit CTL responses in cervical cancer patients (Hara et al., 2005). While E6/75-83 was confirmed to be a weak binder in this study (Fig. 21 C and Tab. 14), E6/91-100 was below the cutoff of testing and thus not even considered in this study. The peptides E7/61-69 and E7/67-76, which have been described as CTL epitopes (Jang et al., 2012), were both tested for their binding affinity. The first one did not bind while the second showed weak binding affinity to HLA-A24 (Fig. 21 C and Tab. 15).

IL-2 secretion detected in the supernatants of PBMCs stimulated with either E6/87-95var, E6/49-57, or E7/56-65 on day seven of culture indicated T cell proliferation which was significantly increased in comparison to unstimulated PBMCs (Fig. 32 B). As bulk PBMC were used in this experiment, IL-2 secretion could not be assigned to a specific cell type. IL-2 synthesis by $CD8^+$ T cells is comparatively weak and the responses of these cells often require help from $CD4^+$ T cells (Boyman and Sprent, 2012). NKT cells have also been reported to secrete IL-2, however to a lesser extent (Jiang et al., 2005). However, it can be safely assumed that the secreted IL-2 is mainly derived from activated $CD8^+$ T cells, because HLA class I-restricted peptides were used for stimulation.

In order to show the clonality of generated peptide-specific long-term T cell lines, TCR sequencing of $CD8^+$ T cells was performed in collaboration with Eliana Ruggiero of the Division of Translational Oncology (G100, Christoph von Kalle, DKFZ) for cell lines generated from donor 3. Results could

only be obtained for TCR sequencing of E6/49-75-specific $CD8^+$ T cells for both the α- and β-chain and for the α-chain of E6/87-95var-specific $CD8^+$ T cells (Fig. 32). Monoclonality for the α-chain was shown for the E6/87-95var-specific $CD8^+$ T cell line. E6/49-75-specific $CD8^+$ T cells were polyclonal for the α- and β-chain and thus a new T cell line was generated for subsequent assays. So far, the technique does not allow to determine which α-chain belongs to which β-chain. The method is currently still under development and aims at an assignment of these two chains to each other. Moreover, TCR sequencing does not allow to conclude any peptide sequences of the recognized HLA/peptide complexes. One step further than testing for clonality would be the determination of specificity of $CD8^+$ T cells. This could be done by multimer stainings (Altman et al., 1996). As this approach requires a specific multimer to be manufactured for each HLA/peptide complex to be tested, it was omitted at this stage of this study.

As another approach to test specific recognition, IFNγ secretion by peptide-specific long-term $CD8^+$ T cells upon co-culture with autologous peptide-pulsed B cells was monitored in ELISpot assays. To this end, eleven peptide-specific long-term T cell lines were generated, $CD8^+$ T cells isolated and co-cultured with autologous peptide-pulsed B cells. IFNγ secretion upon recognition of their cognate peptide was shown to be significant in E6/87-95var- and E6/49-59-specific $CD8^+$ T cell lines from donor 1 (Fig. 34 C). In case of donor 2, E6/87-95var- and E6/49-57-specific $CD8^+$ T cell lines showed significant IFNγ secretion, and all four peptide-specific $CD8^+$ T cell lines of donor 3 were shown to be significantly positive for IFNγ in ELISpots (Fig. 34 A, B and C). Hence, all four tested candidate peptides were capable of inducing CTL specific responses in some donors. One peptide, E6/87-95var, elicited responses in all donors tested, and thus seems to be a very promising candidate to be included into a vaccine. To our knowledge all three donors were healthy at the time of blood donation. Differences in strength of immune reactions between different donors can be accounted to different histories concerning a potential transient infection with HPV16 and due to the different strength of immune responses by immune cells varying amongst individuals.

To find direct evidence for cytotoxic activity of peptide-specific T cells, the potential to actively kill autologous B cells pulsed with the respective peptide was analyzed. Cytotoxicity assays were successfully performed with E7/56-65-specific T cells. These cells were able to kill autologous B cell that were pulsed with E7/56-65 (Fig. 35). Therefore, these results give a first hint that the E7/56-65 peptide might present a potent HPV16 vaccine candidate. However, results should be reproduced with E7/56-65 specfic T cell lines from other HLA-A24 positive donors. Moreover it would be desirable to test the specific cytolytic activity of $CD8^+$ T cells by depletion of $CD4^+$ T cells and to use HLA-matched HPV16-transfomed cancer cells as target cells, which naturally present T cell epitopes. The latter approach was followed in this study by taking HLA-24 positive SiHa cells as target cells. Unfortunately, no reliable results could be produced due to paucity of effector T cells. Besides E7/56-65-specific T cells, also E6/87-95var-specific T cells were tested for their cytolytic activity. However,

cytotoxicity assay results were not consistent with these cells. Cytolytic activity could also be tested with other methods for validation. Potential approaches include FACS staining for cytolytic markers such as CD107a, perforin and granzyme B (Tschopp et al., 1986; Heusel et al., 1994; Aktas et al., 2009). Perforin and granzyme B secretion can also be analyzed by ELISpot assays.

In summary, functional characterization of E6/87-95var-, E6/49-57-, E6/49-59- and E7/56-65-specific T cell lines confirmed these peptides as $CD8^+$ T cell epitopes and therefore as potential candidates for a therapeutic HPV16 vaccine or as targets for immunomonitoring. Especially E7/56-65 was determined as a promising candidate as cytolytic activity could be demonstrated with E7/56-65-specific T cells.

4.6 Conclusions and future perspectives

In the present study, potential HPV16 E6 and E7-derived $CD8^+$ T cell epitopes restricted by HLA-A3, HLA-A11 and HLA-A24 were investigated. Candidate peptides were first identified with diversified *in silico* prediction approaches that determined the potential of peptides to bind to designated HLA types. Peptides were subsequently experimentally validated for binding in cellular binding assays. After assessment of immunogenicity of candidate peptides, functional assays were performed to confirm the potential of these $CD8^+$ T cell epitopes as vaccine candidates or for other purposes, such as immunomonitoring.

Several aspects need to be taken into consideration for the development of a synthetic short peptide vaccine. These include issues of HLA-restriction of $CD8^+$ T cell epitopes, efficacy of immune responses and potential tolerance induction (Van de Wall et al., 2014).

HLA-restriction implicates that only patients which carry matching HLA alleles would benefit from a specific epitope single-peptide vaccine. Thus, inclusion of multiple peptides covering several different HLA alleles or of a peptide that is not only restricted by a single HLA allele, would be beneficial to a broader cohort of patients. The approach of administering multiple synthetic short peptides together is already pursued in ongoing peptide vaccination studies. Up to four synthetic short peptides are currently used in one dose for treatment of melanoma patients (NIH, NCT01970358 and NCT02035956) (Fritsch et al., 2014). It is belived that this number can be increased to up to twenty peptides in one dose when adminstered in groups of five at different sides of the body (personal communication, Dr. Catherine J.Wu, Harvard Medical School, Cambridge, MA, USA). In the given example, the vaccines were developed as a personalized treatment, where all HLA types of the patient were determined. A similar approach could be also employed for patients that have HPV16-driven malignancies. The patients could be HLA-typed and then vaccinated with a HLA-specific vaccine consisting of multiple HLA-restricted synthetic short peptides. This will soon be a valid option, as HLA typing costs will decrease. The second option would be to include at least one peptide for every HLA supertype to ensure that every vaccinated patient is likely to react with at least one vaccine

peptide. Next to the investigation of HLA-A3, HLA-A11 and HLA-A24, our laboratory is currently also working other HLA supertypes such as HLA-A2, HLA-B7 and HLA-B15. The combination of those six HLA supertypes allows > 95% population coverage (Gonzalez-Galarza et al., 2015).

Another issue that needs to be considered in case of HPV16 vaccines are the different existing variants. As discussed before (section 4.1) several HPV16 variants were identified in our HPV16-positive cell line collection (Tab. 27) and included into T cell epitope prediction, cellular peptide-binding assays (section 3.2) and into immunogenicity screening and functional assays (section 3.4 and 3.5). One of the most promising candidates discovered in this study, E6/87-95var, is indeed derived from an European Prototype-1 sequence that carries an exchange from leucine to valine at position 90 of the E6 protein. Therefore, a potential HPV16 peptide vaccine should include peptides derived from the most prevalent HPV16 variants. In terms of a personalized peptide vaccine, the HPV16 variant present in lesions or the tumor of a patient could be determined and then a matching vaccine could be administered.

Peptide vaccines including only peptides of $CD8^+$ T cell epitopes have been shown to be less effective than longer peptides or proteins in creating long-term memory responses and might even lead to tolerance, because of presentation by non-professional APCs (Bijker et al., 2007). This is due to binding of short peptides to all HLA complexes on the surface of nucleated cells, as they do not require processing by APCs. Only properly activated DCs express the necessary costimulatory receptors to activate naïve T cells and therefore, exogenously loaded synthetic short peptides have been reported to confer tolerance (Toes et al., 1996). Moreover, accumulating data suggest that both cytotoxic $CD8^+$ T cell and $CD4^+$ T helper (T_H) cell responses play a pivotal role in the control and clearance of HPV infections (Nakagawa et al., 2000; van der Burg et al., 2002; Welters et al., 2003; Grabowska et al., 2015). The contribution of $CD4^+$ T cells towards tumor eradication is multifaceted. They contribute by supplying help to CTL immune responses and memory T cell responses (Williams et al., 2006a; Wiesel and Oxenius, 2012). Moreover, they have been shown to prevent peptide-specific tolerance (Shafer-Weaver et al., 2009). $CD4^+$ T cells have also been shown to display cytolytic activity and can thus directly kill tumor cells by themselves (Mumberg et al., 1999; Corthay et al., 2005; Perez-Diez et al., 2007). In HPV-induced lesions, HLA class I surface expression can be reduced as a result of HPV immune evasion strategies (Grabowska and Riemer, 2012), therefore exploiting cytolytic activitity of $CD4^+$ T cells is an important option. HLA class II molecules have been shown to be expressed in high-grade cervical lesions and cervical carcinoma (Zhou et al., 2006). Thus the inclusion of HLA class II-restricted epitopes, next to CTL epitopes, into a multi-peptide vaccine would allow for induction and/or activation of tumor antigen-specific effector $CD4^+$ T cells. Together with antigen-specific $CD8^+$ T cells, those cells could exert more efficient anti-tumor immune responses (van Hall and van der Burg, 2012). Different approaches could be followed to this end: one could combine HLA class I and HLA class II peptide-epitopes into one vaccine or use CTL epitopes with a

$CD4^+$ T_H epitope in one synthetic long peptide. The elongation of CTL peptides would also contribute against the potential tolerizing effect of short peptides and restrict presentation to professional APCs (Bijker et al., 2007; Bijker et al., 2008). However, this approach woul bear the risk of generating eptitopes that are not presented by tumor cells.

As synthetic short peptides or peptides in general, even if $CD4^+$ T_H epitopes are included, are poorly immunogenic when administered alone, appropriate immunostimulatory signals are needed for potent activation of APCs. To this end, various adjuvants that can activate DCs were tested in our laboratory *in vitro*. The two most promising adjuvants MPLA, a ligand for TLR4, and R848, a ligand for TLR7/8, were analyzed *in vivo* in HLA-A2.1-/HLA-DR1-transgenic H-2 class I-/class II-knockout mice. Mice were subcutaneously vaccinated with the HLA-A2-restricted E7/11-19 peptide emulsified in Montanide ISA51 in association with either MPLA alone, R848 alone, or MPLA and R848 in combination. The most immunogenic formulations will be evaluated for anti-tumor efficacy (project of Dr. Hadeel Khallouf). The findings of this project could later be translated to the HLA-A24-restricted peptides that were identified in this study, as a similar HLA-A*24:02 mouse model is available (Boucherma et al., 2013).

A therapeutic HPV16 vaccine consisting of nine E6 and four E7 overlapping SLPs formulated with the adjuvant Montanide 51 has been tested in various clinical trials (Kenter et al., 2008; Kenter et al., 2009; de Vos van Steenwijk et al., 2012; van Poelgeest et al., 2013; de Vos van Steenwijk et al., 2014). Durable or complete regression could be observed for some VIN3 patients (Kenter et al., 2009), no clinical responses, however, were reported in patients with advanced cervical carcinoma (van Poelgeest et al., 2013). Despite the latter results, these SLP vaccines were shown to be safe and capable of inducing desired T cell responses. Thus, the authors propose therapeutic SLP vaccination in combination with other therapies that target regulatory mechanisms and local immunosuppression in the tumor microenviroment (Van de Wall et al., 2014). This idea, the combination with other therapies, is one of the latest developments in cancer immunotherapy and peptide vaccination seems to be an optimal candidate for this purpose (Melero et al., 2014). In the past, cyclophosphamide, which leads to depletion of T_{reg} cells, was already successfully combined with peptide vaccination. For example, RCC patients showed prolonged survival upon combination of the peptide vaccine IMA901 and a single dose of cyclophosphamide (Walter et al., 2012). Conventional cancer therapies such as chemotherapy, surgery and radiotherapy are also easily combinable with immunotherapies. Immunotherapy can especially contribute to eliminate residual disease or to prevent recurrence. In the field of therapeutic HPV vaccination, a recent preclinical study has reported the beneficial combination of cisplatin and a SLP HPV16 vaccine in mice (van der Sluis et al., 2015). Moreover, several clinical studies were performed that combine vaccination with other immunotherapy approaches. The sequence optimized gp100 peptide that was developed by Rosenberg and colleagues in the 1990s (Rosenberg et al., 1998), was used in combination with high-dose systemic IL-2

administration, that showed an improved outcome in an phase III trial with metastatic melanoma (Schwartzentruber et al., 2011). Moreover, the gp100 peptide was also tested in combination with ipilimumab in a melanoma trial. This combination of immune checkpoint CTLA-4 blockage with the peptide vaccine did not lead to superior results in comparison with ipilimumab treatment alone (Hodi et al., 2010). For a novel minimal epitope HPV16 vaccine which could include the identified peptides of this study, ongoing reseach thus provides numerous ideas of potential combinational therapy approaches.

Next to combinational therapy, another current innovation in the field of cancer vaccination is the personalized treatment strategy. This approach is especially challenging, since not only every patient is different but also each tumor has its unique set of genomic and epigenomic alterations. The resulting antigens are named neoantigens – a newly available class of immunogens based on the personal, exquisitely tumor-specific mutations found uniquely in each tumor (Fritsch et al., 2014). Rosenberg and colleagues have developed a new method that allows the identification of tumor antigens recognized by tumor infiltrating T cells of individual patients. This screening approach involved mining whole-exome sequence data to identify mutated proteins expressed in patient tumors, subsequent *in silico* prediction using the prediction server NetMHCpan (Nielsen et al., 2007) to identify candidate mutated T cell epitopes and evaluation for recognition by TILs (Robbins et al., 2013). This approach was extended to a tandem minigene library screening, which successfully identified mutated antigens in two melanoma patients and one patient with epithelial cancer. Subsequent adoptive TIL therapy with purified T cells against the mutated antigens showed regression or prolonged stabilization of disease. (Lu et al., 2014; Tran et al., 2014). Wu and colleagues followed a similar approach (Fritsch et al., 2014) and two clinical trials have been initiated to directly test the concept of a neoantigen vaccine (NIH, NCT01970358 and NCT02035956). In order to refine the *in silico* peptide predictions in such approaches, it would be worthwhile to extend the use of prediction servers by not only using one single one but multiple servers as done in this study.

In conclusion, the four HPV16 E6 and E7 $CD8^+$ T cell epitopes that were identified to be immunogenic in this study are promising candidates to be applied as part of a synthetic short peptide HPV16 peptide vaccine. Being HLA-A24-restricted, additional minimal epitopes specific for additional HLA supertypes would need to be included if this vaccine should be applicable for a wide range of patients without the need of prior HLA typing. To improve desired T cell responses upon vaccination, the synthetic short peptides need to be administered in a vaccine formulation with appropriate $CD4^+$ T_H epitopes and in context of adjuvants. Moreover, the identified $CD8^+$ T cell epitopes, that have been shown to be immunogenic, could be employed for immunomonitoring and for the development of other immunotherapies.

5. References

Abban, C.Y. and Meneses, P.I., 2010, Usage of heparan sulfate, integrins, and FAK in HPV16 infection. Virology 403, 1-16.

Aguirre-Ghiso, J.A., 2007, Models, mechanisms and clinical evidence for cancer dormancy. Nature reviews. Cancer 7, 834-46.

Aktas, E., Kucuksezer, U.C., Bilgic, S., Erten, G. and Deniz, G., 2009, Relationship between CD107a expression and cytotoxic activity. Cellular immunology 254, 149-54.

Alberts, B.J., A.; Lewis, J.; Raff, M.; Roberts, K.; Walter, P. 2007. Molecular Biology of the Cell. Garland Science, New York.

Alcaraz, C., De Diego, M., Pastor, M.J. and Escribano, J.M., 1990, Comparison of a radioimmunoprecipitation assay to immunoblotting and ELISA for detection of antibody to African swine fever virus. Journal of veterinary diagnostic investigation : official publication of the American Association of Veterinary Laboratory Diagnosticians, Inc 2, 191-6.

Allan, R.S., Waithman, J., Bedoui, S., Jones, C.M., Villadangos, J.A., Zhan, Y., Lew, A.M., Shortman, K., Heath, W.R. and Carbone, F.R., 2006, Migratory dendritic cells transfer antigen to a lymph node-resident dendritic cell population for efficient CTL priming. Immunity 25, 153-62.

Altman, J.D., Moss, P.A., Goulder, P.J., Barouch, D.H., McHeyzer-Williams, M.G., Bell, J.I., McMichael, A.J. and Davis, M.M., 1996, Phenotypic analysis of antigen-specific T lymphocytes. Science 274, 94-6.

Amador-Molina, A., Gonzalez-Montoya, J.L., Garcia-Carranca, A., Mohar, A. and Lizano, M., 2013, Intratypic changes of the E1 gene and the long control region affect ori function of human papillomavirus type 18 variants. The Journal of general virology 94, 393-402.

Amigorena, S. and Savina, A., 2010, Intracellular mechanisms of antigen cross presentation in dendritic cells. Current opinion in immunology 22, 109-17.

Andreasen, S.O., Christensen, J.E., Marker, O. and Thomsen, A.R., 2000, Role of CD40 ligand and CD28 in induction and maintenance of antiviral CD8+ effector T cell responses. J Immunol 164, 3689-97.

Antinore, M.J., Birrer, M.J., Patel, D., Nader, L. and McCance, D.J., 1996, The human papillomavirus type 16 E7 gene product interacts with and trans-activates the AP1 family of transcription factors. The EMBO journal 15, 1950-60.

Appleman, L.J., Berezovskaya, A., Grass, I. and Boussiotis, V.A., 2000, CD28 costimulation mediates T cell expansion via IL-2-independent and IL-2-dependent regulation of cell cycle progression. J Immunol 164, 144-51.

Apter, D., Wheeler, C.M., Paavonen, J., Castellsague, X., Garland, S.M., Skinner, S.R., Naud, P., Salmeron, J., Chow, S.N., Kitchener, H.C., Teixeira, J.C., Jaisamrarn, U., Limson, G., Szarewski, A., Romanowski, B., Aoki, F.Y., Schwarz, T.F., Poppe, W.A., Bosch, F.X., Mindel, A., de Sutter, P., Hardt, K., Zahaf, T., Descamps, D., Struyf, F., Lehtinen, M., Dubin, G. and for the, H.P.V.P.S.G., 2015, Efficacy of HPV-16/18 AS04-adjuvanted vaccine against cervical infection and precancer in young women: final event-driven analysis of the randomised, double-blind PATRICIA trial. Clinical and vaccine immunology : CVI.

Ashrafi, G.H., Haghshenas, M.R., Marchetti, B., O'Brien, P.M. and Campo, M.S., 2005, E5 protein of human papillomavirus type 16 selectively downregulates surface HLA class I. International journal of cancer. Journal international du cancer 113, 276-83.

Atkins, M.B., Lotze, M.T., Dutcher, J.P., Fisher, R.I., Weiss, G., Margolin, K., Abrams, J., Sznol, M., Parkinson, D., Hawkins, M., Paradise, C., Kunkel, L. and Rosenberg, S.A., 1999, High-dose recombinant interleukin 2 therapy for patients with metastatic melanoma: analysis of 270 patients treated between 1985 and 1993. Journal of clinical oncology : official journal of the American Society of Clinical Oncology 17, 2105-16.

Aucouturier, J., Dupuis, L., Deville, S., Ascarateil, S. and Ganne, V., 2002, Montanide ISA 720 and 51: a new generation of water in oil emulsions as adjuvants for human vaccines. Expert review of vaccines 1, 111-8.

Bagarazzi, M.L., Yan, J., Morrow, M.P., Shen, X., Parker, R.L., Lee, J.C., Giffear, M., Pankhong, P., Khan, A.S., Broderick, K.E., Knott, C., Lin, F., Boyer, J.D., Draghia-Akli, R., White, C.J.,

Kim, J.J., Weiner, D.B. and Sardesai, N.Y., 2012, Immunotherapy against HPV16/18 generates potent TH1 and cytotoxic cellular immune responses. Science translational medicine 4, 155ra138.

Baker, T.S., Newcomb, W.W., Olson, N.H., Cowsert, L.M., Olson, C. and Brown, J.C., 1991, Structures of bovine and human papillomaviruses. Analysis by cryoelectron microscopy and three-dimensional image reconstruction. Biophysical journal 60, 1445-56.

Baldwin, P.J., van der Burg, S.H., Boswell, C.M., Offringa, R., Hickling, J.K., Dobson, J., Roberts, J.S., Latimer, J.A., Moseley, R.P., Coleman, N., Stanley, M.A. and Sterling, J.C., 2003, Vaccinia-expressed human papillomavirus 16 and 18 e6 and e7 as a therapeutic vaccination for vulval and vaginal intraepithelial neoplasia. Clinical cancer research : an official journal of the American Association for Cancer Research 9, 5205-13.

Banchereau, J. and Steinman, R.M., 1998, Dendritic cells and the control of immunity. Nature 392, 245-52.

Berg, M., Wingender, G., Djandji, D., Hegenbarth, S., Momburg, F., Hammerling, G., Limmer, A. and Knolle, P., 2006, Cross-presentation of antigens from apoptotic tumor cells by liver sinusoidal endothelial cells leads to tumor-specific CD8+ T cell tolerance. European journal of immunology 36, 2960-70.

Bergant Marusic, M., Ozbun, M.A., Campos, S.K., Myers, M.P. and Banks, L., 2012, Human papillomavirus L2 facilitates viral escape from late endosomes via sorting nexin 17. Traffic 13, 455-67.

Bernard, H.U., 2005, The clinical importance of the nomenclature, evolution and taxonomy of human papillomaviruses. Journal of clinical virology : the official publication of the Pan American Society for Clinical Virology 32 Suppl 1, S1-6.

Bevan, M.J., 2006, Cross-priming. Nature immunology 7, 363-5.

Bierer, B.E., Sleckman, B.P., Ratnofsky, S.E. and Burakoff, S.J., 1989, The biologic roles of CD2, CD4, and CD8 in T-cell activation. Annual review of immunology 7, 579-99.

Bijker, M.S., van den Eeden, S.J., Franken, K.L., Melief, C.J., Offringa, R. and van der Burg, S.H., 2007, CD8+ CTL priming by exact peptide epitopes in incomplete Freund's adjuvant induces a vanishing CTL response, whereas long peptides induce sustained CTL reactivity. J Immunol 179, 5033-40.

Bijker, M.S., van den Eeden, S.J., Franken, K.L., Melief, C.J., van der Burg, S.H. and Offringa, R., 2008, Superior induction of anti-tumor CTL immunity by extended peptide vaccines involves prolonged, DC-focused antigen presentation. European journal of immunology 38, 1033-42.

Bonanni, P., Bechini, A., Donato, R., Capei, R., Sacco, C., Levi, M. and Boccalini, S., 2015, Human papilloma virus vaccination: impact and recommendations across the world. Therapeutic advances in vaccines 3, 3-12.

Borysiewicz, L.K., Fiander, A., Nimako, M., Man, S., Wilkinson, G.W., Westmoreland, D., Evans, A.S., Adams, M., Stacey, S.N., Boursnell, M.E., Rutherford, E., Hickling, J.K. and Inglis, S.C., 1996, A recombinant vaccinia virus encoding human papillomavirus types 16 and 18, E6 and E7 proteins as immunotherapy for cervical cancer. Lancet 347, 1523-7.

Bos, R. and Sherman, L.A., 2010, CD4+ T-cell help in the tumor milieu is required for recruitment and cytolytic function of CD8+ T lymphocytes. Cancer research 70, 8368-77.

Bosch, F.X. and de Sanjose, S., 2003, Chapter 1: Human papillomavirus and cervical cancer--burden and assessment of causality. Journal of the National Cancer Institute. Monographs, 3-13.

Boscolo-Rizzo, P., Del Mistro, A., Bussu, F., Lupato, V., Baboci, L., Almadori, G., MC, D.A.M. and Paludetti, G., 2013, New insights into human papillomavirus-associated head and neck squamous cell carcinoma. Acta otorhinolaryngologica Italica : organo ufficiale della Societa italiana di otorinolaringologia e chirurgia cervico-facciale 33, 77-87.

Boucherma, R., Kridane-Miledi, H., Bouziat, R., Rasmussen, M., Gatard, T., Langa-Vives, F., Lemercier, B., Lim, A., Berard, M., Benmohamed, L., Buus, S., Rooke, R. and Lemonnier, F.A., 2013, HLA-A*01:03, HLA-A*24:02, HLA-B*08:01, HLA-B*27:05, HLA-B*35:01, HLA-B*44:02, and HLA-C*07:01 monochain transgenic/H-2 class I null mice: novel versatile preclinical models of human T cell responses. J Immunol 191, 583-93.

Bourgault Villada, I., Moyal Barracco, M., Berville, S., Bafounta, M.L., Longvert, C., Premel, V., Villefroy, P., Jullian, E., Clerici, T., Paniel, B., Maillere, B., Choppin, J. and Guillet, J.G., 2010, Human papillomavirus 16-specific T cell responses in classic HPV-related vulvar intra-

epithelial neoplasia. Determination of strongly immunogenic regions from E6 and E7 proteins. Clinical and experimental immunology 159, 45-56.
Bouvard, V., Baan, R., Straif, K., Grosse, Y., Secretan, B., El Ghissassi, F., Benbrahim-Tallaa, L., Guha, N., Freeman, C., Galichet, L., Cogliano, V. and Group, W.H.O.I.A.f.R.o.C.M.W., 2009, A review of human carcinogens--Part B: biological agents. The lancet oncology 10, 321-2.
Boyman, O. and Sprent, J., 2012, The role of interleukin-2 during homeostasis and activation of the immune system. Nat Rev Immunol 12, 180-90.
Brady, C.S., Bartholomew, J.S., Burt, D.J., Duggan-Keen, M.F., Glenville, S., Telford, N., Little, A.M., Davidson, J.A., Jimenez, P., Ruiz-Cabello, F., Garrido, F. and Stern, P.L., 2000, Multiple mechanisms underlie HLA dysregulation in cervical cancer. Tissue antigens 55, 401-11.
Brito, L.A., Malyala, P. and O'Hagan, D.T., 2013, Vaccine adjuvant formulations: a pharmaceutical perspective. Seminars in immunology 25, 130-45.
Bromberg, J.F., Horvath, C.M., Wen, Z., Schreiber, R.D. and Darnell, J.E., Jr., 1996, Transcriptionally active Stat1 is required for the antiproliferative effects of both interferon alpha and interferon gamma. Proceedings of the National Academy of Sciences of the United States of America 93, 7673-8.
Bromley, S.K., Burack, W.R., Johnson, K.G., Somersalo, K., Sims, T.N., Sumen, C., Davis, M.M., Shaw, A.S., Allen, P.M. and Dustin, M.L., 2001, The immunological synapse. Annual review of immunology 19, 375-96.
Buck, C.B., Cheng, N., Thompson, C.D., Lowy, D.R., Steven, A.C., Schiller, J.T. and Trus, B.L., 2008, Arrangement of L2 within the papillomavirus capsid. Journal of virology 82, 5190-7.
Bui, H.H., Sidney, J., Peters, B., Sathiamurthy, M., Sinichi, A., Purton, K.A., Mothe, B.R., Chisari, F.V., Watkins, D.I. and Sette, A., 2005, Automated generation and evaluation of specific MHC binding predictive tools: ARB matrix applications. Immunogenetics 57, 304-14.
Bunce, M., 2003, PCR-sequence-specific primer typing of HLA class I and class II alleles. Methods Mol Biol 210, 143-71.
Burk, R.D., Chen, Z., Harari, A., Smith, B.C., Kocjan, B.J., Maver, P.J. and Poljak, M., 2011, Classification and nomenclature system for human Alphapapillomavirus variants: general features, nucleotide landmarks and assignment of HPV6 and HPV11 isolates to variant lineages. Acta dermatovenerologica Alpina, Pannonica, et Adriatica 20, 113-23.
Burk, R.D., Chen, Z. and Van Doorslaer, K., 2009, Human papillomaviruses: genetic basis of carcinogenicity. Public health genomics 12, 281-90.
Burk, R.D., Harari, A. and Chen, Z., 2013, Human papillomavirus genome variants. Virology 445, 232-43.
Burnet, M., 1957, Cancer; a biological approach. I. The processes of control. British medical journal 1, 779-86.
Busch, C., Geisler, J., Knappskog, S., Lillehaug, J.R. and Lonning, P.E., 2010, Alterations in the p53 pathway and p16INK4a expression predict overall survival in metastatic melanoma patients treated with dacarbazine. The Journal of investigative dermatology 130, 2514-6.
Calis, J.J., Maybeno, M., Greenbaum, J.A., Weiskopf, D., De Silva, A.D., Sette, A., Kesmir, C. and Peters, B., 2013, Properties of MHC class I presented peptides that enhance immunogenicity. PLoS computational biology 9, e1003266.
Campo, M.S., Graham, S.V., Cortese, M.S., Ashrafi, G.H., Araibi, E.H., Dornan, E.S., Miners, K., Nunes, C. and Man, S., 2010, HPV-16 E5 down-regulates expression of surface HLA class I and reduces recognition by CD8 T cells. Virology 407, 137-42.
Carreno, B.M. and Collins, M., 2002, The B7 family of ligands and its receptors: new pathways for costimulation and inhibition of immune responses. Annual review of immunology 20, 29-53.
Celis, E., Fikes, J., Wentworth, P., Sidney, J., Southwood, S., Maewal, A., Del Guercio, M.F., Sette, A. and Livingston, B., 1994, Identification of potential CTL epitopes of tumor-associated antigen MAGE-1 for five common HLA-A alleles. Molecular immunology 31, 1423-30.
Cerwenka, A. and Lanier, L.L., 2001, Natural killer cells, viruses and cancer. Nat Rev Immunol 1, 41-9.
Chen, X.S., Garcea, R.L., Goldberg, I., Casini, G. and Harrison, S.C., 2000, Structure of small virus-like particles assembled from the L1 protein of human papillomavirus 16. Molecular cell 5, 557-67.

Chen, Z., Terai, M., Fu, L., Herrero, R., DeSalle, R. and Burk, R.D., 2005, Diversifying selection in human papillomavirus type 16 lineages based on complete genome analyses. Journal of virology 79, 7014-23.

Chien, Y.H. and Konigshofer, Y., 2007, Antigen recognition by gammadelta T cells. Immunological reviews 215, 46-58.

Chow, L.T., Broker, T.R. and Steinberg, B.M., 2010, The natural history of human papillomavirus infections of the mucosal epithelia. APMIS : acta pathologica, microbiologica, et immunologica Scandinavica 118, 422-49.

Clarke, S.L., Betts, G.J., Plant, A., Wright, K.L., El-Shanawany, T.M., Harrop, R., Torkington, J., Rees, B.I., Williams, G.T., Gallimore, A.M. and Godkin, A.J., 2006, CD4+CD25+FOXP3+ regulatory T cells suppress anti-tumor immune responses in patients with colorectal cancer. PloS one 1, e129.

Collins, S., Mazloomzadeh, S., Winter, H., Blomfield, P., Bailey, A., Young, L.S. and Woodman, C.B., 2002, High incidence of cervical human papillomavirus infection in women during their first sexual relationship. BJOG : an international journal of obstetrics and gynaecology 109, 96-8.

Conesa-Zamora, P., 2013, Immune responses against virus and tumor in cervical carcinogenesis: treatment strategies for avoiding the HPV-induced immune escape. Gynecologic oncology 131, 480-8.

Corthay, A., Skovseth, D.K., Lundin, K.U., Rosjo, E., Omholt, H., Hofgaard, P.O., Haraldsen, G. and Bogen, B., 2005, Primary antitumor immune response mediated by CD4+ T cells. Immunity 22, 371-83.

Croft, M., 2003, Costimulation of T cells by OX40, 4-1BB, and CD27. Cytokine & growth factor reviews 14, 265-73.

Croft, M. and Swain, S.L., 1991a, B cell response to fresh and effector T helper cells. Role of cognate T-B interaction and the cytokines IL-2, IL-4, and IL-6. J Immunol 146, 4055-64.

Croft, M. and Swain, S.L., 1991b, B cell response to T helper cell subsets. II. Both the stage of T cell differentiation and the cytokines secreted determine the extent and nature of helper activity. J Immunol 147, 3679-89.

Crooks, G.E., Hon, G., Chandonia, J.M. and Brenner, S.E., 2004, WebLogo: a sequence logo generator. Genome research 14, 1188-90.

Crosbie, E.J., Einstein, M.H., Franceschi, S. and Kitchener, H.C., 2013, Human papillomavirus and cervical cancer. Lancet 382, 889-99.

Cuschieri, K.S., Cubie, H.A., Whitley, M.W., Seagar, A.L., Arends, M.J., Moore, C., Gilkisson, G. and McGoogan, E., 2004, Multiple high risk HPV infections are common in cervical neoplasia and young women in a cervical screening population. Journal of clinical pathology 57, 68-72.

Dai, L.C., West, K., Littaua, R., Takahashi, K. and Ennis, F.A., 1992, Mutation of human immunodeficiency virus type 1 at amino acid 585 on gp41 results in loss of killing by CD8+ A24-restricted cytotoxic T lymphocytes. Journal of virology 66, 3151-4.

Daling, J.R., Madeleine, M.M., Johnson, L.G., Schwartz, S.M., Shera, K.A., Wurscher, M.A., Carter, J.J., Porter, P.L., Galloway, D.A. and McDougall, J.K., 2004, Human papillomavirus, smoking, and sexual practices in the etiology of anal cancer. Cancer 101, 270-80.

Davidson, E.J., Boswell, C.M., Sehr, P., Pawlita, M., Tomlinson, A.E., McVey, R.J., Dobson, J., Roberts, J.S., Hickling, J., Kitchener, H.C. and Stern, P.L., 2003, Immunological and clinical responses in women with vulval intraepithelial neoplasia vaccinated with a vaccinia virus encoding human papillomavirus 16/18 oncoproteins. Cancer research 63, 6032-41.

Davidson, E.J., Faulkner, R.L., Sehr, P., Pawlita, M., Smyth, L.J., Burt, D.J., Tomlinson, A.E., Hickling, J., Kitchener, H.C. and Stern, P.L., 2004, Effect of TA-CIN (HPV 16 L2E6E7) booster immunisation in vulval intraepithelial neoplasia patients previously vaccinated with TA-HPV (vaccinia virus encoding HPV 16/18 E6E7). Vaccine 22, 2722-9.

De Groot, A.S., Bosma, A., Chinai, N., Frost, J., Jesdale, B.M., Gonzalez, M.A., Martin, W. and Saint-Aubin, C., 2001, From genome to vaccine: in silico predictions, ex vivo verification. Vaccine 19, 4385-95.

De Groot, A.S., Rivera, D.S., McMurry, J.A., Buus, S. and Martin, W., 2008, Identification of immunogenic HLA-B7 "Achilles' heel" epitopes within highly conserved regions of HIV. Vaccine 26, 3059-71.

de Villiers, E.M., 2013, Cross-roads in the classification of papillomaviruses. Virology 445, 2-10.
de Villiers, E.M., Fauquet, C., Broker, T.R., Bernard, H.U. and zur Hausen, H., 2004, Classification of papillomaviruses. Virology 324, 17-27.
de Vos van Steenwijk, P.J., Ramwadhdoebe, T.H., Lowik, M.J., van der Minne, C.E., Berends-van der Meer, D.M., Fathers, L.M., Valentijn, A.R., Oostendorp, J., Fleuren, G.J., Hellebrekers, B.W., Welters, M.J., van Poelgeest, M.I., Melief, C.J., Kenter, G.G. and van der Burg, S.H., 2012, A placebo-controlled randomized HPV16 synthetic long-peptide vaccination study in women with high-grade cervical squamous intraepithelial lesions. Cancer immunology, immunotherapy : CII 61, 1485-92.
de Vos van Steenwijk, P.J., van Poelgeest, M.I., Ramwadhdoebe, T.H., Lowik, M.J., Berends-van der Meer, D.M., van der Minne, C.E., Loof, N.M., Stynenbosch, L.F., Fathers, L.M., Valentijn, A.R., Oostendorp, J., Osse, E.M., Fleuren, G.J., Nooij, L., Kagie, M.J., Hellebrekers, B.W., Melief, C.J., Welters, M.J., van der Burg, S.H. and Kenter, G.G., 2014, The long-term immune response after HPV16 peptide vaccination in women with low-grade pre-malignant disorders of the uterine cervix: a placebo-controlled phase II study. Cancer immunology, immunotherapy : CII 63, 147-60.
de Wilde, J., Wilting, S.M., Meijer, C.J., van de Wiel, M.A., Ylstra, B., Snijders, P.J. and Steenbergen, R.D., 2008, Gene expression profiling to identify markers associated with deregulated hTERT in HPV-transformed keratinocytes and cervical cancer. International journal of cancer. Journal international du cancer 122, 877-88.
Dell, G., Wilkinson, K.W., Tranter, R., Parish, J., Leo Brady, R. and Gaston, K., 2003, Comparison of the structure and DNA-binding properties of the E2 proteins from an oncogenic and a non-oncogenic human papillomavirus. Journal of molecular biology 334, 979-91.
Dengjel, J., Schoor, O., Fischer, R., Reich, M., Kraus, M., Muller, M., Kreymborg, K., Altenberend, F., Brandenburg, J., Kalbacher, H., Brock, R., Driessen, C., Rammensee, H.G. and Stevanovic, S., 2005, Autophagy promotes MHC class II presentation of peptides from intracellular source proteins. Proceedings of the National Academy of Sciences of the United States of America 102, 7922-7.
Dessen, A., Lawrence, C.M., Cupo, S., Zaller, D.M. and Wiley, D.C., 1997, X-ray crystal structure of HLA-DR4 (DRA*0101, DRB1*0401) complexed with a peptide from human collagen II. Immunity 7, 473-81.
Dickmann, J. 2012 Characterization of HPV16 variants in HPV16-transformed cell lines based on gene specific PCR. Bachelor Thesis. University of Heidelberg.
Disis, M.L., Gooley, T.A., Rinn, K., Davis, D., Piepkorn, M., Cheever, M.A., Knutson, K.L. and Schiffman, K., 2002, Generation of T-cell immunity to the HER-2/neu protein after active immunization with HER-2/neu peptide-based vaccines. Journal of clinical oncology : official journal of the American Society of Clinical Oncology 20, 2624-32.
DKFZ. 2012 Krebsatlas. online database: www.krebsatlas.de, (access date: 20150328)
Dong, C., Juedes, A.E., Temann, U.A., Shresta, S., Allison, J.P., Ruddle, N.H. and Flavell, R.A., 2001, ICOS co-stimulatory receptor is essential for T-cell activation and function. Nature 409, 97-101.
Doorbar, J., 2005, The papillomavirus life cycle. Journal of clinical virology : the official publication of the Pan American Society for Clinical Virology 32 Suppl 1, S7-15.
Doorbar, J., 2006, Molecular biology of human papillomavirus infection and cervical cancer. Clinical science 110, 525-41.
Doorbar, J., Quint, W., Banks, L., Bravo, I.G., Stoler, M., Broker, T.R. and Stanley, M.A., 2012, The biology and life-cycle of human papillomaviruses. Vaccine 30 Suppl 5, F55-70.
Drijkoningen, M., De Wolf-Peeters, C., Degreef, H. and Desmet, V., 1988, Epidermal Langerhans cells, dermal dendritic cells, and keratinocytes in viral lesions of skin and mucous membranes: an immunohistochemical study. Archives of dermatological research 280, 220-7.
Dudley, M.E., Wunderlich, J.R., Robbins, P.F., Yang, J.C., Hwu, P., Schwartzentruber, D.J., Topalian, S.L., Sherry, R., Restifo, N.P., Hubicki, A.M., Robinson, M.R., Raffeld, M., Duray, P., Seipp, C.A., Rogers-Freezer, L., Morton, K.E., Mavroukakis, S.A., White, D.E. and Rosenberg, S.A., 2002, Cancer regression and autoimmunity in patients after clonal repopulation with antitumor lymphocytes. Science 298, 850-4.

Dunn, G.P., Bruce, A.T., Ikeda, H., Old, L.J. and Schreiber, R.D., 2002, Cancer immunoediting: from immunosurveillance to tumor escape. Nature immunology 3, 991-8.

Dunn, G.P., Old, L.J. and Schreiber, R.D., 2004, The immunobiology of cancer immunosurveillance and immunoediting. Immunity 21, 137-48.

Dunne, E.F., Unger, E.R., Sternberg, M., McQuillan, G., Swan, D.C., Patel, S.S. and Markowitz, L.E., 2007, Prevalence of HPV infection among females in the United States. JAMA : the journal of the American Medical Association 297, 813-9.

Durst, M., Gissmann, L., Ikenberg, H. and zur Hausen, H., 1983, A papillomavirus DNA from a cervical carcinoma and its prevalence in cancer biopsy samples from different geographic regions. Proceedings of the National Academy of Sciences of the United States of America 80, 3812-5.

EMBL-EBI. IPD-IMGT/HLA database: https://www.ebi.ac.uk/ipd/imgt/hla/ , (access: 20150331), Hinxton, Cambridgeshire.

Escobar, H., Crockett, D.K., Reyes-Vargas, E., Baena, A., Rockwood, A.L., Jensen, P.E. and Delgado, J.C., 2008, Large scale mass spectrometric profiling of peptides eluted from HLA molecules reveals N-terminal-extended peptide motifs. J Immunol 181, 4874-82.

Evander, M., Edlund, K., Gustafsson, A., Jonsson, M., Karlsson, R., Rylander, E. and Wadell, G., 1995, Human papillomavirus infection is transient in young women: a population-based cohort study. The Journal of infectious diseases 171, 1026-30.

Fahey, L.M., Raff, A.B., Da Silva, D.M. and Kast, W.M., 2009, A major role for the minor capsid protein of human papillomavirus type 16 in immune escape. J Immunol 183, 6151-6.

Faint, J.M., Annels, N.E., Curnow, S.J., Shields, P., Pilling, D., Hislop, A.D., Wu, L., Akbar, A.N., Buckley, C.D., Moss, P.A., Adams, D.H., Rickinson, A.B. and Salmon, M., 2001, Memory T cells constitute a subset of the human CD8+CD45RA+ pool with distinct phenotypic and migratory characteristics. J Immunol 167, 212-20.

Falk, K., Rotzschke, O., Stevanovic, S., Jung, G. and Rammensee, H.G., 1991, Allele-specific motifs revealed by sequencing of self-peptides eluted from MHC molecules. Nature 351, 290-6.

Fallon, P.G., Ballantyne, S.J., Mangan, N.E., Barlow, J.L., Dasvarma, A., Hewett, D.R., McIlgorm, A., Jolin, H.E. and McKenzie, A.N., 2006, Identification of an interleukin (IL)-25-dependent cell population that provides IL-4, IL-5, and IL-13 at the onset of helminth expulsion. The Journal of experimental medicine 203, 1105-16.

Ferlay, J., Soerjomataram, I., Ervik, M., Dikshit, R., Eser, S., Mathers, C., Rebelo, M., Parkin, D.M., Forman, D. and Bray, F. 2012 GLOBOCAN 2012 v1.0, Cancer Incidence and Mortality Worldwide: IARC CancerBase No. 11 In. International Agency for Research on Cancer (IARC), Lyon, France.

Fiander, A.N., Tristram, A.J., Davidson, E.J., Tomlinson, A.E., Man, S., Baldwin, P.J., Sterling, J.C. and Kitchener, H.C., 2006, Prime-boost vaccination strategy in women with high-grade, noncervical anogenital intraepithelial neoplasia: clinical results from a multicenter phase II trial. International journal of gynecological cancer : official journal of the International Gynecological Cancer Society 16, 1075-81.

Finnen, R.L., Erickson, K.D., Chen, X.S. and Garcea, R.L., 2003, Interactions between papillomavirus L1 and L2 capsid proteins. Journal of virology 77, 4818-26.

Fisk, B., Blevins, T.L., Wharton, J.T. and Ioannides, C.G., 1995, Identification of an immunodominant peptide of HER-2/neu protooncogene recognized by ovarian tumor-specific cytotoxic T lymphocyte lines. The Journal of experimental medicine 181, 2109-17.

Fontenot, J.D. and Rudensky, A.Y., 2005, A well adapted regulatory contrivance: regulatory T cell development and the forkhead family transcription factor Foxp3. Nature immunology 6, 331-7.

Frazer, I.H., 2010, Measuring serum antibody to human papillomavirus following infection or vaccination. Gynecologic oncology 118, S8-11.

Frazer, I.H., Leggatt, G.R. and Mattarollo, S.R., 2011, Prevention and treatment of papillomavirus-related cancers through immunization. Annual review of immunology 29, 111-38.

Frazer, I.H., Quinn, M., Nicklin, J.L., Tan, J., Perrin, L.C., Ng, P., O'Connor, V.M., White, O., Wendt, N., Martin, J., Crowley, J.M., Edwards, S.J., McKenzie, A.W., Mitchell, S.V., Maher, D.W., Pearse, M.J. and Basser, R.L., 2004, Phase 1 study of HPV16-specific immunotherapy with

E6E7 fusion protein and ISCOMATRIX adjuvant in women with cervical intraepithelial neoplasia. Vaccine 23, 172-81.

Fremont, D.H., Matsumura, M., Stura, E.A., Peterson, P.A. and Wilson, I.A., 1992, Crystal structures of two viral peptides in complex with murine MHC class I H-2Kb. Science 257, 919-27.

Friedl, F., Kimura, I., Osato, T. and Ito, Y., 1970, Studies on a new human cell line (SiHa) derived from carcinoma of uterus. I. Its establishment and morphology. Proceedings of the Society for Experimental Biology and Medicine. Society for Experimental Biology and Medicine 135, 543-5.

Fritsch, E.F., Hacohen, N. and Wu, C.J., 2014, Personal neoantigen cancer vaccines: The momentum builds. Oncoimmunology 3, e29311.

Future I/II Study Group, Dillner, J., Kjaer, S.K., Wheeler, C.M., Sigurdsson, K., Iversen, O.E., Hernandez-Avila, M., Perez, G., Brown, D.R., Koutsky, L.A., Tay, E.H., Garcia, P., Ault, K.A., Garland, S.M., Leodolter, S., Olsson, S.E., Tang, G.W., Ferris, D.G., Paavonen, J., Lehtinen, M., Steben, M., Bosch, F.X., Joura, E.A., Majewski, S., Munoz, N., Myers, E.R., Villa, L.L., Taddeo, F.J., Roberts, C., Tadesse, A., Bryan, J.T., Maansson, R., Lu, S., Vuocolo, S., Hesley, T.M., Barr, E. and Haupt, R., 2010, Four year efficacy of prophylactic human papillomavirus quadrivalent vaccine against low grade cervical, vulvar, and vaginal intraepithelial neoplasia and anogenital warts: randomised controlled trial. BMJ 341, c3493.

Gabrilovich, D.I., Chen, H.L., Girgis, K.R., Cunningham, H.T., Meny, G.M., Nadaf, S., Kavanaugh, D. and Carbone, D.P., 1996, Production of vascular endothelial growth factor by human tumors inhibits the functional maturation of dendritic cells. Nature medicine 2, 1096-103.

Ganguly, N., 2012, Human papillomavirus-16 E5 protein: oncogenic role and therapeutic value. Cellular oncology 35, 67-76.

Ganguly, N. and Parihar, S.P., 2009, Human papillomavirus E6 and E7 oncoproteins as risk factors for tumorigenesis. Journal of biosciences 34, 113-23.

Garcia, F., Petry, K.U., Muderspach, L., Gold, M.A., Braly, P., Crum, C.P., Magill, M., Silverman, M., Urban, R.G., Hedley, M.L. and Beach, K.J., 2004, ZYC101a for treatment of high-grade cervical intraepithelial neoplasia: a randomized controlled trial. Obstetrics and gynecology 103, 317-26.

Garland, S.M., 2014, The Australian experience with the human papillomavirus vaccine. Clinical therapeutics 36, 17-23.

Gattinoni, L., Klebanoff, C.A. and Restifo, N.P., 2012, Paths to stemness: building the ultimate antitumour T cell. Nature reviews. Cancer 12, 671-84.

Gattinoni, L., Lugli, E., Ji, Y., Pos, Z., Paulos, C.M., Quigley, M.F., Almeida, J.R., Gostick, E., Yu, Z., Carpenito, C., Wang, E., Douek, D.C., Price, D.A., June, C.H., Marincola, F.M., Roederer, M. and Restifo, N.P., 2011, A human memory T cell subset with stem cell-like properties. Nature medicine 17, 1290-7.

Geginat, J., Lanzavecchia, A. and Sallusto, F., 2003, Proliferation and differentiation potential of human CD8+ memory T-cell subsets in response to antigen or homeostatic cytokines. Blood 101, 4260-6.

Gillison, M.L., Koch, W.M., Capone, R.B., Spafford, M., Westra, W.H., Wu, L., Zahurak, M.L., Daniel, R.W., Viglione, M., Symer, D.E., Shah, K.V. and Sidransky, D., 2000, Evidence for a causal association between human papillomavirus and a subset of head and neck cancers. Journal of the National Cancer Institute 92, 709-20.

Gissmann, L., deVilliers, E.M. and zur Hausen, H., 1982a, Analysis of human genital warts (condylomata acuminata) and other genital tumors for human papillomavirus type 6 DNA. International journal of cancer. Journal international du cancer 29, 143-6.

Gissmann, L., Diehl, V., Schultz-Coulon, H.J. and zur Hausen, H., 1982b, Molecular cloning and characterization of human papilloma virus DNA derived from a laryngeal papilloma. Journal of virology 44, 393-400.

Gissmann, L. and zur Hausen, H., 1980, Partial characterization of viral DNA from human genital warts (Condylomata acuminata). International journal of cancer. Journal international du cancer 25, 605-9.

GlaxoSmithKline Vaccine HPV Study Group, Romanowski, B., de Borba, P.C., Naud, P.S., Roteli-Martins, C.M., De Carvalho, N.S., Teixeira, J.C., Aoki, F., Ramjattan, B., Shier, R.M., Somani, R., Barbier, S., Blatter, M.M., Chambers, C., Ferris, D., Gall, S.A., Guerra, F.A.,

Harper, D.M., Hedrick, J.A., Henry, D.C., Korn, A.P., Kroll, R., Moscicki, A.B., Rosenfeld, W.D., Sullivan, B.J., Thoming, C.S., Tyring, S.K., Wheeler, C.M., Dubin, G., Schuind, A., Zahaf, T., Greenacre, M. and Sgriobhadair, A., 2009, Sustained efficacy and immunogenicity of the human papillomavirus (HPV)-16/18 AS04-adjuvanted vaccine: analysis of a randomised placebo-controlled trial up to 6.4 years. Lancet 374, 1975-85.

Gnjatic, S., Nishikawa, H., Jungbluth, A.A., Gure, A.O., Ritter, G., Jager, E., Knuth, A., Chen, Y.T. and Old, L.J., 2006, NY-ESO-1: review of an immunogenic tumor antigen. Advances in cancer research 95, 1-30.

Gonzalez-Galarza, F.F., Takeshita, L.Y., Santos, E.J., Kempson, F., Maia, M.H., Silva, A.L., Ghattaoraya, G.S., Alfirevic, A., Jones, A.R. and Middleton, D., 2015, Allele frequency net 2015 update: new features for HLA epitopes, KIR and disease and HLA adverse drug reaction associations. Nucleic Acid Research 28, D784-8.

Gorelik, L. and Flavell, R.A., 2002, Transforming growth factor-beta in T-cell biology. Nat Rev Immunol 2, 46-53.

Gowthaman, U., Chodisetti, S.B., Parihar, P. and Agrewala, J.N., 2010, Evaluation of different generic in silico methods for predicting HLA class I binding peptide vaccine candidates using a reverse approach. Amino acids 39, 1333-42.

Grabowska, A.K., Kaufmann, A.M. and Riemer, A.B., 2015, Identification of promiscuous HPV16-derived T helper cell epitopes for therapeutic HPV vaccine design. International journal of cancer. Journal international du cancer 136, 212-24.

Grabowska, A.K. and Riemer, A.B., 2012, The invisible enemy - how human papillomaviruses avoid recognition and clearance by the host immune system. The open virology journal 6, 249-56.

Grakoui, A., Bromley, S.K., Sumen, C., Davis, M.M., Shaw, A.S., Allen, P.M. and Dustin, M.L., 1999, The immunological synapse: a molecular machine controlling T cell activation. Science 285, 221-7.

Greenwald, R.J., Freeman, G.J. and Sharpe, A.H., 2005, The B7 family revisited. Annual review of immunology 23, 515-48.

Gromme, M. and Neefjes, J., 2002, Antigen degradation or presentation by MHC class I molecules via classical and non-classical pathways. Molecular immunology 39, 181-202.

Grunhagen, D.J., de Wilt, J.H., Graveland, W.J., Verhoef, C., van Geel, A.N. and Eggermont, A.M., 2006, Outcome and prognostic factor analysis of 217 consecutive isolated limb perfusions with tumor necrosis factor-alpha and melphalan for limb-threatening soft tissue sarcoma. Cancer 106, 1776-84.

Grupp, S.A., Kalos, M., Barrett, D., Aplenc, R., Porter, D.L., Rheingold, S.R., Teachey, D.T., Chew, A., Hauck, B., Wright, J.F., Milone, M.C., Levine, B.L. and June, C.H., 2013, Chimeric antigen receptor-modified T cells for acute lymphoid leukemia. N Engl J Med 368, 1509-18.

Guerder, S., Meyerhoff, J. and Flavell, R., 1994, The role of the T cell costimulator B7-1 in autoimmunity and the induction and maintenance of tolerance to peripheral antigen. Immunity 1, 155-66.

Haen, S.P. and Rammensee, H.G., 2013, The repertoire of human tumor-associated epitopes--identification and selection of antigens and their application in clinical trials. Current opinion in immunology 25, 277-83.

Hagensee, M.E., Yaegashi, N. and Galloway, D.A., 1993, Self-assembly of human papillomavirus type 1 capsids by expression of the L1 protein alone or by coexpression of the L1 and L2 capsid proteins. Journal of virology 67, 315-22.

Hajdu, S.I., 2011, A note from history: landmarks in history of cancer, part 1. Cancer 117, 1097-102.

Hanahan, D. and Weinberg, R.A., 2000, The hallmarks of cancer. Cell 100, 57-70.

Hanahan, D. and Weinberg, R.A., 2011, Hallmarks of cancer: the next generation. Cell 144, 646-74.

Haniffa, M., Shin, A., Bigley, V., McGovern, N., Teo, P., See, P., Wasan, P.S., Wang, X.N., Malinarich, F., Malleret, B., Larbi, A., Tan, P., Zhao, H., Poidinger, M., Pagan, S., Cookson, S., Dickinson, R., Dimmick, I., Jarrett, R.F., Renia, L., Tam, J., Song, C., Connolly, J., Chan, J.K., Gehring, A., Bertoletti, A., Collin, M. and Ginhoux, F., 2012, Human tissues contain CD141hi cross-presenting dendritic cells with functional homology to mouse CD103+ nonlymphoid dendritic cells. Immunity 37, 60-73.

Hanley, J.A. and McNeil, B.J., 1982, The meaning and use of the area under a receiver operating characteristic (ROC) curve. Radiology 143, 29-36.

Hansen, T.H. and Bouvier, M., 2009, MHC class I antigen presentation: learning from viral evasion strategies. Nat Rev Immunol 9, 503-13.

Hara, M., Matsueda, S., Tamura, M., Takedatsu, H., Tanaka, M., Kawano, K., Mochizuki, K., Kamura, T., Itoh, K. and Harada, M., 2005, Identification of human papillomavirus 16-E6 protein-derived peptides with the potential to generate cytotoxic T-lymphocytes toward human leukocyte antigen-A24+ cervical cancer. International journal of oncology 27, 1371-9.

Harper, D.M., Franco, E.L., Wheeler, C., Ferris, D.G., Jenkins, D., Schuind, A., Zahaf, T., Innis, B., Naud, P., De Carvalho, N.S., Roteli-Martins, C.M., Teixeira, J., Blatter, M.M., Korn, A.P., Quint, W., Dubin, G. and GlaxoSmithKline, H.P.V.V.S.G., 2004, Efficacy of a bivalent L1 virus-like particle vaccine in prevention of infection with human papillomavirus types 16 and 18 in young women: a randomised controlled trial. Lancet 364, 1757-65.

Hasim, A., Abudula, M., Aimiduo, R., Ma, J.Q., Jiao, Z., Akula, G., Wang, T. and Abudula, A., 2012, Post-transcriptional and epigenetic regulation of antigen processing machinery (APM) components and HLA-I in cervical cancers from Uighur women. PloS one 7, e44952.

Hassan, C., Chabrol, E., Jahn, L., Kester, M.G., de Ru, A.H., Drijfhout, J.W., Rossjohn, J., Falkenburg, J.H., Heemskerk, M.H., Gras, S. and van Veelen, P.A., 2015, Naturally processed non-canonical HLA-A*02:01 presented peptides. The Journal of biological chemistry 290, 2593-603.

Haug, M., Dannecker, L., Schepp, C.P., Kwok, W.W., Wernet, D., Buckner, J.H., Kalbacher, H., Dannecker, G.E. and Holzer, U., 2005, The heat shock protein Hsp70 enhances antigen-specific proliferation of human CD4+ memory T cells. European journal of immunology 35, 3163-72.

Hemmi, H., Takeuchi, O., Kawai, T., Kaisho, T., Sato, S., Sanjo, H., Matsumoto, M., Hoshino, K., Wagner, H., Takeda, K. and Akira, S., 2000, A Toll-like receptor recognizes bacterial DNA. Nature 408, 740-5.

Henderson, J., Sebag, M., Rhim, J., Goltzman, D. and Kremer, R., 1991, Dysregulation of parathyroid hormone-like peptide expression and secretion in a keratinocyte model of tumor progression. Cancer research 51, 6521-8.

Henkart, P.A., 1994, Lymphocyte-mediated cytotoxicity: two pathways and multiple effector molecules. Immunity 1, 343-6.

Heusel, J.W., Wesselschmidt, R.L., Shresta, S., Russell, J.H. and Ley, T.J., 1994, Cytotoxic lymphocytes require granzyme B for the rapid induction of DNA fragmentation and apoptosis in allogeneic target cells. Cell 76, 977-87.

Hildesheim, A., Herrero, R., Wacholder, S., Rodriguez, A.C., Solomon, D., Bratti, M.C., Schiller, J.T., Gonzalez, P., Dubin, G., Porras, C., Jimenez, S.E. and Lowy, D.R., 2007, Effect of human papillomavirus 16/18 L1 viruslike particle vaccine among young women with preexisting infection: a randomized trial. JAMA : the journal of the American Medical Association 298, 743-53.

Hodi, F.S., O'Day, S.J., McDermott, D.F., Weber, R.W., Sosman, J.A., Haanen, J.B., Gonzalez, R., Robert, C., Schadendorf, D., Hassel, J.C., Akerley, W., van den Eertwegh, A.J., Lutzky, J., Lorigan, P., Vaubel, J.M., Linette, G.P., Hogg, D., Ottensmeier, C.H., Lebbe, C., Peschel, C., Quirt, I., Clark, J.I., Wolchok, J.D., Weber, J.S., Tian, J., Yellin, M.J., Nichol, G.M., Hoos, A. and Urba, W.J., 2010, Improved survival with ipilimumab in patients with metastatic melanoma. N Engl J Med 363, 711-23.

Hoffmann, T.K., Sonkoly, E., Hauser, U., van Lierop, A., Whiteside, T.L., Klussmann, J.P., Hafner, D., Schuler, P., Friebe-Hoffmann, U., Scheckenbach, K., Erjala, K., Grenman, R., Schipper, J., Bier, H. and Balz, V., 2008, Alterations in the p53 pathway and their association with radio- and chemosensitivity in head and neck squamous cell carcinoma. Oral oncology 44, 1100-9.

Hoof, I., Peters, B., Sidney, J., Pedersen, L.E., Sette, A., Lund, O., Buus, S. and Nielsen, M., 2009, NetMHCpan, a method for MHC class I binding prediction beyond humans. Immunogenetics 61, 1-13.

Horvath, C.A., Boulet, G.A., Renoux, V.M., Delvenne, P.O. and Bogers, J.P., 2010, Mechanisms of cell entry by human papillomaviruses: an overview. Virol J 7, 11.

Howlader, N., Noone, A.M., Krapcho, M., Garshell, J., Neyman, N., Altekruse, S.F., Kosary, C.L., Yu, M., Ruhl, J., Tatalovich, Z., Cho, H., Mariotto, A., Lewis, D.R., Chen, H.S., Feuer, E.J.

and Cronin, K.A.e., 2013, SEER Cancer Statistics Review, 1975-2010. National Cancer Institute. Bethesda, MD.

Hu, X., Chakraborty, N.G., Sporn, J.R., Kurtzman, S.H., Ergin, M.T. and Mukherji, B., 1996, Enhancement of cytolytic T lymphocyte precursor frequency in melanoma patients following immunization with the MAGE-1 peptide loaded antigen presenting cell-based vaccine. Cancer research 56, 2479-83.

IARC. 2007 IARC Monographs on the Evaluation of Carcinogenic Risks to Humans - Human Papillomaviruses. In, Vol. 90. World Health Organization, Lyon, France, p. 423-465.

Ikeda, H., Old, L.J. and Schreiber, R.D., 2002, The roles of IFN gamma in protection against tumor development and cancer immunoediting. Cytokine & growth factor reviews 13, 95-109.

Jainchill, J.L., Aaronson, S.A. and Todaro, G.J., 1969, Murine sarcoma and leukemia viruses: assay using clonal lines of contact-inhibited mouse cells. Journal of virology 4, 549-53.

Jang, S., Kim, Y.T., Chung, H.W., Lee, K.R., Lim, J.B. and Lee, K., 2012, Identification of novel immunogenic human leukocyte antigen-A 2402-binding epitopes of human papillomavirus type 16 E7 for immunotherapy against human cervical cancer. Cancer 118, 2173-83.

Jankovic, D., Sher, A. and Yap, G., 2001, Th1/Th2 effector choice in parasitic infection: decision making by committee. Current opinion in immunology 13, 403-9.

Jemal, A., Bray, F., Center, M.M., Ferlay, J., Ward, E. and Forman, D., 2011, Global cancer statistics. CA: a cancer journal for clinicians 61, 69-90.

Jeon, S., Allen-Hoffmann, B.L. and Lambert, P.F., 1995, Integration of human papillomavirus type 16 into the human genome correlates with a selective growth advantage of cells. Journal of virology 69, 2989-97.

Jiang, S., Game, D.S., Davies, D., Lombardi, G. and Lechler, R.I., 2005, Activated CD1d-restricted natural killer T cells secrete IL-2: innate help for CD4+CD25+ regulatory T cells? European journal of immunology 35, 1193-200.

Johansson, C., Somberg, M., Li, X., Backstrom Winquist, E., Fay, J., Ryan, F., Pim, D., Banks, L. and Schwartz, S., 2012, HPV-16 E2 contributes to induction of HPV-16 late gene expression by inhibiting early polyadenylation. The EMBO journal 31, 3212-27.

Johnson, K.M., Kines, R.C., Roberts, J.N., Lowy, D.R., Schiller, J.T. and Day, P.M., 2009, Role of heparan sulfate in attachment to and infection of the murine female genital tract by human papillomavirus. Journal of virology 83, 2067-74.

Joura, E.A., Giuliano, A.R., Iversen, O.E., Bouchard, C., Mao, C., Mehlsen, J., Moreira, E.D., Jr., Ngan, Y., Petersen, L.K., Lazcano-Ponce, E., Pitisuttithum, P., Restrepo, J.A., Stuart, G., Woelber, L., Yang, Y.C., Cuzick, J., Garland, S.M., Huh, W., Kjaer, S.K., Bautista, O.M., Chan, I.S., Chen, J., Gesser, R., Moeller, E., Ritter, M., Vuocolo, S., Luxembourg, A. and Broad Spectrum, H.P.V.V.S., 2015, A 9-valent HPV vaccine against infection and intraepithelial neoplasia in women. N Engl J Med 372, 711-23.

Kammer, C., Warthorst, U., Torrez-Martinez, N., Wheeler, C.M. and Pfister, H., 2000, Sequence analysis of the long control region of human papillomavirus type 16 variants and functional consequences for P97 promoter activity. The Journal of general virology 81, 1975-81.

Kanodia, S., Da Silva, D.M. and Kast, W.M., 2008, Recent advances in strategies for immunotherapy of human papillomavirus-induced lesions. International journal of cancer. Journal international du cancer 122, 247-59.

Kanodia, S., Fahey, L.M. and Kast, W.M., 2007, Mechanisms used by human papillomaviruses to escape the host immune response. Current cancer drug targets 7, 79-89.

Kantoff, P.W., Higano, C.S., Shore, N.D., Berger, E.R., Small, E.J., Penson, D.F., Redfern, C.H., Ferrari, A.C., Dreicer, R., Sims, R.B., Xu, Y., Frohlich, M.W., Schellhammer, P.F. and Investigators, I.S., 2010, Sipuleucel-T immunotherapy for castration-resistant prostate cancer. N Engl J Med 363, 411-22.

Karbach, J., Neumann, A., Atmaca, A., Wahle, C., Brand, K., von Boehmer, L., Knuth, A., Bender, A., Ritter, G., Old, L.J. and Jager, E., 2011, Efficient in vivo priming by vaccination with recombinant NY-ESO-1 protein and CpG in antigen naive prostate cancer patients. Clinical cancer research : an official journal of the American Association for Cancer Research 17, 861-70.

Karosiene, E., Lundegaard, C., Lund, O. and Nielsen, M., 2012, NetMHCcons: a consensus method for the major histocompatibility complex class I predictions. Immunogenetics 64, 177-86.

Kast, W.M., Brandt, R.M., Sidney, J., Drijfhout, J.W., Kubo, R.T., Grey, H.M., Melief, C.J. and Sette, A., 1994, Role of HLA-A motifs in identification of potential CTL epitopes in human papillomavirus type 16 E6 and E7 proteins. J Immunol 152, 3904-12.

Kaufmann, A.M., Stern, P.L., Rankin, E.M., Sommer, H., Nuessler, V., Schneider, A., Adams, M., Onon, T.S., Bauknecht, T., Wagner, U., Kroon, K., Hickling, J., Boswell, C.M., Stacey, S.N., Kitchener, H.C., Gillard, J., Wanders, J., Roberts, J.S. and Zwierzina, H., 2002, Safety and immunogenicity of TA-HPV, a recombinant vaccinia virus expressing modified human papillomavirus (HPV)-16 and HPV-18 E6 and E7 genes, in women with progressive cervical cancer. Clinical cancer research : an official journal of the American Association for Cancer Research 8, 3676-85.

Keam, S.J. and Harper, D.M., 2008, Human papillomavirus types 16 and 18 vaccine (recombinant, AS04 adjuvanted, adsorbed) [Cervarix]. Drugs 68, 359-72.

Keller, A.M., Xiao, Y., Peperzak, V., Naik, S.H. and Borst, J., 2009, Costimulatory ligand CD70 allows induction of CD8+ T-cell immunity by immature dendritic cells in a vaccination setting. Blood 113, 5167-75.

Kenter, G.G., Welters, M.J., Valentijn, A.R., Lowik, M.J., Berends-van der Meer, D.M., Vloon, A.P., Drijfhout, J.W., Wafelman, A.R., Oostendorp, J., Fleuren, G.J., Offringa, R., van der Burg, S.H. and Melief, C.J., 2008, Phase I immunotherapeutic trial with long peptides spanning the E6 and E7 sequences of high-risk human papillomavirus 16 in end-stage cervical cancer patients shows low toxicity and robust immunogenicity. Clinical cancer research : an official journal of the American Association for Cancer Research 14, 169-77.

Kenter, G.G., Welters, M.J., Valentijn, A.R., Lowik, M.J., Berends-van der Meer, D.M., Vloon, A.P., Essahsah, F., Fathers, L.M., Offringa, R., Drijfhout, J.W., Wafelman, A.R., Oostendorp, J., Fleuren, G.J., van der Burg, S.H. and Melief, C.J., 2009, Vaccination against HPV-16 oncoproteins for vulvar intraepithelial neoplasia. N Engl J Med 361, 1838-47.

Kessler, J.H., Benckhuijsen, W.E., Mutis, T., Melief, C.J., van der Burg, S.H. and Drijfhout, J.W., 2004, Competition-based cellular peptide binding assay for HLA class I. Current protocols in immunology / edited by John E. Coligan ... [et al.] Chapter 18, Unit 18 12.

Kessler, J.H., Mommaas, B., Mutis, T., Huijbers, I., Vissers, D., Benckhuijsen, W.E., Schreuder, G.M., Offringa, R., Goulmy, E., Melief, C.J., van der Burg, S.H. and Drijfhout, J.W., 2003, Competition-based cellular peptide binding assays for 13 prevalent HLA class I alleles using fluorescein-labeled synthetic peptides. Human immunology 64, 245-55.

Khallouf, H., Grabowska, A.K. and Riemer, A.B., 2014, Therapeutic Vaccine Strategies against Human Papillomavirus. Vaccines 2, 422-462.

Khong, H.T. and Restifo, N.P., 2002, Natural selection of tumor variants in the generation of "tumor escape" phenotypes. Nature immunology 3, 999-1005.

Kim, J.M., Rasmussen, J.P. and Rudensky, A.Y., 2007, Regulatory T cells prevent catastrophic autoimmunity throughout the lifespan of mice. Nature immunology 8, 191-7.

Kines, R.C., Thompson, C.D., Lowy, D.R., Schiller, J.T. and Day, P.M., 2009, The initial steps leading to papillomavirus infection occur on the basement membrane prior to cell surface binding. Proceedings of the National Academy of Sciences of the United States of America 106, 20458-63.

Kisselev, A.F., Akopian, T.N., Woo, K.M. and Goldberg, A.L., 1999, The sizes of peptides generated from protein by mammalian 26 and 20 S proteasomes. Implications for understanding the degradative mechanism and antigen presentation. The Journal of biological chemistry 274, 3363-71.

Kiyono, T., Foster, S.A., Koop, J.I., McDougall, J.K., Galloway, D.A. and Klingelhutz, A.J., 1998, Both Rb/p16INK4a inactivation and telomerase activity are required to immortalize human epithelial cells. Nature 396, 84-8.

Klein, L., Kyewski, B., Allen, P.M. and Hogquist, K.A., 2014, Positive and negative selection of the T cell repertoire: what thymocytes see (and don't see). Nat Rev Immunol 14, 377-91.

Klencke, B., Matijevic, M., Urban, R.G., Lathey, J.L., Hedley, M.L., Berry, M., Thatcher, J., Weinberg, V., Wilson, J., Darragh, T., Jay, N., Da Costa, M. and Palefsky, J.M., 2002, Encapsulated plasmid DNA treatment for human papillomavirus 16-associated anal dysplasia: a Phase I study of ZYC101. Clinical cancer research : an official journal of the American Association for Cancer Research 8, 1028-37.

Klingelhutz, A.J. and Roman, A., 2012, Cellular transformation by human papillomaviruses: lessons learned by comparing high- and low-risk viruses. Virology 424, 77-98.

Kloetzel, P.M. and Ossendorp, F., 2004, Proteasome and peptidase function in MHC-class-I-mediated antigen presentation. Current opinion in immunology 16, 76-81.

Koebel, C.M., Vermi, W., Swann, J.B., Zerafa, N., Rodig, S.J., Old, L.J., Smyth, M.J. and Schreiber, R.D., 2007, Adaptive immunity maintains occult cancer in an equilibrium state. Nature 450, 903-7.

Koenig, S., Fuerst, T.R., Wood, L.V., Woods, R.M., Suzich, J.A., Jones, G.M., de la Cruz, V.F., Davey, R.T., Jr., Venkatesan, S., Moss, B. and et al., 1990, Mapping the fine specificity of a cytolytic T cell response to HIV-1 nef protein. J Immunol 145, 127-35.

Koopmann, J.O., Post, M., Neefjes, J.J., Hammerling, G.J. and Momburg, F., 1996, Translocation of long peptides by transporters associated with antigen processing (TAP). European journal of immunology 26, 1720-8.

Kreider, J.W. and Bartlett, G.L., 1981, The Shope papilloma-carcinoma complex of rabbits: a model system of neoplastic progression and spontaneous regression. Advances in cancer research 35, 81-110.

Kreimer, A.R., Clifford, G.M., Boyle, P. and Franceschi, S., 2005, Human papillomavirus types in head and neck squamous cell carcinomas worldwide: a systematic review. Cancer epidemiology, biomarkers & prevention : a publication of the American Association for Cancer Research, cosponsored by the American Society of Preventive Oncology 14, 467-75.

Kruger, E. and Kloetzel, P.M., 2012, Immunoproteasomes at the interface of innate and adaptive immune responses: two faces of one enzyme. Current opinion in immunology 24, 77-83.

Ku, J.L., Kim, W.H., Park, H.S., Kang, S.B. and Park, J.G., 1997, Establishment and characterization of 12 uterine cervical-carcinoma cell lines: common sequence variation in the E7 gene of HPV-16-positive cell lines. International journal of cancer. Journal international du cancer 72, 313-20.

Kubo, R.T., Sette, A., Grey, H.M., Appella, E., Sakaguchi, K., Zhu, N.Z., Arnott, D., Sherman, N., Shabanowitz, J., Michel, H. and et al., 1994, Definition of specific peptide motifs for four major HLA-A alleles. J Immunol 152, 3913-24.

Kumar, A., Commane, M., Flickinger, T.W., Horvath, C.M. and Stark, G.R., 1997, Defective TNF-alpha-induced apoptosis in STAT1-null cells due to low constitutive levels of caspases. Science 278, 1630-2.

Kurts, C., Robinson, B.W. and Knolle, P.A., 2010, Cross-priming in health and disease. Nat Rev Immunol 10, 403-14.

Laemmli, U.K., 1970, Cleavage of structural proteins during the assembly of the head of bacteriophage T4. Nature 227, 680-5.

Lajer, C.B. and von Buchwald, C., 2010, The role of human papillomavirus in head and neck cancer. APMIS : acta pathologica, microbiologica, et immunologica Scandinavica 118, 510-9.

Larsen, M.V., Lelic, A., Parsons, R., Nielsen, M., Hoof, I., Lamberth, K., Loeb, M.B., Buus, S., Bramson, J. and Lund, O., 2010, Identification of CD8+ T cell epitopes in the West Nile virus polyprotein by reverse-immunology using NetCTL. PloS one 5, e12697.

Larsen, M.V., Lundegaard, C., Lamberth, K., Buus, S., Brunak, S., Lund, O. and Nielsen, M., 2005, An integrative approach to CTL epitope prediction: a combined algorithm integrating MHC class I binding, TAP transport efficiency, and proteasomal cleavage predictions. European journal of immunology 35, 2295-303.

Larsen, M.V., Lundegaard, C., Lamberth, K., Buus, S., Lund, O. and Nielsen, M., 2007, Large-scale validation of methods for cytotoxic T-lymphocyte epitope prediction. BMC bioinformatics 8, 424.

Lee, D.W., Anderson, M.E., Wu, S. and Lee, J.H., 2008, Development of an adenoviral vaccine against E6 and E7 oncoproteins to prevent growth of human papillomavirus-positive cancer. Archives of otolaryngology--head & neck surgery 134, 1316-23.

Lee, J.H., Yi, S.M., Anderson, M.E., Berger, K.L., Welsh, M.J., Klingelhutz, A.J. and Ozbun, M.A., 2004, Propagation of infectious human papillomavirus type 16 by using an adenovirus and Cre/LoxP mechanism. Proceedings of the National Academy of Sciences of the United States of America 101, 2094-9.

Lehoux, M., D'Abramo, C.M. and Archambault, J., 2009, Molecular mechanisms of human papillomavirus-induced carcinogenesis. Public health genomics 12, 268-80.

Lenz, P., Thompson, C.D., Day, P.M., Bacot, S.M., Lowy, D.R. and Schiller, J.T., 2003, Interaction of papillomavirus virus-like particles with human myeloid antigen-presenting cells. Clinical immunology 106, 231-7.

Leong, C.M., Doorbar, J., Nindl, I., Yoon, H.S. and Hibma, M.H., 2010, Loss of epidermal Langerhans cells occurs in human papillomavirus alpha, gamma, and mu but not beta genus infections. The Journal of investigative dermatology 130, 472-80.

Lesterhuis, W.J., Haanen, J.B. and Punt, C.J., 2011, Cancer immunotherapy--revisited. Nature reviews. Drug discovery 10, 591-600.

Liebig, T.M., Fiedler, A., Zoghi, S., Shimabukuro-Vornhagen, A. and von Bergwelt-Baildon, M.S., 2009, Generation of human CD40-activated B cells. Journal of visualized experiments : JoVE.

Lin, H.H., Ray, S., Tongchusak, S., Reinherz, E.L. and Brusic, V., 2008, Evaluation of MHC class I peptide binding prediction servers: applications for vaccine research. BMC immunology 9, 8.

Liou, G.Y. and Storz, P., 2010, Reactive oxygen species in cancer. Free radical research 44, 479-96.

Longworth, M.S. and Laimins, L.A., 2004, Pathogenesis of human papillomaviruses in differentiating epithelia. Microbiology and molecular biology reviews : MMBR 68, 362-72.

Lowy, D.R., Solomon, D., Hildesheim, A., Schiller, J.T. and Schiffman, M., 2008, Human papillomavirus infection and the primary and secondary prevention of cervical cancer. Cancer 113, 1980-93.

Lu, Y.C., Yao, X., Crystal, J.S., Li, Y.F., El-Gamil, M., Gross, C., Davis, L., Dudley, M.E., Yang, J.C., Samuels, Y., Rosenberg, S.A. and Robbins, P.F., 2014, Efficient identification of mutated cancer antigens recognized by T cells associated with durable tumor regressions. Clinical cancer research : an official journal of the American Association for Cancer Research 20, 3401-10.

Lund, O., Nascimento, E.J., Maciel, M., Jr., Nielsen, M., Larsen, M.V., Lundegaard, C., Harndahl, M., Lamberth, K., Buus, S., Salmon, J., August, T.J. and Marques, E.T., Jr., 2011, Human leukocyte antigen (HLA) class I restricted epitope discovery in yellow fewer and dengue viruses: importance of HLA binding strength. PloS one 6, e26494.

Lund, O., Nielsen, M., Kesmir, C., Petersen, A.G., Lundegaard, C., Worning, P., Sylvester-Hvid, C., Lamberth, K., Roder, G., Justesen, S., Buus, S. and Brunak, S., 2004, Definition of supertypes for HLA molecules using clustering of specificity matrices. Immunogenetics 55, 797-810.

Lundegaard, C., Lamberth, K., Harndahl, M., Buus, S., Lund, O. and Nielsen, M., 2008a, NetMHC-3.0: accurate web accessible predictions of human, mouse and monkey MHC class I affinities for peptides of length 8-11. Nucleic acids research 36, W509-12.

Lundegaard, C., Lund, O. and Nielsen, M., 2008b, Accurate approximation method for prediction of class I MHC affinities for peptides of length 8, 10 and 11 using prediction tools trained on 9mers. Bioinformatics 24, 1397-8.

Macdonald, W.A., Purcell, A.W., Mifsud, N.A., Ely, L.K., Williams, D.S., Chang, L., Gorman, J.J., Clements, C.S., Kjer-Nielsen, L., Koelle, D.M., Burrows, S.R., Tait, B.D., Holdsworth, R., Brooks, A.G., Lovrecz, G.O., Lu, L., Rossjohn, J. and McCluskey, J., 2003, A naturally selected dimorphism within the HLA-B44 supertype alters class I structure, peptide repertoire, and T cell recognition. The Journal of experimental medicine 198, 679-91.

Madden, D.R., Garboczi, D.N. and Wiley, D.C., 1993, The antigenic identity of peptide-MHC complexes: a comparison of the conformations of five viral peptides presented by HLA-A2. Cell 75, 693-708.

Maier, R., Falk, K., Rotzschke, O., Maier, B., Gnau, V., Stevanovic, S., Jung, G., Rammensee, H.G. and Meyerhans, A., 1994, Peptide motifs of HLA-A3, -A24, and -B7 molecules as determined by pool sequencing. Immunogenetics 40, 306-8.

Malagon, T., Drolet, M., Boily, M.C., Franco, E.L., Jit, M., Brisson, J. and Brisson, M., 2012, Cross-protective efficacy of two human papillomavirus vaccines: a systematic review and meta-analysis. The Lancet infectious diseases 12, 781-9.

Maldonado, L., Teague, J.E., Morrow, M.P., Jotova, I., Wu, T.C., Wang, C., Desmarais, C., Boyer, J.D., Tycko, B., Robins, H.S., Clark, R.A. and Trimble, C.L., 2014, Intramuscular therapeutic vaccination targeting HPV16 induces T cell responses that localize in mucosal lesions. Science translational medicine 6, 221ra13.

Manning, J., Indrova, M., Lubyova, B., Pribylova, H., Bieblova, J., Hejnar, J., Simova, J., Jandlova, T., Bubenik, J. and Reinis, M., 2008, Induction of MHC class I molecule cell surface expression and epigenetic activation of antigen-processing machinery components in a murine model for human papilloma virus 16-associated tumours. Immunology 123, 218-27.

Marzo, A.L., Klonowski, K.D., Le Bon, A., Borrow, P., Tough, D.F. and Lefrancois, L., 2005, Initial T cell frequency dictates memory CD8+ T cell lineage commitment. Nature immunology 6, 793-9.

Masopust, D., Vezys, V., Marzo, A.L. and Lefrancois, L., 2001, Preferential localization of effector memory cells in nonlymphoid tissue. Science 291, 2413-7.

McLaughlin-Drubin, M.E., Crum, C.P. and Munger, K., 2011, Human papillomavirus E7 oncoprotein induces KDM6A and KDM6B histone demethylase expression and causes epigenetic reprogramming. Proceedings of the National Academy of Sciences of the United States of America 108, 2130-5.

Medina, D.M., Valencia, A., de Velasquez, A., Huang, L.M., Prymula, R., Garcia-Sicilia, J., Rombo, L., David, M.P., Descamps, D., Hardt, K., Dubin, G. and Group, H.P.V.S., 2010, Safety and immunogenicity of the HPV-16/18 AS04-adjuvanted vaccine: a randomized, controlled trial in adolescent girls. The Journal of adolescent health : official publication of the Society for Adolescent Medicine 46, 414-21.

Melero, I., Gaudernack, G., Gerritsen, W., Huber, C., Parmiani, G., Scholl, S., Thatcher, N., Wagstaff, J., Zielinski, C., Faulkner, I. and Mellstedt, H., 2014, Therapeutic vaccines for cancer: an overview of clinical trials. Nature reviews. Clinical oncology 11, 509-24.

Melief, C.J. and van der Burg, S.H., 2008, Immunotherapy of established (pre)malignant disease by synthetic long peptide vaccines. Nature reviews. Cancer 8, 351-60.

Michaud, D.S., Langevin, S.M., Eliot, M., Nelson, H.H., Pawlita, M., McClean, M.D. and Kelsey, K.T., 2014, High-risk HPV types and head and neck cancer. International journal of cancer. Journal international du cancer 135, 1653-61.

Middleton, D., Menchaca, L., Rood, H. and Komerofsky, R., 2003, New allele frequency database: http://www.allelefrequencies.net. Tissue antigens 61, 403-7.

Miyagi, J., Kinjo, T., Tsuhako, K., Higa, M., Iwamasa, T., Kamada, Y. and Hirayasu, T., 2001, Extremely high Langerhans cell infiltration contributes to the favourable prognosis of HPV-infected squamous cell carcinoma and adenocarcinoma of the lung. Histopathology 38, 355-67.

Modis, Y., Trus, B.L. and Harrison, S.C., 2002, Atomic model of the papillomavirus capsid. The EMBO journal 21, 4754-62.

Momburg, F., Roelse, J., Hammerling, G.J. and Neefjes, J.J., 1994, Peptide size selection by the major histocompatibility complex-encoded peptide transporter. The Journal of experimental medicine 179, 1613-23.

Moody, C.A. and Laimins, L.A., 2010, Human papillomavirus oncoproteins: pathways to transformation. Nature reviews. Cancer 10, 550-60.

Mora, M., Donati, C., Medini, D., Covacci, A. and Rappuoli, R., 2006, Microbial genomes and vaccine design: refinements to the classical reverse vaccinology approach. Current opinion in microbiology 9, 532-6.

Morgan, R.A., Chinnasamy, N., Abate-Daga, D., Gros, A., Robbins, P.F., Zheng, Z., Dudley, M.E., Feldman, S.A., Yang, J.C., Sherry, R.M., Phan, G.Q., Hughes, M.S., Kammula, U.S., Miller, A.D., Hessman, C.J., Stewart, A.A., Restifo, N.P., Quezado, M.M., Alimchandani, M., Rosenberg, A.Z., Nath, A., Wang, T., Bielekova, B., Wuest, S.C., Akula, N., McMahon, F.J., Wilde, S., Mosetter, B., Schendel, D.J., Laurencot, C.M. and Rosenberg, S.A., 2013, Cancer regression and neurological toxicity following anti-MAGE-A3 TCR gene therapy. J Immunother 36, 133-51.

Morishima, S., Akatsuka, Y., Nawa, A., Kondo, E., Kiyono, T., Torikai, H., Nakanishi, T., Ito, Y., Tsujimura, K., Iwata, K., Ito, K., Kodera, Y., Morishima, Y., Kuzushima, K. and Takahashi, T., 2007, Identification of an HLA-A24-restricted cytotoxic T lymphocyte epitope from human papillomavirus type-16 E6: the combined effects of bortezomib and interferon-gamma on the presentation of a cryptic epitope. International journal of cancer. Journal international du cancer 120, 594-604.

Mork, J., Lie, A.K., Glattre, E., Hallmans, G., Jellum, E., Koskela, P., Moller, B., Pukkala, E., Schiller, J.T., Youngman, L., Lehtinen, M. and Dillner, J., 2001, Human papillomavirus infection as a risk factor for squamous-cell carcinoma of the head and neck. N Engl J Med 344, 1125-31.

Mosmann, T.R. and Coffman, R.L., 1989, TH1 and TH2 cells: different patterns of lymphokine secretion lead to different functional properties. Annual review of immunology 7, 145-73.

Mota, F., Rayment, N., Chong, S., Singer, A. and Chain, B., 1999, The antigen-presenting environment in normal and human papillomavirus (HPV)-related premalignant cervical epithelium. Clinical and experimental immunology 116, 33-40.

Muderspach, L., Wilczynski, S., Roman, L., Bade, L., Felix, J., Small, L.A., Kast, W.M., Fascio, G., Marty, V. and Weber, J., 2000, A phase I trial of a human papillomavirus (HPV) peptide vaccine for women with high-grade cervical and vulvar intraepithelial neoplasia who are HPV 16 positive. Clinical cancer research : an official journal of the American Association for Cancer Research 6, 3406-16.

Mullis, K., Faloona, F., Scharf, S., Saiki, R., Horn, G. and Erlich, H., 1986, Specific enzymatic amplification of DNA in vitro: the polymerase chain reaction. Cold Spring Harbor symposia on quantitative biology 51 Pt 1, 263-73.

Mumberg, D., Monach, P.A., Wanderling, S., Philip, M., Toledano, A.Y., Schreiber, R.D. and Schreiber, H., 1999, CD4(+) T cells eliminate MHC class II-negative cancer cells in vivo by indirect effects of IFN-gamma. Proceedings of the National Academy of Sciences of the United States of America 96, 8633-8.

Munger, K., Yee, C.L., Phelps, W.C., Pietenpol, J.A., Moses, H.L. and Howley, P.M., 1991, Biochemical and biological differences between E7 oncoproteins of the high- and low-risk human papillomavirus types are determined by amino-terminal sequences. Journal of virology 65, 3943-8.

Munoz, N., Castellsague, X., de Gonzalez, A.B. and Gissmann, L., 2006, Chapter 1: HPV in the etiology of human cancer. Vaccine 24 Suppl 3, S3/1-10.

Murali-Krishna, K., Altman, J.D., Suresh, M., Sourdive, D.J., Zajac, A.J., Miller, J.D., Slansky, J. and Ahmed, R., 1998, Counting antigen-specific CD8 T cells: a reevaluation of bystander activation during viral infection. Immunity 8, 177-87.

Murphy, K.T., P.; Walport, M. 2007. Janeway's Immunobiology. Garland Science, New York.

Nakagawa, M., Stites, D.P., Patel, S., Farhat, S., Scott, M., Hills, N.K., Palefsky, J.M. and Moscicki, A.B., 2000, Persistence of human papillomavirus type 16 infection is associated with lack of cytotoxic T lymphocyte response to the E6 antigens. The Journal of infectious diseases 182, 595-8.

Narisawa-Saito, M. and Kiyono, T., 2007, Basic mechanisms of high-risk human papillomavirus-induced carcinogenesis: roles of E6 and E7 proteins. Cancer science 98, 1505-11.

Neefjes, J., Jongsma, M.L., Paul, P. and Bakke, O., 2011, Towards a systems understanding of MHC class I and MHC class II antigen presentation. Nat Rev Immunol 11, 823-36.

Nicholls, P.K., Moore, P.F., Anderson, D.M., Moore, R.A., Parry, N.R., Gough, G.W. and Stanley, M.A., 2001, Regression of canine oral papillomas is associated with infiltration of CD4+ and CD8+ lymphocytes. Virology 283, 31-9.

Niebler, M., Qian, X., Hofler, D., Kogosov, V., Kaewprag, J., Kaufmann, A.M., Ly, R., Bohmer, G., Zawatzky, R., Rosl, F. and Rincon-Orozco, B., 2013, Post-translational control of IL-1beta via the human papillomavirus type 16 E6 oncoprotein: a novel mechanism of innate immune escape mediated by the E3-ubiquitin ligase E6-AP and p53. PLoS pathogens 9, e1003536.

Nielsen, M., Lundegaard, C., Blicher, T., Lamberth, K., Harndahl, M., Justesen, S., Roder, G., Peters, B., Sette, A., Lund, O. and Buus, S., 2007, NetMHCpan, a method for quantitative predictions of peptide binding to any HLA-A and -B locus protein of known sequence. PloS one 2, e796.

Nielsen, M., Lundegaard, C., Lund, O. and Kesmir, C., 2005, The role of the proteasome in generating cytotoxic T-cell epitopes: insights obtained from improved predictions of proteasomal cleavage. Immunogenetics 57, 33-41.

Nielsen, M., Lundegaard, C., Worning, P., Lauemoller, S.L., Lamberth, K., Buus, S., Brunak, S. and Lund, O., 2003, Reliable prediction of T-cell epitopes using neural networks with novel sequence representations. Protein science : a publication of the Protein Society 12, 1007-17.

NIH. 2015 ClinicalTrials.gov. https://clinicaltrials.gov/, (access date: 20150409).

Nussbaum, A.K., Dick, T.P., Keilholz, W., Schirle, M., Stevanovic, S., Dietz, K., Heinemeyer, W., Groll, M., Wolf, D.H., Huber, R., Rammensee, H.G. and Schild, H., 1998, Cleavage motifs of the yeast 20S proteasome beta subunits deduced from digests of enolase 1. Proceedings of the National Academy of Sciences of the United States of America 95, 12504-9.

O'Brien, P.M. and Saveria Campo, M., 2002, Evasion of host immunity directed by papillomavirus-encoded proteins. Virus research 88, 103-17.

O'Garra, A. and Arai, N., 2000, The molecular basis of T helper 1 and T helper 2 cell differentiation. Trends in cell biology 10, 542-50.

Okun, M.M., Day, P.M., Greenstone, H.L., Booy, F.P., Lowy, D.R., Schiller, J.T. and Roden, R.B., 2001, L1 interaction domains of papillomavirus l2 necessary for viral genome encapsidation. Journal of virology 75, 4332-42.

Pandiyan, P., Zheng, L., Ishihara, S., Reed, J. and Lenardo, M.J., 2007, CD4+CD25+Foxp3+ regulatory T cells induce cytokine deprivation-mediated apoptosis of effector CD4+ T cells. Nature immunology 8, 1353-62.

Park, W.H. and Schroder, M.C., 1932, Diphtheria Toxin-Antitoxin and Toxoid : A Comparison. American journal of public health and the nation's health 22, 7-16.

Parker, D.C., 1993, T cell-dependent B cell activation. Annual review of immunology 11, 331-60.

Parker, K.C., Bednarek, M.A. and Coligan, J.E., 1994, Scheme for ranking potential HLA-A2 binding peptides based on independent binding of individual peptide side-chains. J Immunol 152, 163-75.

Parkin, D.M., 2006, The global health burden of infection-associated cancers in the year 2002. International journal of cancer. Journal international du cancer 118, 3030-44.

Pashine, A., Valiante, N.M. and Ulmer, J.B., 2005, Targeting the innate immune response with improved vaccine adjuvants. Nature medicine 11, S63-8.

Pattillo, R.A., Hussa, R.O., Story, M.T., Ruckert, A.C., Shalaby, M.R. and Mattingly, R.F., 1977, Tumor antigen and human chorionic gonadotropin in CaSki cells: a new epidermoid cervical cancer cell line. Science 196, 1456-8.

Paul, S., Weiskopf, D., Angelo, M.A., Sidney, J., Peters, B. and Sette, A., 2013, HLA Class I Alleles Are Associated with Peptide-Binding Repertoires of Different Size, Affinity, and Immunogenicity. J Immunol.

Peaper, D.R., Wearsch, P.A. and Cresswell, P., 2005, Tapasin and ERp57 form a stable disulfide-linked dimer within the MHC class I peptide-loading complex. The EMBO journal 24, 3613-23.

Pepperl, S., Benninger-Doring, G., Modrow, S., Wolf, H. and Jilg, W., 1998, Immediate-early transactivator Rta of Epstein-Barr virus (EBV) shows multiple epitopes recognized by EBV-specific cytotoxic T lymphocytes. Journal of virology 72, 8644-9.

Perez-Diez, A., Joncker, N.T., Choi, K., Chan, W.F., Anderson, C.C., Lantz, O. and Matzinger, P., 2007, CD4 cells can be more efficient at tumor rejection than CD8 cells. Blood 109, 5346-54.

Peters, B., Bui, H.H., Frankild, S., Nielson, M., Lundegaard, C., Kostem, E., Basch, D., Lamberth, K., Harndahl, M., Fleri, W., Wilson, S.S., Sidney, J., Lund, O., Buus, S. and Sette, A., 2006, A community resource benchmarking predictions of peptide binding to MHC-I molecules. PLoS computational biology 2, e65.

Peters, B., Bulik, S., Tampe, R., Van Endert, P.M. and Holzhutter, H.G., 2003, Identifying MHC class I epitopes by predicting the TAP transport efficiency of epitope precursors. J Immunol 171, 1741-9.

Peters, B. and Sette, A., 2005, Generating quantitative models describing the sequence specificity of biological processes with the stabilized matrix method. BMC bioinformatics 6, 132.

Piccart-Gebhart, M.J., Procter, M., Leyland-Jones, B., Goldhirsch, A., Untch, M., Smith, I., Gianni, L., Baselga, J., Bell, R., Jackisch, C., Cameron, D., Dowsett, M., Barrios, C.H., Steger, G., Huang, C.S., Andersson, M., Inbar, M., Lichinitser, M., Lang, I., Nitz, U., Iwata, H., Thomssen, C., Lohrisch, C., Suter, T.M., Ruschoff, J., Suto, T., Greatorex, V., Ward, C., Straehle, C., McFadden, E., Dolci, M.S., Gelber, R.D. and Herceptin Adjuvant Trial Study, T., 2005, Trastuzumab after adjuvant chemotherapy in HER2-positive breast cancer. N Engl J Med 353, 1659-72.

Piette, J., Neel, H. and Marechal, V., 1997, Mdm2: keeping p53 under control. Oncogene 15, 1001-10.

Pim, D. and Banks, L., 2010, Interaction of viral oncoproteins with cellular target molecules: infection with high-risk vs low-risk human papillomaviruses. APMIS : acta pathologica, microbiologica, et immunologica Scandinavica 118, 471-93.

Poljak, M., 2012, Prophylactic human papillomavirus vaccination and primary prevention of cervical cancer: issues and challenges. Clinical microbiology and infection : the official publication of the European Society of Clinical Microbiology and Infectious Diseases 18 Suppl 5, 64-9.

Porter, D.L., Levine, B.L., Kalos, M., Bagg, A. and June, C.H., 2011, Chimeric antigen receptor-modified T cells in chronic lymphoid leukemia. N Engl J Med 365, 725-33.

Pyeon, D., Pearce, S.M., Lank, S.M., Ahlquist, P. and Lambert, P.F., 2009, Establishment of human papillomavirus infection requires cell cycle progression. PLoS pathogens 5, e1000318.

Qin, Z. and Blankenstein, T., 2000, CD4+ T cell--mediated tumor rejection involves inhibition of angiogenesis that is dependent on IFN gamma receptor expression by nonhematopoietic cells. Immunity 12, 677-86.

Radulovic, S., Brankovic-Magic, M., Malisic, E., Jankovic, R., Dobricic, J., Plesinac-Karapandzic, V., Maciag, P.C. and Rothman, J., 2009, Therapeutic cancer vaccines in cervical cancer: phase I study of Lovaxin-C. Journal of B.U.ON. : official journal of the Balkan Union of Oncology 14 Suppl 1, S165-8.

Raff, A.B., Woodham, A.W., Raff, L.M., Skeate, J.G., Yan, L., Da Silva, D.M., Schelhaas, M. and Kast, W.M., 2013, The evolving field of human papillomavirus receptor research: a review of binding and entry. Journal of virology 87, 6062-72.

Ragin, C.C., Reshmi, S.C. and Gollin, S.M., 2004, Mapping and analysis of HPV16 integration sites in a head and neck cancer cell line. International journal of cancer. Journal international du cancer 110, 701-9.

Rammensee, H., Bachmann, J., Emmerich, N.P., Bachor, O.A. and Stevanovic, S., 1999, SYFPEITHI: database for MHC ligands and peptide motifs. Immunogenetics 50, 213-9.

Rammensee, H.G., 1995, Chemistry of peptides associated with MHC class I and class II molecules. Current opinion in immunology 7, 85-96.

Rammensee, H.G., Falk, K. and Rotzschke, O., 1993, MHC molecules as peptide receptors. Current opinion in immunology 5, 35-44.

Reits, E., Neijssen, J., Herberts, C., Benckhuijsen, W., Janssen, L., Drijfhout, J.W. and Neefjes, J., 2004, A major role for TPPII in trimming proteasomal degradation products for MHC class I antigen presentation. Immunity 20, 495-506.

Ressing, M.E., Sette, A., Brandt, R.M., Ruppert, J., Wentworth, P.A., Hartman, M., Oseroff, C., Grey, H.M., Melief, C.J. and Kast, W.M., 1995, Human CTL epitopes encoded by human papillomavirus type 16 E6 and E7 identified through in vivo and in vitro immunogenicity studies of HLA-A*0201-binding peptides. J Immunol 154, 5934-43.

Ressing, M.E., van Driel, W.J., Brandt, R.M., Kenter, G.G., de Jong, J.H., Bauknecht, T., Fleuren, G.J., Hoogerhout, P., Offringa, R., Sette, A., Celis, E., Grey, H., Trimbos, B.J., Kast, W.M. and Melief, C.J., 2000, Detection of T helper responses, but not of human papillomavirus-specific cytotoxic T lymphocyte responses, after peptide vaccination of patients with cervical carcinoma. J Immunother 23, 255-66.

Restifo, N.P., Dudley, M.E. and Rosenberg, S.A., 2012, Adoptive immunotherapy for cancer: harnessing the T cell response. Nat Rev Immunol 12, 269-81.

Richardson, H., Kelsall, G., Tellier, P., Voyer, H., Abrahamowicz, M., Ferenczy, A., Coutlee, F. and Franco, E.L., 2003, The natural history of type-specific human papillomavirus infections in female university students. Cancer epidemiology, biomarkers & prevention : a publication of the American Association for Cancer Research, cosponsored by the American Society of Preventive Oncology 12, 485-90.

Riemer, A.B., Keskin, D.B., Zhang, G., Handley, M., Anderson, K.S., Brusic, V., Reinhold, B. and Reinherz, E.L., 2010, A conserved E7-derived cytotoxic T lymphocyte epitope expressed on human papillomavirus 16-transformed HLA-A2+ epithelial cancers. The Journal of biological chemistry 285, 29608-22.

Robbins, P.F., Lu, Y.C., El-Gamil, M., Li, Y.F., Gross, C., Gartner, J., Lin, J.C., Teer, J.K., Cliften, P., Tycksen, E., Samuels, Y. and Rosenberg, S.A., 2013, Mining exomic sequencing data to identify mutated antigens recognized by adoptively transferred tumor-reactive T cells. Nature medicine 19, 747-52.

Rollier, C.S., Reyes-Sandoval, A., Cottingham, M.G., Ewer, K. and Hill, A.V., 2011, Viral vectors as vaccine platforms: deployment in sight. Current opinion in immunology 23, 377-82.

Romond, E.H., Perez, E.A., Bryant, J., Suman, V.J., Geyer, C.E., Jr., Davidson, N.E., Tan-Chiu, E., Martino, S., Paik, S., Kaufman, P.A., Swain, S.M., Pisansky, T.M., Fehrenbacher, L., Kutteh, L.A., Vogel, V.G., Visscher, D.W., Yothers, G., Jenkins, R.B., Brown, A.M., Dakhil, S.R., Mamounas, E.P., Lingle, W.L., Klein, P.M., Ingle, J.N. and Wolmark, N., 2005, Trastuzumab plus adjuvant chemotherapy for operable HER2-positive breast cancer. N Engl J Med 353, 1673-84.

Rosenberg, S.A., 2011, Cell transfer immunotherapy for metastatic solid cancer--what clinicians need to know. Nature reviews. Clinical oncology 8, 577-85.

Rosenberg, S.A., Lotze, M.T., Muul, L.M., Leitman, S., Chang, A.E., Ettinghausen, S.E., Matory, Y.L., Skibber, J.M., Shiloni, E., Vetto, J.T. and et al., 1985, Observations on the systemic administration of autologous lymphokine-activated killer cells and recombinant interleukin-2 to patients with metastatic cancer. N Engl J Med 313, 1485-92.

Rosenberg, S.A., Lotze, M.T., Yang, J.C., Aebersold, P.M., Linehan, W.M., Seipp, C.A. and White, D.E., 1989, Experience with the use of high-dose interleukin-2 in the treatment of 652 cancer patients. Annals of surgery 210, 474-84; discussion 484-5.

Rosenberg, S.A., Yang, J.C., Schwartzentruber, D.J., Hwu, P., Marincola, F.M., Topalian, S.L., Restifo, N.P., Dudley, M.E., Schwarz, S.L., Spiess, P.J., Wunderlich, J.R., Parkhurst, M.R., Kawakami, Y., Seipp, C.A., Einhorn, J.H. and White, D.E., 1998, Immunologic and therapeutic evaluation of a synthetic peptide vaccine for the treatment of patients with metastatic melanoma. Nature medicine 4, 321-7.

Rous, P. and Beard, J.W., 1935, The Progression to Carcinoma of Virus-Induced Rabbit Papillomas (Shope). The Journal of experimental medicine 62, 523-48.

Russell, J.H. and Ley, T.J., 2002, Lymphocyte-mediated cytotoxicity. Annual review of immunology 20, 323-70.

Sabbatini, P., Tsuji, T., Ferran, L., Ritter, E., Sedrak, C., Tuballes, K., Jungbluth, A.A., Ritter, G., Aghajanian, C., Bell-McGuinn, K., Hensley, M.L., Konner, J., Tew, W., Spriggs, D.R., Hoffman, E.W., Venhaus, R., Pan, L., Salazar, A.M., Diefenbach, C.M., Old, L.J. and Gnjatic, S., 2012, Phase I trial of overlapping long peptides from a tumor self-antigen and poly-ICLC shows rapid induction of integrated immune response in ovarian cancer patients. Clinical cancer research : an official journal of the American Association for Cancer Research 18, 6497-508.

Saiki, R.K., Scharf, S., Faloona, F., Mullis, K.B., Horn, G.T., Erlich, H.A. and Arnheim, N., 1985, Enzymatic amplification of beta-globin genomic sequences and restriction site analysis for diagnosis of sickle cell anemia. Science 230, 1350-4.

Sakaguchi, S., Sakaguchi, N., Asano, M., Itoh, M. and Toda, M., 1995, Immunologic self-tolerance maintained by activated T cells expressing IL-2 receptor alpha-chains (CD25). Breakdown of a single mechanism of self-tolerance causes various autoimmune diseases. J Immunol 155, 1151-64.

Sallusto, F., Lenig, D., Forster, R., Lipp, M. and Lanzavecchia, A., 1999, Two subsets of memory T lymphocytes with distinct homing potentials and effector functions. Nature 401, 708-12.

Sambrook, J. and Gething, M.J., 1989, Protein structure. Chaperones, paperones. Nature 342, 224-5.

Santin, A.D., Bellone, S., Palmieri, M., Ravaggi, A., Romani, C., Tassi, R., Roman, J.J., Burnett, A., Pecorelli, S. and Cannon, M.J., 2006, HPV16/18 E7-pulsed dendritic cell vaccination in cervical cancer patients with recurrent disease refractory to standard treatment modalities. Gynecologic oncology 100, 469-78.

Santin, A.D., Bellone, S., Palmieri, M., Zanolini, A., Ravaggi, A., Siegel, E.R., Roman, J.J., Pecorelli, S. and Cannon, M.J., 2008, Human papillomavirus type 16 and 18 E7-pulsed dendritic cell vaccination of stage IB or IIA cervical cancer patients: a phase I escalating-dose trial. Journal of virology 82, 1968-79.

Sapp, M. and Bienkowska-Haba, M., 2009, Viral entry mechanisms: human papillomavirus and a long journey from extracellular matrix to the nucleus. The FEBS journal 276, 7206-16.

Sapp, M., Fligge, C., Petzak, I., Harris, J.R. and Streeck, R.E., 1998, Papillomavirus assembly requires trimerization of the major capsid protein by disulfides between two highly conserved cysteines. Journal of virology 72, 6186-9.

Scarinci, I.C., Garcia, F.A., Kobetz, E., Partridge, E.E., Brandt, H.M., Bell, M.C., Dignan, M., Ma, G.X., Daye, J.L. and Castle, P.E., 2010, Cervical cancer prevention: new tools and old barriers. Cancer 116, 2531-42.

Schelhaas, M., Shah, B., Holzer, M., Blattmann, P., Kuhling, L., Day, P.M., Schiller, J.T. and Helenius, A., 2012, Entry of human papillomavirus type 16 by actin-dependent, clathrin- and lipid raft-independent endocytosis. PLoS pathogens 8, e1002657.

Schenkel, J.M., Fraser, K.A., Vezys, V. and Masopust, D., 2013, Sensing and alarm function of resident memory CD8(+) T cells. Nature immunology 14, 509-13.

Schiffman, M., Castle, P.E., Jeronimo, J., Rodriguez, A.C. and Wacholder, S., 2007, Human papillomavirus and cervical cancer. Lancet 370, 890-907.

Schiller, J.T., Day, P.M. and Kines, R.C., 2010, Current understanding of the mechanism of HPV infection. Gynecologic oncology 118, S12-7.

Schlecht, N.F., Kulaga, S., Robitaille, J., Ferreira, S., Santos, M., Miyamura, R.A., Duarte-Franco, E., Rohan, T.E., Ferenczy, A., Villa, L.L. and Franco, E.L., 2001, Persistent human papillomavirus infection as a predictor of cervical intraepithelial neoplasia. JAMA : the journal of the American Medical Association 286, 3106-14.

Schlecker, E., Stojanovic, A., Eisen, C., Quack, C., Falk, C.S., Umansky, V. and Cerwenka, A., 2012, Tumor-infiltrating monocytic myeloid-derived suppressor cells mediate CCR5-dependent recruitment of regulatory T cells favoring tumor growth. J Immunol 189, 5602-11.

Schmitt, M. and Pawlita, M., 2011, The HPV transcriptome in HPV16 positive cell lines. Molecular and cellular probes 25, 108-13.

Schreiber, R.D., Old, L.J. and Smyth, M.J., 2011, Cancer immunoediting: integrating immunity's roles in cancer suppression and promotion. Science 331, 1565-70.

Schultze, J.L., Cardoso, A.A., Freeman, G.J., Seamon, M.J., Daley, J., Pinkus, G.S., Gribben, J.G. and Nadler, L.M., 1995, Follicular lymphomas can be induced to present alloantigen efficiently: a conceptual model to improve their tumor immunogenicity. Proceedings of the National Academy of Sciences of the United States of America 92, 8200-4.

Schultze, J.L., Grabbe, S. and von Bergwelt-Baildon, M.S., 2004, DCs and CD40-activated B cells: current and future avenues to cellular cancer immunotherapy. Trends in immunology 25, 659-64.

Schultze, J.L., Michalak, S., Seamon, M.J., Dranoff, G., Jung, K., Daley, J., Delgado, J.C., Gribben, J.G. and Nadler, L.M., 1997, CD40-activated human B cells: an alternative source of highly efficient antigen presenting cells to generate autologous antigen-specific T cells for adoptive immunotherapy. The Journal of clinical investigation 100, 2757-65.

Schwartzentruber, D.J., Lawson, D.H., Richards, J.M., Conry, R.M., Miller, D.M., Treisman, J., Gailani, F., Riley, L., Conlon, K., Pockaj, B., Kendra, K.L., White, R.L., Gonzalez, R., Kuzel, T.M., Curti, B., Leming, P.D., Whitman, E.D., Balkissoon, J., Reintgen, D.S., Kaufman, H., Marincola, F.M., Merino, M.J., Rosenberg, S.A., Choyke, P., Vena, D. and Hwu, P., 2011, gp100 peptide vaccine and interleukin-2 in patients with advanced melanoma. N Engl J Med 364, 2119-27.

Schwarz, T.F., Flamaing, J., Rumke, H.C., Penzes, J., Juergens, C., Wenz, A., Jayawardene, D., Giardina, P., Emini, E.A., Gruber, W.C. and Schmoele-Thoma, B., 2011, A randomized, double-blind trial to evaluate immunogenicity and safety of 13-valent pneumococcal conjugate vaccine given concomitantly with trivalent influenza vaccine in adults aged >/=65 years. Vaccine 29, 5195-202.

Seliger, B., Maeurer, M.J. and Ferrone, S., 2000, Antigen-processing machinery breakdown and tumor growth. Immunology today 21, 455-64.

Sette, A. and Rappuoli, R., 2010, Reverse vaccinology: developing vaccines in the era of genomics. Immunity 33, 530-41.

Sette, A. and Sidney, J., 1999, Nine major HLA class I supertypes account for the vast preponderance of HLA-A and -B polymorphism. Immunogenetics 50, 201-12.

Sette, A., Sidney, J., del Guercio, M.F., Southwood, S., Ruppert, J., Dahlberg, C., Grey, H.M. and Kubo, R.T., 1994, Peptide binding to the most frequent HLA-A class I alleles measured by quantitative molecular binding assays. Molecular immunology 31, 813-22.

Shafer-Weaver, K.A., Watkins, S.K., Anderson, M.J., Draper, L.J., Malyguine, A., Alvord, W.G., Greenberg, N.M. and Hurwitz, A.A., 2009, Immunity to murine prostatic tumors: continuous

provision of T-cell help prevents CD8 T-cell tolerance and activates tumor-infiltrating dendritic cells. Cancer research 69, 6256-64.
Shedlock, D.J. and Shen, H., 2003, Requirement for CD4 T cell help in generating functional CD8 T cell memory. Science 300, 337-9.
Sheets, E.E., Urban, R.G., Crum, C.P., Hedley, M.L., Politch, J.A., Gold, M.A., Muderspach, L.I., Cole, G.A. and Crowley-Nowick, P.A., 2003, Immunotherapy of human cervical high-grade cervical intraepithelial neoplasia with microparticle-delivered human papillomavirus 16 E7 plasmid DNA. American journal of obstetrics and gynecology 188, 916-26.
Shirota, H. and Klinman, D.M., 2014, Recent progress concerning CpG DNA and its use as a vaccine adjuvant. Expert review of vaccines 13, 299-312.
Shope, R.E. and Hurst, E.W., 1933, Infectious Papillomatosis of Rabbits : With a Note on the Histopathology. The Journal of experimental medicine 58, 607-24.
Sidney, J., Assarsson, E., Moore, C., Ngo, S., Pinilla, C., Sette, A. and Peters, B., 2008, Quantitative peptide binding motifs for 19 human and mouse MHC class I molecules derived using positional scanning combinatorial peptide libraries. Immunome research 4, 2.
Sims, G.P., Rowe, D.C., Rietdijk, S.T., Herbst, R. and Coyle, A.J., 2010, HMGB1 and RAGE in inflammation and cancer. Annual review of immunology 28, 367-88.
Singh-Jasuja, H., Emmerich, N.P. and Rammensee, H.G., 2004, The Tubingen approach: identification, selection, and validation of tumor-associated HLA peptides for cancer therapy. Cancer immunology, immunotherapy : CII 53, 187-95.
Slifka, M.K. and Whitton, J.L., 2000, Antigen-specific regulation of T cell-mediated cytokine production. Immunity 12, 451-7.
Smith, B., Chen, Z., Reimers, L., van Doorslaer, K., Schiffman, M., Desalle, R., Herrero, R., Yu, K., Wacholder, S., Wang, T. and Burk, R.D., 2011, Sequence imputation of HPV16 genomes for genetic association studies. PloS one 6, e21375.
Smith, C.M., Wilson, N.S., Waithman, J., Villadangos, J.A., Carbone, F.R., Heath, W.R. and Belz, G.T., 2004, Cognate CD4(+) T cell licensing of dendritic cells in CD8(+) T cell immunity. Nature immunology 5, 1143-8.
Smith, F.O., Downey, S.G., Klapper, J.A., Yang, J.C., Sherry, R.M., Royal, R.E., Kammula, U.S., Hughes, M.S., Restifo, N.P., Levy, C.L., White, D.E., Steinberg, S.M. and Rosenberg, S.A., 2008, Treatment of metastatic melanoma using interleukin-2 alone or in conjunction with vaccines. Clinical cancer research : an official journal of the American Association for Cancer Research 14, 5610-8.
Smyth, L.J., Van Poelgeest, M.I., Davidson, E.J., Kwappenberg, K.M., Burt, D., Sehr, P., Pawlita, M., Man, S., Hickling, J.K., Fiander, A.N., Tristram, A., Kitchener, H.C., Offringa, R., Stern, P.L. and Van Der Burg, S.H., 2004, Immunological responses in women with human papillomavirus type 16 (HPV-16)-associated anogenital intraepithelial neoplasia induced by heterologous prime-boost HPV-16 oncogene vaccination. Clinical cancer research : an official journal of the American Association for Cancer Research 10, 2954-61.
Smyth, M.J., Cretney, E., Takeda, K., Wiltrout, R.H., Sedger, L.M., Kayagaki, N., Yagita, H. and Okumura, K., 2001, Tumor necrosis factor-related apoptosis-inducing ligand (TRAIL) contributes to interferon gamma-dependent natural killer cell protection from tumor metastasis. The Journal of experimental medicine 193, 661-70.
Soerjomataram, I., Lortet-Tieulent, J., Parkin, D.M., Ferlay, J., Mathers, C., Forman, D. and Bray, F., 2012, Global burden of cancer in 2008: a systematic analysis of disability-adjusted life-years in 12 world regions. Lancet 380, 1840-50.
Solares, A.M., Baladron, I., Ramos, T., Valenzuela, C., Borbon, Z., Fanjull, S., Gonzalez, L., Castillo, D., Esmir, J., Granadillo, M., Batte, A., Cintado, A., Ale, M., Fernandez de Cossio, M.E., Ferrer, A., Torrens, I. and Lopez-Saura, P., 2011, Safety and Immunogenicity of a Human Papillomavirus Peptide Vaccine (CIGB-228) in Women with High-Grade Cervical Intraepithelial Neoplasia: First-in-Human, Proof-of-Concept Trial. ISRN obstetrics and gynecology 2011, 292951.
Sorokin, A.V., Kim, E.R. and Ovchinnikov, L.P., 2009, Proteasome system of protein degradation and processing. Biochemistry. Biokhimiia 74, 1411-42.

Spoden, G., Freitag, K., Husmann, M., Boller, K., Sapp, M., Lambert, C. and Florin, L., 2008, Clathrin- and caveolin-independent entry of human papillomavirus type 16--involvement of tetraspanin-enriched microdomains (TEMs). PloS one 3, e3313.
Stanley, M., 2006a, Immune responses to human papillomavirus. Vaccine 24 Suppl 1, S16-22.
Stanley, M., 2008, Immunobiology of HPV and HPV vaccines. Gynecologic oncology 109, S15-21.
Stanley, M., Pinto, L.A. and Trimble, C., 2012, Human papillomavirus vaccines--immune responses. Vaccine 30 Suppl 5, F83-7.
Stanley, M.A., 2006b, Human papillomavirus vaccines. Rev Med Virol 16, 139-49.
Stanley, M.A., 2012, Epithelial cell responses to infection with human papillomavirus. Clinical microbiology reviews 25, 215-22.
Stanley, M.A., Pett, M.R. and Coleman, N., 2007, HPV: from infection to cancer. Biochemical Society transactions 35, 1456-60.
Stauffer, Y., Raj, K., Masternak, K. and Beard, P., 1998, Infectious human papillomavirus type 18 pseudovirions. Journal of molecular biology 283, 529-36.
Steenbergen, R.D., Hermsen, M.A., Walboomers, J.M., Joenje, H., Arwert, F., Meijer, C.J. and Snijders, P.J., 1995, Integrated human papillomavirus type 16 and loss of heterozygosity at 11q22 and 18q21 in an oral carcinoma and its derivative cell line. Cancer research 55, 5465-71.
Steinman, R.M., 1991, The dendritic cell system and its role in immunogenicity. Annual review of immunology 9, 271-96.
Steller, M.A., Gurski, K.J., Murakami, M., Daniel, R.W., Shah, K.V., Celis, E., Sette, A., Trimble, E.L., Park, R.C. and Marincola, F.M., 1998, Cell-mediated immunological responses in cervical and vaginal cancer patients immunized with a lipidated epitope of human papillomavirus type 16 E7. Clinical cancer research : an official journal of the American Association for Cancer Research 4, 2103-9.
Stern, P.L., van der Burg, S.H., Hampson, I.N., Broker, T.R., Fiander, A., Lacey, C.J., Kitchener, H.C. and Einstein, M.H., 2012, Therapy of human papillomavirus-related disease. Vaccine 30 Suppl 5, F71-82.
Stevanovic, S., 2002, Identification of tumour-associated T-cell epitopes for vaccine development. Nature reviews. Cancer 2, 514-20.
Stoltze, L., Schirle, M., Schwarz, G., Schroter, C., Thompson, M.W., Hersh, L.B., Kalbacher, H., Stevanovic, S., Rammensee, H.G. and Schild, H., 2000, Two new proteases in the MHC class I processing pathway. Nature immunology 1, 413-8.
Stout, R.D. and Bottomly, K., 1989, Antigen-specific activation of effector macrophages by IFN-gamma producing (TH1) T cell clones. Failure of IL-4-producing (TH2) T cell clones to activate effector function in macrophages. J Immunol 142, 760-5.
Stranzl, T., Larsen, M.V., Lundegaard, C. and Nielsen, M., 2010, NetCTLpan: pan-specific MHC class I pathway epitope predictions. Immunogenetics 62, 357-68.
Su, J.H., Wu, A., Scotney, E., Ma, B., Monie, A., Hung, C.F. and Wu, T.C., 2010, Immunotherapy for cervical cancer: Research status and clinical potential. BioDrugs : clinical immunotherapeutics, biopharmaceuticals and gene therapy 24, 109-29.
Suzich, J.A., Ghim, S.J., Palmer-Hill, F.J., White, W.I., Tamura, J.K., Bell, J.A., Newsome, J.A., Jenson, A.B. and Schlegel, R., 1995, Systemic immunization with papillomavirus L1 protein completely prevents the development of viral mucosal papillomas. Proceedings of the National Academy of Sciences of the United States of America 92, 11553-7.
Swets, J.A., 1988, Measuring the accuracy of diagnostic systems. Science 240, 1285-93.
Sylvester-Hvid, C., Nielsen, M., Lamberth, K., Roder, G., Justesen, S., Lundegaard, C., Worning, P., Thomadsen, H., Lund, O., Brunak, S. and Buus, S., 2004, SARS CTL vaccine candidates; HLA supertype-, genome-wide scanning and biochemical validation. Tissue antigens 63, 395-400.
Szarewski, A., 2012, Cervarix(R): a bivalent vaccine against HPV types 16 and 18, with cross-protection against other high-risk HPV types. Expert review of vaccines 11, 645-57.
Tabora, N., Melchers, W.J., van Doorn, L.J., Quint, W. and Ferrera, A., 2010, Molecular Variants of HPV Type 16 E6 Among Honduran Women. International journal of gynecological cancer : official journal of the International Gynecological Cancer Society 20, 323-8.

Tan, S., de Vries, E.G., van der Zee, A.G. and de Jong, S., 2012, Anticancer drugs aimed at E6 and E7 activity in HPV-positive cervical cancer. Current cancer drug targets 12, 170-84.
Tanaka, K., 2009, The proteasome: overview of structure and functions. Proceedings of the Japan Academy. Series B, Physical and biological sciences 85, 12-36.
Tato, C.M. and O'Shea, J.J., 2006, Immunology: what does it mean to be just 17? Nature 441, 166-8.
Tey, S.K., 2014, Adoptive T-cell therapy: adverse events and safety switches. Clinical & translational immunology 3, e17.
Thery, C. and Amigorena, S., 2001, The cell biology of antigen presentation in dendritic cells. Current opinion in immunology 13, 45-51.
Thomsen, M., Lundegaard, C., Buus, S., Lund, O. and Nielsen, M., 2013, MHCcluster, a method for functional clustering of MHC molecules. Immunogenetics 65, 655-65.
Thorpe, G.H. and Kricka, L.J., 1986, Enhanced chemiluminescent reactions catalyzed by horseradish peroxidase. Methods in enzymology 133, 331-53.
Toes, R.E., Offringa, R., Blom, R.J., Melief, C.J. and Kast, W.M., 1996, Peptide vaccination can lead to enhanced tumor growth through specific T-cell tolerance induction. Proceedings of the National Academy of Sciences of the United States of America 93, 7855-60.
Tosato, G. and Cohen, J.I., 2007, Generation of Epstein-Barr Virus (EBV)-immortalized B cell lines. Current protocols in immunology / edited by John E. Coligan ... [et al.] Chapter 7, Unit 7 22.
Tran, E., Turcotte, S., Gros, A., Robbins, P.F., Lu, Y.C., Dudley, M.E., Wunderlich, J.R., Somerville, R.P., Hogan, K., Hinrichs, C.S., Parkhurst, M.R., Yang, J.C. and Rosenberg, S.A., 2014, Cancer immunotherapy based on mutation-specific CD4+ T cells in a patient with epithelial cancer. Science 344, 641-5.
Tschopp, J., Masson, D. and Stanley, K.K., 1986, Structural/functional similarity between proteins involved in complement- and cytotoxic T-lymphocyte-mediated cytolysis. Nature 322, 831-4.
Tu, J.J., Kuhn, L., Denny, L., Beattie, K.J., Lorincz, A. and Wright, T.C., Jr., 2006, Molecular variants of human papillomavirus type 16 and risk for cervical neoplasia in South Africa. International journal of gynecological cancer : official journal of the International Gynecological Cancer Society 16, 736-42.
Uyttenhove, C., Pilotte, L., Theate, I., Stroobant, V., Colau, D., Parmentier, N., Boon, T. and Van den Eynde, B.J., 2003, Evidence for a tumoral immune resistance mechanism based on tryptophan degradation by indoleamine 2,3-dioxygenase. Nature medicine 9, 1269-74.
van Bogaert, L., 2013, Are the currently existing anti-human papillomavirus vaccines appropriate for the developing world? Annals of medical and health sciences research 3, 306-12.
Van de Wall, S., Nijman, H.W. and Daemen, T., 2014, HPV-specific immunotherapy: key role for immunomodulators. Anti-cancer agents in medicinal chemistry 14, 265-79.
Van den Eynde, B.J. and Morel, S., 2001, Differential processing of class-I-restricted epitopes by the standard proteasome and the immunoproteasome. Current opinion in immunology 13, 147-53.
van der Bruggen, P., Traversari, C., Chomez, P., Lurquin, C., De Plaen, E., Van den Eynde, B., Knuth, A. and Boon, T., 1991, A gene encoding an antigen recognized by cytolytic T lymphocytes on a human melanoma. Science 254, 1643-7.
van der Burg, S.H., de Jong, A., Welters, M.J., Offringa, R. and Melief, C.J., 2002, The status of HPV16-specific T-cell reactivity in health and disease as a guide to HPV vaccine development. Virus research 89, 275-84.
van der Sluis, T.C., van Duikeren, S., Huppelschoten, S., Jordanova, E.S., Beyranvand Nejad, E., Sloots, A., Boon, L., Smit, V.T., Welters, M.J., Ossendorp, F., van de Water, B., Arens, R., van der Burg, S.H. and Melief, C.J., 2015, Vaccine-induced tumor necrosis factor-producing T cells synergize with Cisplatin to promote tumor cell death. Clinical cancer research : an official journal of the American Association for Cancer Research 21, 781-94.
van Hall, T. and van der Burg, S.H., 2012, Mechanisms of peptide vaccination in mouse models: tolerance, immunity, and hyperreactivity. Advances in immunology 114, 51-76.
van Poelgeest, M.I., Welters, M.J., van Esch, E.M., Stynenbosch, L.F., Kerpershoek, G., van Persijn van Meerten, E.L., van den Hende, M., Lowik, M.J., Berends-van der Meer, D.M., Fathers, L.M., Valentijn, A.R., Oostendorp, J., Fleuren, G.J., Melief, C.J., Kenter, G.G. and van der Burg, S.H., 2013, HPV16 synthetic long peptide (HPV16-SLP) vaccination therapy of patients with advanced or recurrent HPV16-induced gynecological carcinoma, a phase II trial. J Transl Med 11, 88.

Vanky, F., Klein, E., Willems, J., Book, K., Ivert, T., Peterffy, A., Nilsonne, U., Kreicbergs, A. and Aparisi, T., 1986, Lysis of autologous tumor cells by blood lymphocytes tested at the time of surgery. Correlation with the postsurgical clinical course. Cancer immunology, immunotherapy : CII 21, 69-76.

Vanneman, M. and Dranoff, G., 2012, Combining immunotherapy and targeted therapies in cancer treatment. Nature reviews. Cancer 12, 237-51.

Vaslin, B., Claverie, J.M., Benveniste, O., Barre-Sinoussi, F.C. and Dormont, D., 1994, Nef and Gag synthetic peptide priming of antibody responses to HIV type 1 antigens in mice and primates. AIDS research and human retroviruses 10, 1241-50.

Veiga-Fernandes, H., Walter, U., Bourgeois, C., McLean, A. and Rocha, B., 2000, Response of naive and memory CD8+ T cells to antigen stimulation in vivo. Nature immunology 1, 47-53.

Veldhoen, M., Hocking, R.J., Atkins, C.J., Locksley, R.M. and Stockinger, B., 2006, TGFbeta in the context of an inflammatory cytokine milieu supports de novo differentiation of IL-17-producing T cells. Immunity 24, 179-89.

Vesely, M.D., Kershaw, M.H., Schreiber, R.D. and Smyth, M.J., 2011, Natural innate and adaptive immunity to cancer. Annual review of immunology 29, 235-71.

Vial, T. and Descotes, J., 2003, Immunosuppressive drugs and cancer. Toxicology 185, 229-40.

Vignali, D.A., Collison, L.W. and Workman, C.J., 2008, How regulatory T cells work. Nat Rev Immunol 8, 523-32.

Villa, L.L., Costa, R.L., Petta, C.A., Andrade, R.P., Ault, K.A., Giuliano, A.R., Wheeler, C.M., Koutsky, L.A., Malm, C., Lehtinen, M., Skjeldestad, F.E., Olsson, S.E., Steinwall, M., Brown, D.R., Kurman, R.J., Ronnett, B.M., Stoler, M.H., Ferenczy, A., Harper, D.M., Tamms, G.M., Yu, J., Lupinacci, L., Railkar, R., Taddeo, F.J., Jansen, K.U., Esser, M.T., Sings, H.L., Saah, A.J. and Barr, E., 2005, Prophylactic quadrivalent human papillomavirus (types 6, 11, 16, and 18) L1 virus-like particle vaccine in young women: a randomised double-blind placebo-controlled multicentre phase II efficacy trial. The lancet oncology 6, 271-8.

Villadangos, J.A., 2001, Presentation of antigens by MHC class II molecules: getting the most out of them. Molecular immunology 38, 329-46.

Virolainen, E., Vanharanta, R. and Carey, T.E., 1984, Steroid hormone receptors in human squamous carcinoma cell lines. International journal of cancer. Journal international du cancer 33, 19-25.

Vlad, A.M., Kettel, J.C., Alajez, N.M., Carlos, C.A. and Finn, O.J., 2004, MUC1 immunobiology: from discovery to clinical applications. Advances in immunology 82, 249-93.

Volpers, C., Sapp, M., Snijders, P.J., Walboomers, J.M. and Streeck, R.E., 1995, Conformational and linear epitopes on virus-like particles of human papillomavirus type 33 identified by monoclonal antibodies to the minor capsid protein L2. The Journal of general virology 76 (Pt 11), 2661-7.

von Andrian, U.H. and Mackay, C.R., 2000, T-cell function and migration. Two sides of the same coin. N Engl J Med 343, 1020-34.

von Bergwelt-Baildon, M., Shimabukuro-Vornhagen, A., Popov, A., Klein-Gonzalez, N., Fiore, F., Debey, S., Draube, A., Maecker, B., Menezes, I., Nadler, L.M. and Schultze, J.L., 2006, CD40-activated B cells express full lymph node homing triad and induce T-cell chemotaxis: potential as cellular adjuvants. Blood 107, 2786-9.

Walter, S., Weinschenk, T., Stenzl, A., Zdrojowy, R., Pluzanska, A., Szczylik, C., Staehler, M., Brugger, W., Dietrich, P.Y., Mendrzyk, R., Hilf, N., Schoor, O., Fritsche, J., Mahr, A., Maurer, D., Vass, V., Trautwein, C., Lewandrowski, P., Flohr, C., Pohla, H., Stanczak, J.J., Bronte, V., Mandruzzato, S., Biedermann, T., Pawelec, G., Derhovanessian, E., Yamagishi, H., Miki, T., Hongo, F., Takaha, N., Hirakawa, K., Tanaka, H., Stevanovic, S., Frisch, J., Mayer-Mokler, A., Kirner, A., Rammensee, H.G., Reinhardt, C. and Singh-Jasuja, H., 2012, Multipeptide immune response to cancer vaccine IMA901 after single-dose cyclophosphamide associates with longer patient survival. Nature medicine 18, 1254-61.

Ward, M.J., Thirdborough, S.M., Mellows, T., Riley, C., Harris, S., Suchak, K., Webb, A., Hampton, C., Patel, N.N., Randall, C.J., Cox, H.J., Jogai, S., Primrose, J., Piper, K., Ottensmeier, C.H., King, E.V. and Thomas, G.J., 2014, Tumour-infiltrating lymphocytes predict for outcome in HPV-positive oropharyngeal cancer. British journal of cancer 110, 489-500.

Wearsch, P.A. and Cresswell, P., 2007, Selective loading of high-affinity peptides onto major histocompatibility complex class I molecules by the tapasin-ERp57 heterodimer. Nature immunology 8, 873-81.

Wearsch, P.A. and Cresswell, P., 2008, The quality control of MHC class I peptide loading. Current opinion in cell biology 20, 624-31.

Weenink, S.M. and Gautam, A.M., 1997, Antigen presentation by MHC class II molecules. Immunology and cell biology 75, 69-81.

Weide, B., Derhovanessian, E., Pflugfelder, A., Eigentler, T.K., Radny, P., Zelba, H., Pfohler, C., Pawelec, G. and Garbe, C., 2010, High response rate after intratumoral treatment with interleukin-2: results from a phase 2 study in 51 patients with metastasized melanoma. Cancer 116, 4139-46.

Welters, M.J., de Jong, A., van den Eeden, S.J., van der Hulst, J.M., Kwappenberg, K.M., Hassane, S., Franken, K.L., Drijfhout, J.W., Fleuren, G.J., Kenter, G., Melief, C.J., Offringa, R. and van der Burg, S.H., 2003, Frequent display of human papillomavirus type 16 E6-specific memory t-Helper cells in the healthy population as witness of previous viral encounter. Cancer research 63, 636-41.

Welters, M.J., Kenter, G.G., de Vos van Steenwijk, P.J., Lowik, M.J., Berends-van der Meer, D.M., Essahsah, F., Stynenbosch, L.F., Vloon, A.P., Ramwadhdoebe, T.H., Piersma, S.J., van der Hulst, J.M., Valentijn, A.R., Fathers, L.M., Drijfhout, J.W., Franken, K.L., Oostendorp, J., Fleuren, G.J., Melief, C.J. and van der Burg, S.H., 2010, Success or failure of vaccination for HPV16-positive vulvar lesions correlates with kinetics and phenotype of induced T-cell responses. Proceedings of the National Academy of Sciences of the United States of America 107, 11895-9.

White, J.S., Weissfeld, J.L., Ragin, C.C., Rossie, K.M., Martin, C.L., Shuster, M., Ishwad, C.S., Law, J.C., Myers, E.N., Johnson, J.T. and Gollin, S.M., 2007, The influence of clinical and demographic risk factors on the establishment of head and neck squamous cell carcinoma cell lines. Oral oncology 43, 701-12.

WHO. 2008, The global burden of disease: 2004 update. World Health Organization, Geneva, Swiss

WHO. 2014, World Cancer Report 2014. IARC, Lyon, France

Wiesel, M. and Oxenius, A., 2012, From crucial to negligible: functional CD8(+) T-cell responses and their dependence on CD4(+) T-cell help. European journal of immunology 42, 1080-8.

Williams, M.A., Holmes, B.J., Sun, J.C. and Bevan, M.J., 2006a, Developing and maintaining protective CD8+ memory T cells. Immunological reviews 211, 146-53.

Williams, M.A., Tyznik, A.J. and Bevan, M.J., 2006b, Interleukin-2 signals during priming are required for secondary expansion of CD8+ memory T cells. Nature 441, 890-3.

Winer, R.L., Kiviat, N.B., Hughes, J.P., Adam, D.E., Lee, S.K., Kuypers, J.M. and Koutsky, L.A., 2005, Development and duration of human papillomavirus lesions, after initial infection. The Journal of infectious diseases 191, 731-8.

Woodman, C.B., Collins, S.I. and Young, L.S., 2007, The natural history of cervical HPV infection: unresolved issues. Nature reviews. Cancer 7, 11-22.

Xi, L.F., Koutsky, L.A., Hildesheim, A., Galloway, D.A., Wheeler, C.M., Winer, R.L., Ho, J. and Kiviat, N.B., 2007, Risk for high-grade cervical intraepithelial neoplasia associated with variants of human papillomavirus types 16 and 18. Cancer epidemiology, biomarkers & prevention : a publication of the American Association for Cancer Research, cosponsored by the American Society of Preventive Oncology 16, 4-10.

Xue, Y., Lim, D., Zhi, L., He, P., Abastado, J.P. and Thierry, F., 2012, Loss of HPV16 E2 Protein Expression Without Disruption of the E2 ORF Correlates with Carcinogenic Progression. The open virology journal 6, 163-72.

Yaciuk, J.C., Skaley, M., Bardet, W., Schafer, F., Mojsilovic, D., Cate, S., Stewart, C.J., McMurtrey, C., Jackson, K.W., Buchli, R., Olvera, A., Cedeno, S., Plana, M., Mothe, B., Brander, C., West, J.T. and Hildebrand, W.H., 2014, Direct interrogation of viral peptides presented by the class I HLA of HIV-infected T cells. Journal of virology 88, 12992-3004.

Yewdell, J.W. and Bennink, J.R., 2001, Cut and trim: generating MHC class I peptide ligands. Current opinion in immunology 13, 13-8.

Zehbe, I., Wilander, E., Delius, H. and Tommasino, M., 1998, Human papillomavirus 16 E6 variants are more prevalent in invasive cervical carcinoma than the prototype. Cancer research 58, 829-33.

Zeng, G., Li, Y., El-Gamil, M., Sidney, J., Sette, A., Wang, R.F., Rosenberg, S.A. and Robbins, P.F., 2002, Generation of NY-ESO-1-specific CD4+ and CD8+ T cells by a single peptide with dual MHC class I and class II specificities: a new strategy for vaccine design. Cancer research 62, 3630-5.

Zhang, G.L., Ansari, H.R., Bradley, P., Cawley, G.C., Hertz, T., Hu, X., Jojic, N., Kim, Y., Kohlbacher, O., Lund, O., Lundegaard, C., Magaret, C.A., Nielsen, M., Papadopoulos, H., Raghava, G.P., Tal, V.S., Xue, L.C., Yanover, C., Zhu, S., Rock, M.T., Crowe, J.E., Panayiotou, C., Polycarpou, M.M., Duch, W. and Brusic, V., 2011, Machine learning competition in immunology - Prediction of HLA class I binding peptides. Journal of immunological methods 374, 1-4.

Zhang, G.L., Bozic, I., Kwoh, C.K., August, J.T. and Brusic, V., 2007, Prediction of supertype-specific HLA class I binding peptides using support vector machines. Journal of immunological methods 320, 143-54.

Zhang, L., Conejo-Garcia, J.R., Katsaros, D., Gimotty, P.A., Massobrio, M., Regnani, G., Makrigiannakis, A., Gray, H., Schlienger, K., Liebman, M.N., Rubin, S.C. and Coukos, G., 2003, Intratumoral T cells, recurrence, and survival in epithelial ovarian cancer. N Engl J Med 348, 203-13.

Zheng, Z.M. and Baker, C.C., 2006, Papillomavirus genome structure, expression, and post-transcriptional regulation. Frontiers in bioscience : a journal and virtual library 11, 2286-302.

Zhou, J.H., Ye, F., Chen, H.Z., Zhou, C.Y., Lu, W.G. and Xie, X., 2006, Altered expression of cellular membrane molecules of HLA-DR, HLA-G and CD99 in cervical intraepithelial neoplasias and invasive squamous cell carcinoma. Life sciences 78, 2643-9.

Zhou, X.Y., Yashiro-Ohtani, Y., Nakahira, M., Park, W.R., Abe, R., Hamaoka, T., Naramura, M., Gu, H. and Fujiwara, H., 2002, Molecular mechanisms underlying differential contribution of CD28 versus non-CD28 costimulatory molecules to IL-2 promoter activation. J Immunol 168, 3847-54.

Zuna, R.E., Tuller, E., Wentzensen, N., Mathews, C., Allen, R.A., Shanesmith, R., Dunn, S.T., Gold, M.A., Wang, S.S., Walker, J. and Schiffman, M., 2011, HPV16 variant lineage, clinical stage, and survival in women with invasive cervical cancer. Infectious agents and cancer 6, 19.

zur Hausen, H., 1977, Human papillomaviruses and their possible role in squamous cell carcinomas. Curr Top Microbiol Immunol 78, 1-30.

zur Hausen, H., 2002, Papillomaviruses and cancer: from basic studies to clinical application. Nature reviews. Cancer 2, 342-50.

zur Hausen, H., Gissmann, L., Steiner, W., Dippold, W. and Dreger, I., 1975, Human papilloma viruses and cancer. Bibliotheca haematologica, 569-71.

Zwaveling, S., Ferreira Mota, S.C., Nouta, J., Johnson, M., Lipford, G.B., Offringa, R., van der Burg, S.H. and Melief, C.J., 2002, Established human papillomavirus type 16-expressing tumors are effectively eradicated following vaccination with long peptides. J Immunol 169, 350-8.

References

6. Abbreviations

aa	amino acid
Ag	antigen
Ab	antibody
APC	antigen presenting cell
A_{ROC}	area under the ROC curve
bp	base pairs
BSA	bovine serum albumin
C-terminus	carboxyl-terminus
°C	degree Celsius
cDNA	complementary DNA
CIN	cervical intraepithelial neoplasia
CMV	cytomegalovirus
CO_2	carbon dioxide
CTL	cytotoxic T lymphocyte
Da	Dalton
DC	dendritic cell
ddH_20	double distilled water
dNTP	deoxyribonucleoside triphosphate
DMEM	Dulbecco´s Modified Eagle Medium
DMSO	dimethyl sulfoxide
DNA	deoxyribonucleic acid
dNTP	deoxynucleoside triphosphate
ds	double-stranded
EBV	Epstein-Barr virus
EDTA	ethylenediaminetetraacetic acid
ELISA	Enzyme Linked Immunosorbent Assay
ELISpot	Enzyme Linked Immuno Spot
ER	endoplasmic reticulum
et al.	*et alii, at aliae, et alia*
FACS	fluorescence-activated cell sorting
FCS	fetal calf serum
FDA	Food and Drug Administration
FITC	fluorescein isothiocyanate
Fig.	figure
for	forward
FSC	forward scatter
Gy	Gray
hr	hour
HEPES	4-(2-hydroxyethyl)-1-piperazineethanesulfonic acid
HLA	human leukocyte antigen
HIV	human immunodeficiency virus
HPV	human papillomavirus
HNSCC	head and neck squamous cell carcinoma
HS	human serum
IC_{50}	half maximal inhibitory concentration
IFN	interferon
IL	interleukin
kb	kilo base pairs
kDa	kilo Dalton
LPS	lipopolysaccharide
M	molarity
mAb	monoclonal antibody
Mg	magnesium

MHC	major histocompatibility complex
MFI	mean fluorescent intensity
min	minute
mM	millimolar
mRNA	messenger RNA
MS	mass spectrometry
MW	molecular weight
N-terminus	amino-terminus
nm	nanometer
No.	number
nt	nucleotide
o/n	overnight
ORF	open reading frame
PAGE	polyacrylamide gel electrophoresis
PBS	phosphate buffered saline
PCR	polymerase chain reaction
PFA	paraformaldehyde
pH	*pondus hydrogenii*
PHA	phytohaemagglutinin
RNA	ribonucleic acid
RNase	ribonuclease
rpm	rounds per minute
ROC	receiver operating characteristic
RT	room temperature
sec	second(s)
SDS	sodium dodecyl sulfate
SNT	supernatant
ss	single-stranded
SCC	squamous cell carcinoma
SSC	side scatter
Tab.	table
Taq	*Thermus aquaticus*
TCR	T cell receptor
temp	temperature
TGF-β	transforming growth factor beta
TLR	Toll-like receptor
TNFα	tumor necrosis factor alpha
T_{reg}	regulatory T cell
Tris	Tris(hydroxylmethyl)-aminomethane
U	unit
UV	ultraviolet
UTR	untranslated region
V	Volt
VIN	vuval intraepithelial neoplasia
VLP	virus like particle
WHO	Word Health Organisation
WB	Western blot
w/o	without
wt	wild type
x	times, -fold

7. Appendix

Table 22 I Predicted and experimental binding affinities to HLA-A3 for HPV16 E6 peptides. Peptides are sorted by the actual binding affinity as determined in the cellular binding assays. Binding affinities are color-coded according to their predicted and experimental binding strength. NetMHC and IEDB servers indicate binding affinities as IC50 [nM] and the average is displayed in the third column from the left. SYFPEITHI and BIMAS show scores as arbitrary units. Dashes indicate that the peptide length was not supported by the respective server and empty cells indicate that the chosen cutoff for the individual prediction server was exceeded. *Italic* highlighting indicates peptides that were determined to be potential binders by motif analysis. The code colors dark blue, blue and light blue indicate strong, intermediate and weak binders, repectively. Individual recommended ([a], [b], [c]) and self-determined ([d], [e], [f]) binding affinities: [a]: strong: < 5µM, intermediate: 5-15µM, weak: 15-100µM, non: > 100µM; [b]: strong: < 50nM, weak: 50-500nM, non: > 500nM; [c, d]: strong: < 50nM, intermediate: 50-500nM, weak: 500-5000nM, non: > 500nM; [e]: strong: > 28, intermediate: 28-24, weak: 24-20, non: < 20; [f]: strong: > 40, intermediate: 40-15, weak: 15-5, non: < 5; exp: experimental

peptide	length	exp. IC50 [µM][a]	NetMHC[b]	NetMHC Pan[b]	NetMHC cons[b]	IEDB ann[c]	IEDB smm[c]	IEDB arb[c]	IEDB smmpmbec[c]	IEDB netmhcpan[c]	average IC50[d]	SYFPEITHI[e]	BIMAS[f]
E6/106-115	10	2,02	41	226,95	247,81	41,36	67,50	7,14	61,13	156,47	106,17	29	45,00
E6/107-115	9	4,67	369	265,28		369,90	394,83	68,51	419,57	233,50	302,94	24	3,00
E6/68-77	10	9,29	192	1928,44	2065,97	192,32	498,02	435,08	645,69	2812,19	1096,21	20	0,30
E6/89-99	11	10,06	180	151,91	129,48	-	-	-	-	257,38	179,69	-	-
E6/59-67	9	10,95	472	416,41		472,50	623,06	231,10	676,12	537,16	489,76	28	2,00
E6/75-84	10	11,72	156	1186,57	801,61	156,11	324,35	425,85	261,56	1158,05	558,76	11	0,09
E6/33-41	9	14,69	270	262,48	226,04	270,73	287,34	80,16	322,75	249,16	246,08	23	40,50
E6/92-101	10	17,33	1204	1612,76	2169,05	1204,66	731,56	329,44	799,32	1602,13	1206,61	11	9,00
E6/93-101	9	20,10	315	399,88		315,88	422,99	63,61	520,21	543,00	368,65	13	6,75
E6/129-138	10	21,01	1196	2780,96	2593,00	1196,21	1104,10	602,75	1017,99	1637,18	1516,02	10	0,05
E6/37-46	10	30,56	263	273,59	190,11	263,35	203,86	99,80	240,54	241,20	221,93	21	4,00
E6/68-75	8	34,39	540	358,87		-	-	-	-	384,09	427,65	-	-
E6/125-133	9	34,95	3630	6798,29	3472,75	3630,59	2353,77	3408,25	2254,04	7131,08	4084,85	15	0,02
E6/84-91	8	58,09	3308	1139,38	1145,59	-	-	-	-	1145,59	1684,64	-	-
E6/75-83	9	61,37	515	1508,88	739,13	515,50	638,82	107,74	561,92	605,05	649,01	17	0,09
E6/8-18	11	64,67	10489	3280,96	4701,59	-	-	-	-	4625,90	5774,36	-	-
E6/32-41	10	non-binder	1396	14176,57	12183,00	1396,37	1043,81	1636,43	1064,57	13797,25	5836,75	22	8,10
E6/79-88	10	non-binder	290	387,18		290,89	611,86	737,87	434,00	525,66	468,21	18	5,40
E6/143-151	9	non-binder	1106	569,75		1106,78	636,84	536,52	962,03	704,01	803,13	10	4,00
E6/113-122	10	non-binder	4435	3642,54	5743,49	4435,20	1838,79	2130,07	3568,73	3416,85	3651,33	15	0,90
E6/58-67	10	non-binder	2933	4442,73	7208,66	2933,61	2025,29	9580,25	2450,65	7054,34	4828,57	17	0,60
E6/89-97	9	non-binder	6110	3827,94	4062,65	6110,91	8139,51	351,81	7649,44	7446,48	5462,34	20	0,30
E6/139-148	10	non-binder	4519	12100,85	12517,05	4519,88	3554,74	1149,95	4200,95	12653,21	6901,95	7	0,20
E6/142-151	10	non-binder	1179	8307,51	6978,43	1179,31	1579,16	2652,43	1455,73	9047,59	4047,40	14	0,06
E6/144-153	10	non-binder	802	2598,42	3745,99	802,87	645,64	1009,96	927,35	3685,69	1777,24	8	0,00
E6/34-41	8	non-binder	890	645,94	605,05	-	-	-	-	330,10	617,77	-	-
E6/37-47	11	non-binder	438	553,77		-	-	-	-	446,91	479,56	-	-
E6/94-101	8	non-binder	1621	1083,36	1103,02	-	-	-	-	759,40	1141,69	-	-
E6/79-86	8	non-binder	625	876,57	797,29	-	-	-	-	855,38	788,56	-	-
E6/73-83	11	non-binder	3039	1474,46	1709,59	-	-	-	-	1097,07	1830,03	-	-
E6/143-153	11	non-binder	2095	937,27	989,90	-	-	-	-	1145,59	1291,94	-	-
E6/122-129	8	non-binder	1018	1962,79	1501,43	-	-	-	-	1347,45	1457,42	-	-
E6/129-136	8	non-binder	3383	3240,86	3099,81	-	-	-	-	1785,20	2877,22	-	-
E6/75-85	11	non-binder	4743	4742,80	2889,29	-	-	-	-	2496,64	3717,93	-	-
E6/48-55	8	non-binder	1279	3485,82	2510,18	-	-	-	-	2579,01	2463,50	-	-
E6/72-79	8	non-binder	1304	1830,91	1445,63	-	-	-	-	2607,06	1796,90	-	-
E6/144-151	8	non-binder	2840	1955,47	2607,06	-	-	-	-	2607,06	2502,40	-	-
E6/144-154	11	non-binder	1774	1804,62	2277,27	-	-	-	-	2751,98	2151,97	-	-
E6/29-39	11	non-binder	5068	2509,08	2430,01	-	-	-	-	2751,98	3189,77	-	-
E6/105-115	11	non-binder	3259	4248,75	3491,59	-	-	-	-	3066,45	3516,45	-	-
E6/81-91	11	non-binder	5663	4106,89	2443,19	-	-	-	-	4196,68	4102,44	-	-
E6/43-52	10	non-binder	25750	25316,84	20589,91	25750,01	14125,77		15501,17	25289,19	21760,41	21	27,00
E6/44-52	9	non-binder	20826	28515,92	22818,90	20826,74				24218,04	23441,12	20	18,00
E6/134-142	9	non-binder	7073	7947,14	7169,76	7073,45	4326,94	9135,07	3656,74	7945,94	6791,00	20	0,60
E6/68-76	9	non-binder	19386	19172,91	17985,29	19386,32	18709,61	1400,54	18176,88	19295,70	16689,16	22	0,40
E6/52-61	10	non-binder	12813	5963,81	6755,55	12813,99	10303,64		10169,68	5620,54	9205,74	13	0,40
E6/116-124	9	non-binder	20579	34734,94	27131,77	20579,11		4757,86		34237,82	23670,08	20	0,30
E6/67-75	9	non-binder	11316	7262,05	5805,97	11316,13	5024,17	646,45	5845,77	6610,93	6728,43	10	0,30
E6/89-98	10	non-binder	9136	9659,52	9146,01	9136,42	1253,81		2951,06	13648,77	7847,37	20	0,23
E6/70-79	10	non-binder	10487	19563,23	13947,35	10487,43	336,97	1743,07	670,51	20589,91	9728,18	13	0,18
E6/74-83	10	non-binder	8274	17006,16	18279,56	8274,43	2583,73	6050,70	1981,89	13356,59	9475,88	9	0,03
E6/38-46	9	non-binder	11173	16412,45	9195,62	11173,30	5396,69	513,86	5189,70	18279,56	9666,77	7	0,01
E6/53-62	10	non-binder	1563	5092,70	6062,77	1563,50	1998,50	1226,80	1959,75	5932,98	3175,00	15	0,01

E6/144-152	9	non-binder	20362	21299,45	21500,59	20362,93	30300,51	510,49	23586,76	25017,04	20367,47	5	0,00
E6/52-62	11	non-binder	6243	2392,09	2889,29	-	-	-	-	2264,98	3447,34	-	-
E6/43-50	8	non-binder	6273	4147,55	4174,04	-	-	-	-	4727,10	4830,42	-	-
E6/91-101	11	not tested	-	-	-	-	-	-	-	14722,66	14722,66	-	-
E6/93-103	11	not tested	-	-	-	-	-	-	-	29745,37	29745,37	-	-

Table 23 I Predicted and experimental binding affinities to HLA-A3 for HPV16 E7 peptides. Peptides are sorted by the actual binding affinity as determined in the cellular binding assays. Binding affinities are color-coded according to their predicted and experimental binding strength. NetMHC and IEDB servers indicate binding affinities as IC50 [nM] and the average is displayed in the third column from the left. SYFPEITHI and BIMAS show scores as arbitrary units. Dashes indicate that the peptide length was not supported by the respective server and empty cells indicate that the chosen cutoff for the individual prediction server was exceeded. *Italic* highlighting indicates peptides that were determined to be potential binders by motif analysis. The code colors dark blue, blue and light blue indicate strong, intermediate and weak binders, repectively. Individual recommended ([a], [b], [c]) and self-determined ([d], [e], [f]) binding affinities: [a]: strong: < 5µM, intermediate: 5-15µM, weak: 15-100µM, non: > 100µM; [b]: strong: < 50nM, weak: 50-500nM, non: > 500nM; [c, d]: strong: < 50nM, intermediate: 50-500nM, weak: 500-5000nM, non: > 500nM; [e]: strong: > 28, intermediate: 28-24, weak: 24-20, non: < 20; [f]: strong: > 40, intermediate: 40-15, weak: 15-5, non: < 5; exp: experimental

peptide	length	exp. IC50 [µM][a]	NetMHC[b]	NetMHC Pan[b]	NetMHC cons[b]	IEDB ann[c]	IEDB smm[c]	IEDB arb[c]	IEDB smmpmbec[c]	IEDB netmhcpan[c]	average IC50[d]	SYFPEITHI[e]	BIMAS[f]
E7/88-97	10	2,22	62	133,49		62,91	87,26	64,11	75,34	100,41	83,65	19	1,80
E7/89-97	9	3,16	36	65,03	40,03	36,28	39,74	9,86	44,80	58,45	41,28	21	2,00
E7/87-97	11	6,32	2796	1049,93	1610,82	-	-	-	-	953,12	1602,47	-	-
E7/52-60	9	15,84	3679	3049,31	2737,14	3679,87	1434,87	46,98	1128,23	2722,37	2309,72	13	0,06
E7/53-60	8	17,88	487	252,83	222,40	-	-	-	-	249,16	302,85	-	-
E7/50-60	11	28,96	1070	930,26	582,56	-	-	-	-	659,75	810,64	-	-
E7/63-73	11	non-binder	2006	861,66	979,25	-	-	-	-	837,07	1170,99	-	-
E7/51-60	10	non-binder	6879	999,09	984,56	6879,10	739,80	600,69	707,95	554,88	2293,13	11	0,40
E7/68-77	10	non-binder	7694	1190,51	1654,99	7694,16	7128,74		7941,86	1469,28	4967,65	20	0,40
E7/77-84	8	non-binder	11355	2852,50	4909,54	-	-	-	-	4382,30	5874,83	-	-
E7/63-71	9	non-binder	14702	9471,40	8119,76	14702,13	4011,61	1354,36	3837,88	10191,11	8298,78	18	0,00
E7/85-93	9	non-binder	17045	8957,97	9295,66	17045,71	5608,92	1939,76	4616,44	9346,08	9231,94	16	0,05
E7/19-27	9	non-binder	14706	12456,79	9396,78	14706,74	11798,37	1130,34	11925,05	19088,05	11901,01	11	0,00
E7/55-63	9	non-binder	22433	18782,24	16583,46	22433,09	9020,44	364,83	8466,23	16404,99	14311,03	11	0,00
E7/18-26	9	non-binder	22248	21121,82	19611,42	22248,42	16096,73	1003,08	19681,74	24481,50	18311,59	12	0,00
E7/71-80	10	non-binder	30342	14322,65	9865,62	30342,51	5997,96	-	34043,30	16583,46	20213,93	16	0,00
E7/31-40	10	non-binder	36295		35559,24	36295,07					36049,77	17	0,00
E7/18-25	8	non-binder	4701	6228,96	6062,77	-	-	-	-	5997,52	5747,56	-	-
E7/69-77	9	not tested	6693	5265,77	5869,13	6693,85	2238,76	1625,60	2293,64	7131,08	4726,35	10	0,12
E7/36-43	8	not tested	30697		38565,12	-	-	-	-		34631,06	-	-
E7/42-50	9	not tested	25939		33504,88	25939,19		19863,93			26311,75	5	0,00
E7/68-75	8	not tested	25613	27753,19	23192,26	-	-	-	-	31398,89	26989,33	-	-
E7/41-50	10	not tested	37421		37132,00	37420,98					37324,66	1	0,00

Table 24 I Predicted and experimental binding affinities to HLA-A11 for HPV16 E6 peptides. Peptides are sorted by the actual binding affinity as determined in the cellular binding assays. Binding affinities are color-coded according to their predicted and experimental binding strength. NetMHC and IEDB servers indicate binding affinities as IC50 [nM] and theaverage is displayed in the third column from the left. SYFPEITHI and BIMAS show scores as arbitrary units. Dashes indicate that the peptide length was not supported by the respective server and empty cells indicate that the chosen cutoff for the individual prediction server was exceeded. *Italic* highlighting indicates peptides that were determined to be potential binders by motif analysis. The code colors dark blue, blue and light blue indicate strong, intermediate and weak binders, repectively. Individual recommended ([a], [b], [c]) and self-determined ([d], [e], [f]) binding affinities: [a]: strong: < 5µM, intermediate: 5-15µM, weak: 15-100µM, non: > 100µM; [b]: strong: < 50nM, weak: 50-500nM, non: > 500nM; [c, d]: strong: < 50nM, intermediate: 50-500nM, weak: 500-5000nM, non: > 500nM; [e]: strong: > 22, intermediate: 22-19, weak: 19-15, non: < 15; [f]: strong: > 6, intermediate: 6-4, weak: 4-0.4, non: < 0.4; exp: experimental

peptide	length	exp. IC50 [µM][a]	NetMHC[b]	NetMHC Pan[b]	NetMHC cons[b]	IEDB ann[c]	IEDB smm[c]	IEDB arb[c]	IEDB smmpmbec[c]	IEDB netmhcpan[c]	average IC50[d]	SYFPEITHI[e]	BIMAS[f]
E6/106-115	10	1,36	162	269,21	214,14	162,29	136,93	141,45	122,15	146,63	169,35	17	0,60
E6/52-62	11	2,67	697	207,33	350,34	-	-	-	-	216,47	367,78	-	-
E6/93-101	9	3,99	13	12,85		13,45	18,99	5,79	23,70	11,91	14,24	21	3,00
E6/9-18	10	4,06	4381	5330,69	5590,22	4381,30	1072,84	4102,43	2000,83	3975,68	3854,37	11	0,60
E6/92-101	10	4,19	33	38,54	41,12	33,29	35,94	4,85	35,97	61,70	35,55	23	6,00
E6/68-77	10	4,80	553	716,37	492,62	553,46	586,96	718,05	710,85	810,33	642,70	15	0,01
E6/33-41	9	4,98	28	70,84	29,25	28,26	69,85	35,47	71,48	48,11	47,66	18	1,20
E6/107-115	9	5,21	2376	488,95	1017,05	2376,57	813,86	47,11	658,10	427,98	1025,70	16	0,40
E6/94-101	8	6,03	471	253,84	314,41	-	-	-	-	277,63	329,22	-	-

E6/32-41	10	6,80	241	1935,47	1164,33	241,09	252,54	136,24	188,70	1946,61	763,25	18	0,36
E6/34-41	8	8,34	337	406,29	311,03	-	-	-	-	238,60	323,23	-	-
E6/68-75	8	9,72	35	49,15	27,56	-	-	-	-	30,21	35,48	-	-
E6/68-78	11	11,51	4129	7887,81	5900,97	-	-	-	-	7446,48	6341,07	-	-
E6/67-75	9	12,64	2496	1056,96	1255,95	2496,66	778,33	55,93	826,29	953,12	1239,91	12	0,30
E6/105-115	11	14,75	6791	3538,34	4778,52	-	-	-	-	3454,02	4640,47	-	-
E6/59-67	9	18,78	288	314,32	279,13	288,41	388,74	260,66	424,89	396,76	330,11	10	0,04
E6/48-55	8	27,75	98	253,51	165,16	-	-	-	-	159,89	169,14	-	-
E6/37-46	10	36,49	407	73,66		407,58	272,27	383,80	353,86	51,34	278,50	24	1,60
E6/91-101	11	43,48	5502	3009,38	4651,00	-	-	-	-	4830,50	4498,22	-	-
E6/53-62	10	47,68	3076	2576,04	4551,43	3076,75	3578,01	3060,57	3182,41	3066,45	3270,96	18	0,04
E6/68-76	9	48,82	11564	16297,43	13648,77	11564,68	3300,57	317,03	3581,45	16946,23	9652,52	19	0,04
E6/79-88	10	48,83	400	268,76	208,42	400,07	725,63	433,32	525,14	384,09	418,18	6	0,02
E6/144-154	11	54,36	637	264,36	425,67	-	-	-	-	466,68	448,43	-	-
E6/69-79	11	58,43	9918	7208,82	6434,51	-	-	-	-	3766,31	6831,91	-	-
E6/89-99	11	64,75	521	497,78	585,72	-	-	-	-	659,75	566,06	-	-
E6/80-88	9	65,36	1681	3848,74	4174,04	1681,37	2408,44	3199,22	2166,99	4727,10	2985,86	10	0,00
E6/139-148	10	82,74	6496	1308,96	2469,77	6496,13	3084,13	4590,76	2944,84	1904,94	3661,94	18	0,20
E6/37-47	11	non-binder	505	192,50	289,91	-	-	-	-	137,41	281,21	-	-
E6/144-151	8	non-binder	422	253,28	324,79	-	-	-	-	461,65	365,43	-	-
E6/144-153	10	non-binder	481	488,27	1011,56	481,63	549,10	881,39	936,25	883,60	714,10	18	0,00
E6/75-84	10	non-binder	1089	702,01	1067,79	1089,97	824,95	1580,65	821,98	912,75	1011,14	9	0,24
E6/29-39	11	non-binder	1071	1186,02	1017,05	-	-	-	-	1073,58	1086,91	-	-
E6/72-79	8	non-binder	1922	932,32	958,29	-	-	-	-	963,49	1194,02	-	-
E6/8-18	11	non-binder	1596	1032,98	1067,79	-	-	-	-	1209,27	1226,51	-	-
E6/143-151	9	non-binder	2474	350,56	700,21	2474,40	1184,39	1472,28	2136,48	492,62	1410,62	14	0,08
E6/79-86	8	non-binder	1692	1000,90	1501,43	-	-	-	-	1654,99	1462,33	-	-
E6/113-122	10	non-binder	3304	1705,71	2510,18	3304,32	911,52	1270,13	1784,73	1501,43	2036,50	13	0,60
E6/143-153	11	non-binder	5384	704,49	1854,10	-	-	-	-	932,72	2218,83	0	-
E6/77-84	8	non-binder	4477	1289,30	2403,86	-	-	-	-	2216,49	2596,66	-	-
E6/75-83	9	non-binder	5128	4394,98	5182,46	5128,19	1926,12	533,51	2270,04	2443,19	3375,81	3	0,01
E6/122-129	8	non-binder	5791	2564,73	3646,02	-	-	-	-	2781,92	3695,92	-	-
E6/84-91	8	non-binder	8998	2588,75	5044,15	-	-	-	-	3033,45	4916,09	-	-
E6/38-46	9	non-binder	8266	6396,26	5774,65	8266,38	1908,89	409,42	2588,80	6903,33	5064,22	14	0,16
E6/81-91	11	non-binder	8103	4421,13	4936,17	-	-	-	-	3529,57	5247,47	-	-
E6/58-67	10	non-binder	4404	3309,07	5295,83	4404,78	2635,19	14072,03	3429,32	4526,88	5259,64	6	0,01
E6/92-99	8	non-binder	7104	4033,48	5620,54	-	-	-	-	4429,97	5297,00	-	-
E6/129-136	8	non-binder	11469	3887,26	6610,93	-	-	-	-	4106,84	6518,51	-	-
E6/28-36	9	non-binder	11296	9443,97	4727,10	11296,68	1765,21	390,99	3029,02	15044,73	7124,21	18	0,00
E6/89-97	9	non-binder	9881	6574,05	5238,84	9881,33	5600,87	992,73	5513,92	13356,59	7129,92	15	0,00
E6/73-83	11	non-binder	15003	4493,70	8032,38	-	-	-	-	4382,30	7977,84	-	-
E6/70-79	10	non-binder	13842	13324,55	8853,90	13842,41	440,77	2042,62	760,54	11479,16	8073,24	11	0,04
E6/75-85	11	non-binder	13502	7981,50	9972,95	-	-	-	-	7131,08	9646,88	-	-
E6/129-138	10	non-binder	13372	4436,52	7818,02	13372,06	16548,24	17666,36	19967,66	4478,16	12207,38	9	0,04
E6/64-72	9	non-binder	17607	15901,68	15457,23	17607,61	9264,62	533,00	8441,33	19932,31	13093,10	14	0,12
E6/48-56	9	non-binder	17492	21324,51	16673,41	17492,35	3192,61	714,36	3153,46	28485,48	13566,02	14	0,00
E6/101-109	9	non-binder	21637	16001,61	16316,49	21637,34	2904,36	1874,55	2891,90	25842,40	13638,21	13	0,36
E6/88-97	10	non-binder	22481	11223,96	12249,09	22481,32	5992,45		11213,93	19505,61	15021,05	16	0,00
E6/29-37	9	non-binder	24187	21596,42	15541,08	24187,40	6275,95	1118,56	4949,49	27875,69	15716,45	14	0,00
E6/28-37	10	non-binder	30761	15625,01	10699,58	30761,66	4304,45		3250,97	21269,21	16667,41	17	0,00
E6/140-148	9	non-binder	21145	13694,63	15290,89	21145,42	30041,50	552,60	21296,52	10757,62	16740,52	8	0,00
E6/144-152	9	non-binder	23240	19612,34	19295,70	23240,87	14560,43	1017,81	15983,85	23957,42	17613,55	10	0,00
E6/134-142	9	non-binder	24314	11254,35	13872,10	24314,92	23048,16	28377,77	19392,44	14722,66	19912,05	15	0,08
E6/71-79	9	non-binder	22417	29957,47	22818,90	22417,68	18089,75	218,84	12892,88	33144,32	20244,61	11	0,01
E6/145-153	9	non-binder	24229	19723,50	20149,14	24229,18	37241,87	1030,74	30689,30	22209,93	22437,83	11	0,00
E6/27-36	10	non-binder	28156	22669,63	18780,76	28155,93	6162,05		26553,41	28178,94	22665,24	17	0,00
E6/81-89	9	non-binder	25002	32280,41	27575,71	25002,43	29460,31	1493,11	13228,82	27575,71	22702,31	3	0,00
E6/116-124	9	non-binder	28702	32709,34	28178,94	28702,82		5008,77		33144,32	26074,37	15	0,00
E6/18-25	8	non-binder	29754	32976,28	29425,27	-	-	-	-	36931,66	32271,80	-	-
E6/63-73	11	non-binder	29590		35176,57	-	-	-	-	-	32383,29	-	-
E6/52-61	10	non-binder	3972	3617,43	4242,33	3972,80	1876,44		2167,22	2264,98	3159,03	6	0,01
E6/65-75	11	not tested	10642	9950,92	9447,76	-	-	-	-	13212,86	10813,38	-	-
E6/31-41	11	not tested	12779	24988,00	6330,92	-	-	-	-	6682,85	7996,18	-	-
E6/66-75	10	not tested	24988	24839,38	9447,76	24988,09	5440,22		7380,68	23444,56	18451,97	14	0,04

Table 25 I Predicted and experimental binding affinities to HLA-A11 for HPV16 E7 peptides. Peptides are sorted by the actual binding affinity as determined in the cellular binding assays. Binding affinities are color-coded according to their predicted and experimental binding strength. NetMHC and IEDB servers indicate binding affinities as IC50 [nM] and theaverage is displayed in the third column from the left. SYFPEITHI and BIMAS show scores as arbitrary units. Dashes indicate that the peptide length was not supported by the respective server and empty cells indicate that the chosen cutoff for the individual prediction server was exceeded. *Italic* highlighting indicates peptides that were determined to be potential binders by motif analysis. The code colors dark blue, blue and light blue indicate strong, intermediate and weak binders, repectively. Individual recommended ([a], [b], [c]) and self-determined ([d], [e], [f]) binding affinities: [a]: strong: < 5µM, intermediate: 5-15µM, weak: 15-100µM, non: > 100µM; [b]: strong: < 50nM, weak: 50-500nM, non: > 500nM; [c, d]: strong: < 50nM, intermediate: 50-500nM, weak: 500-5000nM, non: > 500nM; [e]: strong: > 22, intermediate: 22-19, weak: 19-15, non: < 15; [f]: strong: > 6, intermediate: 6-4, weak: 4-0.4, non: < 0.4; exp: experimental

peptide	length	exp. IC50 [µM][a]	NetMHC[b]	NetMHC Pan[b]	NetMHC cons[b]	IEDB ann[c]	IEDB smm[c]	IEDB arb[c]	IEDB smmpmbec[c]	IEDB netmhcpan[c]	average IC50[d]	SYFPEITHI[e]	BIMAS[f]
E7/88-97	10	2,22	62	133,49		62,91	87,26	64,11	75,34	100,41	83,65	19	1,80
E7/89-97	9	3,16	36	65,03	40,03	36,28	39,74	9,86	44,80	58,45	41,28	21	2,00
E7/87-97	11	6,32	2796	1049,93	1610,82	-	-	-	-	953,12	1602,47	-	-
E7/52-60	9	15,84	3679	3049,31	2737,14	3679,87	1434,87	46,98	1128,23	2722,37	2309,72	13	0,06
E7/53-60	8	17,88	487	252,83	222,40	-	-	-	-	249,16	302,85	-	-
E7/50-60	11	28,96	1070	930,26	582,56	-	-	-	-	659,75	810,64	-	-
E7/63-73	11	non-binder	2006	861,66	979,25	-	-	-	-	837,07	1170,99	-	-
E7/51-60	10	non-binder	6879	999,09	984,56	6879,10	739,80	600,69	707,95	554,88	2293,13	11	0,40
E7/68-77	10	non-binder	7694	1190,51	1654,99	7694,16	7128,74		7941,86	1469,28	4967,65	20	0,40
E7/77-84	8	non-binder	11355	2852,50	4909,54	-	-	-	-	4382,30	5874,83	-	-
E7/63-71	9	non-binder	14702	9471,40	8119,76	14702,13	4011,61	1354,36	3837,88	10191,11	8298,78	18	0,00
E7/85-93	9	non-binder	17045	8957,97	9295,66	17045,71	5608,92	1939,76	4616,44	9346,08	9231,94	16	0,05
E7/19-27	9	non-binder	14706	12456,79	9396,78	14706,74	11798,37	1130,34	11925,05	19088,05	11901,01	11	0,00
E7/55-63	9	non-binder	22433	18782,24	16583,46	22433,09	9020,44	364,83	8466,23	16404,99	14311,03	11	0,00
E7/18-26	9	non-binder	22248	21121,82	19611,42	22248,42	16096,73	1003,08	19681,74	24481,50	18311,59	12	0,00
E7/71-80	10	non-binder	30342	14322,65	9865,62	30342,51	5997,96	-	34043,30	16583,46	20213,93	16	0,00
E7/31-40	10	non-binder	36295		35559,24	36295,07					36049,77	17	0,00
E7/18-25	8	non-binder	4701	6228,96	6062,77	-	-	-	-	5997,52	5747,56	-	-
E7/69-77	9	not tested	6693	5265,77	5869,13	6693,85	2238,76	1625,60	2293,64	7131,08	4726,35	10	0,12
E7/36-43	8	not tested	30697		38565,12	-	-	-	-		34631,06	-	-
E7/42-50	9	not tested	25939		33504,88	25939,19		19863,93			26311,75	5	0,00
E7/68-75	8	not tested	25613	27753,19	23192,26	-	-	-	-	31398,89	26989,33	-	-
E7/41-50	10	not tested	37421		37132,00	37420,98					37324,66	1	0,00

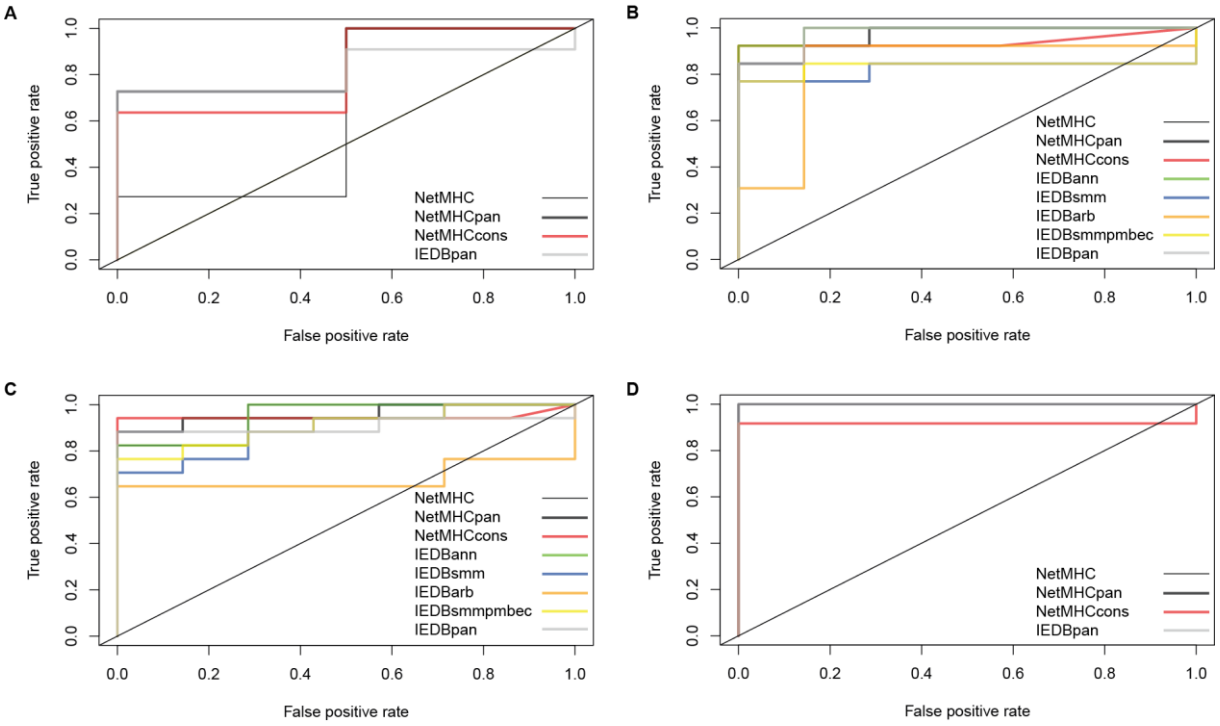

Figure 37 I Evaluation of prediction server performance for peptide predictions of 8mers, 9mers, 10mers and 11mers binding to HLA-A3 by ROC analysis. The rates of true positive predictions are plotted as a function of the rate of false positive predictions. **A** Analysis for 8mers (n=13). **B** Analysis of 9mers (n=20). **C** Analysis of 10mers (n=24). **D** Analysis of 11mers (n=14). Some curves are slightly overlayed.

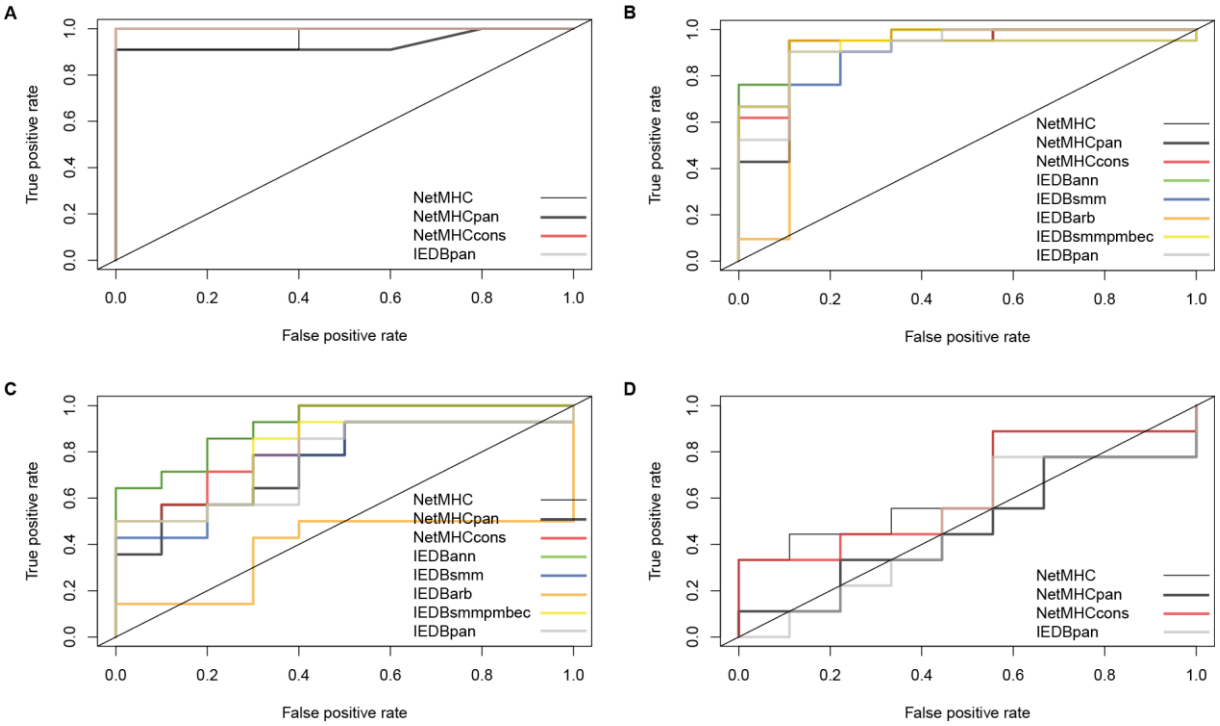

Figure 38 I Evaluation of prediction server performance for peptide predictions of 8mers, 9mers, 10mers and 11mers binding to HLA-A11 by ROC analysis. The rates of true positive predictions are plotted as a function of the rate of false positive predictions. **A** Analysis for 8mers (n=16). **B** Analysis of 9mers (n=30). **C** Analysis of 10mers (n=24). **D** Analysis of 11mers (n=18). Some curves are slightly overlayed.

Lineage	Isolate #	NCBI#	Nucleotide exchanges in the E6 open reading frame																			Nucleotide exchanges in the E7 open reading frame							Resulting amino acid exchanges	
	Position of change		83	109	131	132	143	145	146	162	176	178	233	286	289	335	350	403	433	457	532	618	647	732	789	795	843	846	E6	E7
E-1	HPV16Ref	NC_001526	A	T	A	G	C	G	T	A	G	T	G	T	A	C	T	A	G	T	A	A	A	T	T	T	T	T		
E-1	AS411b	HQ644236	-	-	-	-	-	-	-	-	-	-	-	-	-	-	-	-	-	-	-	-	-	-	-	-	-	-		
E-1	Qv02234b	HQ644259	-	-	-	-	-	-	-	-	-	-	-	-	-	-	-	-	-	-	-	-	-	-	-	-	-	-		
E-1	Qv11074b	HQ644267	-	-	-	-	-	-	-	-	-	-	-	-	-	-	-	-	-	-	-	-	-	-	-	-	-	-		
E-1	Qv11687b	HQ644268	-	-	-	-	-	-	-	-	-	-	-	-	-	-	G	-	-	-	-	-	-	-	-	-	-	-	L83V	
E-1	Qv13956b	HQ644271	-	-	-	-	-	-	-	-	A	-	-	-	-	-	G	-	-	-	-	-	-	-	-	-	-	-	D25N, L83V	
E-1	Qv15521b	AY686581	-	-	-	-	-	-	-	-	-	-	-	-	-	-	-	-	-	-	-	-	-	-	-	-	-	-		
E-1	Qv16936b	AY686580	-	-	-	-	-	-	-	-	-	-	-	-	-	-	G	-	-	-	-	-	-	-	-	-	-	-	L83V	
E-1	Qv17286b	HQ644272	-	-	-	-	-	-	-	-	-	-	-	-	-	-	-	-	-	-	-	-	-	-	-	-	-	-		
E-1	Qv17722b	AY686584	-	-	-	-	-	-	-	-	-	-	-	-	-	-	-	-	-	c	-	-	-	-	-	-	-	-		
E-1	Qv18158b	AY686583	-	-	-	-	-	-	-	-	A	-	-	-	-	-	G	-	-	-	-	-	-	-	-	-	-	-	D25N, L83V	
E-1	Qv19110b	HQ644274	-	-	-	-	-	-	-	-	-	-	-	-	-	-	-	-	-	-	-	-	-	-	-	-	-	-		
E-1	Qv24723b	HQ644280	-	-	-	-	-	-	-	-	-	-	-	-	-	-	G	-	-	-	-	-	-	-	-	-	-	-	L83V	
E-1	Qv25054b	HQ644282	-	-	-	-	-	-	-	-	-	-	-	-	-	-	G	-	-	-	-	-	-	-	-	-	-	-	L83V	
E-1	Qv25086b	HQ644283	-	-	-	-	-	-	-	-	-	-	-	-	-	-	G	-	-	-	-	-	-	-	-	-	-	-	L83V	
E-1	Qv28131b	HQ644284	-	-	-	-	-	-	-	-	-	-	-	-	-	-	-	-	-	-	-	-	-	-	-	-	-	-		
E-1	Qv33501b	HQ644286	-	-	-	-	-	-	-	-	-	-	-	-	-	-	G	-	-	-	-	-	-	-	-	-	-	-	L83V	
E-1	Qv35943b	HQ644287	-	-	-	-	-	-	G	-	-	-	-	-	-	-	-	-	-	-	-	-	-	-	-	-	-	-	L15V	
E-1	Z032b	HQ644297	-	-	-	-	-	-	-	-	-	-	-	-	-	-	-	-	-	-	-	-	-	-	-	-	-	-		
E-2	W0122	AF536179	-	-	G	-	-	-	-	-	-	-	-	-	-	-	G	-	-	-	-	-	-	-	-	-	-	-	R10T, L83V	
E-A	AS097b	HQ644234	-	-	-	-	-	-	-	-	-	G	-	-	-	-	-	-	-	-	-	-	G	-	-	-	c	c	D25E	N29S
E-A	AS310b	HQ644235	-	-	-	-	-	-	-	-	-	G	-	-	-	-	-	-	-	-	-	-	G	-	-	-	-	c	D25E	N29S
E-A	IN/Qv151168b	HQ644248	-	-	-	-	-	-	-	G	-	G	-	-	-	-	-	-	-	-	-	-	G	-	-	-	-	c	Q20R, D25E	N29S
E-A	INJP0168b	HQ644251	-	-	-	-	-	-	-	G	-	G	-	-	-	-	-	-	-	-	-	-	G	-	-	-	-	c	Q20R, D25E	N29S
E-A	Qv02706b	HQ644261	-	-	-	-	-	-	-	-	-	G	-	-	-	-	-	-	-	-	-	-	G	-	-	-	-	c	D25E	N29S
E-A	W0724b	AF534061	-	-	-	-	-	-	-	-	-	G	-	-	-	-	-	-	-	-	-	-	G	-	-	-	-	c	D25E	N29S
Af-1	BF215b	HQ644238	C	-	-	C	G	T	-	-	-	-	-	a	g	T	-	-	-	-	-	-	-	-	c	g	-	-	M(-6)L, R10T, Q14D, H78Y	
Af-1	BF325b	HQ644240	C	-	-	C	G	T	-	-	-	-	-	a	g	T	-	-	-	-	-	-	-	-	c	g	-	-	M(-6)L, R10T, Q14D, H78Y	
Af-1	R872b	AF472508	C	-	-	C	G	T	-	-	-	-	-	a	g	T	-	-	-	-	-	g	-	-	c	g	-	-	M(-6)L, R10T, Q14D, H78Y	
Af-1	Rw768b	HQ644290	C	-	-	C	G	T	-	-	-	-	-	a	g	T	-	-	-	-	-	-	-	-	c	g	-	-	M(-6)L, R10T, Q14D, H78Y	
Af-1	Rw918b	HQ644293	C	-	-	C	G	T	-	-	-	-	-	a	g	T	-	-	-	-	-	-	-	-	c	g	-	-	M(-6)L, R10T, Q14D, H78Y	
Af-1	W0236b	AF536180	C	-	-	C	G	T	-	-	-	-	-	a	g	T	-	-	-	-	-	-	-	-	c	g	-	-	M(-6)L, R10T, Q14D, H78Y	
Af-1	Z016b	HQ644296	C	-	-	C	G	T	-	-	-	-	-	a	g	T	-	-	-	-	-	-	-	-	c	g	-	-	M(-6)L, R10T, Q14D, H78Y	
Af-1	Z109b	HQ644298	-	-	G	-	G	T	-	-	-	-	-	a	g	T	-	-	-	-	-	-	G	-	c	g	-	-	R10T, Q14D, H78Y	N29S
Af-1	Z122b	HQ644299	C	-	-	C	G	T	-	-	-	-	-	a	g	T	-	-	-	-	-	-	-	-	c	g	-	-	M(-6)L, R10T, Q14D, H78Y	
Af-2	BF039b	HQ644237	-	c	-	T	G	T	-	-	-	-	-	a	g	T	-	g	-	-	-	-	G	-	c	g	-	-	R10I,Q14D,H78Y	N29S
Af-2	BF236b	HQ644239	-	c	-	T	G	T	-	-	-	-	-	a	g	T	-	g	-	-	-	-	G	-	c	g	-	-	R10I,Q14D,H78Y	N29S
Af-2	IN221688b	HQ644249	-	c	-	T	G	T	-	-	-	-	-	a	g	T	-	g	-	-	-	-	G	-	c	g	-	-	R10I,Q14D,H78Y	N29S
Af-2	IN272098b	HQ644250	-	c	-	T	G	T	-	-	-	-	-	a	g	T	-	g	-	-	-	-	G	-	c	g	-	-	R10I,Q14D,H78Y	N29S
Af-2	R460b	AF472509	-	c	-	T	G	T	-	-	-	-	-	a	g	T	-	g	-	-	-	-	G	-	c	g	-	-	R10I,Q14D,H78Y	N29S
Af-2	Rw851b	HQ644291	-	c	-	T	G	T	-	-	-	-	-	a	g	T	-	g	-	-	-	-	G	-	c	g	-	-	R10I,Q14D,H78Y	N29S
Af-2	Rw862b	HQ644292	-	c	-	T	G	T	-	-	-	-	-	a	g	T	-	g	-	-	-	-	G	-	c	g	-	-	R10I,Q14D,H78Y	N29S
NA1	Qv00512	HQ644257	-	-	-	-	-	T	-	-	-	-	-	a	g	T	G	-	-	-	-	-	-	-	c	g	-	-	Q14H, H78Y, L83V	
AA1	IN000078b	HQ644247	-	-	-	-	-	T	-	-	-	-	A	a	g	T	G	-	-	-	g	-	-	c	c	g	-	-	Q14H, D44N, H78Y, L83V	
AA1	Qv00079b	HQ644253	-	-	-	-	-	T	-	-	-	-	-	a	g	T	G	-	-	-	g	-	-	c	c	g	-	-	Q14H, H78Y, L83V	
AA1	Qv00346b	HQ644255	-	-	-	-	-	T	-	-	-	-	-	a	g	T	G	-	-	-	g	-	-	c	c	g	-	-	Q14H, H78Y, L83V	
AA1	Qv00995b	AF402678	-	-	-	-	-	T	-	-	-	-	-	a	g	T	G	-	a	-	g	-	-	c	c	g	-	-	Q14H, H78Y, L83V	
AA1	Qv04917b	HQ644265	-	-	-	-	-	T	-	-	-	-	-	a	g	T	G	-	-	-	g	-	-	c	c	g	-	-	Q14H, H78Y, L83V	
AA1	Qv13040b	HQ644269	-	-	-	-	-	T	-	-	-	-	-	a	g	T	G	-	-	-	g	-	-	c	c	g	-	-	Q14H, H78Y, L83V	
AA1	Qv21730b	HQ644276	-	-	-	-	-	T	-	-	-	-	-	a	g	T	G	-	-	-	g	-	-	c	c	g	-	-	Q14H, H78Y, L83V	
AA1	Qv23856b	HQ644278	-	-	-	-	-	T	-	-	-	-	-	a	g	T	G	-	-	-	g	-	-	c	c	g	-	-	Q14H, H78Y, L83V	
AA1	Qv33364b	HQ644285	-	-	-	-	-	T	-	-	-	-	-	a	g	T	G	-	-	-	g	-	-	c	c	g	-	-	Q14H, H78Y, L83V	
AA1	Rw649b	HQ644288	-	-	-	-	-	T	-	-	-	-	-	a	g	T	G	-	-	-	g	-	-	c	c	g	-	-	Q14H, H78Y, L83V	
AA1	Rw677b	HQ644289	-	-	-	-	-	T	-	-	-	-	-	a	g	T	G	-	-	-	g	-	-	c	c	g	-	-	Q14H, H78Y, L83V	
AA2	Qv00124b	HQ644254	-	-	-	-	-	T	-	-	-	-	-	a	g	T	G	-	-	-	-	-	-	c	c	g	-	-	Q14H, H78Y, L83V	
AA2	Qv13791b	HQ644270	-	-	-	-	-	T	-	-	-	-	-	a	g	T	G	-	-	-	g	-	-	c	c	g	-	-	Q14H, H78Y, L83V	
AA2	Qv15321b	AY686579	-	-	-	-	-	T	-	-	-	-	-	a	g	T	G	-	-	-	g	-	-	c	c	g	-	-	Q14H, H78Y, L83V	
AA2	Qv15351b	AY686582	-	-	-	-	-	T	-	-	-	-	-	a	g	T	G	-	-	-	-	-	-	c	c	g	-	-	Q14H, H78Y, L83V	
AA2	Qv19067b	HQ644273	-	-	-	-	-	T	-	-	-	-	-	a	g	T	G	-	-	-	-	-	-	c	c	g	-	-	Q14H, H78Y, L83V	
AA2	Qv22478b	HQ644277	-	-	-	-	-	T	-	-	-	-	-	a	g	T	G	-	-	-	-	-	-	c	c	g	-	-	Q14H, H78Y, L83V	
AA2	Qv23890b	HQ644279	-	-	-	-	-	T	-	-	-	-	-	a	g	T	G	-	-	-	-	-	-	c	c	g	-	-	Q14H, H78Y, L83V	
AA2	Qv24898b	HQ644281	-	-	-	-	-	T	-	-	-	-	-	a	g	T	G	-	-	-	-	-	-	c	c	g	-	-	Q14H, H78Y, L83V	

Table 26 I Classification of 62 HPV16 whole genome sequences to distinct HPV16 variants. HPV16 sequences were kindly provided by Robert D. Burk (Burk et al., 2011). The right column indicates the variant lineage (E: European, Af-1: African-1, Af-2: African-2, AA: Asian American) and the sublineages where applicable (E-1: European Prototype 1, E-2: European Prototype 2, E-A: European Asian; NA-1: North American-1, AA1: Asian-American-1, AA2: Asian-American-2). The isolate numbers were generated by Robert D. Burk. The prefix indicates the location the sample was obtained from: AS: Taiwan, BK: Burkina Faso, IN/INJP: Thailand, Qv: Costa Rica, R: USA (HAPI study), Rw: Rwanda, W: USA (WIHS study), Z: Zambia. The b after the number refers to the whole genome sequence being available.

The first 1000bp of the HPV16 sequences were analyzed in this multiple sequence alignment. Exchanges within the E6 and the E7 ORF (nucleotides 83-559 and 562-858, respectively) with regard to the HPV16 reference sequence (HPV16Ref, NC_001526) are displayed. The first row displays exchanges in position counted from the first nucleotide in the reference sequence. The second row indicates the nucleotide of the reference sequence (HPV16Ref) at the given position. Dashes (-) within the table indicate no exchange. Lowercase letters refer to silent mutations whereas capital letters indicate non-synonymous mutations. Resulting amino acid exchanges for E6 and E7 are listed in the last two columns, respectively. The positions of change are counted from the first amino acid in the actual protein, i.e. the second methionine in the coding sequence of E6 (encoded by nucleotides 104-106) and the first methionine in the coding sequence of E7 (encoded by nucleotides 562-564). Shading in the same light color (lineage assignment, isolate number and NCBI number) states that sequences are identical within the E6 and E7 ORF. Exchanges distinguishing a variant from the others are shaded yellow. Those shared between two variants (light orange) and those shared among all non-European variants (dark orange) are indicated. The T350G exchange (blue) does not correlate with a specific variant as it is present in some European and all Asian variants.

Table 27 I Cell lines with their HLA type and designated HPV16 variant including nucleotide and amino acid exchanges in comparison to the HPV16 reference sequence. The first column indicates the cell line, the second its HLA types, the third the identified HPV16 variant and the last two columns nucleotide exchanges in the E6 and E7 open reading frame (ORF), respectively. Resulting amino acid changes are included in (). "New" states that this amino acid change was not included in the 62 sequences supplied from Robert D. Burk (Burk et al., 2011). n.a.: not applicable, sil: silent mutation, XX: new allele

Cell line	HLA type	HPV16 variant	exchanges within E6 ORF	exchanges within E7 ORF
HPV16Ref		European Prototype 1		
CaSki	A*02:01, A*03:01; B*07:02, B*37:01; C07, -	European Prototype 2	A131G (R10T), T350G (L83V)	-
SiHa	A*24:02, - ; B*40:02, - ; C03, -	European Prototype 1	T350G (L83V), A442C (E113D, new)	A645C (new, L28F)
Marqu	A*02:01, -; B*27:02, -;C*02:02 ,-	European Prototype 1	-	n.a.
SNU 703	A*02:01, A*02:06; B*35:01, B*40:06	European (Asian)	T178G (D25E)	A647G (N29S), T846C (sil)
SNU 902	A*01:01, A*11:01; B*07:05, B*35:01	European (Asian)	T178G (D25E)	A647G (N29S), C749T (new, S63F), T846C (sil)
SNU 1299	A*02:01, A*33:03; B*27:05, B*44:03	Asian-American	G145T (Q14D), T286A (sil), A289G (sil), C335T (H78Y), T350G (L83V), A532G (sil)	T732C, T789C, T795G, all: sil
SCC090	A*02:01, A*03:01; B*44:03, B*51:01	European Prototype 2	A131G (R10T), T350G (L83V)	-
SCC152	A*02:01, A*03:01; B*44:03, B*51:01	European Prototype 2	A131G (R10T), T350G (L83V)	-
SCC154	A*25:01, -; B*44:02, B*44:03	Asian-American	G145T (Q14D), T286A (sil), A288G (sil), C335T (H78Y), T350G (L83V), A532G (sil)	T732C, T789C, T795G, all: sil

93VU147T	A*03:01, -; B*07:02, -	European Prototype 1	-	-
UM-SCC-47	A*01:01, A*23:01; B*37:01, B*45:01	African-2	T109C (sil), G132T (R10I), C143G (Q14D), G145T, G188C (new, E29Q), C285G (new, A61G), T286A (sil), A289G (sil), C335T (H78Y), A403G (sil)	A647G (N29S), T789C (sil), T795G (sil)
UD-SCC2	A*25:01,-; B*18N	European Prototype 1	-	C712A (new, H51N)
C66#3	A*02:01, A*30:02; B*18:01, B*35:03	European Prototype 1	C256T (sil,new), T350G (L83V)	-
C66#7	A*02:01, A*30:02; B*18:01, B*35:03	European Prototype 1	C265T (sil, new), T350G (L83V)	-
FK16A	A*01:01, A*24:02; B*07:02, B*0801	European Prototype 1	-	-
HPK 1A	A*02:01, A*03:01; B*40:01,B*55:01	European Prototype 1	-	-
MRI-H-196	A*02:XX, A*03:01; B*07:02 ,B*51:01	European Prototype 1	T350G (L83V)	-
SNU 1000	A*02:01, A*11:01; B*40:02, -	European (Asian)	T178G (D25E), T183G (I27R)	A647G (N29S), T846C (sil)
W12 20861	A*11:01, A*24:02; B*15:01, B*51:01	European Prototype 1	C256T (sil,new), T350G (L83V)	-
W12 20863	A*11:01, A*24:02; B*15:01, B*51:01	European Prototype 1	C256T (sil,new), T350G (L83V)	-
SNU 1005	A*24:02, - ; B*52:01, -	European (Asian)	T178G (D25E)	A647G (N29S), T846C (sil)
Goerke	A*01:01, - ; B*37:01	European Prototype 1	-	-
879	A*02:01, A*31:01; B*39:XX, B*40:01	European Prototype 1	-	-
866	A*02:01, A*68:01; B*15:01, B*27:05	African-2	T109C (sil), G132T (R10I), C143G (Q14D in combi), G145T (Q14D in combi), T256A (sil),T286A (sil), A289G (sil), C335T (H78Y), A403G (sil)	A647G (N29S), C765T (new, sil), T789C (sil), T795G (sil)
915	A*03:01, - ; B*14:XX, -	European Prototype 1	-	-
SNU 17	A*02:06, - , B*48:01, -	European (Asian)	T178G (D25E)	A647G (N29S), T828C (new,sil), T846C (sil)

Table 28 I Blood donor characteristics and HLA types. Questions marks indicate HLA types that are not known. * HLA typing was available only for two digits.

Donor	gender	age	HLA class I	HLA class II
1*	male	24	A*23, A*24; B*18, B*44; ?	DRB1*04, DRB1*07; ?
2	female	24	A*24:02, ?	?
3	female	37	A*24:02, A*26:02; B*35:03, B*51:08; ?, ?	DRB1*04:08, DRB1*13:01; DQB1*03:04, DQB1*06:03; DRB3*02:02, DRB4*01; DPB1*09:02, DRB1*15:01